

**FLOOD RISK MAPPING FOR
NAKHON RATCHASIMA MUNICIPALITY**



**A Thesis Submitted in Fulfillment of the Requirements for the
Degree of Doctor of Philosophy in Civil Engineering**

Suranaree University of Technology

Academic Year 2017

การสร้างแผนที่เสี่ยงภัยน้ำท่วมสำหรับเทศบาลนครนครราชสีมา



นางสาวหฤทัย มาศโค้ง

วิทยานิพนธ์นี้เป็นส่วนหนึ่งของการศึกษาตามหลักสูตรปริญญาวิศวกรรมศาสตรดุษฎีบัณฑิต

สาขาวิชาวิศวกรรมโยธา

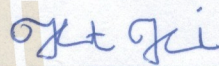
มหาวิทยาลัยเทคโนโลยีสุรนารี

ปีการศึกษา 2560

**FLOOD RISK MAPPING FOR
NAKHON RATCHASIMA MUNICIPALITY**

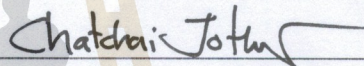
Suranaree University of Technology has approved this thesis submitted in partial fulfillment of the requirements for the Degree of Doctor of Philosophy.

Thesis Examining Committee



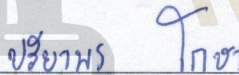
(Asst. Prof. Dr. Kittiwet Kuntiyawichai)

Chairperson



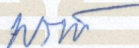
(Assoc. Prof. Dr. Chatchai Jothityangkoon)

Member (Thesis Advisor)



(Asst. Prof. Dr. Preeyaphorn Kosa)

Member



(Asst. Prof. Dr. Pornpot Tanseng)

Member



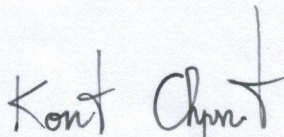
(Asst. Prof. Dr. Mongkol Jiravacharadet)

Member



(Prof. Dr. Santi Maensiri)

Vice Rector for Academic Affairs
and Internationalization



(Assoc. Prof. Ft. Lt. Dr. Kontorn Chamniprasart)

Dean of Institute of Engineering

หฤทัย มาศโค้ง : การสร้างแผนที่เสี่ยงภัยน้ำท่วมสำหรับเทศบาลนครนครราชสีมา
(FLOOD RISK MAPPING FOR NAKHON RATCHASIMA MUNICIPALITY)

อาจารย์ที่ปรึกษา : รองศาสตราจารย์ ดร.ฉัตรชัย โชติษฐียงกูร, 138 หน้า

วิทยานิพนธ์ฉบับนี้มีวัตถุประสงค์เพื่อศึกษาสภาพปัญหา ทำความเข้าใจ เหตุการณ์น้ำท่วมในอดีตในพื้นที่เทศบาลเมืองนครราชสีมา โดยเฉพาะเหตุการณ์ปี พ.ศ.2553 และปรับแก้ข้อมูลสภาพการเกิดน้ำท่วมในอดีตให้มีความถูกต้องแม่นยำขึ้น ข้อมูลที่ได้นี้ได้ถูกนำมาใช้สำหรับการพัฒนาแบบจำลองน้ำท่วม เพื่อสร้างแผนที่น้ำท่วม (Flood Hazard Map) ที่คาบการเกิดซ้ำต่าง ๆ 5 10 15 25 50 และ 100 ปี ตลอดจนพัฒนาแบบจำลอง และเครื่องมือสำหรับสร้างแผนที่เสี่ยงภัยน้ำท่วม (Flood Risk Map) เพื่อใช้ในโปรแกรม ArcGIS

ข้อมูลความลึกน้ำท่วมสูงสุดจากการสำรวจหลังจากเหตุการณ์น้ำท่วมเมื่อปี พ.ศ.2553 ถูกนำมาสร้างเป็นแผนที่น้ำท่วม (Flood Event Map) เพื่อทำความเข้าใจสภาพปัญหาจริงของการเกิดน้ำท่วม รวมถึงการวิเคราะห์ข้อมูลทางอุตุ-อุทกวิทยาของพื้นที่ศึกษาด้วย พบว่าแผนที่น้ำท่วมจากสำนักงานพัฒนาเทคโนโลยีอวกาศและภูมิสารสนเทศ (องค์การมหาชน) เป็นแผนที่น้ำท่วมที่แสดงเพียงพื้นที่น้ำท่วม (Flood Extend Map) ไม่ได้แสดงถึงความลึกน้ำท่วม อีกทั้งยังไม่สามารถแสดงถึงพื้นที่น้ำท่วมที่เป็นจริงในพื้นที่ศึกษาได้ และข้อมูลอัตราการไหลในขณะที่เกิดน้ำล้นตลิ่งแล้ว ไม่สามารถตรวจวัดได้ ดังนั้นเพื่อสร้างแผนที่น้ำท่วมที่แสดงถึงผลกระทบที่มีความแม่นยำมากขึ้น จึงใช้แบบจำลองทางชลศาสตร์ คือ โปรแกรม HecRAS V5 จำลองแผนที่น้ำท่วม โดยสร้างข้อมูลกายภาพ (Geometric data) เช่น ร่องลำนํ้า (Channel) และพื้นที่ราบน้ำท่วม (Floodplain) ของพื้นที่ศึกษาจากแผนที่ความสูงเชิงตัวเลข (DEM) ด้วยเครื่องมือ Hec-GeoRAS ในโปรแกรม ArcGIS ก่อนจะส่งออกข้อมูลทางกายภาพ เพื่อนำเข้าแบบจำลองแผนที่น้ำท่วม ซึ่งข้อมูลทางกายภาพของพื้นที่ศึกษา ได้นำเส้นโค้งความสัมพันธ์ระหว่างระดับน้ำและปริมาณน้ำ (Rating curve) ใช้เพื่อสอบเทียบการไหลในร่องน้ำ พบว่าค่าสัมประสิทธิ์ความขรุขระ (Manning's n) ที่เหมาะสมในแบบจำลองอยู่ระหว่าง 0.020-0.035 (ขึ้นอยู่กับระดับของร่องน้ำ) และของพื้นที่ราบน้ำท่วมขึ้นอยู่กับประเภทของการใช้ประโยชน์ที่ดิน จากผลการจำลองแผนที่น้ำท่วม และแผนที่น้ำท่วมจากการสำรวจ สามารถทำความเข้าใจกายภาพของการเกิดน้ำล้นตลิ่งในพื้นที่ที่ศึกษาได้ว่าเป็นเหตุการณ์น้ำท่วมที่มีอัตราการสูงสุดไหลในลำน้ำที่คาบการเกิดซ้ำ 50 ปี (อัตราการไหลเท่ากับ $217 \text{ m}^3/\text{s}$) และยังสามารถสร้างเส้นโค้งความสัมพันธ์ระหว่างระดับน้ำ และปริมาณน้ำ ที่ระดับน้ำล้นตลิ่งไปยังพื้นที่ราบน้ำท่วมของสถานีวัดน้ำท่า M.164 ได้ สามารถใช้ปรับแก้กราฟอุทก (Hydrograph) จากข้อมูลตรวจวัด ในช่วงเวลาเกิดน้ำล้นตลิ่งให้ถูกต้องแม่นยำยิ่งขึ้น

การจำลองแผนที่คุณลักษณะพื้นที่เสี่ยงภัยน้ำท่วมดำเนินการต่อจากข้อมูลแผนที่น้ำท่วมและการเปลี่ยนแปลงการใช้ประโยชน์ที่ดิน แผนที่น้ำท่วมที่ใช้ถูกจำลองจากข้อมูลการไหลแบบไม่คงที่ (Unsteady flow) ใช้กราฟอูทกที่ถูกปรับแก้แล้ว และแผนที่การใช้ประโยชน์ที่ดินของปี พ.ศ. 2565 ทำนายโดยแบบจำลอง CA-Markov จากแผนที่การใช้ประโยชน์ที่ดินปี พ.ศ.2555 และ ปี พ.ศ. 2560 ซึ่งพบว่า พื้นที่การใช้ประโยชน์ที่ดินประเภทที่อยู่อาศัย และพื้นที่เศรษฐกิจของปี พ.ศ.2565 เพิ่มขึ้น ร้อยละ 9.05 และ ร้อยละ 11.92 ตามลำดับ จากปี พ.ศ.2555 ส่งผลให้มีพื้นที่เสี่ยงภัยน้ำท่วมสูงสุด เพิ่มขึ้นร้อยละ 53 ด้วย แผนที่เสี่ยงภัยน้ำท่วมยังมีประโยชน์เพื่อที่นำไปใช้สำหรับการวางผังเมือง ตลอดจนการวางแผนเพื่อรับมือกับภัยน้ำท่วมในอนาคตได้อย่างแม่นยำ



สาขาวิชา วิศวกรรมโยธา

ปีการศึกษา 2560

ลายมือชื่อนักศึกษา

ลายมือชื่ออาจารย์ที่ปรึกษา

HARUETAI MASKONG : FLOOD RISK MAPPING FOR

NAKHON RATCHASIMA MUNICIPALITY. THESIS ADVISOR : ASSOC.

PROF. CHATCHAI JOTHITYANGKOON, Ph.D., 138 PP.

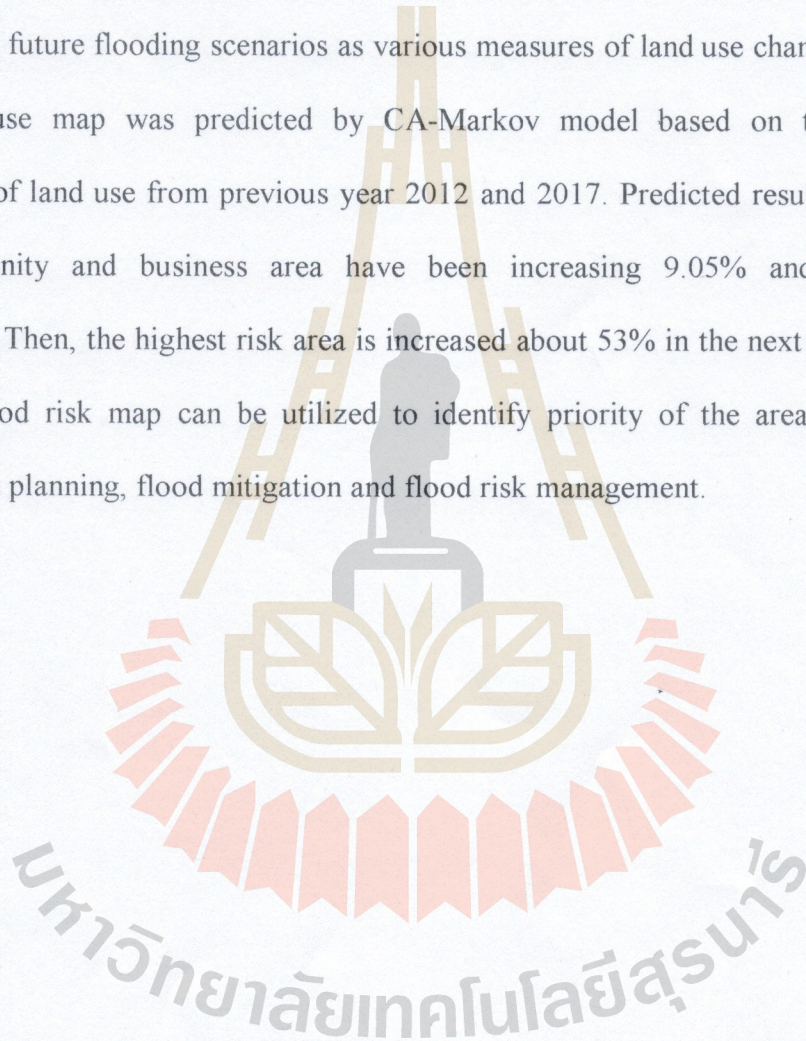
FLOOD MANAGEMENT / FLOOD HAZARD MAP / FLOOD RISK / RIVER
FLOOD / GIS APPLICATION TOOL /

The objectives of this dissertation are to collect historical flood properties, to understand flood behavior and to improve the accuracy of recorded flood in the municipality of Nakhon Ratchasima, particularly, past flood in 2010. This information has been used for developing flood inundation model to generate flood hazard maps with the maximum discharge value at the observed station (M.164) for return periods of 5, 10, 15, 25, 50, and 100 years. Then, develop an application tool in ArcGIS to generate flood risk map.

To construct the flood hazard map from available observed flood map of the small flood affected area, HecRAS V.5 and GIS tool are used to formulate and delineate flood hazard map for future scenarios of flood properties. For a simulation, input physical parameters were generated by Hec-GeoRAS in ArcGIS based on DEM ($5 \times 5 \text{ m}^2$). A range of calibrated Manning's n in a main channel was obtained from fitting exercise with observed Rating curve. It was found that the n values between 0.020-0.035 (vary with elevation of main channel) are suitable values. Manning's n in floodplain depending upon the type of land cover that were estimated by the land-use map. Observed and simulated flood map with precise information can be used to understand flood behavior in urban area and to improve the accuracy of recorded flood area from satellite images. For the 2010 flooding event in the concerning area, the

simulated flood hazard map subjected to the discharge of 50 years return period ($217 \text{ m}^3/\text{s}$) is almost identical with the observed flood map from the surveying. These results confirmed that the recorded hydrograph at M.164 was underestimated values then the new hydrograph was proposed.

Simulated flood characteristic flood risk maps were derived based on existing and different future flooding scenarios as various measures of land use change. Future 2022 land use map was predicted by CA-Markov model based on the spatial distribution of land use from previous year 2012 and 2017. Predicted results showed that community and business area have been increasing 9.05% and 11.92%, respectively. Then, the highest risk area is increased about 53% in the next decade. In addition, flood risk map can be utilized to identify priority of the area for flood preparedness planning, flood mitigation and flood risk management.



School of Civil Engineering

Academic Year 2017

Student's Signature Hanvetai M.

Advisor's Signature Chatchai John

ACKNOWLEDGEMENTS

I would like to express my highest gratitude to my supervisor, Assoc. Prof. Dr. Chatchai Jothityangkoon, for his supervision, encouragement and support, all of which have been given to me with his endless kindness. The examining committee has played a significant role in the completion of my thesis. I am grateful to Asst. Prof. Dr. Kittiwet Kuntiyawichai for serving as the chair of the Ph.D. thesis examining committee. I would also like to thank Asst. Prof. Dr. Preeyaphorn Kosa, Asst. Prof. Dr. Pornpot Tanseng, and Asst. Prof. Dr. Mongkol Jiravacharadet for serving as Ph.D. thesis examiners.

I would like to acknowledge the valuable supervision from Asst. Prof. Dr. Jurgen Komma and Prof. Dr. Gunter Bloeschl during my 8-month visit to the Vienna University of Technology, Austria.

I acknowledge the help and encouragement from Asst. Prof. Chow Hirunteeyakul, Dr. Nattaporn Charoentham, Dr. Chayakrit Phetchuay, Dr. Wisitsak Tabyang, Dr. Cherdsak Suksiripattanapong, Dr. Apichat Suddeepong, Miss. Nattiya Wonglakorn, Mr. Mathagul Metham, Mr. Nart Sooksil and Mr. Nivech Sertjantuk. I am very grateful to Mr. Thitikorn Aphibunsuwan for supporting, understanding and encouraging which made my study more than just successful.

Finally, I would like to appreciate my family and my brother Mr. Piyawut Maskong for their love, support, understanding, and providing me the opportunity to pursue my graduate studies.

Haruetai Maskong

TABLE OF CONTENTS

	Page
ABSTRACT IN THAI.....	I
ABSTRACT IN ENGLISH.....	III
ACKNOWLEDGEMENTS.....	V
TABLE OF CONTENTS.....	VI
LIST OF TABLES.....	XI
LIST OF FIGURES.....	XII
CHAPTER	
1 INTRODUCTION.....	1
1.1 Problem background and importance of the study.....	1
1.2 Research objective.....	7
1.3 Scope and limitations of study.....	8
1.4 Benefit of study.....	9
1.5 Thesis structure.....	9
1.6 References.....	10

TABLE OF CONTENTS (Continued)

	Page
2 BASIC CONCEPTS AND LITERATURE REVIEW	11
2.1 Introduction.....	11
2.2 Runoff generation processes.....	13
2.3 Hydrologic model.....	23
2.3.1 Type of the model.....	23
2.3.2 Rainfall-runoff model.....	27
2.3.3 Water balance concept.....	33
2.3.4 Water balance concept based on watershed	34
2.3.5 Channel Routing.....	36
2.4 Tool of Flood mapping.....	37
2.5 Review of the relevant research works.....	40
2.6 Reference.....	51
3 MATERIALS AND METHODS	57
3.1 Data preparation.....	57
3.1.1 Basin characteristic of study area.....	57
3.1.2 Hydrological and Geological data.....	64
3.1.3 Surveying and collecting data.....	64
3.2 Development of the flood map model.....	65
3.3 Development of the flood risk model.....	66

TABLE OF CONTENTS (Continued)

	Page
4 THE DEVELOPMENT OF A SIMPLE DISTRIBUTED HYDROLOGICAL MODEL BASED ON UP-SCALING FROM PIXEL TO CATCHMENT SCALE.....	68
4.1 Summary.....	68
4.2 Introduction.....	69
4.3 Methodology.....	71
4.3.1 Soil-water moisture and water balance.....	72
4.3.2 Evapotranspiration.....	74
4.3.3 Runoff generation process.....	75
4.3.4 Routing processes at the pixel scale.....	76
4.3.5 Topography.....	78
4.3.5 Soil properties.....	79
4.4 Results and discussion.....	80
4.5 Conclusions.....	83
4.6 References.....	85

TABLE OF CONTENTS (Continued)

	Page
5 FLOOD HAZARD MAPPING USING ON-SITE SURVEYED FLOOD MAP, HECRAS V.5 AND GIS TOOL: A CASE STUDY OF NAKHON RATCHASIMA MUNICIPALITY, THAILAND.....	87
5.1 Summary.....	87
5.2 Introduction.....	88
5.3 Study area and dataset.....	91
5.4 Methodology.....	94
5.5 Review of flood experiences.....	95
5.6 Modeling approach for numerical simulation	96
5.7 Results and discussion.....	98
5.7.1 Observed annual maximum discharge.....	98
5.7.2 Roughness coefficients (Manning's n)	99
5.7.3 Flood hazard map.....	101
5.8 Correction of flood hydrograph.....	106
5.9 Conclusions.....	106
5.10 References.....	107

TABLE OF CONTENTS (Continued)

	Page
6 THE DEVELOPMENT OF A GIS TOOL APPLICATION FOR FLOOD RISK MAPPING: A CASE STUDY OF NAKHON RATCHASIMA MUNICIPALITY, THAILAND.....	111
6.1 Summary.....	111
6.2 Introduction.....	112
6.3 Methodology.....	112
6.3.1 Input data.....	112
6.3.2 Flood Risk model.....	116
6.3.3 GIS application tool.....	122
6.4 Results and discussion.....	123
6.5 Conclusions.....	132
6.6 References.....	133
7 CONCLUSION AND RECOMMENDATION.....	135
7.1 Conclusions.....	135
7.2 Recommendation.....	137
BIOGRAPHY.....	138

LIST OF TABLES

Table	Page
2.1	The disaster vulnerability factors.....48
3.1	List of sub-basins of upper Mun River Basin and their properties.....60
3.2	Data types agencies and available records for upper Mun River Basin.....60
3.3	List of land use type and its area for Lam Takong River Basin.....63
5.1	Observed annual maximum discharges for different return period at M.164.....99
5.2	Comparison between calculated and simulated Rating curve.....100
5.3	The value of the manning roughness (n)101
6.1	Classification of the flood depth.....121
6.2	Classification of the flood velocity.....121
6.3	Classification of the type of Land use that affected by flood.....122
6.4	Covering area for different Land use type in years 2012, 2017 and 2022 based on Figure 6.4, 6.5 and 6.10.....124
6.5	The rating risk area in year 2012 for different Land use type.....127
6.6	The rating risk area in year 2017 for different Land use type.....128
6.7	The rating risk area in year 2022 for different Land use type.....129

LIST OF FIGURES

Figure	Page
1.1	Satellite image of 2011 flooding in Ayutthaya And Pathum Thani Provinces2
1.2	Boundary and location of Nakhon Ratchasima province and upper Mun river basin5
1.3	Boundary and location of study area in Nakhon Ratchasima Municipality, Nakhon Ratchasima province, Thailand6
2.1	Pathway Pathways followed by subsurface runoff on hillslopes.14
2.2	Classification of runoff generation processes15
2.3	Rainfall, runoff, infiltration and surface storage during a natural rainstorm.....19
2.4	Schematic of a watershed discretization and associated flow network in sub-watershed (left) and in grid-based artificial units (right).....24
2.5	Rainfall-runoff models using effective rainfall..... 26
2.6	Rainfall-runoff model using a surface water budget 26

LIST OF FIGURES (Continued)

Figure	Page
2.7 Flood prediction process	29
2.8 Relationship of runoff to rainfall in SCS method	32
2.9 Hydrological cycle	32
2.10 The components of flood risk	50
2.11 The reduction of flood risk.....	50
3.1 Conceptual framework of the research methodology and processes.....	58
3.2 Upper Mun river basin.....	59
3.3 DEM of Lam Takong basin	61
3.4 Land use of Lam Takong basin	61
3.5 Stream network of Lam Takong basin.....	62
3.6 Hydrological and geological station of Lam Takong basin.....	62
4.1 Conceptual description of the hydrological processes in hillslope pixels	71
4.2 Schematic diagram of the pixel-based model structure of single soil column.....	75
4.3 Multi inflow directions upstream of pixel E and only one outflow direction from pixel E depending on its elevation (100).	78

LIST OF FIGURES (Continued)

Figure	Page
4.4	Estimation of Hortonian overland flow based on Green-Ampt equation.....80
4.5	Water balance of input and output water from a pixel82
4.6	Output hydrograph form pixels based on combination of pixel and channel routing processes84
5.1	The boundary and location of the study area (a) Nakhon Ratchasima Province (b) Nakhon Ratchasima Municipality.....92
5.2	Land use of Nakhon Ratchasima Municipality93
5.3	DEM of Nakhon Ratchasima Municipality.....93
5.4	Flowchart of the study step, which is a conceptual framework of this study.....94
5.5	The 2010 surveyed point of flooding of Nakhon Ratchasima Municipality.....96
5.6	Comparison of Rating curve between calculated and simulated.100
5.7	Simulated flood hazard area at the return periods (a) T=5 years, (b) T=10 years, (c) T=15 years, (d) T=25 years, (e) T=50 years and (f) T=100 years.....102
5.8	Comparison of flood depth between surveyed flood and simulated flood.....105
5.9	Adjusted hydrograph in 2010 flood event at M.164105

LIST OF FIGURES (Continued)

Figure	Page
6.1	Flowchart of the study step for flood risk mapping.....113
6.2	Simulated Rating curve at M164.....113
6.3	Generated runoff hydrograph for T=50 years (2010 flood event).....114
6.4	Land use in 2012 Map of Nakhon Ratchasima Municipality115
6.5	Land use in 2017 Map of Nakhon Ratchasima Municipality115
6.6	The components of flood risk.....117
6.7	The reduction of flood risk118
6.8	The model structure in the flood risk application tool.....122
6.9	The flood risk application tool is applied in ArcGIS.....123
6.10	The 2022 Land use map of Nakhon Ratchasima Municipality.....124
6.11	The 2022 classification of simulated flood depth at the return periods 50 years based on risk rating scale for Nakhon Ratchasima Municipality.....125
6.12	The 2022 classification of simulated flood velocity at the return periods 50 years based on risk rating scale for Nakhon Ratchasima Municipality126
6.13	The 2012 Flood Risk Map of Nakhon Ratchasima Municipality.....130
6.14	The 2017 Flood Risk Map of Nakhon Ratchasima Municipality.....130
6.15	The 2022 Flood Risk Map of Nakhon Ratchasima Municipality.....131
6.16	The 2022 Flood Risk Map with 2017 avail photo of Nakhon Ratchasima Municipality.....133

CHAPTER I

INTRODUCTION

1.1 Problem background and importance of the study

The worst flood in five decades in Thailand occurred in 2011. It began in late July by the rainfall of tropical storm Nock-ten, flood water moved through the provinces of Northern and Central Thailand along the Mekong and Chao Phraya river basins. By October flood water reached the Chao Phraya river and inundated parts of the capital city of Bangkok. Figure 1.1 showed flood inundated area in Ayutthaya and Pathum Thani Provinces in Central Thailand on 23 October 2011 (right), compared to before the flooding on 11 July 2011 (left). In October, the Chao Phraya River had overflowed onto nearby floodplains, especially southwest of the river. Paddy fields, roads, and buildings had all been submerged by flood water. Fast flooding and flood water persevered inundation in some areas lasted until mid-January 2012. The flood resulted in a total of 815 deaths (with 3 missing) and 13.6 million people affected. Sixty-five of Thailand's 77 provinces were declared flood disaster zones, and over 20,000 square kilometers of farmland was damaged (Emergency Operation Center for Flood, 2012). The World Bank estimated that the economic loss exceeded 1,425 billion baht. Most of these were manufacturing industries, as seven major industrial estates were inundated by as much 3 meters depth during the floods (World Bank, 2011). Disruptions of manufacturing supply chains affected regional automobile production and caused a global shortage of hard disk drives which lasted throughout

2012. Thai government was unprepared for the long duration and severity of the floods, and many communities felt that the Flood Response Operation Center (FROC), which was established to coordinate emergency rescue and provide regular communications to the public, was inadequate. The Thai Government was blamed by the public that decision making on flood water management had done was carried out based on political interest and without reliable projection of flood inundated area for flood warning.



(a) 11 July 2011

(b) 23 October 2011

Figure 1.1 Satellite images of the 2011 flooding in Ayutthaya and Pathum Thani Provinces (NASA Earth Observatory, 2011)

Peak floods often occur with a frequency results in loss life and property, agricultures and industries. In 2010, Nakhon Ratchasima province located in the upper Mun River basin as shown in figure 1.2, received excessive rainfall in successive during day 14 – 16 October 2010. Majority of floodplain area in Nakhon Ratchasima province suffered from this serious flooding event. Heavy rains caused large amount of runoff flow into both upstream and downstream of all reservoirs in Nakhon Ratchasima province including Lamtakong and Lamphrapkloeng Dams. With ongoing water flowing into these reservoirs until excess it capacity, the water level was higher than the level of emergency service spillway which in turn caused severe uncontrolled flood flow into many municipalities downstream. Moreover, most of the rain could not be retarded by wetland, water then flow rapidly over lands into canals and combined with overflow water from many dams. The combination of these events caused widespread flooding on floodplain in lower basin including Muang Nakhon ratchasima district, Pukthongchai district and Chaloemphrakiat district etc. Flood water from tributary of Mun River was drained slowly into Mun River because the water level in Mun River was higher than the water level in tributary's canals and there are a lot of obstructions in the canal which resulted in reduce flow speed.

There are two types of flood protection methods to alleviate flood: (1) structural measures and (2) non-structural measures. The structural measures are a hard tool for flood control use levees and floodwalls, by-pass floodways, retarding basins and flood storage area, flood mitigation reservoirs and drainage systems modifications etc. to reduce flood peaks. The non-structural measures are a soft tool for flood management, including of land use management, flood forecasting and flood warning etc. Both measures should be used together to mitigate disaster efficiently.

After flood disaster in year 2011, there are a number of adhoc organizations were established by government. GISTDA (Geo-Informatics and Space Technology Development Agency) is a public organization under the Ministry of Science and Technology. GISTDA provides the satellite image archive for the Emergency Operation Center for Flood, Storm and Landslide (EOC). The EOC supports broad aspect of information for situation monitoring and evaluation to the provincial Flood Relief Operations Center (FROC). GISTDA not only supplies daily information from satellite images about the flooded areas but also sending experts in geo-informatics technology to help analyze satellites images, GISTDA also derives flood maps for other agencies working under FROC. Flood map can present spatial data of inundation area and expansion of flood boundary. However, it cannot evaluate flood depth and flood duration. In order to protect or at least mitigate the effect of flooding problems, physical characteristic of inundation area combine with consequent impact have to be defined in the form of a flood risk map. The flood risk map will help the responsible authorities to target on the area with higher risk where flood mitigation plan have to be effectively implemented. Flood map and flood risk map will give public tangible imagery of its impaction the flood on their community.

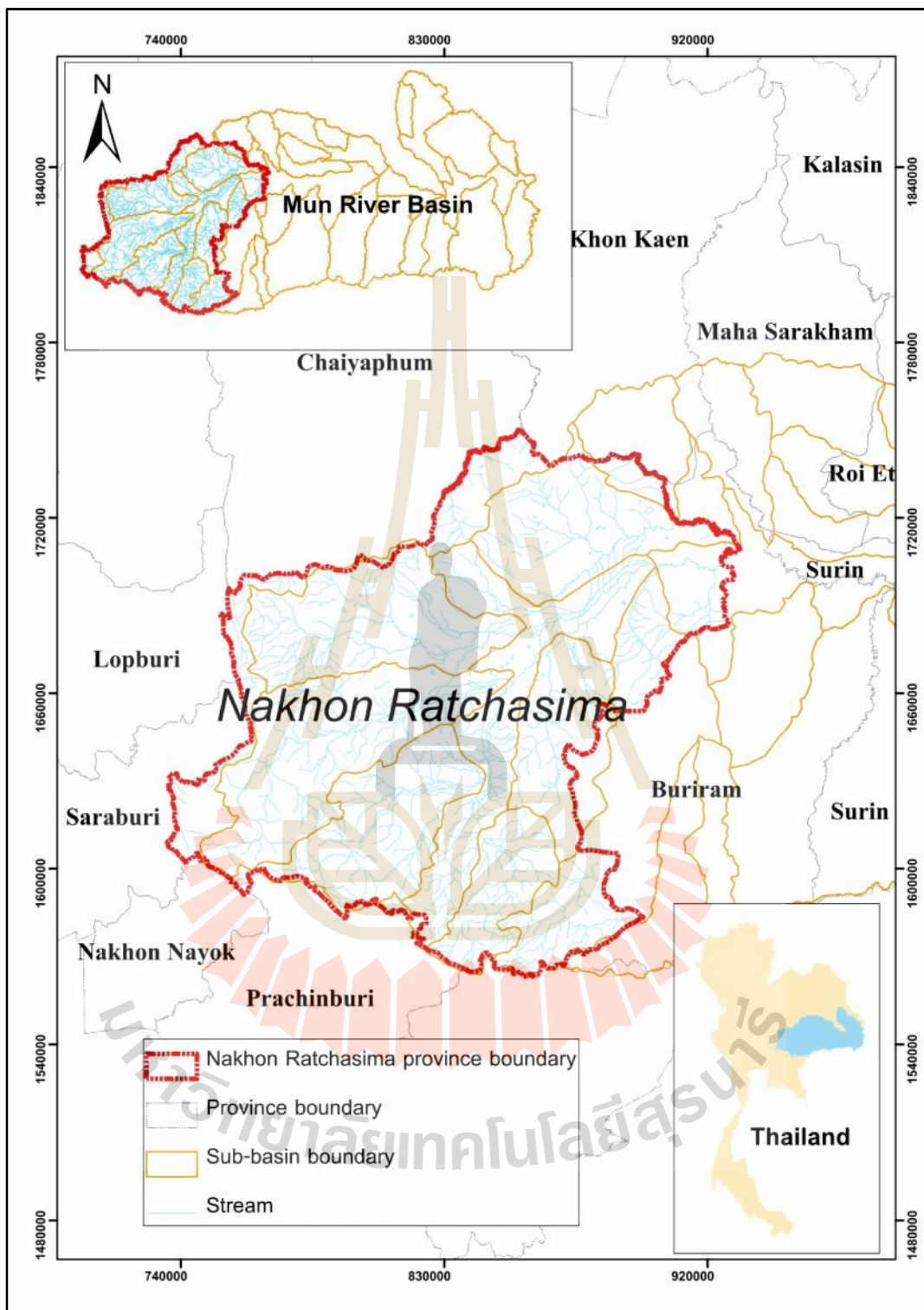


Figure 1.2 Boundary and location of Nakhon Ratchasima Province and upper Mun River Basin.

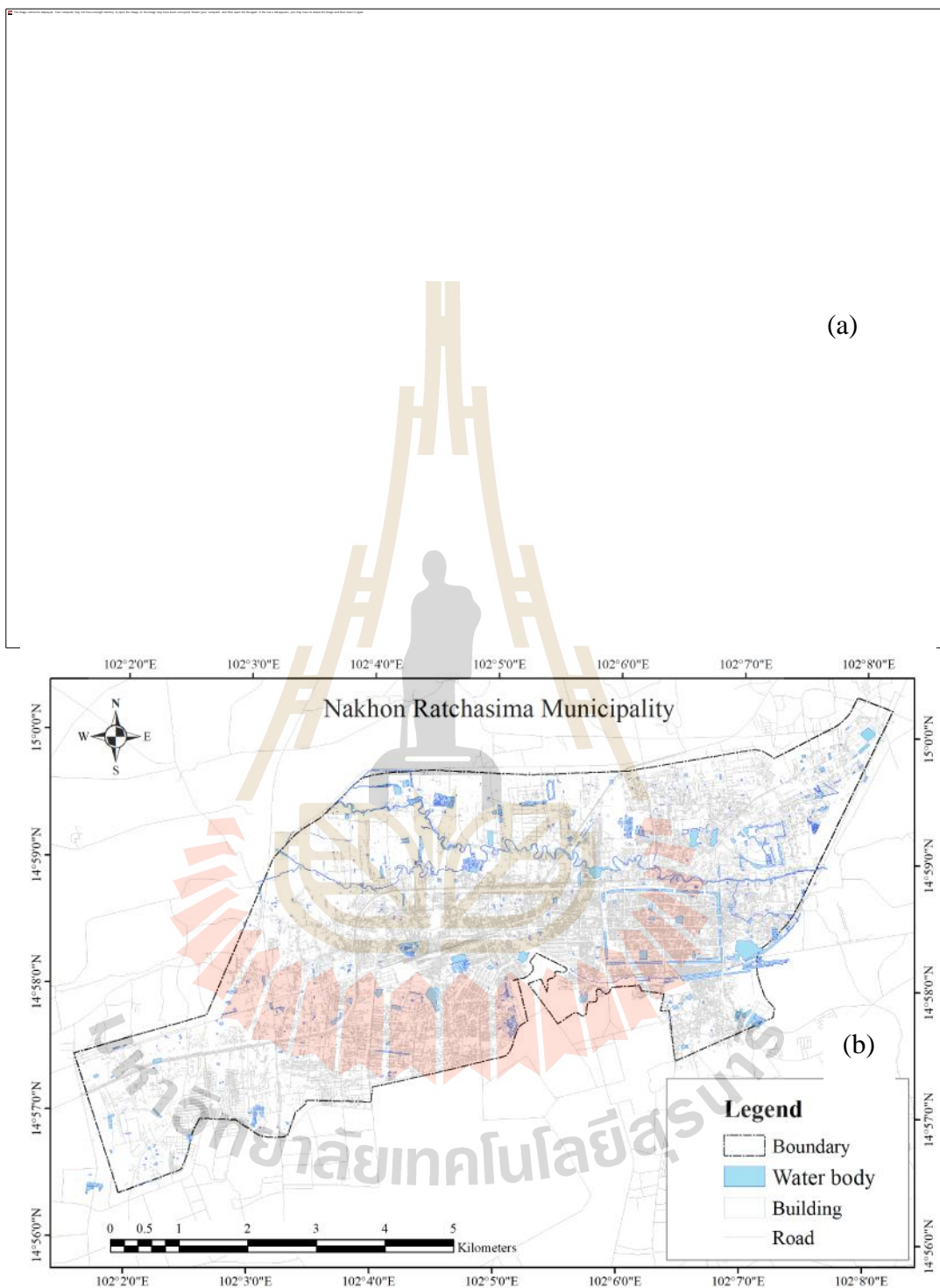


Figure 1.3 The boundary and location of the study area (a) Nakhon Ratchasima Province (b) Nakhon Ratchasima Municipality

1.2 Research objectives

Nakhon Ratchasima Municipality show in Figure 1.3 is located at the downstream of the Lam Ta Kong River as the urban center of Nakhon Ratchasima Province. There has suffered from flooding in 1978, 1996, 2002 and 2010 (Weeraya and Jirawat, 2012). Thus, the objectives of this study are as follows :

1.2.1 Collect historical flood extent and delineate observed flood map in the Nakhon Ratchasima Municipality, particularly, past flood in 2010.

1.2.2 Develop the simple distributed model that could investigate the combined effect of climate, soil, vegetation and topography on the runoff generation processes at the catchment scale in a quantitative way.

1.2.3 Construct a flood hazard map from available observed flood map of the small flood affected area with specified return periods.

1.2.4 Understand flood behavior in urban area and to improve the accuracy of recorded flood map.

1.2.5 Derive flood risk maps based on different future flooding scenarios including various measures of flood protection system land use change.

1.2.6 Develop an application tool in ArcGIS to generate flood risk map.

1.3 Scope and limitations of study

1.3.1 Study area is the Nakhon Ratchasima Municipality in Nakhon Ratchasima Province, Thailand. Upstream and downstream boundary are Khon Chum Watergates and Khoi Ngam Watergates, respectively.

1.3.2 HEC-RAS V.5 as a hybrid 1D2D model is used to quantified flood extent, depth and velocity. Flood map simulation are considered as steady flow at the observed station (M.164) for return period of 5, 10, 15, 25, 50 and 100 years.

1.3.3 The Topographic map with scale 1:50,000 (L7018 WGS84) is obtained from the Royal Thai Survey Department (RTSD) .

1.3.4 The Digital Elevation Model (DEM) 5x5 m² resolution is obtained from the Land Development Department (LDD) in the year 2008.

1.3.5 The soil data is collected from the Land Development Department (LDD) and the Department of Groundwater Resources (DGR).

1.3.6 The rainfall data and the weather data are provided by the Thai Meteorological Department (TMD) between the years 1982-2013. There are 23 rainfall stations and 6 weather stations.

1.3.7 The runoff data is provided by the Royal Irrigation Department (RID) between the years 1982-2013 for 12 stations.

1.4 Benefit of study

1.4.1 Observed flood map with precise information (i.e. area, depth, duration) can be used to understand flood behavior in urban area and to improve the accuracy of recorded flood map from satellite images.

1.4.2 Flood risk map can be identified and utilized as a tool for flood preparedness planning, flood mitigation, and flood risk management.

1.5 Thesis structure

The thesis is divided into 7 chapters Chapter I to VII are as follows:

Chapter I “Introduction” present the problem background and importance of the study, research objective, scope and limitation of study, benefits of study and thesis structure.

Chapter II “Basic concepts and literature review” consists of the descriptions of flooding and flood map, hydraulic model and literature reviews.

Chapter III “Data and methodology” summarize about collected data, surveyed data and description of methodology.

Chapter IV “The development of a simple distributed hydrological model based on up-scaling from pixel to catchment scale”

Chapter V “Flood hazard mapping using on-site surveyed flood map, HEC-RAS V.5 and GIS tool: a case study of Nakhon Ratchasima Municipality, Thailand”

Chapter VI “The development of a GIS tool application for flood risk mapping: a case study of Nakhon Ratchasima Municipality, Thailand”

Chapter VII “Conclusion and Recommendation” contains conclusion of the study and recommendations.

1.6 References

Emergency Operation Center for Flood, Storm and Landslide (2012). **Flood, storm and landslide situation report**. Retrieved 25 January 2012 (in Thai)

NASA Earth Observatory (2011). **2011 flooding in Ayutthaya Province-EO-1 merged** [Online]. Available:http://upload.wikimedia.org/wikipedia/commons/e/ec/2011_flooding_in_Ayutthaya_Province-EO-1_merged.jpg. [Accessed: 15 November 2013]

Weeraya,. M. and Jirawat, K. (2012). **The study of flood relief measures of upper Mun River Basin in Nakhon Ratchasima by Mike 11 Model**. In The 10th National Kasetsart University Kamphaeng Saen Conference, December 6-7, Kasetsart University Kamphaen, Nakhon Pathom.

World Bank (2011). **The World Bank Supports Thailand's Post-Floods Recovery Effort** [online]. Available: <http://www.worldbank.org/en/news/feature/2011/12/13/world-bank-supports-thailands-post-floods-recovery-effort>. [Accessed: 15 November 2013]

CHAPTER II

BASIC CONCEPTS AND LITERATURE REVIEW

This chapter summarizes the results of literature review carried out to understanding of the flood phenomenon, concepts of the flood risk model, which include recent research results and application of the flood risk map.

2.1 Introduction

Since the prehistoric times, floods interactions have evolved include a version to flood risk, flood defense and flood risk management, all serve as mindset or a paradigm. Flood is a general and temporary condition of partial or complete inundation of normally dry land from overflow of inland or tidal waters from the unusual and rapid accumulation or runoff of surface waters from any source. The impacts of major floods may considerably increase in the future, since society is becoming more vulnerable to the damage and disruption caused by floods, and because floods may become more serious and more frequent due to climatic changes.

Flood can be defined as an overflow, or accumulation, of substantial water volume that inundates the land (which is not normally submerged). Floods are well-known natural hazard that sometimes can lead to devastated consequences like loss of human lives or costly damage to the properties. In general, floods can be divided into 5 main types, which are (Ghosh, S.N., 2006) :

1. *River flood* is the major cause of flooding extensive areas as a result of heavy rains in the catchment areas as well as local areas thereby increasing the river level.

2. *Flash flood* occur due to heavy rain in hilly areas which cause local rivers and small streams to rise to dangerous level within a short period of time (6-12 hours). Heavy and continuous rains in local areas can cause flash floods.

3. *Urban flood* occur due to local heavy rain up to 100 mm or more in a day over the city and larger towns can cause damaging and disruptive flooding due to poor drainage and rapid runoff.

4. *Strom surge or tidal flooding* occurs during tropical disturbances, developing to cyclones and crossing surrounding coastlines. Cyclone induced storm surges have devastating consequences in coastal areas and such surge induced floods may extend many kilometers inland.

5. *Floods arising due to failure of dam* is the large number of large and small dams are constructed to store water for various purposes. Due to poor maintenance and due to exceptionally high precipitation, a severe flood may result causing failure of the dam. This causes a surging water front travelling with high velocity causing destruction of properties and loss of life.

Primary effects of flooding are physical damage to properties, buildings, roads, and to natural resources, due to the drowning and subsequence epidemics or water-borne diseases. Its secondary effects include, water-supply contamination, spread of the water-borne diseases, diminishing of crop supply. Moreover, flooding can cause long-term effect by corrupting natural resources and fertility of the ecosystem along with sustainable use of fertile land. High cost for recovering of the severely-damaged buildings, infrastructure and human illness is also a concerned issue.

2.2 Runoff generation processes

The rainfall – runoff question is also at the heart of the interface linking meteorology and hydrology. The temporal and spatial scales associated with surface water inputs, given as output from meteorological processes have profound effects on the hydrological processes that partition water inputs at the earth surface. High intensity short duration rainfall is much more likely to exceed the capacity of the soil to infiltrate water and result in overland flow than a longer less intense rainfall. A cross section (Figure 2.1) through a hillslope that demonstrate in detail of the pathways infiltrated water. Infiltrated water may flow through the matrix of the soil in the inter-granular pores and small structural voids. Infiltrated water may also flow through larger voids referred to as macropores. Macropores include pipes that are open passageways in the soil caused by decaying roots and burrowing animals. Macropores also include larger structural voids within the soil matrix that serve as preferential pathways for subsurface flow. The permeability of the soil matrix may differ between soil horizons and this may lead to the buildup of a saturated wedge above a soil horizon interface. Water in these saturated wedges may flow laterally through the soil matrix or enter macropores and be carried rapidly to the stream as subsurface storm flow in the form of interflow.

With background on the pathways followed by infiltrated water can inspect the processes involved in the generation of runoff (Figure 2.2). Each process has a different response to rainfall or snowmelt in the volume of runoff produced, the peak discharge rate, and the timing of contributions to stream flow in the channel. The relative importance of each process is affected by climate, geology, topography, soil

characteristics, vegetation, and land use. The dominant process may vary between large and small storms.

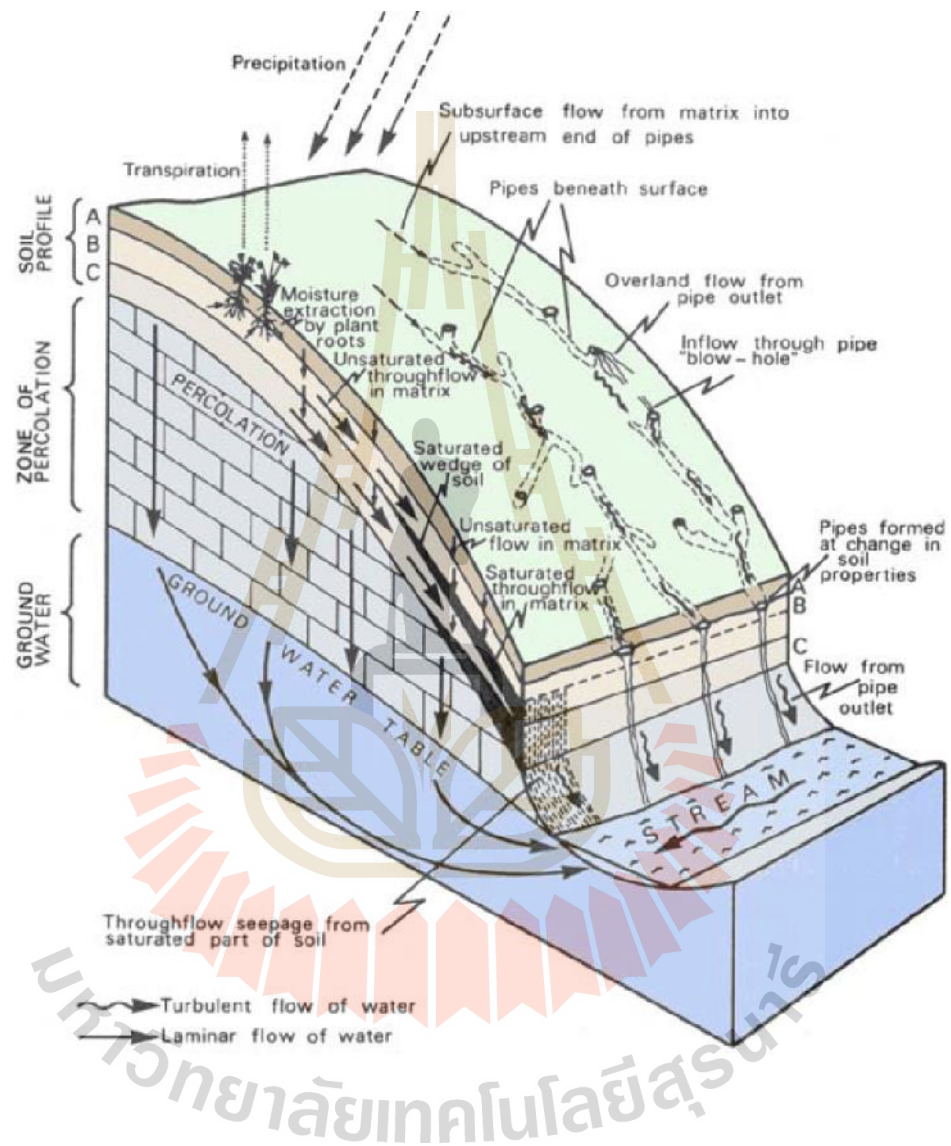


Figure 2.1 Pathway Pathways followed by subsurface runoff on hillslopes

(Tarboton, D.G., 2003)

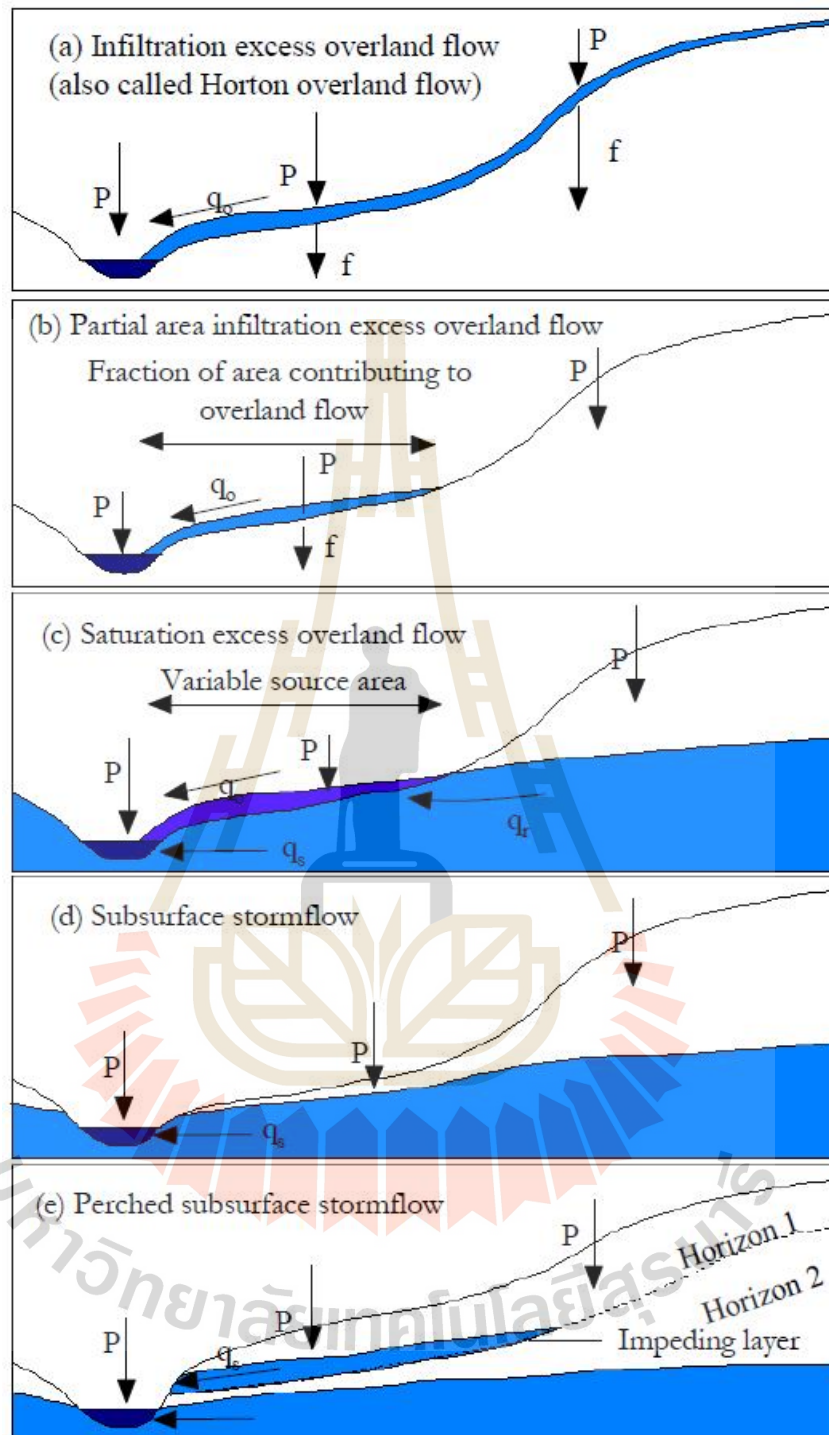


Figure 2.2 Classification of runoff generation processes (Beven, 2000)

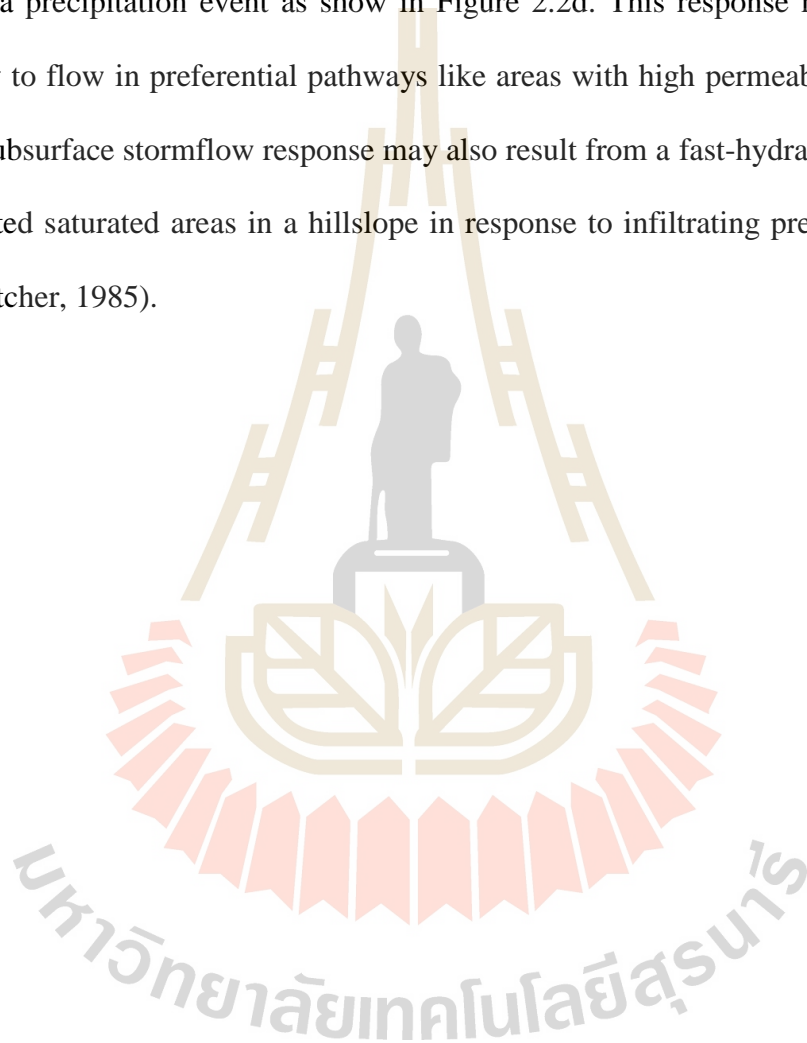
The infiltration excess overland flow processes is illustrated in Figure 2.2a. There is a maximum limiting rate at which a soil in a given condition can absorb surface water input. This process called “Horton” overland flow, named after one of the founding fathers of quantitative hydrology. As the infiltration capacity of the soil, infiltration capacity is also referred to as infiltrability. When surface water input exceeds infiltration capacity the excess water accumulates on the soil surface and fills small depressions. Water in depression storage does not directly contribute to overland flow runoff; it either evaporates or infiltrates later. With continued surface water input, the depression storage capacity is filled, and water spills over to run down slope as an irregular sheet or to converge into rivulets of overland flow. The amount of water stored on the hillside in the process of flowing down slope is called surface detention. The transition from depression storage to surface detention and overland flow is not sharp, because some depressions may fill and contribute to overland flow before others. Figure 2.3 illustrates the response, in terms of runoff from a hillside plot due to rainfall rate exceeding infiltration capacity with the filling of depression storage and increase in, and draining of, water in surface detention during a storm. Note, in Figure 2.3, that infiltration capacity declines during the storm, due to the pores being filled with water reducing the capillary forces drawing water into pores. Due to spatial variability of the soil properties affecting infiltration capacity and due to spatial variability of surface water inputs, infiltration excess runoff does not necessarily occur over a whole drainage basin during a storm or surface water input event. Betson (1964) pointed out that the area contributing to infiltration excess runoff may only be a small portion of the watershed. This idea has

become known as the partial-area concept of infiltration excess overland flow and is illustrated in Figure 2.2b.

Infiltration excess overland flow occurs anywhere that surface water input exceeds the infiltration capacity of the surface. This occurs most frequently in areas devoid of vegetation or possessing only a thin cover. Semi-arid rangelands and cultivated fields in regions with high rainfall intensity are places where this process can be observed. It can also be seen where the soil has been compacted or topsoil removed. Infiltration excess overland flow is particularly obvious on paved urban areas. In most humid regions infiltration capacities are high because vegetation protects the soil from rain-packing and dispersal, and because the supply of humus and the activity of micro fauna create an open soil structure. Under such conditions surface water input intensities generally do not exceed infiltration capacities and infiltration excess runoff is rare.

Overland flow can occur due to surface water input on areas that are already saturated. This is referred to as saturation excess overland flow, illustrated in Figure 2.2c. Saturation excess overland flow occurs in locations where infiltrating water completely saturates the soil profile until there is no space for any further water to infiltrate. The complete saturation of a soil profile resulting in the water table rising to the surface is referred to as saturation from below. Once saturation from below occurs at a location all further surface water input at that location becomes overland flow runoff.

Subsurface stormflow is a runoff producing mechanism operating in most upland terrains. Subsurface stormflow describes a runoff generation processes in the hillslope close to the soil surface that result in a stream channel hydrograph response during a precipitation event as show in Figure 2.2d. This response may be coupled directly to flow in preferential pathways like areas with high permeability. However, rapid subsurface stormflow response may also result from a fast-hydraulic response of connected saturated areas in a hillslope in response to infiltrating precipitation (Burt and Butcher, 1985).



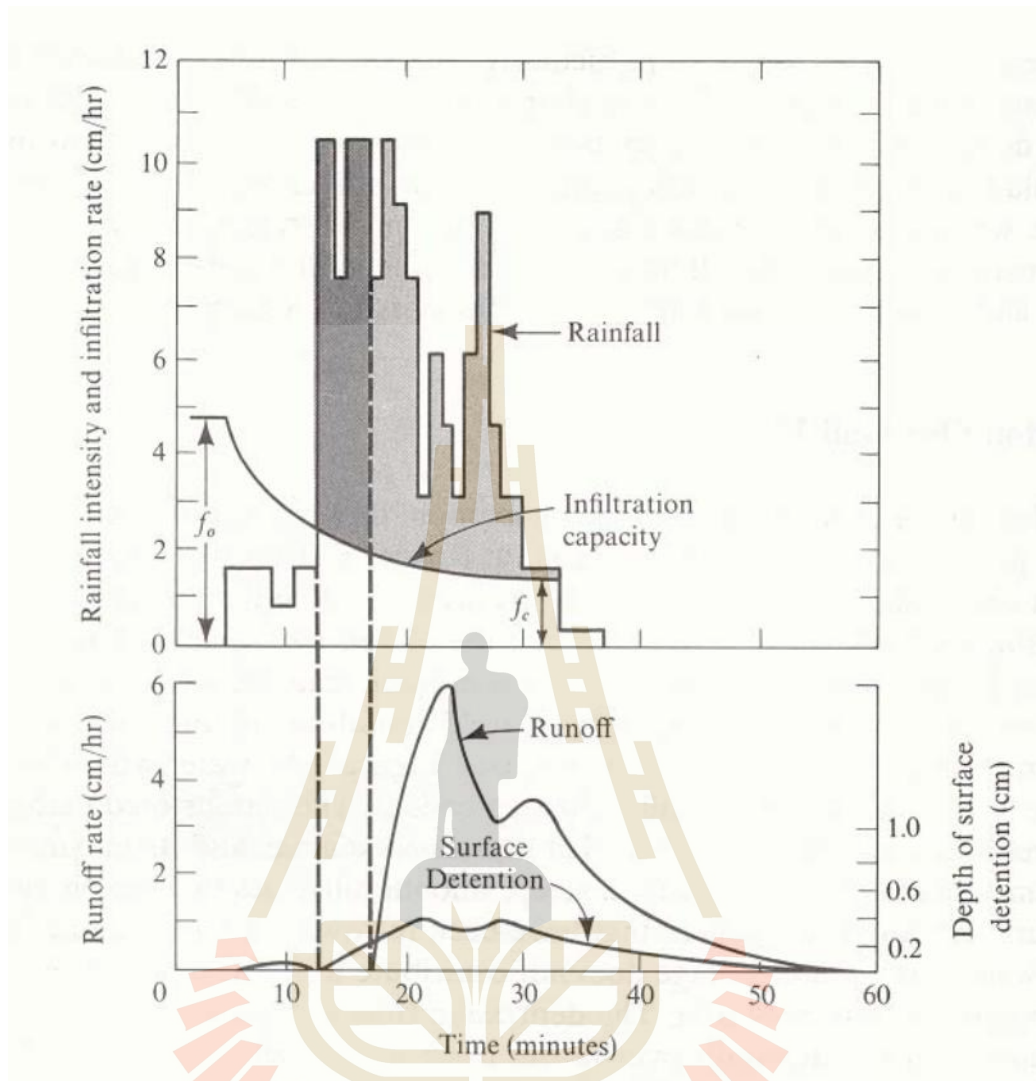


Figure 2.3 Rainfall, runoff, infiltration and surface storage during a natural rainstorm (Dunne and Leopold, 1978)

A hydrologic model was used development by Jothityangkoon et al (2001).

The water balance equation for revised, single bucket model is as follows:

$$\frac{ds(t)}{dt} = p(t) - q_{ss}(t) - q_{se}(t) - e_b(t) - e_v(t) \quad (2.1)$$

where $s(t)$ is the volume of soil moisture storage, $p(t)$ is the rainfall input rate, $q_{ss}(t)$ is subsurface runoff, $q_{se}(t)$ is saturation excess runoff rate, $e_b(t)$ is bare soil evaporation rate and $e_v(t)$ is the transpiration rate. Details of the four outflow rates (ones with a negative sign on the right hand side of Eq. 2.1) can be described as follows:

Subsurface runoff

The subsurface runoff term, q_{ss} , was determined using the relation:

$$q_{ss} = \frac{(s - s_f)}{t_c} \quad \text{if } s > s_f \quad (2.2a)$$

$$q_{ss} = 0 \quad \text{if } s < s_f \quad (2.2b)$$

Where s_f is the soil-moisture storage at field capacity, and t_c is a catchment response time with respect to the subsurface flow. The threshold storage, s_f , is assumed to be equal to $S_f = f_c D$, where f_c is soil's field capacity, and D is average effective soil depth. The reason for the use of field capacity is that often when the moisture content is less than the field capacity, capillary forces are larger than those of gravity and drainage is prevented.

In theory, the catchment response time, t_c , defines average traveling time of the induced runoff within the catchment to reach catchment's outlet. For the subsurface flow, this value can be estimated by the Darcy's law for idealized triangular representation of the unconfined aquifer within a hillslope, assuming that the hydraulic gradient can be approximated by slope of ground surface. This gives:

$$t_c = \frac{LW}{2K_s \tan S} \quad (2.3)$$

where W is the average soil porosity, L is the average hill slope length, $\tan S$ is the average ground surface slope, K_s is the average saturated hydraulic conductivity. However, due to the lack of necessary data, especially the hydraulic conductivity, for performing direct calculation of t_c from Eq. 2.3, its proper value was calibrated to provide the best fit of the simulated discharge to the observed one.

Saturation excess runoff rate

Similarly, the surface runoff term, $q_{se}(t)$, was determined using the relation:

$$q_{se} = (s - S_b) / \Delta t \quad \text{if} \quad s > S_b \quad (2.4a)$$

$$q_{se} = 0 \quad \text{if} \quad s < S_b \quad (2.4b)$$

where S_b is the bucket's soil-moisture storage capacity, given by $S_b = wD$ where w is the average soil porosity, and Δt is the time interval. Eq. 2.4 indicates that the excess surface runoff exists if amount of soil moisture storage is higher than bucket's soil-moisture storage capacity only, otherwise this term will be zero.

Bare soil evaporation rate

The evaporation term, e_b , was estimated through the relation:

$$e_b = \frac{s}{t_e} \quad (2.5)$$

$$t_e = \frac{S_b}{(1-M)e_p} \quad (2.6)$$

where t_e is a characteristic time scale associated with bare soil evaporation, estimated using Eq. 2.6, e_p is potential evaporation rate, and M is fraction of forest vegetation cover. In the original lumped model, M can vary between 0 and 1 as the forest cover can vary significantly basin to basin.

Transpiration rate

$$e_v = Mk_v e_p \quad \text{if} \quad s > s_f \quad (2.7a)$$

$$e_v = \frac{s_f}{t_g} \quad \text{if} \quad s < s_f \quad (2.7b)$$

$$t_g = \frac{s_f}{Mk_v e_p} \quad (2.8)$$

where t_g is a characteristic time scale associated with the transpiration and k_v is a plant transpiration efficiency.

2.3 Hydrologic model

2.3.1 Type of the model

The models are simplified conceptual framework of the water balance at some specific area. Most models were developed using complicated mathematical formulation to operate mainly at basin or catchment scale. They are mostly used for hydrologic prediction and for apposite understanding of hydrologic processes and their consequences. The hydrologic models commonly used nowadays can be divided into two broad categories (Seth, 2006):

(1) *Stochastic model* generates outputs that are at least partially random produces the different output from a given input. In essence, they are black-box systems in nature as their main aim is to link certain input (for instance rainfall) to model output (for instance stream runoff) using some chosen mathematical and statistical concepts where the commonly used are regression, transfer functions, and system identification. The simplest form is the linear model, but it is common to employ non-linear components to represent some general aspects of the catchment's response without moving deeply into real physical processes that might be involved (no/little physical basis required). A well-known example is the ANN model (artificial neural network) which has the ability to model both linear and nonlinear relationships without the need to make any implicit assumptions at first.

(2) *Deterministic models*, this model does not consider randomness. A given input always produces the same output. The model's processes are developed based on definite physical laws and no uncertainties in prediction are admitted. The models are based on our understanding of physics of the hydrological processes which control catchment response and use physically-based equations to describe these

processes. They basically try to represent main physical processes observed in the real world, especially those of surface runoff, subsurface flow, evapotranspiration, and channel flow, but these can go far more complicated.

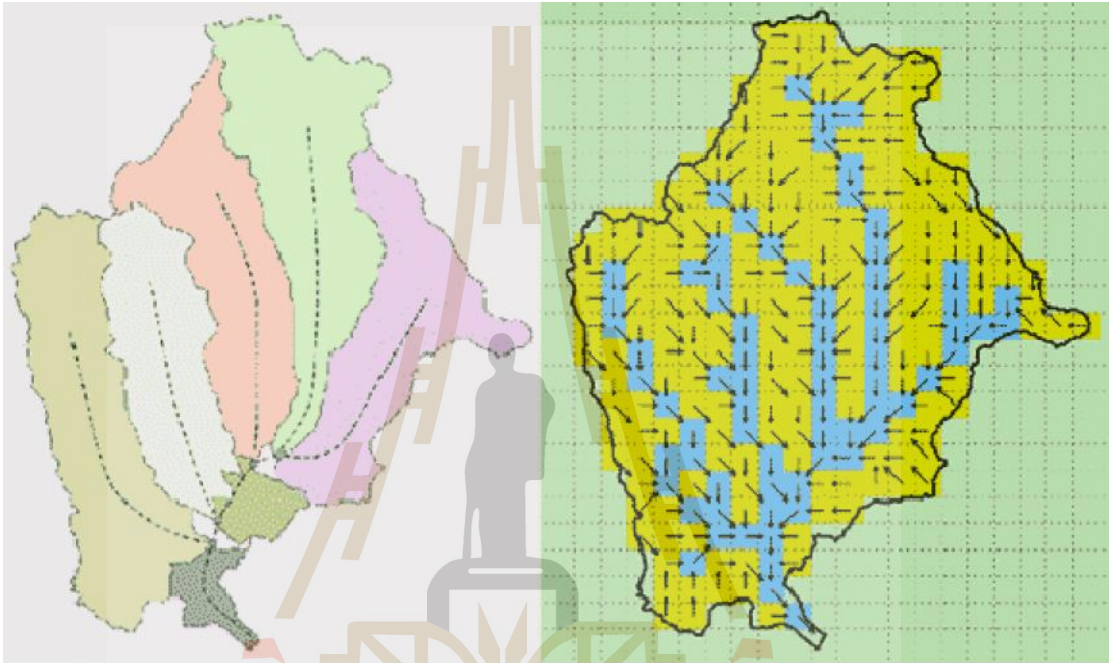


Figure 2.4 Schematic of a watershed discretization and associated flow network in sub-watershed (left) and in grid-based artificial units (right) (CRAHI, 2012).

Deterministic models can be further classified according to whether the model gives a spatially lumped or distributed description of the catchment area, and whether the description of hydrological processes is empirical, conceptual or fully physically based. Two groups of the models generally referred to in literature are (Figure 2.4) (CRAHI, 2012);

lumped model, these models conceptually assume that the transfer of water in the catchment taking place in only few well-defined storages (or lump), each of which has homogeneous property and represents a fundamental unit in the operating process (e.g. rainfall, soil characteristics, vegetation, land use practice). Though, this assumption is rarely fulfilled in reality, their concepts still provide some primary understanding in the water balance details of the examined area. These models can be regarded as in the intermediate position between the full grid-based approach and the empirical black box analysis. There are numerous lumped hydrologic models which are based on concept of a Unit Hydrograph (UH). This concept is valid within a framework which assumes that the watershed is a linear causative and time invariant system where only part of relevant excess rainfall that produces runoff.

The grid-based or distributed models, these models consider the hydrologic process that taking place within area divided into a large amount of small rectangular grids that enables them to describe the hydrologic processes with a fine resolution (e.g. 100-500 m). The equations of the processes are solved in each defined unit (grid) and combined with output from the neighbor. This structure leads to very complex models that require a great amount of information, and at least, up to present, the calibration of a tremendous amount of parameters, if not all the variables may be estimated from field data. This makes the use of the distributed models for realistic runoff forecasting is still rather difficult so far, particularly when performing in the large and heterogeneous area.

In general, the black-box model is appropriate for the preliminary study of the water balance process in the area due to its simple structure and no/little physical data of the area required. However, it gives little information about the actual process and several adjustments in the calculating algorithms might be needed just to fit the output data with the real observed ones. On the contrary, lumped model needs more physical data and knowledge of the hydrological process in the area to work properly. But its capacity is still limited to the analysis at basin/sub-basin scale only. To have model with better spatial resolution, the grid-based model is the most suitable alternative. However, the difficulties in developing such model lie in its need for huge amount of physical data and through knowledge of the hydrological process of the interested area. Therefore, it typically works well for the study in small area.

There are two strategic approaches to build the preferred hydrologic model, the downward (or top-down) and the upward (or bottom-up) approaches. As described by Klemes (1983), the downward (or top-down) approach was applied in the model's developing process. In essence, this kind of work tries to find a concept directly at the level or scale of interest (or higher) and then looks for steps that could have led to it. This is in the contrary to the upward (or bottom-up) approach which tries to combine, by mathematical synthesis, the empirical facts and theoretical knowledge available at a lower level of scale into the theories capable of predicting the response at the higher scale. As a consequence, the simple form of the preferred model will be considered and test first at the preferred scale of interest, then more complexity will be added to the original model to gain higher accuracy in the obtained result until it reaches level of accuracy required.

2.3.2 Rainfall-runoff model

The major input into the rainfall-runoff model is an estimate of rainfall and the output is an estimate of runoff. The intermediate steps that transform rainfall to runoff are the model processes. Among the hydrologic processes typically modeled are: interception, infiltration, evapotranspiration, snowpack and snowmelt, retention and detention storages, soil water movement, and filtration to ground water, overland flow, open channel flow, and subsurface flow (interflow and base flow).

Rainfall runoff models may be grouped in two general classifications that are illustrated in Figures 2.5 and 2.6. The first approach uses the concept of effective rainfall in which a loss model is assumed which divides the rainfall intensity into losses and an effective rainfall hyetograph. The effective rainfall is then used as input to a catchment model to produce the runoff hydrograph. It follows from this approach that the infiltration process ceases at the end of the storm duration. An alternative approach that might be termed a surface water budget model incorporates the loss mechanism into the catchment model. In this way, the incident rainfall hyetograph is used as input and the estimation of infiltration and other losses is made as an integral part of the calculation of runoff. This approach implies that infiltration will continue to occur as long as the average depth of excess water on the surface is finite. Clearly, this may continue after the cessation of rainfall.

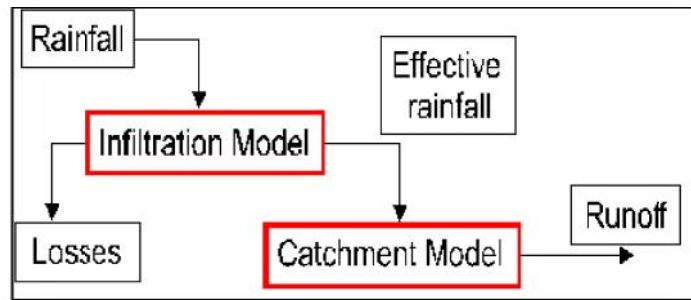


Figure 2.5 Rainfall-runoff models using effective rainfall (Alan, 2010)

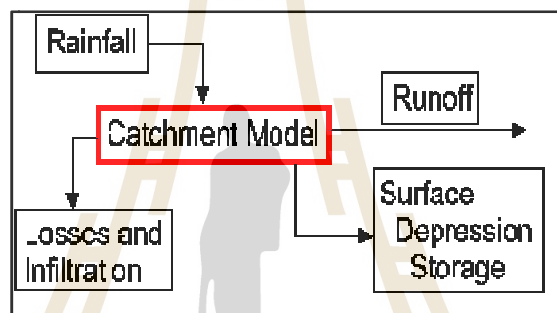


Figure 2.6 Rainfall-runoff model using a surface water budget (Alan, 2010)

Examples of the rainfall-runoff model

Unit hydrograph model

Unit hydrograph shows the temporal change in flow per unit of runoff.

The unit hydrograph is a useful tool in the process of predicting the impact of precipitation on streamflow. The role of unit hydrograph theory in the flood prediction process (Figure 2.7) is to provide an estimate of streamflow given an amount precipitation. The Unit Hydrograph provides us with a way to estimate runoff, and is an integral part of many hydrologic modeling systems.

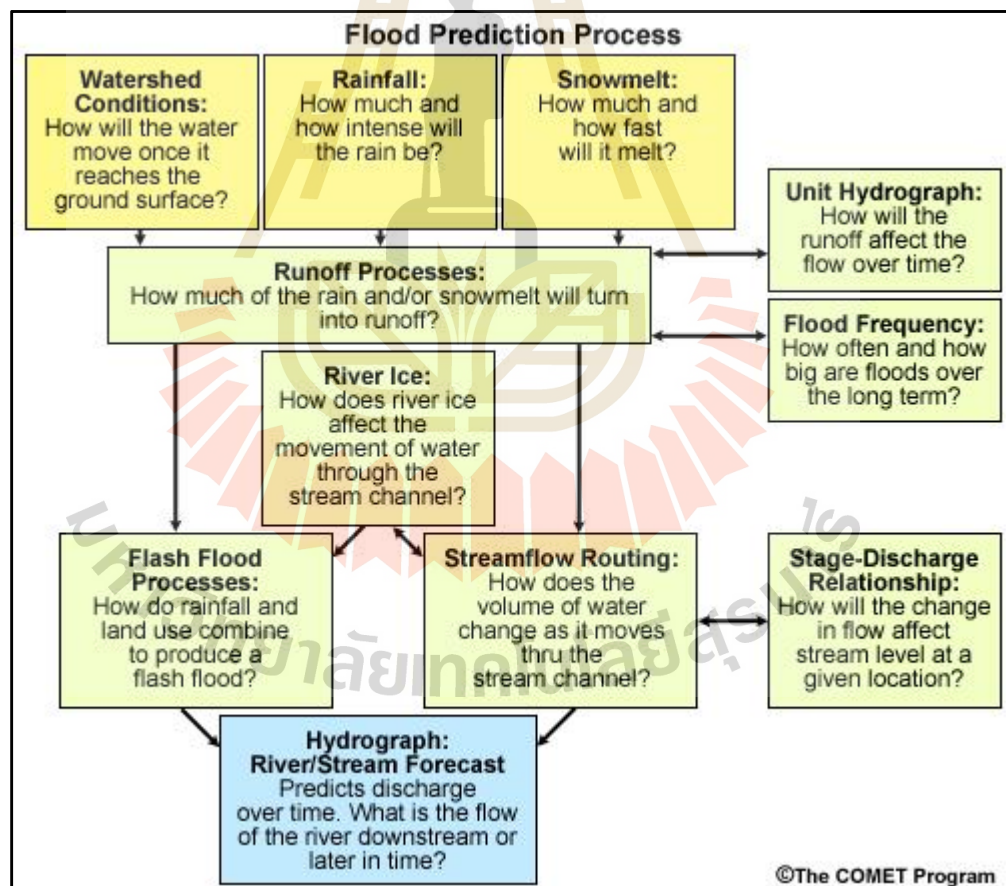


Figure 2.7 Flood prediction process (NOAA National Weather Service (NWS), 2010)

Curve Number model

The Curve Number (CN) method was developed to estimate total storm runoff from total storm rainfall. This method estimates direct runoff, which consists of channel runoff, surface runoff, and unknown proportion subsurface runoff. Generally, the CN method is well suited for small watershed (Tekeli et al., 2007). In contrast, it is not restricted to use for only small watersheds. It can be applied equally well to other large areas if the geographic variations of storm rainfall, soil, and land use are taken into account. So that with increasing availability of finer spatial resolution information from remote sensing data on land use, it is possible to use CN method for large areas with better accuracy (Chatterjee et al., 2001).

The model was developed to provide a consistent basis for estimating the amounts of runoff under varying land use and soil types (Rallison and Miller, 1981).

The SCS curve number equation is (Soil Conservation Service, 1972)

$$Q_{surf} = \frac{(R_{day} - I_a)^2}{(R_{day} - I_a + S)} \quad (2.9)$$

Where Q_{surf} is the accumulated runoff or rainfall excess (mm.H₂O),

R_{day} is the rainfall depth for the day (mm.H₂O), I_a is the initial abstractions which includes surface storage, interception and infiltration prior to runoff (mm.H₂O) and S is the retention parameter (mm.H₂O).

The retention parameter varies spatially due to changes in soils, land use, management and slope and temporally due to changes in soil water content. The retention parameter is defined as:

$$S = 25.4 \left[\frac{1000}{CN} - 10 \right] \quad (2.10)$$

Where CN is the curve number for the day. The initial abstractions, I_a is commonly approximated as $0.2S$ and equation 2.9 becomes:

$$Q_{surf} = \frac{(R_{day} - 0.2S)^2}{(R_{day} - 0.8S)} \quad (2.11)$$

Runoff will only occur when $R_{day} > I_a$. A graphical solution of equation 2.11 for different curve number values is presented in Figure 2.8.

มหาวิทยาลัยเทคโนโลยีสุรนารี

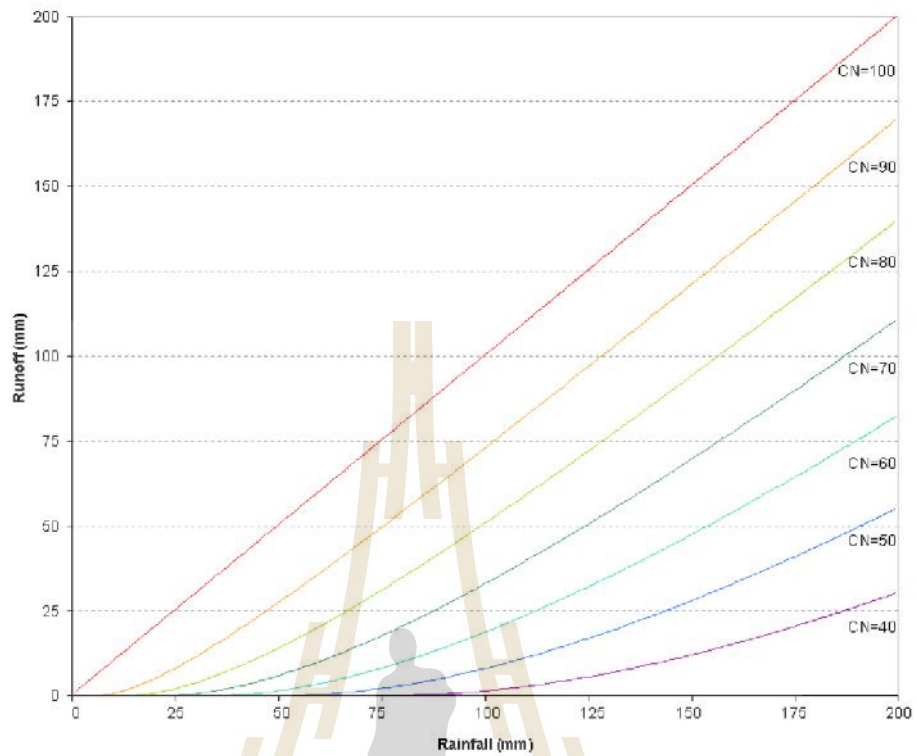


Figure 2.8 Relationship of runoff to rainfall in SCS method (Neitsch et al., 2011)

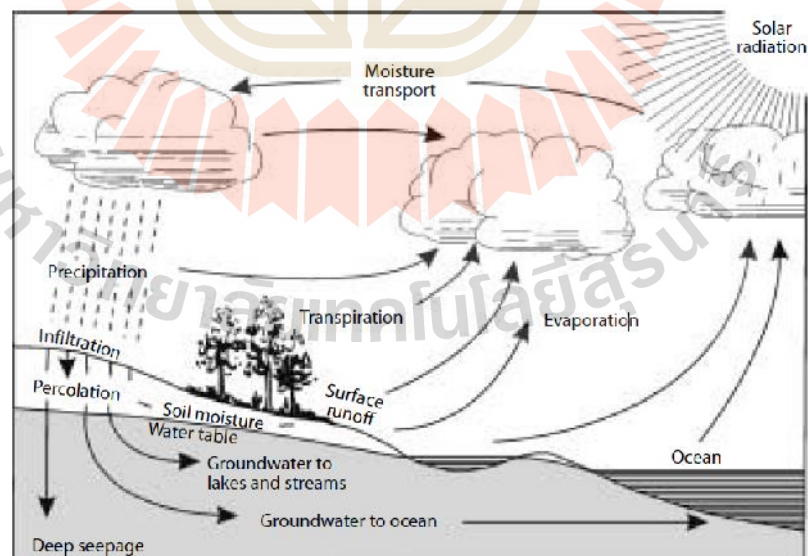


Figure 2.9 Hydrological cycle (Zhang, 2002)

2.3.3 Water balance concept

The natural occurrence of water circulation near the surface of the earth, the hydrological cycle is illustrated in Figure 2.9. The movement of water through the hydrological cycle varies significantly in both time and space. The hydrological cycle emphasizes the four phases: precipitation, evapotranspiration, surface runoff and groundwater. Water balance is based on the law of conservation of mass: any change in the water content of a given soil volume during a specified period must equal the difference between the amount of water added to the soil volume and the amount of water withdrawn from it. In principle, a water balance can be computed for any soil volume, ranging from a small sample of soil to an entire catchment.

When the control volume is the entire catchment, the surface water balance equation can be expressed as:

$$\Delta S = P - Q - ET - R \quad (2.12)$$

where ΔS is the change in spatially averaged catchment water storage, P is the spatially averaged precipitation, Q is the spatially averaged catchment surface runoff, ET is the spatially averaged evapotranspiration and R is the spatially averaged catchment recharge.

The water balance model in Eq. 2.12 is applied to determine amount of the total overland surface runoff over each considered unit area under the prior input data. It then simulates the runoff movement to the neighboring land units before finding its way to the stream channel situated nearby. Flow pattern of the existing

surface runoff usually determined by the topographic elements of the area, especially surface slope and aspect. Primary output from the hydrologic model is hydrographs at varying locations along the waterways to describe quantity, rate and timing of stream flow that results from the associated rain events. These hydrographs then become a key input into the hydraulic model. The hydraulic model simulates the movement of flood waters through waterway reaches, storage elements, and hydraulic structures. It calculates flood levels and flow patterns and also complex effects of backwater, overtopping of embankments, waterway confluences, bridge constructions and other hydraulic structure behavior.

2.3.4 Water balance concept based on watershed

Typically, the watershed can be defined as an enclosed region where the direct precipitation occurs within the confines of its drainage basin and collects into a stream channel, flowing downhill to a common basin outlet. A drainage basin is the physical boundary between watersheds where slope of the watershed diverts all surface runoff to the same drainage outlet. The boundary between watersheds is called a drainage divide. Watershed hydrology deals with the rainfall-runoff relationships found across a drainage basin (Singh 1992).

Watershed runoff is composed of three components: surface runoff, interflow, groundwater runoff (i.e. baseflow). Surface runoff flows over the surface of the watershed and downstream in stream channels to the watershed basin outlet. Interflow is the portion of runoff that infiltrates into the upper soil layers of the watershed and moves laterally until it reaches the stream channel. Interflow moves slower than surface runoff, reaching the stream channel later in time. Base flow percolates through soil until it reaches the water table and then moves laterally until

reaching the stream. Base flow is much slower than both surface runoff and interflow and has little to no impact on flood peaks resulting from a storm (Shultz, 2007).

Surface runoff is composed of two main components: overland flow and channel flow. Overland flow is the portion of runoff which flows over the land surface to the stream channel. Overland flow occurs when the precipitation rate from a storm exceeds the interception capacity of the vegetative canopy, the infiltration capacity of soil on the watershed, and surface storage. Channel flow is the translation of a flood wave as it moves downstream in a stream channel. As runoff moves across a watershed and then downstream to the outlet, it undergoes changes across both the overland flow plane and within the stream channel (Shultz, 2007).

Regarding to general concept of the hydrologic model stated earlier, there are five main factors that contribute the most to variation of the observed channel runoff:

1. Precipitation (e.g. duration, distribution, intensity) is used as the input water resource in the water balance model;
2. Topography (e.g. slope, geologic structure, drainage system) is used to determine general flow direction of the surface runoff;
3. Evapotranspiration (ET) is used to determine rate of water loss due to the evapotranspiration process (depends mostly on the climatic and soil conditions and vegetation cover pattern);
4. Soil infiltration capacity is used to determine the water loss due to the infiltration process (depends mostly on soil type);
5. Land use/land cover (LULC) pattern is used to assist the determination of flow movement, infiltration rate and AET rate the most.

2.3.5 Channel Routing

Hydraulic routing is based on the solution of partial differential equations of unsteady open-channel flow. The equations used are the St. Venant equations or the dynamic wave equations (Chow 1988). The hydraulic models (e.g. dynamic and diffusion wave models) require the gathering of a lot of data related to river geometry and morphology and consume a lot of computer resources in order to solve the Saint-Venant equations numerically.

Governing equations and numerical solution schemes

A complete set of governing equations for reduced complexity two-dimensional flood modelling comprises one of the simplified forms of the momentum equation, and a continuity equation. Continuity (or the law of conservation of mass) relates the volume in a given computational cell to the flows into and out of it during a time step:

$$\frac{\partial V^{i,j}}{\partial t} = Q_x^{i-1,j} - Q_x^{i,j} + Q_y^{i,j-1} - Q_y^{i,j} \quad (2.13)$$

where $V^{i,j}$ is the volume in cell (i, j) , t is the time and $Q_x^{i-1,j}$, $Q_x^{i,j}$, $Q_y^{i,j-1}$ and $Q_y^{i,j}$ describe the volumetric flow rates (either positive or negative) between adjacent floodplain cells in the x and y Cartesian directions respectively. The continuity equation for the cell (i, j) can therefore be written:

$$\frac{\partial h^{i,j}}{\partial t} = \theta \frac{Q_{x,t}^{i-1,j} - Q_{x,t}^{i,j} + Q_{y,t}^{i,j-1} - Q_{y,t}^{i,j}}{\Delta x \Delta y} + (1 - \theta) \frac{Q_{x,t+1}^{i-1,j} - Q_{x,t+1}^{i,j} + Q_{y,t+1}^{i,j-1} - Q_{y,t+1}^{i,j}}{\Delta x \Delta y} \quad (2.14)$$

Where $h^{i,j}$ is the flow depth, Δx and Δy are the grid cell dimensions. The weighting coefficient (θ) is used to determine whether the equation system is solved fully or partially implicitly for $\theta < 1$ or explicitly for $\theta = 1$ (Cunge et al., 1980).

2.4 Tools for Flood mapping

MIKE FLOOD

MIKE FLOOD is the complete toolbox for flood modelling available. It includes a wide selection of 1D and 2D flood simulation engines, which enable user to model virtually any flood problem - whether it involves rivers, floodplains, floods in streets, drainage networks, coastal areas, dam, levee and dike breaches or any combination of these. Where other tools give up, MIKE FLOOD gives results. The core elements in MIKE FLOOD are well-proven models, MIKE 11 for rivers, MIKE URBAN for collection systems and MIKE 21 for 2D surface flow. These are coupled to form a unique and trend-setting three-way coupled modelling tool. MIKE FLOOD is applicable at any scale from a single parking lot to regional models. Independent studies show that you can save months of efforts and create more reliable models by upgrading from standard 1D modelling to MIKE FLOOD.

HAZUS-MH software

HAZUS-MH was developed by the Federal Emergency Management Agency's (FEMA) of USA. HAZUS is a nationally applicable standardized methodology that contains models for estimating potential losses from earthquakes, floods and hurricanes. HAZUS uses Geographic Information Systems (GIS) technology to estimate physical, economic and social impacts of disasters. It graphically illustrates the limits of identified high-risk locations due to earthquake, hurricane and floods. Users can then visualize the spatial relationships between populations and other more permanently fixed geographic assets or resources for the specific hazard being modeled, a crucial function in the pre-disaster planning process. HAZUS is used for mitigation and recovery, as well as preparedness and response. Government planners, GIS specialists and emergency managers use HAZUS to determine losses and the most beneficial mitigation approaches to take to minimize them. HAZUS can be used in the assessment step in the mitigation planning process, which is the foundation for a community's long-term strategy to reduce disaster losses and break the cycle of disaster damage, reconstruction and repeated damage. Being ready will aid in recovery after a natural disaster. As the number of HAZUS users continues to increase, so do the types of uses. Increasingly, HAZUS is being used by states and communities in support of risk assessments that perform economic loss scenarios for certain natural hazards and rapid needs assessments during hurricane response. Other communities are using HAZUS to increase hazard awareness. Emergency managers have also found these map templates helpful to support rapid impact assessment and disaster response.

WMS software

The Watershed Modeling System (WMS) is a modelling system for watershed hydrology and hydraulics. WMS is capable of automated delineation of sub-watershed boundaries and flood extent, and includes graphic display options to aid in understanding the drainage characteristics of terrain surfaces as well as several computation features. WMS is a comprehensive graphical modeling environment for all phases of watershed hydrology and hydraulics. WMS can perform operations such as automated basin delineation, geometric parameter calculations; GIS overlay computations (CN, rainfall depth, roughness coefficients, etc.), cross-section extraction from terrain data, floodplain delineation and mapping, storm drain analysis, runoff, and more.

HEC-RAS

The Hydrologic Engineering Center River Analysis System (HEC-RAS) is free software with a friendly graphical user interface that was successfully used for flood studies (US Army Corps of Engineers, 2014). This software allows the user to perform one-dimensional steady flow, one and two-dimensional unsteady flow calculations, sediment transport/mobile bed computations, and water temperature/water quality modeling. In 2014, a new version of HEC-RAS (HEC-RAS-v5) was released including 2D capabilities. HEC-RAS-v5 can be used either as a fully 2D model or as a hybrid 1D2D model when the main rivers are modelled as 1D and the floodplains are modelled as 2D. Although a hybrid 1D2D model tends to be faster than a 2D model, such 1D2D model requires the user to define the connections between the 1D and the 2D models. Such connections require a prior definition of the overflow locations.

2.5 Review of the relevant research works

Flooding is a critical, yet natural phenomenon with severe economic, social and environmental consequences. Recent years, the results of severe flood events underline the requirements for reliable flood modelling tools that enable us to analyse flood events and develop flood protection measures or flood mitigation strategies in the attempt to prevent the losses of human lives and property, as well as to minimize significant destruction of infrastructure and landscape. Several hydrologic models have been developed and applied to the study of surface runoff characteristics and the associated flooding analysis for the interested areas. Examples of these works are reviewed here as follows.

Werner (2000) indicated that the flood hazard in areas adjacent to rivers may be estimated by applying hydrological/hydraulic models to calculate parameters such as flood extent, depth and duration. However, by using a two-dimensional flow model based on the topography has the drawback that computational requirements are high, making this approach unattractive when applying in, e.g., a decision support system.

Sinnakaudan et al. (2002) found that the Geographic Information System (GIS) is an efficient and interactive spatial decision support tool for flood risk analysis. They had developed the ArcView GIS extension namely AVHEC-6.avx to integrate the HEC-6 hydraulic model within GIS environment. It has the capability of analyzing the computed water surface profiles generated from HEC-6 model and producing a related flood map for the Pari River in the ArcView GIS. The flood risk model was tested using the hydraulic and hydrological data from the Pari River catchment area. The results of this study clearly show that GIS provides an effective environment for flood risk analysis and mapping.

Liu et al. (2003) studied a diffusive transport approach for flow routing in GIS-based flood modelling. This research proposes a GIS-based diffusive transport approach for the determination of rainfall runoff response and flood routing through a catchment. The watershed is represented as a grid cell mesh and routing of runoff from each cell to the basin outlet is accomplished using first passage time response function based on the mean and variance of the flow time distribution derived from the advection–dispersion transport equation. The flow velocity is location dependent and calculated in each cell by using the Manning equation based on the local slope, roughness coefficient and hydraulic radius. The total direct runoff at the basin outlet is obtained by superimposing all contributions from every grid cell.

Jothityangkoon and Sivapalam (2003) developed the distributed rainfall-runoff model to predict extreme flood. It was found from this work that when increase of normal flood condition to the extreme flood condition, the model's results showed that process of the runoff occurrence has changed by increasing of saturation excess overland flood from the increase of the saturated area. The overflowing process of the river bank had the role more than the flowing in the waterway.

Werner et al. (2005) explored the potential for identifying roughness values for distributed land use types using a comprehensive calibration data set of the 1995 flood event in the River Meuse, including gauged levels, flood extent maps and distributed flood plain level observations. The reach studied was modelled using an integrated 1D–2D hydrodynamic model, with floodplain flow modelled in the 2D domain. Detailed information on floodplain land use types is aggregated to form one, two or five classes of floodplain roughness. Sensitivity analysis of model performance against the calibration data shows that as the number of floodplain classes increases,

sensitivity to these roughness values decreases, given allocation of prior roughness values on the basis of constituent land use types and associated roughness values found from literature. Evaluating the identifiability of the roughness in these classes using the Generalised Likelihood Uncertainty Estimation (GLUE) method confirms this insensitivity. As a consequence, application of complex formula to establish roughness values for changed floodplain land use would seem inappropriate, and evaluation of such changes within a probabilistic framework are suggested.

Jothityangkoon et al. (2006) applied the distributed rainfall-runoff model developed in Australia to analyze daily water balance in Lum Pang Chu Watershed, which is sub-catchment of Mun River in the northeast of Thailand. Result of the daily model being developed by using long term water balance concept found that, it was necessary to add more complexity to runoff generation processes from soil-water storage to increase base flow in the stream and receive a better fit to the observed flow duration curve.

Ramlal and Baban (2007) developed a GIS-based hydrologic model to flood management in Trinidad, West Indies. This work uses GIS to map the extent of the flooding, estimate soil loss due to erosion and estimate sediment loading in the rivers in the Caparo River Basin. The results indicate that flooding was caused by several factors including clear cutting of vegetative cover, especially in areas of steep slopes that lead to sediment filled rivers and narrow waterways. Other factors include poor agricultural practices and uncontrolled development in floodplains.

Merwade et al. (2008) studied of GIS techniques for creating river terrain models for hydrodynamic modelling and flood inundation mapping. The objectives of them study are to highlight key issues associated with creating an integrated river terrain, and propose GIS techniques to overcome these issues. Multiple approaches are used to create river terrain models for 2D/3D hydrodynamic modelling and flood inundation mapping. Creating surface representations of river systems is a challenging task because of issues associated with interpolating river bathymetry, and then integrating this bathymetry with surrounding topography. The techniques are presented by mapping and analyzing river channel data in a channel fitted coordinate system; interpolation of river cross-sections to create a 3D mesh for main channel; and integration of interpolated 3D mesh with surrounding topography. Creation of a 3D mesh for the main channel using a channel-fitted coordinate system and subsequent integration with surrounding topography produces a coherent river terrain model, which can be used for 2D/3D hydrodynamic modelling and flood inundation mapping. Since the results from hydraulic and hydrodynamic models are greatly affected by the geometric description of the river channel bathymetry and surrounding topography, an integrated river terrain that accurately describes the main channel and the floodplain along with geomorphologic and engineering features is an important dataset that will improve our ability to accurately model and understand river flow and surrounding hydrologic processes such as surface water/ground water interaction.

Zonensein et al. (2008) presented a quantitative multi-criteria index, named Flood Risk Index (FRI), which is able to overcome some off the inconveniences of traditional flood risk assessment methodologies. The two components of risk (Probability and consequences) are represented by sub-indices, related both to flood properties and to local vulnerability and exposure characteristics, and each sub-index results from the interaction of a number of factors, expressed by indicators. The relative importance of indicators and sub-indices is represented by weights associated to each of them. The concept of risk has variable meaning according to the context in which it is employed and, for that reason, the adopted interpretation must be elucidated prior to any analysis. In engineering, risk is divided in two basic components: one related to the probability of occurrence of a hazardous event and another regarding its consequences. Concerning flood risk, in particular, this is the definition mostly accepted being. Range of the FRI were set up for the sake of simplicity and clarity, it was determined that the FRI should be a dimensionless value, which could range between 0 and 100 – the minimum and maximum risk, respectively. Moreover, in order to operate the indicators that compose FRI, which have varied natures and units, they must be normalized beforehand, converting them into a common range. According to the formulation established next, all indicators have to be adjusted to the same range, assuming values between 0 and 100. Finally, weighted summations and products compose the formulation of FRI. The index constitutes a decision support tool, allowing the rating, identification, and comparison of critical zones, the assessment of different flood risk scenarios, the development of flood risk maps, among other potential uses. The FRI was applied in a GIS.

Chen et al. (2009) developed a GIS-based urban flood inundation model called GUFIM which consists of two components: a storm-runoff model and an inundation model. Cumulative surface runoff, output of the storm-runoff model, serves as input to the inundation model. The storm-runoff model adapts the Green-Ampt model to compute infiltration based on rainfall characteristics, soil properties, and drainage infrastructure conveyance. The basis of the inundation model is a flat-water model. This effort uses publicly available elevation data, storm data, and insurance claim data to develop, implement and verify the model approach.

Rozalis et al. (2010) studied of the assessment of flood hazard by developing a flood hazard map for mid-eastern Dhaka of Bangladesh was carried out by 1D hydrodynamic simulation using both topographic remote sensing data and hydrologic field-observed data. The study demonstrates a simple and effective way to modify the collected DEM. The aim of flood hazard map is to provide residents with the information on the range of possible damage and the disaster prevention activities. The effective use of hazard map can decrease the magnitude of disasters. On the other hand, flood risk map represents the current scenario of that area according to degree of risk. The map provides helpful information about flood risk management and should be useful in assigning priority for the development of high-risk areas.

Masood and Takeuchi (2010) studied of flash floods prediction. Flash floods cause some of the most severe natural disasters. The complexity of flash flood generation processes and their dependency on different factors related to watershed properties and rainfall characteristics make flash flood prediction a difficult task. They used an uncalibrated hydrological model to simulate flow events. The model is based on the well-known SCS curve number method for rainfall–runoff calculations

and on the kinematic wave method for flow routing. Existing data available from maps, GIS and field studies were used to define model parameters, and no further calibration was conducted to obtain a better fit between computed and observed flow data. The model rainfall input was obtained from the high temporal and spatial resolution radar data adjusted to rain gauges. The model shows a generally good capability in predicting flash flood peak discharge in terms of their general level, classified as low, medium or high (all high level events were correctly predicted). It was found that the model mainly well predicts flash floods generated by intense, short-lived convective storm events while model performances for lowland moderate flows generated by more widespread winter storms were quite poor. The degree of urban development was found to have a large impact on runoff amount and peak discharge, with higher sensitivity of moderate and low flow events relative to high flows. Flash flood generation was also found to be very sensitive to the temporal distribution of rain intensity within a specific storm event.

Khatibi (2011) used historical data to model these transitions and to explain. This is a new bottom-up modelling capability based on a set of postulates integrating: (i) systemic thinking where systems are effected by four types of feedback loops to be described in the paper, which include positive/negative feedback; and (ii) evolutionary thinking, where each feedback loop is associated with a “risk mindset.” These mindsets can undergo evolutionary transition from one to the next and the transition is largely driven by natural selection. After an evolutionary transition, lower mindsets do not necessarily disappear but can adapt and coexist with higher order loops. Based on the insight gained, the paper argues that (i) as the loops coexist pluralistically, systems increase in their complexity; (ii) there may be unexpected

dynamic behaviors when a system is interacted with different types of feedback loops; and (iii) currently, these dynamic behaviors are overlooked, suggesting possible loopholes, bottlenecks or barriers and hence the motivation.

Jothityangkoon et al. (2013) studied of the assessing the impact of climate and land use changes on extreme floods in a large tropical catchment. They concern about the safety of large dams designed and built some 50 years ago. In this study distributed rainfall–runoff model appropriate for extreme flood conditions is used to generate revised estimates of the Probable Maximum Flood (PMF) for the Upper Ping River catchment in northern Thailand, upstream of location of the Bhumipol Dam. The model has two components: a continuous water balance model based on a configuration of parameters estimated from climate, soil and vegetation data and a distributed flood routing model based on non-linear storage discharge relationships of the river network under extreme flood conditions. The model is implemented under several alternative scenarios regarding the Probable Maximum Precipitation (PMP) estimates and is also used to estimate the potential effects of both climate change and land use and land cover changes on the extreme floods. These new estimates are compared against estimates using other hydrological models, including the application of the original prediction methods under current conditions. Model simulations and sensitivity analyses indicate that area reasonable Probable Maximum Flood (PMF) at the dam site is $6,311 \text{ m}^3/\text{s}$, which is only slightly higher than the original design flood of $6000 \text{ m}^3/\text{s}$. As part of an uncertainty assessment, the estimated PMF is sensitive to the design method, input PMP, land use changes and the flood plain inundation effect.

Daungthima and Hokao (2013) studied of the Analyzing the Possible Physical Impact of Flood Disasters on Cultural Heritage in Ayutthaya, Thailand. They was reviews of disaster vulnerability factors, found that the most crucial factors may be organized as six groups of factors which are: topography, slope, density of building, distance from the river, drainage system and soil type, and distance to road. Topography refers to current elevation and surface water flow paths. Slope refers to upstream source of flooding, flood susceptibility and overflow sensibility. Density of building refers to land value per floor space and land use. The distance from the river refers to distance of area flooding risk to river. Drainage system and soil refer to vulnerable community and critical, soil erodibility, soil drainage, soil moisture, soil scape in fragile environmental balance and soil composition. Distance to road refers to distance of historical sites to road.

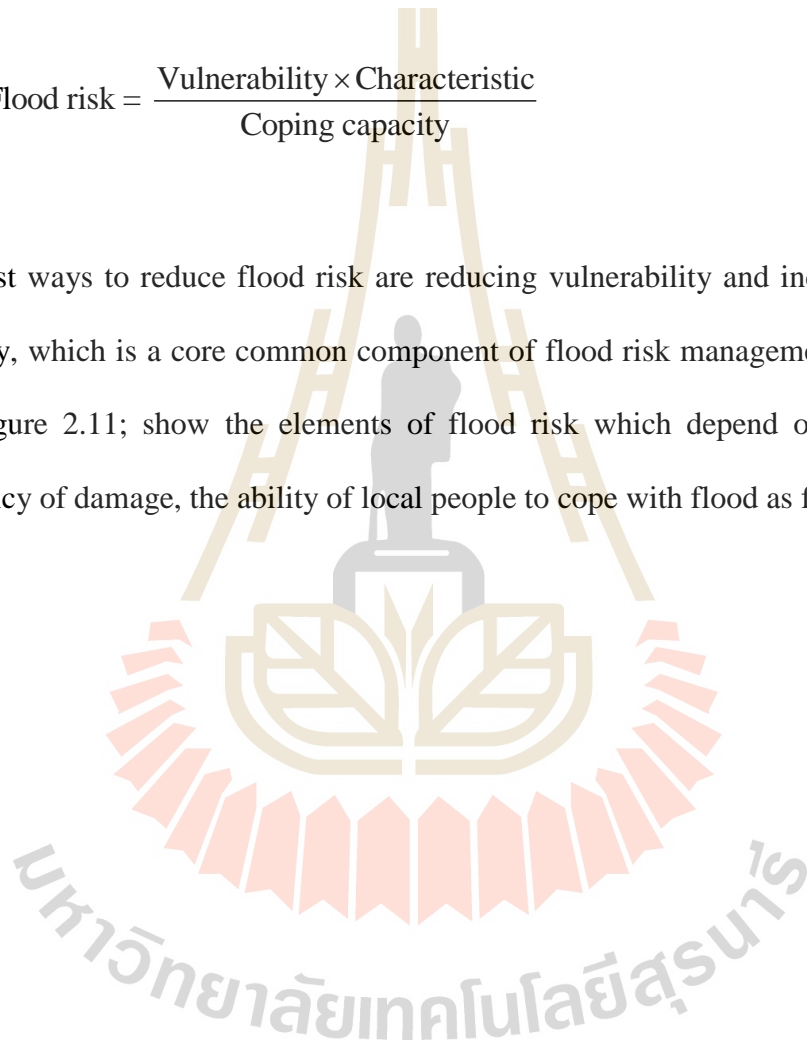
Table 2.1. The disaster vulnerability factors

Factors	Detail of factors
Topography	Current elevation Surface water flow paths
Slope	Upstream source of flooding Flood susceptibility Overflow sensibility
Density of building	Land value per floor space Land use
Distance from the river	Area at risk from flooding
Drainage system & Soil	Vulnerable community and critical infrastructure Soil erodibility Soil drainage Soil moisture Soil scape in fragile environmental balance Soil composition
Distance to road	Distance of historical site to road

Mongkonkerd et al. (2013) determined flood risk not only by vulnerability but also by characteristics and coping capacity to flood exposure. Therefore, the risk of flood is based on three crucial elements which are related as shown in equation 2.15 (the formula of flood risk).

$$\text{Flood risk} = \frac{\text{Vulnerability} \times \text{Characteristic}}{\text{Coping capacity}} \quad (2.15)$$

The best ways to reduce flood risk are reducing vulnerability and increasing coping capacity, which is a core common component of flood risk management. Figure 2.10 and Figure 2.11; show the elements of flood risk which depend on vulnerability, frequency of damage, the ability of local people to cope with flood as follows:



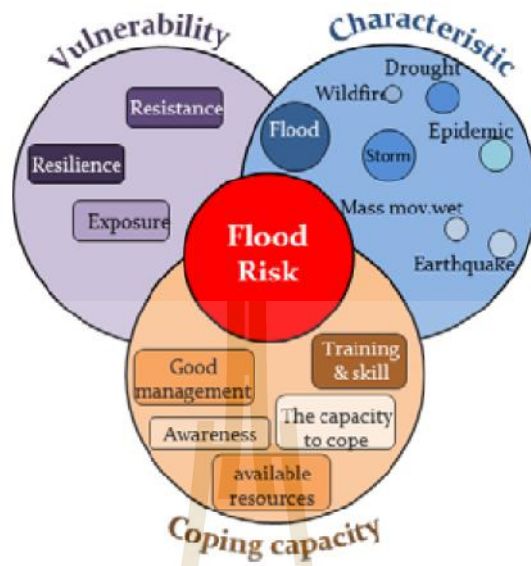


Figure 2.10 The components of flood risk (Daungthima and Hokao., 2013)

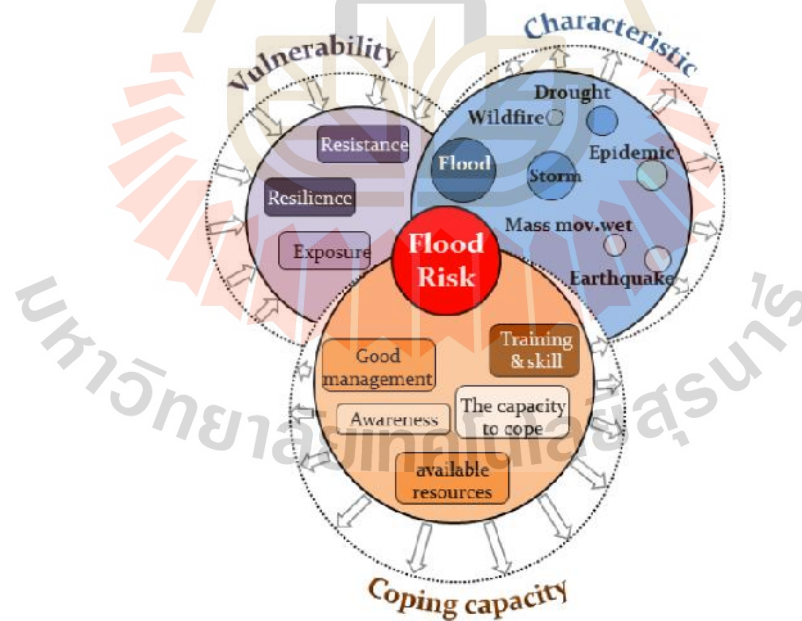


Figure 2.11 The reduction of flood risk (Daungthima and Hokao., 2013)

Vulnerability refers to circumstances of a community or asset that make it susceptible to the damaging effects of a flood. There are many aspects of vulnerability, arising from various physical, social, economic, and environmental factors. Examples may include construction of buildings, inadequate protection of assets, lack of information and awareness.

Characteristic refers to natural disaster occurrence, frequency of damage, duration and maximum water level.

Coping capacity is the ability of people in the community to face and manage the flood using available skills and resources. The capacity to cope requires continuing awareness, resources and good management, both in normal times as well as during crises or adverse conditions.

2.6 References

- Alan A.S. (2010). **Hydrological Theory: Rainfall Runoff Models** [online]. Available: <http://www.alanasmith.com/theory-Calculating-Runoff-Rainfall-Runoff-Models.html>.
- Beven, K. J. (2000). **Rainfall Runoff Modelling: The Primer**, John Wiley, Chichester.
- Betson, R. P. (1964). **What Is Watershed Runoff**. Journal of Geophysical Research, 68: 1541-1552.
- Burt T.P. and Butcher D.P. (1985), **Topographic controls of soil moisture distributions**. Journal of Soil Science, 36(3), 469 – 486.

- Chatterjee, C., Jha, R., Lohani, A. K., Kumar, R., and Singh, R. (2001). **Run-off curve number estimation for a basin using remote sensing and GIS**. Asian-Pacific Remote Sensing and GIS Journal. 14: 1-8.
- Chen, J., Hill, A.A. and Urbano, L.D. (2009). **A GIS-based model for urban flood inundation**. Journal of Hydrology. 373: 184-192.
- Chow, V. T., Maidment, D. R. and Mays L.W (1988). **Applied Hydrology**. McGrawHill International Editions: Singapore. 569 pp.
- CRAHI. (2012). **Type of hydrological models**. [Online]. Available: <http://www.crahi.upc.edu/en/projects/areas-of-expertise/78-tipus-de-models-hydrologics>.
- Cunge, J.A., Holly, F.M., Verwey, A. (1980). **Practical Aspects of Computational River Hydraulics**. Pitman Publishing, London. 420 pp.
- Daungthima, W. and Hokao, K. (2013). **Assessing the flood impacts and the cultural properties vulnerabilities in Ayutthaya, Thailand**. Procedia Environmental Sciences. 17: 739-748.
- Dunne, T. and Leopold, L. B. (1978). **Water in Environmental Planning**. W H Freeman and Co, San Francisco, 818 p.
- Tarboton, D.G. (2003). **Rainfall-Runoff Processes**. Water Research Laboratory, Civil and Environmental Engineering, Utah State University
- Ghosh, S.N. (2006). **Flood Control and Drainage Engineering** 3th edition. Taylor & Francis Group. 357 pp.
- Jothityangkoon, C. and Sivapalan, M. and Farmer, D.L. (2001). **Process controls of water balance variability in a large semiarid catchment: Downward**

- approach to hydrological model development.** Journal of Hydrology. 254: 174-198.
- Jothityangkoon, C. and Sivapalan, M. (2003). **Towards estimation of extreme flood: Examination of the roles of runoff process changes and floodplain flows.** Journal of Hydrology. 281: 206-229.
- Jothityangkoon, C. and Hirunteeyakul, C. (2006). **Hydrological model development for water balance study in subcatchment of Mun River.** School of civil engineering, Suranaree University of Technology.
- Jothityangkoon, C., Hirunteeyakul, C., Boonraed, K. and Sivapalan, M. (2013). **Assessing the impact of climate and land use changes on extreme floods in a large tropical catchment** Journal of Hydrology. 490: 88-105.
- Khatibi, R. (2011). Evolutionary systemic modelling of practices on flood risk, Journal of Hydrology, 401 36–52
- Klemes, V. (1983). **Conceptualisation and scale in hydrology.** Journal of Hydrology. 65: 1-23.
- Liu, Y.B., Gebremeskel, S., Smedt, F.D., Hoffmann, L. and Pfister, L. (2003). **A diffusive transport approach for flow routing in GIS-based flood modeling.** Journal of Hydrology. 283: 91-106.
- Masood, M. and Takeuchi, K. (2010). **Assessment of flood hazard, vulnerability and risk of mid-eastern Dhaka using DEM and 1D hydrodynamic model,** Nat Hazards, 61:757–770.
- Merwade, V., Cook, A., Coonrod, J. (2008). **GIS techniques for creating river terrain models for hydrodynamic modelling and flood inundation mapping,** Environmental Modelling & Software, 23:1300-1311.

- Mongkonkerd, S., Hirunsalee, S., Kanaegae, H. and Denpaiboon, C. (2013). **Comparison of direct monetary flood damage in 2011 to pillar house and non-pillar house in Ayuthhaya, Thailand.** *Procedia Environmental Sciences*, 17: 327-336.
- Neil, M.H., Paul, D.B., Matthew, S.H. and Matthew, D.W.(2007). **Simple spatially-distributed models for predicting flood inundation: A review.** *Geomorphology*, Vol.90, pp.208-225.
- Neitsch, S. L., Arnold, J. G., Kiniry, J. R., and Williams, J. R. (2011). **Soil and Water Assessment Tool theoretical documentation version 2009.** Texas Water Resources Institute, College Station, Texas.
- NOAA National Weather Service (2010). **Unit Hydrograph Theory** [online]. Available:http://stream2.cma.gov.cn/pub/comet/HydrologyFlooding/UnitHydrographTheoryInternationalEdition/comet/hydro/basic_int/unit_hydrograph/print.htm#page_1.0.0.
- Rallison. R. E. and Miller, N. (1981). **Past, present and future SCS runoff procedure.** In V.P. Singh (Ed.), *Rainfall runoff relationship* (pp.353-364). Water Resources Publication, Littleton, Colorado.
- Ramlal, B. and Baban, S.M.J. (2007). **Developing a GIS based integrated approach to flood management in Trinidad, West Indies.** *Journal of Environmental Management*. 88: 1131-1140.
- Rozalis, S., Morin, E., Yair, Y. and Price, C. (2010), **Flash flood prediction using an uncalibrated hydrological model and radar rainfall data in a**

- Mediterranean watershed under changing hydrological conditions**,
Journal of Hydrology, 394:245–255
- Seth, S.M. (2006). **Role of Remote Sensing and GIS inputs in physically based Hydrological Modelling** [Online]. Available: <http://www.gisdevelopment.net/application/nrm/water/overview/wato0006pf.htm>
- Shultz, M.J. (2007). **Comparison of Distributed Versus Lumped Hydrologic Simulation Models Using Stationary and Moving Storm Events Applied to Small Synthetic Rectangular Basins and an Actual Watershed Basin**. Ph.D. THESIS, The University of Texas at Arlington.
- Singh, V.P. (1992). **Elementary Hydrology**. New Jersey: Prentice Hall, Englewood Cliffs.
- Sinnakaudan, S.K., Ghani, A.A., Ahmad, M.S.S. and Zakaria, N.A. (2002). Flood risk mapping for Pari River incorporating sediment transport. **Environmental Modelling & Software**. 18: 119-130.
- Soil Conservation Service (SCS). (1972). **National Engineering Handbook, Section 4: Hydrology**. Department of Agriculture, Washington DC, 762 p.
- Tekeli, T. I., Akgul, S., Dengiz, O., and Akuzum, T. (2007). **Estimation of flood discharge for small watershed using SCS curve number and geographic information system**. International Congress on River Basin Management. Antalya, Turkey.
- US Army Corps of Engineers, (2014). **Hydrologic Engineering Centers River Analysis System (HEC-RAS)**, available at: <http://www.hec.usace.army.mil/software/hec-ras/>[Accessed: 15 November 2014].

Werner, M.G.F. (2000). **Impact of Grid Size in GIS Based Flood Extent Mapping Using a 1D Flow Model**. Elsevier Science Ltd.

Werner, M.G.F., Hunter, N.M. and Bates, P.D. (2005). **Identifiability of distributed floodplain roughness values in flood extent estimation**. Journal of Hydrology, 314 : 139–157

Zhang,L., Walker, G.R and Dawes, W.R.(2002). **Water balance modelling: concepts and applications**. Regional Water and Soil Assessment for Managing Sustainable Agriculture in China and Australia, ACIAR Monograph. No. 84: 31–47.

Zonensein, J., Miguez., M.G., de Magalhaes, L.P.C., Valentin, M.G., and Mascarenhas, F.C.B. (2008). **Flood Risk Index as an Urban Management Tool**. 11th International Conference on Urban Drainage, Edinburgh, Scotland, UK.

CHAPTER III

DATA AND METHODOLOGY

This chapter describes the materials and methodology of risk mapping. Conceptual framework of the research is shown in Figure 3.1. Table 3.1 is represented physical data for basin in the study area. Upper Mun river basin consist of 6 subbasins shown in Figure 3.2 to demonstrate primary collected data, Lam Takong subbasin is chosen to represent methodology process.

3.1 Data preparation

3.1.1 Physical characteristic of study area

Digital Elevation Model (DEM)

The topography of land surface substantially influence on the magnitude and dynamics of surface runoff. To illustrate the shape of land surface, DEM can be used to generate topographic map. The Digital Elevation Model (DEM) (Figure 3.3) contains spatially distributed elevation information to allow an automatic delineation of watershed boundary. Topographic maps from the Royal Thai Survey Department (RTSD) at the scale 1:50,000 and 1:4,000 are used to generate DEM. The relevant parameters can be generated from DEM: slope, flow direction, flow accumulation and stream network. In general, increasing level of spatial resolution can increase the accuracy of the simulated results. Values assigned to any grid cell represent an average value over a number of grid elements.

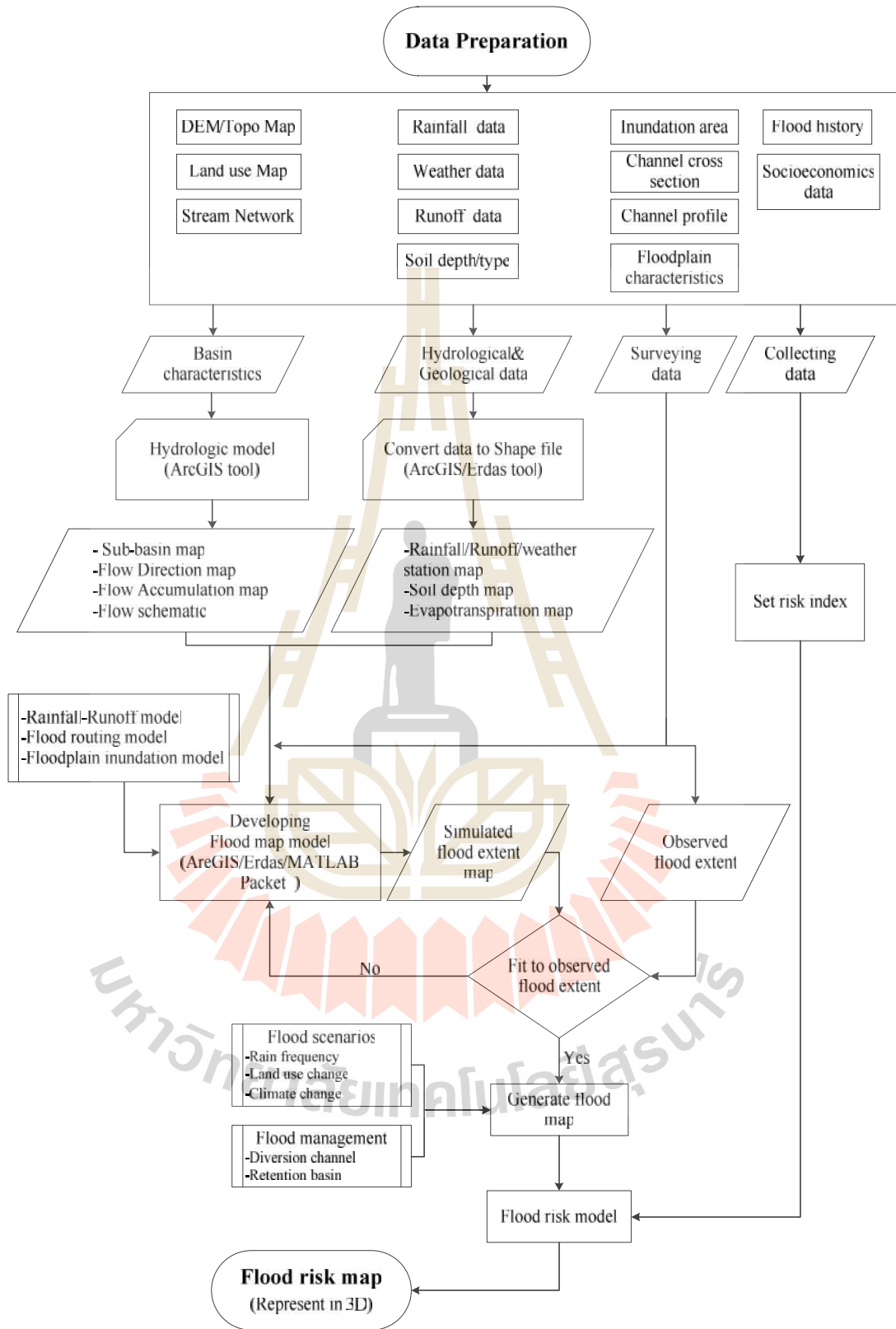


Figure 3.1 Conceptual framework of the research methodology and processes

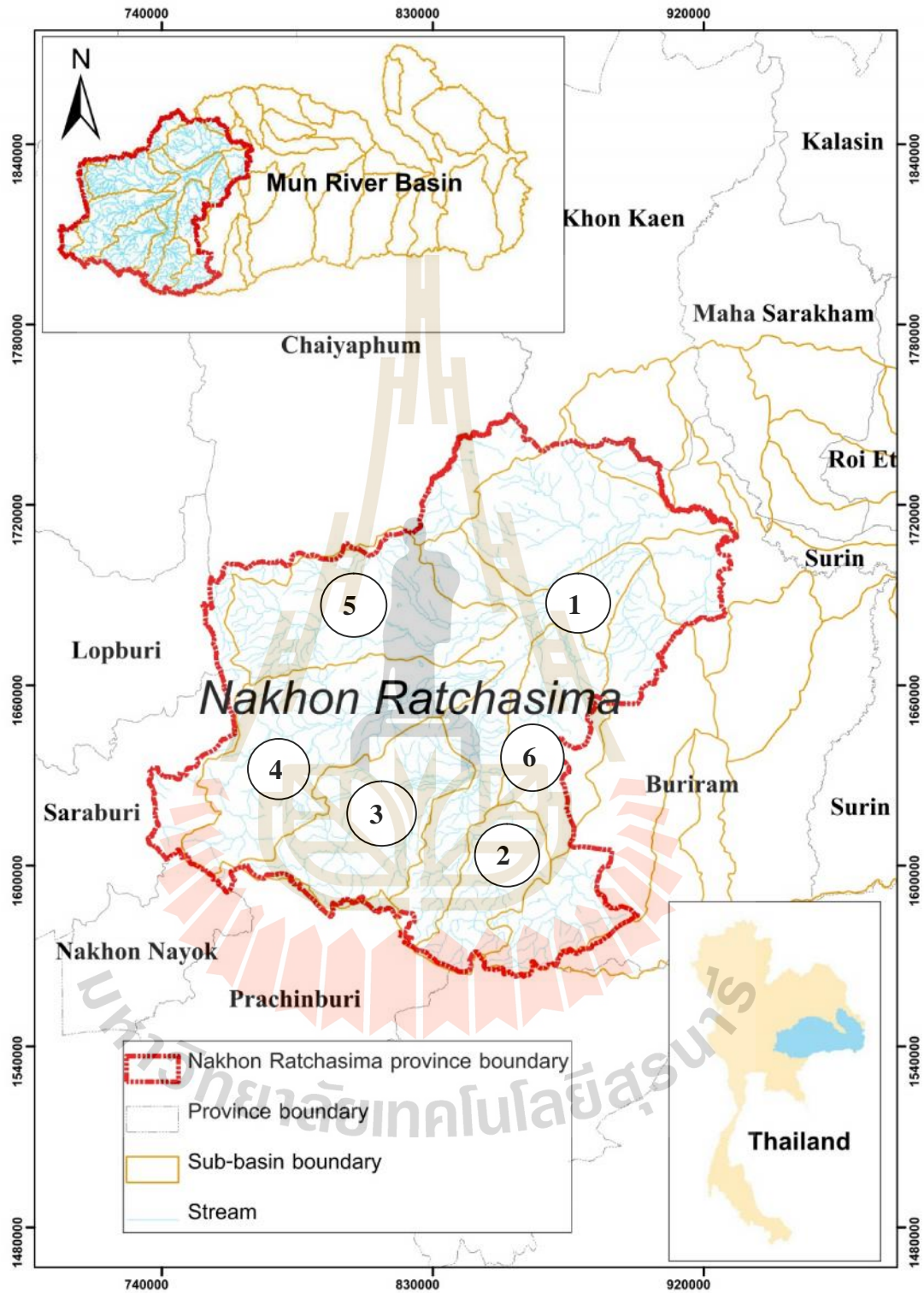


Figure 3.2 Upper Mun River Basin

Table 3.1 List of subbasins of upper Mun River Basin and their properties

Sub-basin no.	Sub-basin name	Area (km ²)	Stream Length (m)
1	Upper part of Lam nam mun	2,811	224
2	Lam sae	1,197	
3	Lam phra phlong	2,277	
4	Lam ta khong	3,315	220
5	Lam Chiang Krai	2,617	178
6	Lam Chak karat	1,642	
Total		13,859	-

Table 3.2 Data types agencies and available records for upper Mun River Basin

Data type	Agency	Period of time
Digital Elevation Model	Land Development Department (LDD)	2004
Land use	Land Development Department (LDD)	2008
Stream network	Land Development Department (LDD)	2008
Rainfall	Thai Meteorology Department (TMD)	1990-2013
Weather	Thai Meteorology Department (TMD)	1990-2013
Runoff	Royal Irrigation Department (RID)	1990-2013
Soil	Land Development Department (LDD)	2008
	Department of Groundwater Resources (DGR)	-

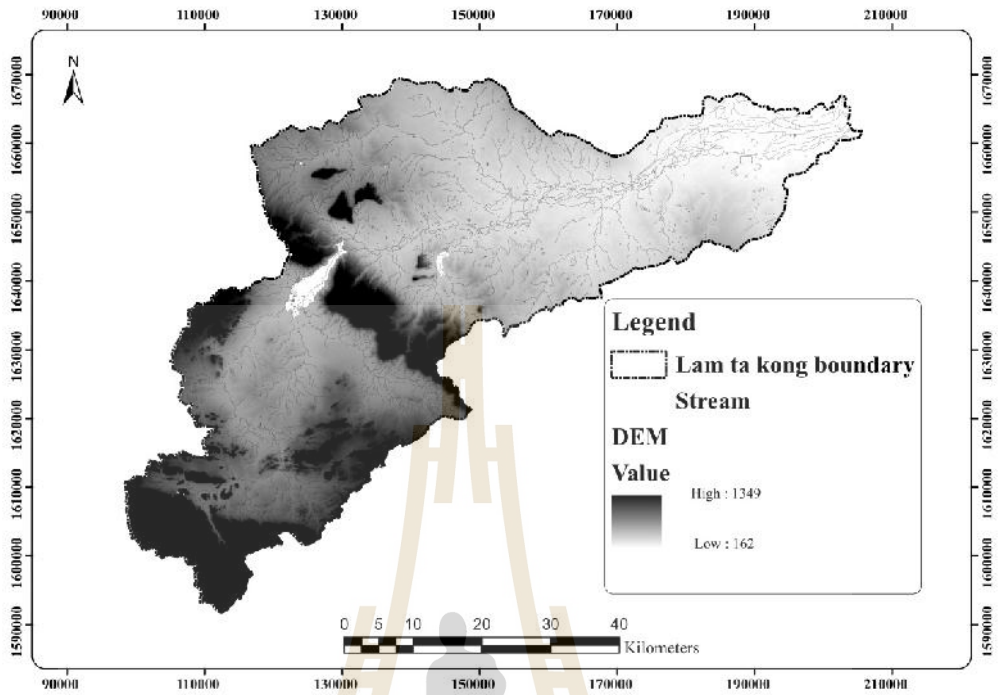


Figure 3.3 DEM of Lam Takong River Basin

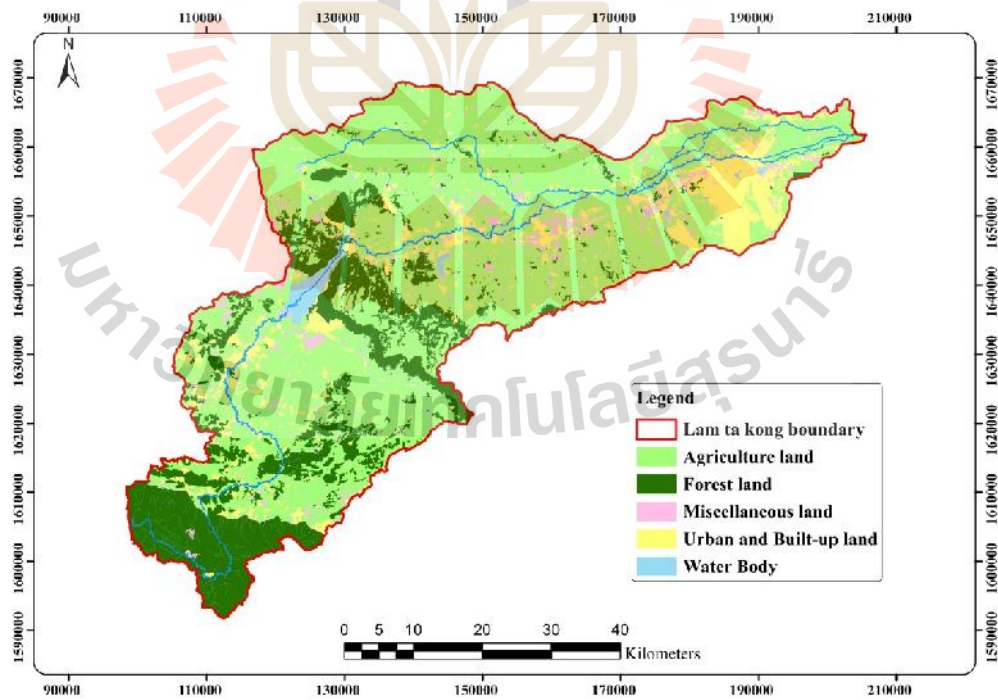


Figure 3.4 Land use of Lam Takong River Basin

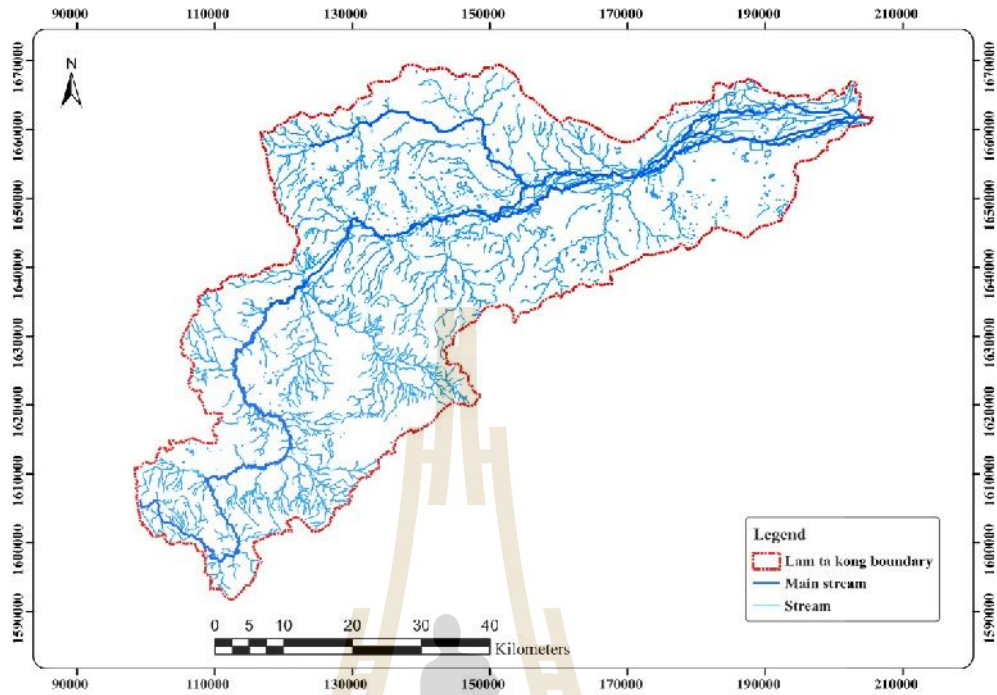


Figure 3.5 Stream network of Lam Takong River Basin

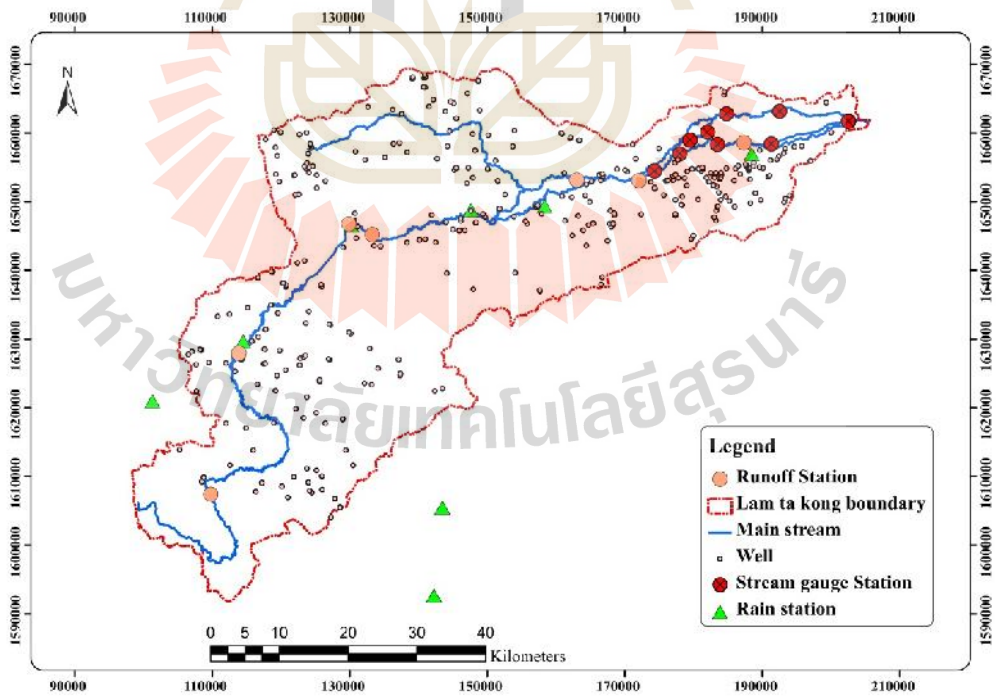


Figure 3.6 Hydrological and geological station of Lam Takong River Basin

Land use and Land cover

Land use and Land cover data are required for rainfall-runoff processes and flood assessment because they indicate the activities on land with different level of flood risk. The digital land use data on scale of 1:50,000 and 1:4000 were obtained from Land Development Department (LDD) in 2008. Five land use types are used in this study (Table 3.3).

Table 3.3 List of land use type and its area for Lam Takong River Basin

Land use types	Area (km²)	% of total area
Agriculture land (A)	2,022	61
Forest land (F)	675	20
Urban and built-up land (U)	400	12
Miscellaneous land (M)	158	5
Water Body (W)	60	2
Total	3,315	100

3.1.2 Hydrological and Geological data

To obtain accurate a real rainfall for the whole basin, rainfall data from a number of rain gauges are required to capture the variability of rainfall in the watershed. In this study in Lam Takong River Basin, rainfall data were collected from 8 stations (Figure 3.6) located within and around the watershed by Thai Meteorology Department (TMD). The runoff data are obtained from Royal Irrigation Department (RID). These data were used for calibrate and validate model parameter. For soil data, there are two main properties to be considered: effective depth of soil layer and soil texture (in term of the soil porosity). Soil data was obtained at the scale of 1:25,000 from LDD. These data were mapped based on original data extracted from 360 boring log of ground water wells (surveyed the Department of Groundwater Resources (DGR) within the Lam Takong area. The effective soil depth for each well is defined as distance from ground to the bedrock level of the well. The porosity will be calculated from the average porosity value of relevant soil textures found at each. Knowledge of effective soil depth and soil porosity data can be used to calculate soil water storage for water balance model.

3.1.3 Surveying and collecting data

Surveying data consist of channel cross section, channel profile, inundation area and floodplain characteristics. Collecting data consist of a simple and accurate method of collating and displaying the relevant extent and level information. After the data has been collected. It was used to produce a map of the flooded area, with peak flood levels at particular locations, if available. A brief accompanying report can detail additional information such as flood mechanism, time and duration of flooding, emergency response and estimated damage. Data and

information on historic flood events is essential to identify where flood risk management measures are required and to efficiently design the most effective system for mitigating the risk. This data is also of benefit to local authorities and other state agencies in functions such as land-use planning, developing the emergency response to future flood events, and assisting in the development of flood map model.

3.2 Construct the flood hazard map model

This part contributes to generating of flood maps for study area during October's flood 2010 based on the simulated flood hazard map. A flood hazard map is simulated by flood map model (Hec-RAS V.5) which is developed from geometric data with ArcGIS/Erdas software packet. The simulated flood hazard map are compared with the observed flood hazard map (of the same event) calibrated with surveying data and collecting data. The result to be re-developed until outcome is significant and acceptable. If the result of flood extent map is acceptable, the product can use for generate flood map process. Flood map is assumed as the flood scenarios (Rain frequency, Land use change and Climate change) and flood management (Diversion channel and Retention basin) for generating the flood map.

3.3 Development of the flood risk model

The purpose of flood risk such assessment is to identify the areas within a development plan that are at risk of flooding base on factors that are relevant to flood risks. Flood risk model was developed by flood map from previous step using GIS raster index model. An index model calculates the index value for each unit area and produces a classified map based on the index values. An index model is similar to a binary model in that both involve multi-criteria evaluation and both depend on map overlay operations in data processing. The concept of risk has variable meaning according to the context in which it is employed and, for that reason, the adopted interpretation must be elucidated prior to any analysis. In engineering, risk is divided in two basic components: one related to the probability of occurrence of a hazardous event and another regarding its consequences. Concerning flood risk, in particular, this is the definition mostly accepted being. Multi-criteria analysis enables a combined assessment, in which aspects of different natures and its relative importance are taken into account without the need of monetary valuation, this approach is recommended for the analysis of flood risk. Indices are an example of multi-criteria analyses and are especially useful and well suited to aid the resolution of decision problems. It is a way to combine information associated to indicators of distinct natures and significances, translating them into a single value. This effect, which must be representative of a real situation, means to reproduce the joint effect of the set of indicators. The properties that characterize an index include:

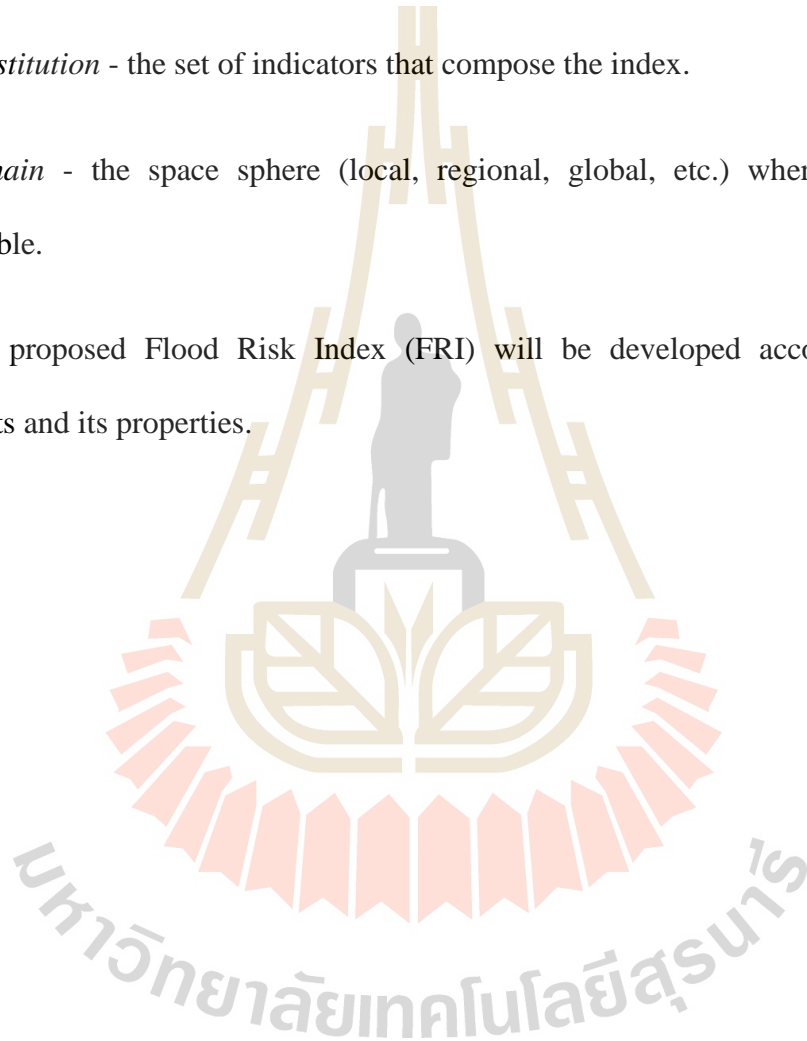
Range - defined by its maximum and minimum extremes, which comprise all the values the index can assume.

Formulation - the mathematical expression that represents the relationship between the set of indicators, which compose the index.

Constitution - the set of indicators that compose the index.

Domain - the space sphere (local, regional, global, etc.) where the index is applicable.

The proposed Flood Risk Index (FRI) will be developed according to these concepts and its properties.



CHAPTER IV

THE DEVELOPMENT OF A SIMPLE DISTRIBUTED HYDROLOGICAL MODEL BASED ON UP-SCALING FROM PIXEL TO CATCHMENT SCALE

4.1 Summary

Spatial units used in the modeling are rectangular grids with 30m-resolution grouped into hillslope and channel pixels. For each hillslope pixel, a simple two-layer soil model is used to simulate the dynamics of soil-water between unsaturated and saturated zones. Soil column of each pixel receives water in form of infiltration into unsaturated zone from precipitation, lateral overland and subsurface discharge from neighboring upstream pixels. It loss water through evapotranspiration and lateral overland and subsurface discharge to downstream pixel. Water column moves out of the grid in only one direction, depending to the steepest slope. Runoff generation is estimated at every pixel including Horton Overland Flow (HOF), Dunne overland flow (DOF), Subsurface Storm Flow (SSF) and infiltration excess runoff given by the Green-Ampt method. The upstream-downstream aggregated interaction of hydrological processes through the catchment scale forming of DOF, SSF and partial saturation area which occurs in the river network. Advantage of this approach is simple, tractable and computationally efficiency that we can carry out for multiple realization of climate- soil- topography combination. This model will be used to

simulate the effects of different combination of climate, soil, and topography on the runoff generation processes through hypothetical catchment and climate combination.

4.2 Introduction

Infiltration excess runoff (or Hortonian Overland Flow, HOF), saturation excess runoff (or Dunne Overland Flow, DOF) and Subsurface Storm Flow (SSF) are the three main and well-known runoff generation processes occurring in headwater catchments (Horton, 1933; Dunne, 1978). Dunne (1978) explained that the relative dominance of given runoff generation mechanisms is controlled by the combination of climate, soil, vegetation and topography. However, this holistic conceptual illustration of climate and landscape controls on runoff generation processes is still explained in a qualitative way. A quasi-distributed model based on TOPMODEL concepts (Beven and Kirkby, 1979) is used to investigate the relative dominance of Hortonian and Dunne overland flow mechanisms (Sivapalan et al., 1987; Larsen et al., 1994; Robison and Sivapalan, 1995). Their work was limited to two mechanisms and operated at event scales, and could not include the effect of antecedent condition and the effect of all conditions of catchments (e.g. steep topography or complex subsurface as assumed in TOPMODEL). Several studies applied semi or fully distributed catchment model in actual catchments that includes all three mechanisms of runoff generation. Mirus and Loague (2013) used a physics-based coupled surface and subsurface model, *InHM*, to investigate climatic and landscape controls on runoff generation. Carrillo et al. (2011) also used a physics-based model, *hsB*, to perform regressions of calibrated parameters associated with vegetation cover, demonstrating the role of vegetation in the co-evolution of catchment properties with climate. Torch

et al. (2013) extended this model to show the response and adaptation of vegetation to climate difference reflected in the long-term water balance exhibited by catchment in respect to Budyko curve. Li et al. (2014) developed a simple distributed hydrologic model to simulate the effects of different combinations of climate, soil, and topography on the runoff generation processes. Limitation of available observed data from highly instrumented catchments and most parameters are obtained by calibration. This prevented the ability of these models to apply to a large population of sites and catchments to obtain general knowledge on what are underlying physical controls on the runoff generation processes. Inspired by the work of (Li et al., 2014), the aim of this study is to further develop the simple distributed model that could investigate the combined effect of climate, soil, vegetation and topography on the runoff generation processes at the catchment scale in a quantitative way.

4.3 Methodology

A schematic illustration of the model is shown in Figure 4.1. Brief description of the procedure for runoff generation simulation are as follows:

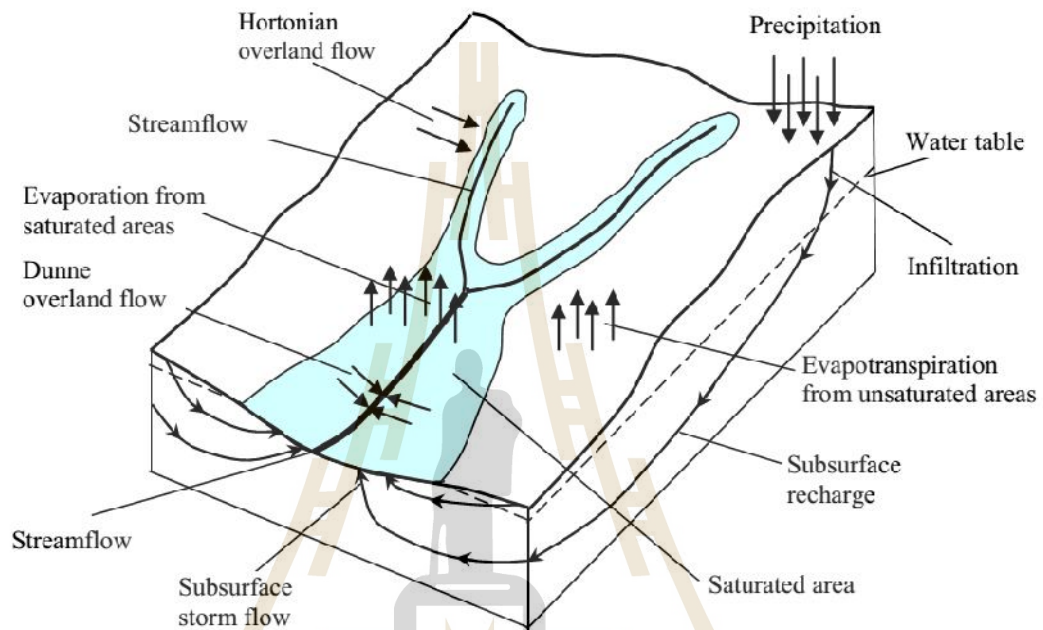


Figure 4.1 Conceptual description of the hydrological processes in hillslope pixels (Li et al., 2014)

- (1) The spatial units are DEM pixels grouped into hillslope pixels and channel pixels. Soil depth and soil hydraulic properties (hydraulic conductivity, porosity etc.) are assigned to each pixel.
- (2) For every pixel and every time step, HOF is estimated based on local infiltration capacity given by Green-Ampt method (1911). Later on soil moisture content is changed and the other two runoff generation mechanisms are possible: DOF and SSF.

(3) A simple two-layer soil model is used to simulate soil-water processes both in unsaturated and saturated layers.

(4) Overland flow is routed to downstream pixels at open channel velocity estimated by Manning's equation and subsurface is routed downstream at a subsurface velocity given by Darcy's law. Apart from river network geometry and soil depth, heterogeneity of other parameters is ignored such as soil properties, vegetation pattern, preferential pathways on the surface and in the subsurface. The details of the model and description of procedure and underlying equation and concepts are provided as following.

4.3.1 Soil-water moisture and water balance

To represent the dynamics of soil-water moisture in the pixel, a water balance equation can be applied at the pixel scale. In this study, the soil-water moisture in the soil column is divided into a ponding, unsaturated and saturated zone. Saturated soil-water moisture in the saturated zone is below the water table in the soil column. There are exchanges between the saturated zone and above unsaturated zone through capillary action and allow the retention of water in the unsaturated zone. Given the depth of unsaturated zone, the steady-state soil moisture profile in the unsaturated zone can be estimated by,

$$\theta_w(Z) = w \left(\frac{D_{us} - Z}{\zeta_a} + 1 \right)^{-\lambda} \quad (4.1)$$

Where $\theta_w(Z)$ is soil moisture in the soil column with a depth Z from the ground surface, ζ_a is bubbling pressure head, and λ is the pore-size distribution index

(Brooks and Corey, 1966). The average soil moisture in the unsaturated zone can be estimated by integrating Equation (4.1),

$$\bar{n} = \frac{w}{1-\beta} \frac{\Gamma_a}{D_{us}} \left[\left(\frac{D_{us}}{\Gamma_a} + 1 \right)^{1-\beta} - 1 \right] \quad (4.2)$$

The total soil water storage is given by,

$$S_{total} = D_{us} \bar{n} + D_s w \quad (4.3)$$

Where D_{us} is variable depth of the unsaturated zone, D_s is variable depth of the saturated zone and summation of D_{us} and D_s is the local soil depth (D), \bar{n} is the average soil moisture in unsaturated zone, and w is the effective porosity of the soil.

$$\frac{dS_s}{dt} = i - q_f - q_{se} - q_{ss} - e \quad (4.4)$$

$$D_{us} = (D - D_s) / \bar{n} \quad (4.5)$$

Where S_s is soil-water moisture in saturated zone ($= D_s w$), i is precipitation rate, q_f is infiltration excess runoff, q_{se} is saturation excess runoff, q_{ss} is subsurface storm flow and e is evapotranspiration rate. Equation (4.2) (4.4) (4.5) are solved for a new set of S_s D_s D_{us} \bar{n} , which satisfy the water balance condition. The new set of these parameters will be used for the next time step to estimate infiltration, evaporation and runoff generation.

4.3.2 Evapotranspiration

During inter-storm period, evapotranspiration is assumed to occur in three types with sequential order from surface unsaturated and saturated zone of the soil. Evaporation from water on the soil surface (if exists) is given by,

$$e_{ss} = \begin{cases} e_p & \text{if } d_w \geq e_p \Delta t \\ d_w / \Delta t & \text{if } d_w < e_p \Delta t \end{cases} \quad (4.6)$$

Where d_w is the local depth of surface water and e_p is the potential evaporation rate. If soil moisture is available for evaporation in the unsaturated zone of the soil column, evapotranspiration is given by,

$$e_{us} = \begin{cases} (e_p - e_{ss}) F_r \frac{n}{W} & \text{if } D_{us}^- \geq (e_p - e_{ss}) \Delta t \\ D_{us}^- / \Delta t & \text{if } D_{us}^- < (e_p - e_{ss}) \Delta t \end{cases} \quad (4.7)$$

Where F_r is the fraction of roots zone in the soil column, assumed to be unity. If soil moisture is still available for evapotranspiration in deeper saturated zone of the soil column. This evapotranspiration is given by,

$$e_{sat} = \begin{cases} 0 & \text{if } D_{us}^- \geq (e_p - e_{ss}) \Delta t \\ (e_p - e_{ss}) - D_{us}^- / \Delta t & \text{if } D_{us}^- < (e_p - e_{ss}) \Delta t \end{cases} \quad (4.8)$$

Potential evaporation demand is fully satisfied when the water table is close to the ground surface or soil surface is saturated during ponding period. Total evapotranspiration from all three zones will not exceed the potential evaporation rate.

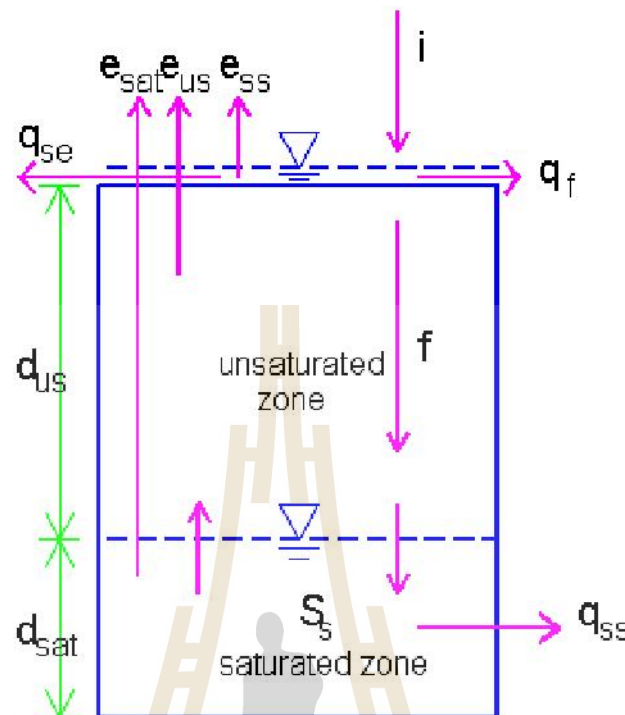


Figure 4.2 Schematic diagram of the pixel-based model structure of single soil column

4.3.3. Runoff generation process

Horton Overland Flow (HOF), saturation excess or Dunne Overland Flow (DOF), Subsurface Storm Flow (SSF) are three mechanisms of runoff generation processes. HOF occurs in a pixel when rainfall intensity exceeds the infiltration capacity. The dynamics of soil moisture in the unsaturated zone influence infiltration rate are estimated by using the Green-Ampt equation. DOF occurs in any pixel when the soil column is completely saturated from bottom, and forming the variable contributing area from a number of saturated pixels. Subsurface storm flow is generated from saturated zone of the pixels governed by saturated soil depth and downstream hydraulic gradient. At the same time, if the soil column receives water

more than lost it, saturated zone in the soil column may increase through the ground surface to generate DOF. In this situation, DOF and SSF are co-exist processes (Figure 4.2).

4.3.4. Routing processes at the pixel scale

The soil column of each pixel receives external water including lateral overland flow and subsurface discharge from neighboring upstream pixels. Routing of both surface and subsurface runoff is carried out based on two assumptions (1) outflow from each pixel will not be affected by inflow water over a short time step, (2) there is only one direction for outflow from each pixel, corresponding to the steepest slope with constant velocity (u), whereas there are 7 possible directions for inflow from its neighboring upstream pixels. Figure 4.3 presents outflow of pixel A, B, G into pixel E and only one outflow of pixel E into pixel I.

Over a short time interval (Δt), the volume of outflow from the grid is $u \cdot \Delta t \cdot \Delta x \cdot h$ equal the change of storage volume in the grid, $\Delta h \cdot \Delta x \cdot \Delta x$, where Δx is grid size in square shape, h is the water depth in the grid, Δh is the change of water depth. Integrating over Δt , the volume of outflow of a grid to downstream grid is,

$$\Delta V = h \left(1 - \exp \left(-u \cdot \frac{\Delta t}{\Delta x} \right) \right) \Delta x^2 \quad (4.9)$$

This routing scheme is applied to both ground surface and saturated zone. Overland flow velocity are estimated based on Manning 's equation as follows:

$$u_s = \frac{1}{n} S_0^{1/2} h_s^{2/3} \quad (4.10)$$

Where u_s is local velocity of overland flow, n is Manning 's coefficient, S_0 is the local surface slope and h_s is the surface water depth. Manning n for hill-slope pixels is 0.1 for grass/pasture range and is 0.06 for channel pixels.

Surface velocity is given by Darcy 's velocity as follows:

$$u_{ss} = k_s S_1 \quad (4.11)$$

Where S_1 is local bedrock slope, k_s is saturated hydraulic conductivity. We assume that subsurface water flows across pixels in only the saturated zone with water table slope parallel to the bedrock slope.

$$q_{ss} = u_{ss} A = k_s S_1 s_s(t) dx / dx^2 \quad (4.12)$$

Where q_{ss} is subsurface flow with the unit in L/T, $s_s(t)$ is soil-water moisture in saturated zone and dx is pixel size in m.

Finally, runoff from HOF, DOF and SSF reach the stream network and then is routed downstream through the channel pixels forming river network. The river network is assumed to be rectangular, width of the channel is estimated based on the hydraulic geometry relationship (Menabde and Sivapalan, 2001):

$$W = aA^b \quad (4.13)$$

Where A is the upstream catchment area corresponding to each river pixel at the catchment outlet, b is a constant parameter, which is 0.45, and a is a coefficient which can be adjusted to provide appropriate channel widths.

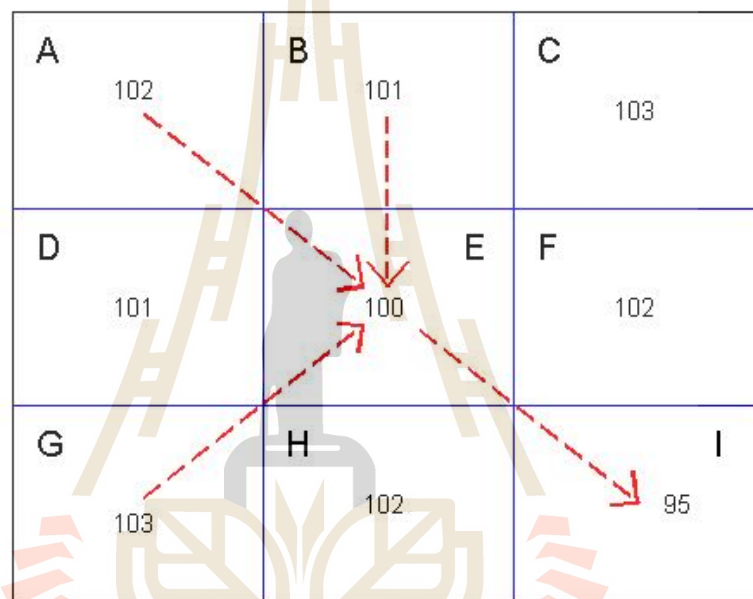


Figure 4.3 Multi inflow directions upstream of pixel E and only one outflow direction from pixel E depending on its elevation (100)

4.3.5. Topography

The topographic structure of a catchment is an important control on the dominance of runoff generation mechanisms. Overall steepness of the hillslope is chosen for this study which is the most dominant control compare to the other distribution of hillslope including convergence/divergence and convexity/concavity. A single realistic catchment is used to create new virtual catchment based on the 30 x

30 m DEM for a small catchment (4,019 pixels, 3.62 km²) located in Lam Ta Klong River Basin, Nakhon Ratchasima province, Thailand. Three types of slope distribution (flat, medium, steep) are generated by multiplying the original pixel slope by a factor.

4.3.6 Soil properties

Required soil properties for the model including saturated hydraulic conductivity, soil depth, effective porosity, wetting front soil suction head, bubbling pressure and pore-size distribution index. These properties vary in space and in multiple scales, and its variability can control the response. Only the first-order control of soil texture is chosen to investigate and leave the other effects to be considered in future research. Soil hydraulic properties are varied according to three texture classes: sand, silt loam and clay loam. Variation of soil depth (Z_x) is assumed to be a linear function of the topographic wetness index ($\ln(a/\tan s)$) (Stieglitz et al., 2003).

$$Z_x = \bar{Z} - (1/f) [\ln(a/\tan s)_x - \bar{\}}] \quad (4.14)$$

Where a is area drained per unit contour length, s is local slope angle, \bar{Z} is mean water table depth (WTD), $\bar{\}}$ is mean watershed value of $\ln(a/\tan s)$, and f is rate of decline of saturated hydraulic conductivity with depth in the soil column. The slope parameter of this function is adjusted to keep the main soil depth over entire catchment under three representative cases of soil depth: shallow, medium and deep with 1.0, 2.5 and 4.0 meters, respectively.

4.4 RESULTS AND DISCUSSION

Figure 4.4 presents simulated results from an infiltration model based on Green-Ampt equation to estimate excess rainfall hyetograph or HOF if the total rainfall of 11.37 cm. falls on a sandy loam soil ($K=1.09$ cm/h, $\Phi=11.01$ cm and $n_e=0.412$) of initial effective saturation 40%.

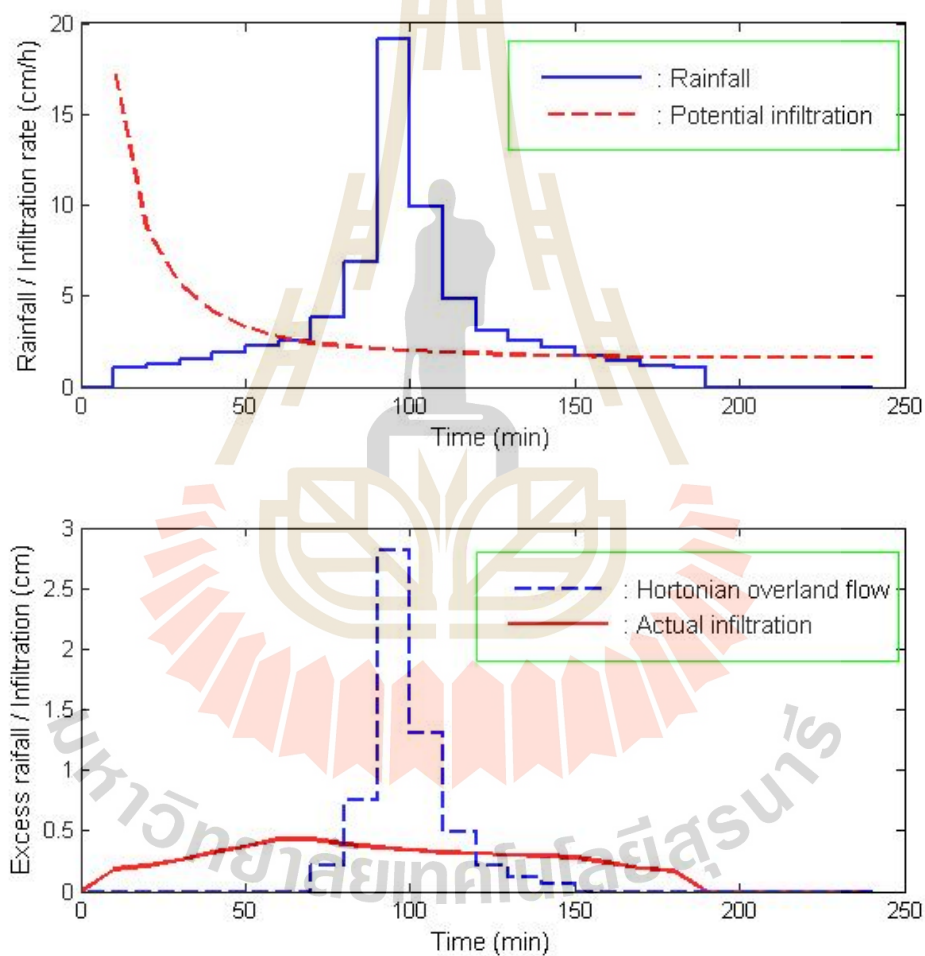


Figure 4.4 Estimation of Hortonian overland flow based on Green-Ampt equation

Model results of water balance in a soil column of pixel show in Figure 4.5. Testing soil is sand with effective porosity = 0.417, bubbling pressure = 0.0726 m, pore-size distribution index = 0.694, hydraulic conductivity = 10^{-6} m/s, soil depth = 1 m and surface slope = 0.10. Climate regime is generated with annual rainfall = 1,000 mm, annual potential evaporation = 500 mm, number of storm = 90 events/year, average rainfall intensity is 0.673 mm/hr. Simulated results in Figure 4.5 shows only 4 input storm events in steady state condition when initial and final saturation soil-water storages are equal. Figure 4.5(b) presents accumulated input and output from soil column of the pixel. Model results in Figure 4.5(b) indicated that HOF hardly coexist with DOF and SSF, very little HOF is generated under condition that supports DOF and SSF.

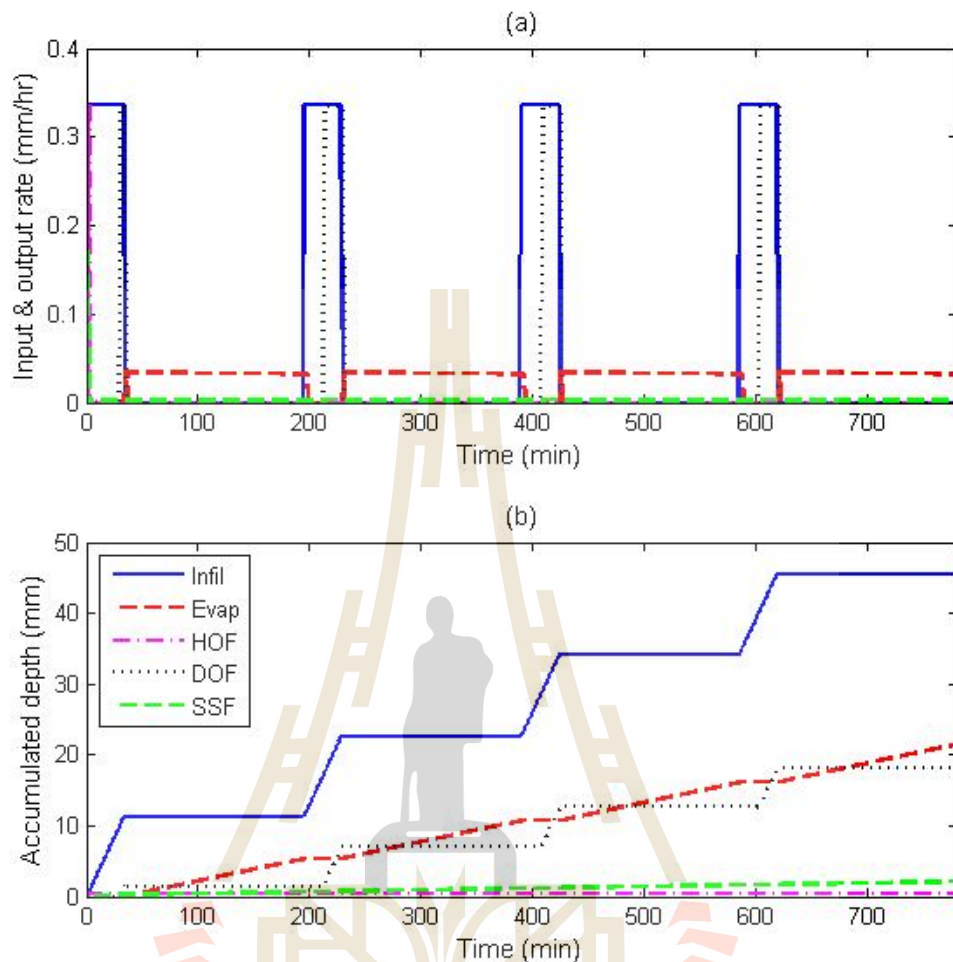


Figure 4.5 Water balance of input and output water from a pixel

Figure 4.6(a) shows topographic map of original DEM from Lam Ta Klong River Basin, the range of soil surface elevation is between 370 to 842 m. If combined overland flow from each pixel is 10 mm/h with duration 10 h, average soil depth = 2.5 m, $K = 10^{-4}$ m/s, $\Delta t = 10$ min, $\bar{Z} = 2$ m, $f = 1$ and $\beta = 5.38$ (for Equation 10). Hillslope and channel routing are carried out with the sequence of its elevation from upstream to downstream, providing downstream discharge at each pixel. For channel geometry,

parameters in Equation (13) $a = 25$ and $b = 0.45$. Figure 4.6 (b) presents discharge hydrograph (in mm) from pixel No.1 the most upstream pixel, pixel No.1652 (344 grids, 0.31 km²), pixel No.3104 (1814 grids, 1.63 km²), pixel No. 3806 (3590 grids, 3.23 km²) and the outlet of the basin, pixel No.4019 (4018 grids, 3.62 km²). Attenuation of downstream hydrographs show realistic manner.

4.5 CONCLUSIONS

A simple distributed hydraulic model is developed at the pixel/soil column scale and upscale to implement at the catchment scale. Applied water balance concept within the pixel and downstream interactions between each pixel allow the runoff generation by three mechanisms: HOF, DOF and SSF. Based on an actual building block of selected DEM, the model can be parameterized for a large set of hypothetical catchments and input climate events. Simulation results are received when all processes are driven to reach a periodic steady state by a sequence of identical climate events. In the next step, this model will be used to investigate the climate, soil and topographic controls on annual water balance in a qualitative way to define dimensionless functional relationships.

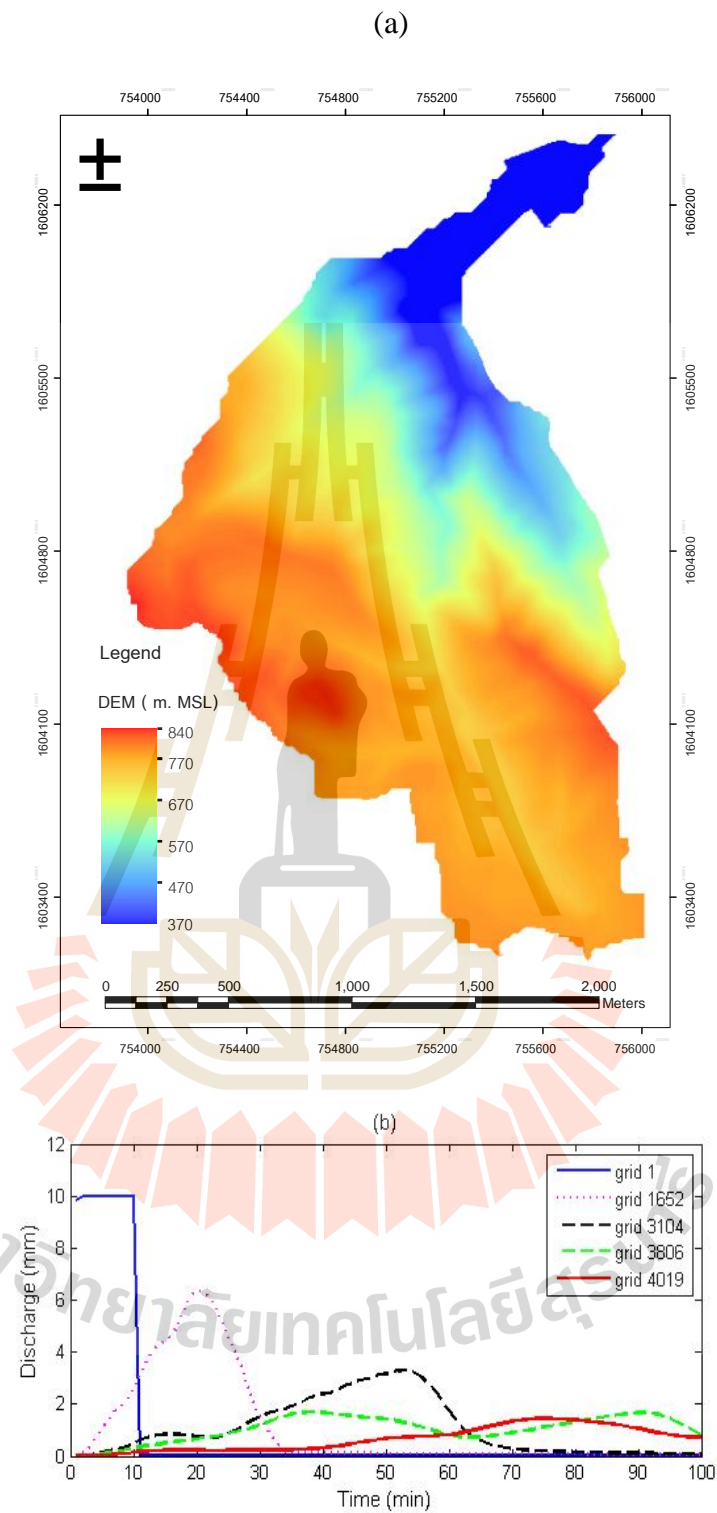


Figure 4.6 Output hydrograph form pixels based on combination of pixel and channel routing processes

4.6 References

- Beven, K.J., and Kirkby, M.J. (1979). **A physically-based variable contributing area model of basin hydrology**, *Hydrol. Sci. J.*, 24(1), 43-69.
- Brooks, R.H., and Corey A.T. (1966). **Properties of porous media affecting fluid flow**, *J. Irrig. Drain. Div. Am. Soc. Civ. Eng.*, IR2, 61–88.
- Carrillo, G., Torch, P.A., Sivapalan, M., Wagener, T., Harman, C., and Sawicz, K. (2011). **Catchment classification: hydrological analysis of catchment behavior through process-based modeling along a climate gradient**, *Hydrol. Earth Syst. Sci.*, 15, 3411-3430, doi:10.5194/hess-15-3411-2011,2011.
- Dunne, T. (1978). **Field studies of hillslope flow processes**, In: *Hillslope Hydrology* (M.J. Kirby, Editor), 227-293, J. Wiley & Son.
- Green, W.H., and Ampt, G.A. (1911). **Studies on soil physics, I. The flow of air and water through soils**, *J. Agric. Sci.*, 4, 1–24.
- Horton, R.E. (1933). **The role of infiltration in the hydrologic cycle**. *Trans. Am. Geophys. Union*.
- Larsen, J.E., Sivapalan, M., Coles, N.A., and Linnet, P.E. (1994). **Similarity analysis of runoff generation processes in real world catchments**, *Water Resour. Res.*, 30(6), 1641-1652.
- Li, H.Y., Sivapalan, M., Tian, F., and Harman, C. (2014). **Functional approach to exploring climatic and landscape controls of runoff generation: 1. Behavioral constraints on runoff volume**, *Water Resour. Res.*, 50, 9300–9322, doi:10.1002/2014WR016307.2014WR016307.

- Menabde, M., and Sivapalan, M. (2001). **Linking space-time variability of river runoff and rainfall fields: a dynamic approach**, *Adv. Water Resour.*, 24(9-10), 1001–1014.
- Mirus, B.B. and Loague, K. (2013). **How runoff begins (and ends): Characterizing hydrologic response at the catchment scale**, *Water Resour. Res.*, 49, 2987-3006, doi:10.1002/wrcr.20218.
- Robinson, J.S., and Sivapalan, M. (1995). **Catchment scale model of runoff generation by aggregation and similarity analysis**, *Hydrol. Process.*, 9, 5/6, 555-574.
- Sivapalan, M., Beven, K. and Wood E.F., (1987). **On hydrologic similarity, 2. A scaled model of storm runoff production**. *Water Resour. Res.*, 23(12), 2266-2278.
- Stieglitz, M., Sherman, J., McNamara, J., Engel, V., Shanley, J. and Kling, G.W. (2003). **An approach to understanding hydrologic connectivity on the hillslope and the implication for nutrient transport**. *Global Biogeochem. Cycles*, 17(4), 1105, doi: 10.1029/ 2003 GB002041.
- Troch, P.A., Carrillo, G., Sivapalan, M., Wagener, T. and Sawicz, K. (2013). **Climate-vegetation-soil interactions and long-term hydrologic partitioning: Signatures of catchment co-evolution**, *Hydrol. Earth Syst. Sci.*, 17, 2209–2217, doi:10.5194/hess-17-2209-2013.

CHAPTER V

**FLOOD HAZARD MAPPING USING ON-SITE
SURVEYED FLOOD MAP, HECRAS V.5 AND
GIS TOOL: A CASE STUDY OF
NAKHON RATCHASIMA MUNICIPALITY,
THAILAND**

5.1 Summary

For a small flood affected area, satellite data normally provides physical properties of flood event with low accuracy information (location and boundary). Flood depth and flood duration cannot be identified from a snapshot of satellite image. Therefore, on-site surveying of historical flood properties and its impact are still essential and this observed flood map is realistic and reliable information for future flood management. The objective of this study is to constructing flood hazard map from available observed flood map of the small flood affected area and use HEC-RAS V.5 and GIS tool to formulate flood hazard map for future scenarios. This method was applied for the municipality of Nakhon Ratchasima, Thailand. For a simulation, input physical parameters were generated by Hec-GeoRAS in ArcGIS based on DEM ($5 \times 5 \text{ m}^2$). A range of calibrated Manning's n in a main channel was obtained from fitting exercise with observed Rating curve. Land-use map was used to

estimate the Manning's n in floodplain depending upon the type of land cover. Simulated results were exported to ArcGIS to delineate water surface on floodplain. Then, the maximum discharge value at the observed station (M.164) for return periods of 5, 10, 15, 25, 50, and 100 years were used as upstream input flood to simulate the flood map. It is found that, for the 2010 flooding event in the concerning area, the simulated flood hazard map subjected to the discharge of 50 years ($217 \text{ m}^3/\text{s}$) return period which is almost identical with the observed flood map from the surveying.

5.2 Introduction

Floods can be considered as the most important natural disaster with higher frequency of occurrence higher than any other natural disaster and affecting more people than the other natural hazards together (ARDC, 2009). Floods are related to social–civil conflicts (Ghimire et al., 2015) environmental problems (Jia and Wenjiao, 2015) and economic losses (Aerts and Botzen, 2011). Floodplains can be defined as the areas that are periodically inundated by the overflow of river (Maskong and Jothityangkoon, 2013). In 2010, Nakhon Ratchasima province received excessive rainfall in successive day during 14 – 16 October 2010. A majority of the floodplain area in Nakhon Ratchasima province suffered from this serious flooding event. Heavy rains caused a large amount of runoff flow into both upstream and downstream of all reservoirs in Nakhon Ratchasima province including Lam Takong and Lam Prapleng Dams. With ongoing water flowing into these reservoirs until excess its capacity, the water level was higher than the level of emergency service spillway which in turn causes severe uncontrolled flood flow into many municipalities downstream. Moreover, most of water flow rapidly over lands into the canal and combined with the

overflow water from many dams. The combination of these events caused widespread flooding on the floodplain in lower basin, including Muang Nakhon Ratchasima district, Pukthongchai district and Chaloeprakiat district, etc. Flood water from tributary of Mun River was drained slowly into Mun River because the water level in Mun River was higher than the water level in tributary canals and there are a lot of obstructions in the canal which resulted in reducing flow speed (Kongjun and Noypairroj, 2011; Ponsan and Panchana, 2011; Reports of Members on the Impact of Tropical Cyclones, 2011).

The river flood modelling is a tool for evaluation and prediction of river flood risk in different scenarios. River flood risk modelling comprise of hydrological modelling, hydraulic modelling, river flood visualization and river flood mapping (Alaghmand, 2009). A flood hazard map is a graphical representation of flood inundation (inundation depths, extent, flow velocity etc.) expected for an event of given probability or several probabilities (APFM, 2013). The flood hazard map will help responsible authorities to target on the area with higher hazard where flood mitigation plans have to be effectively implemented. The flood hazard map will give public tangible imagery of its impact on their community. Flood hazard maps will not prevent floods from occurring, but they are an essential tool for warning and mitigation the damage of property and loss of life caused by floods, and for communicating flood risk. Nowadays, hydraulic simulation tools are available to model channel discharge and flooding in floodplains with 1D and 2D approaches. The Hydrologic Engineering Center River Analysis System (HEC-RAS) is free software with a friendly graphical user interface that was successfully used for flood studies (US Army Corps of Engineers, 2014; Knell et al., 2005; Lian et al., 2013;

Mohammadi et al., 2014), commercial software packages are widely used and distributed such as FLO-2D to simulate floods and flows (FLO-2D software, 2016) and the MIKE packets modelling tools (DHI Group, 2016). One of the most popular hydraulic models is HEC-RAS which announced and released its new HEC-RAS version 5 with 2D capabilities is a great innovation for flood studies (Brunner, 2014). The Flood map event was simulated by the 2D of the HEC-RAS 5 beta that shows good performance when compared with flood extent registered by satellite images (Moya et al., 2016). Furthermore, HEC-RAS has more accurate results of river flood map (flood extent and water depth) in comparison with MIKE11 in urban area. In recent years GIS integrated modelling applications have been made to integrate hydraulic models and GIS to facilitate the manipulation of the model output which led to the establishment of a new branch of hydraulics and hydrology. There are strong grounds for believing that GIS has an important function because natural hazards are multi-dimensional phenomena which have a spatial component [Alaghmand et al., 2013; Congressional Budget Office, 2009; Nakhon Ratchasima City Municipality, 2016]. The flood hazard map can be generated from a variety of tools, for example, (1) using vertical aerial photographs due to lacking of detailed topographic maps (Furdada et al., 2008), (2) using a remote sensing and GIS based flood index (Kabenge et al., 2017), using flood mark data (including flood depth and flood duration) and analytic hierarchy process (Luu et al., 2018).

The available flood map in Thailand from Geo-Informatics and Space Technology Development Agency (GISTDA) can present spatial data of inundation area and expansion of flood boundary. However, it cannot exhibit high resolution of flood depth and flood duration (Maskong and Jothityangkoon, 2013). In order to protect or at least mitigate the effect of flooding problems, physical characteristic of inundation area combining with consequent impact has to be defined in the form of flood hazard map. Therefore, this study aims to simulate flood hazard map from the 2010 flood event in Nakhon Ratchasima Municipality using the 2D capabilities of HEC-RAS V.5 application. The model provides the simulation of the flood extent and flood depth.

5.3 Study area and dataset

Nakhon Ratchasima Municipality is an urban center of Nakhon Ratchasima Province, Thailand where is located at the downstream of the Lam Ta Kong River, which is a tributary of Mun River Basin. The length of main stream of river is 17 km, and study area is 37.5 km² shown in Figure 5.1. The observed daily discharge data of the Lam Ta Kong River at station M.164 is provided by Royal Irrigation Department of Thailand. Mean annual rainfall is 1,373 mm and contributes to 510×10^6 m³ of the total average annual runoff. Figure 5.2 shows that majority of the areas are urban and built-up land-uses, where the population is approximately 136,153 people (Nakhon Ratchasima City Municipality, 2016). The geographic data based on the digital elevation model (DEM) from the Land Development Department of Thailand has a grid cell size of 5×5 m² demonstrating elevation between 172.6-204.6 m.MSL, shown in Figure 5.3.

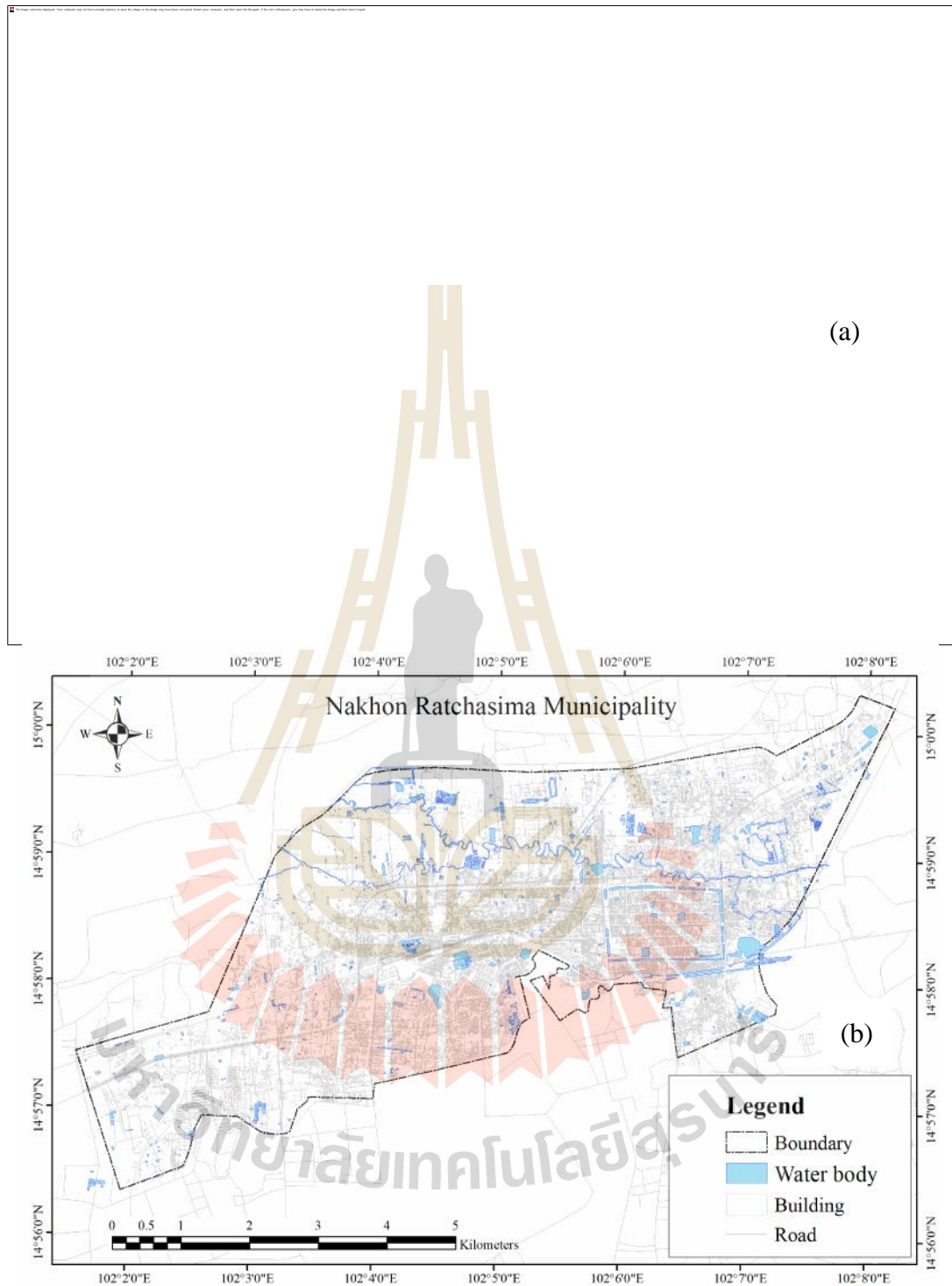


Figure 5.1 The boundary and location of the study area (a) Nakhon Ratchasima Province (b) Nakhon Ratchasima Municipality

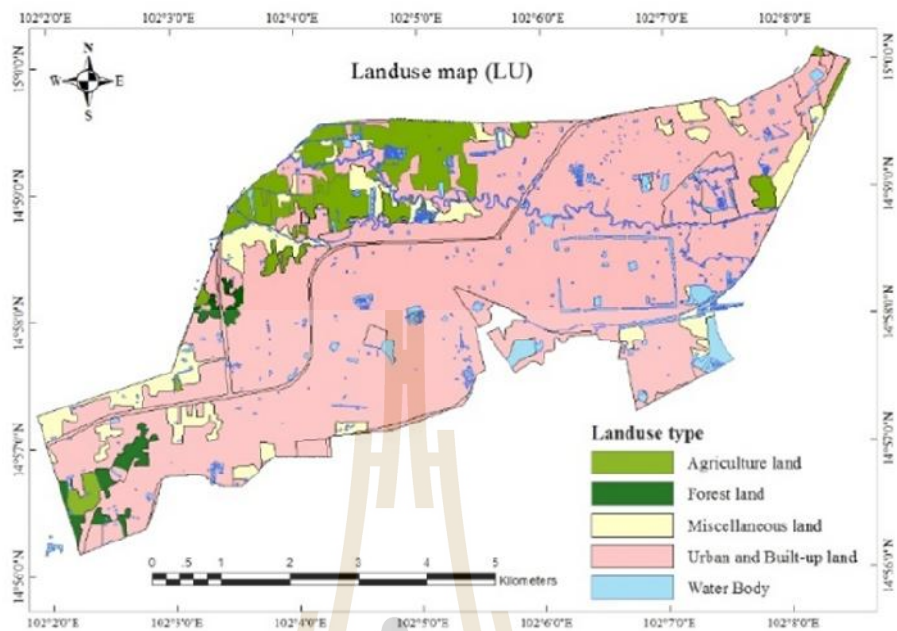


Figure 5.2 Land use of Nakhon Ratchasima Municipality

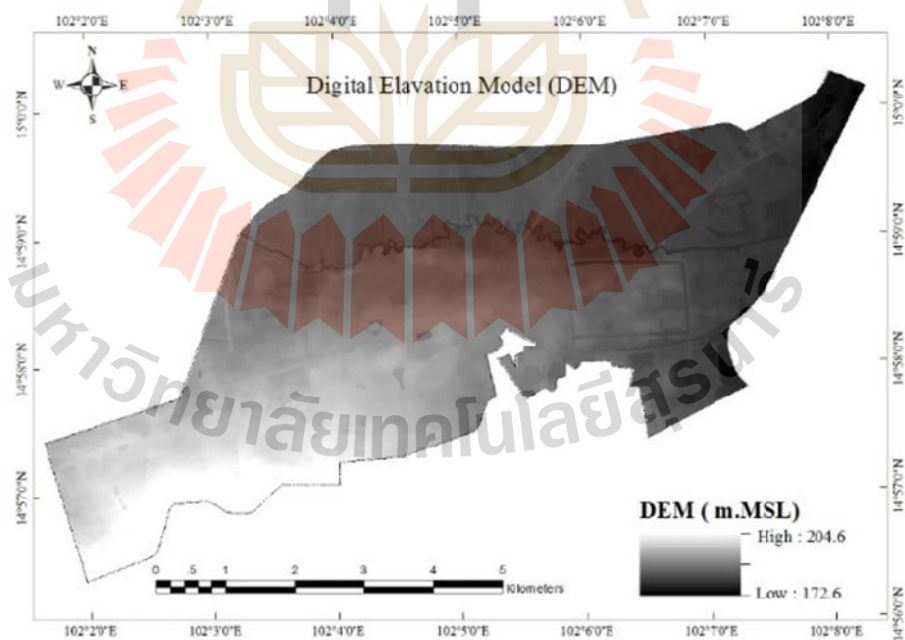


Figure 5.3 DEM of Nakhon Ratchasima Municipality

5.4 Methodology

The methodology for mapping a flood hazard map (shown in Figure 5.4) can be divided into two parts: review of flood and modeling approach for numerical simulation. Important step of these parts has been described below.

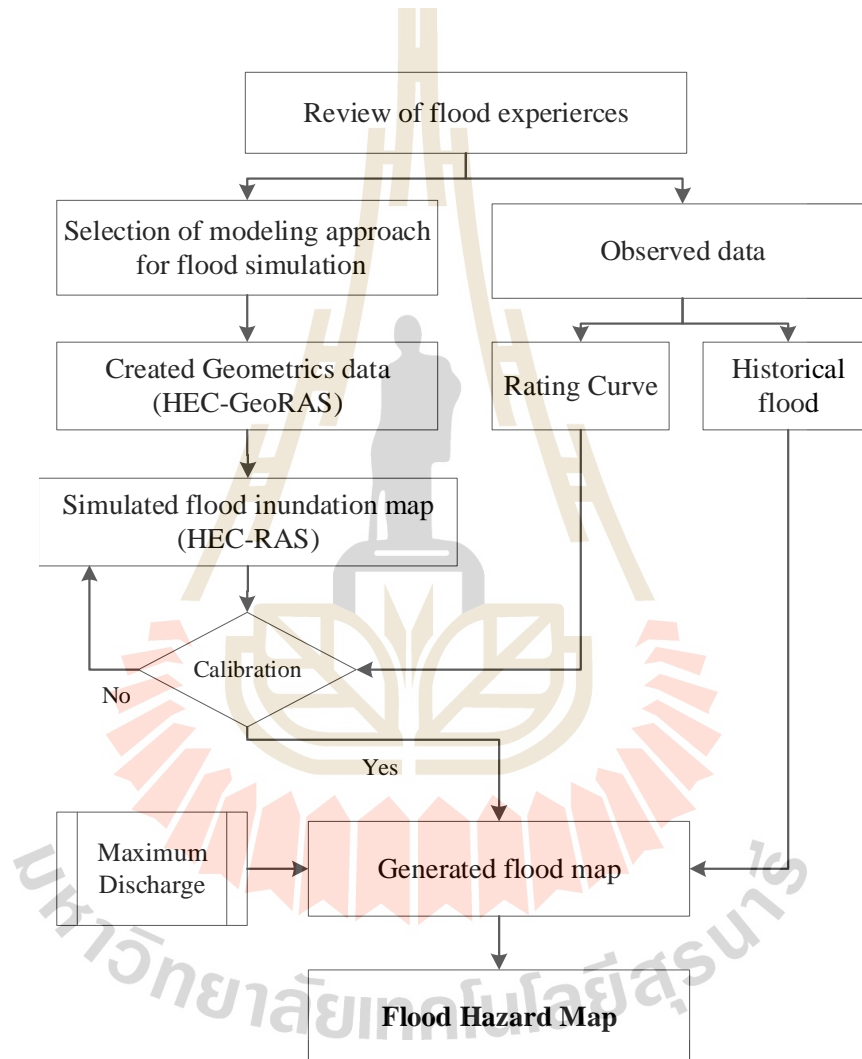


Figure 5.4 Flowchart of the study step, which is a conceptual framework of this study

5.5 Review of flood experiences

The lower northeastern part of Thailand was under low pressure groove during 1-19 October 2010. There was continuous heavy rain, especially in the Khao Yai National Park and covered very large surrounding areas. The accumulated areal rainfall was about 450 mm, which was about 40 % of the annual amount. The maximum 3-day rainfall (14-16 October 2010) in the upstream of Lam Ta Khong Dam was 180.3 mm, while in the downstream was 211.6 mm. The storage of Lam Ta Khong Dam and volume in all reservoirs rose very quickly and its downstream was extensively flooded. The dam operator failed to keep flood water in the reservoir. Since 17 October 2010, excess volume of flood began to overflow the service spillway at +277.30 m.MSL (Kongjun and Noypairoj, 2011; Ponsan and Panchana, 2011; Reports of Members on the Impact of Tropical Cyclones, 2011). Previous study (Maskong and Jothityangkoon, 2013) analyzed water balance of runoff found that accumulated depth of rainfall and volume of surface water in the year 2010 is higher than the other years. The severe scaling of flooding problem can be captured in the form of inundation map. Although, the boundary and location of 2010 flood inundation area is provided by GISTDA, its accuracy is low for small urban area. Figure 5 shown the surveyed point of flooding and the flood map obtained from field surveyed data represents is an inundation area and flood depth of Nakhon Ratchasima Municipality on 2010 flood event. This map can be developed further to include spatial variability of the depth and area and can be used to evaluate the hazard area and mitigation measures.

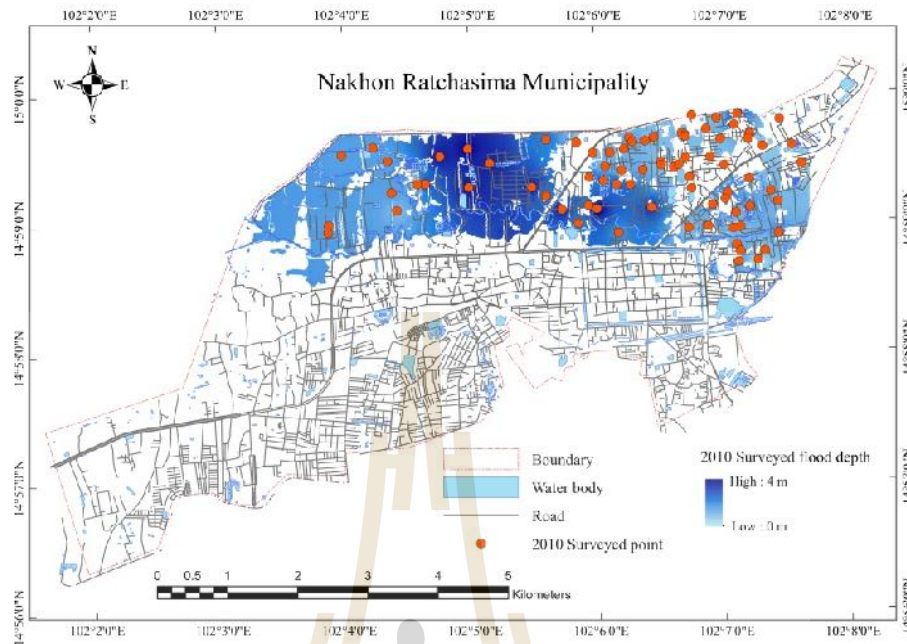


Figure 5.5 The 2010 surveyed point of flooding of Nakhon Ratchasima Municipality
(modified from Maskong and Jothityangkoon, 2013)

5.6 Modeling approach for numerical simulation

A number of hydraulic simulation tools are available to model channel discharge and flooding in a flood plain with 1D and 2D approaches. One of the tools is provided by the Hydrology Engineering Center River Analysis System (HEC-RAS) which is available in public domain. Hence, a new HEC-RAS V.5 model developed by the United States Army Corps of Engineers (USACE) is used in this study to simulate the flood event in Nakhon Ratchasima Municipality. The new HEC-RAS V.5 can solve either the full 2D Saint Venant equations or the 2D diffusive wave equations.

$$\frac{\partial u}{\partial t} + \frac{\partial p}{\partial x} + \frac{\partial q}{\partial y} = 0 \quad (5.1)$$

$$\frac{\partial p}{\partial t} + \frac{\partial}{\partial x} \left(\frac{p^2}{h} \right) + \frac{\partial}{\partial y} \left(\frac{pq}{h} \right) = \frac{n^2 pg \sqrt{p^2 + q^2}}{h^2} - gh \frac{\partial u}{\partial x} + pf + \frac{\partial}{\partial x} (h\tau_{xx}) + \frac{\partial}{\partial y} (h\tau_{xy}) \quad (5.2)$$

$$\frac{\partial q}{\partial t} + \frac{\partial}{\partial y} \left(\frac{q^2}{h} \right) + \frac{\partial}{\partial x} \left(\frac{pq}{h} \right) = \frac{n^2 qg \sqrt{p^2 + q^2}}{h^2} - gh \frac{\partial u}{\partial y} + qf + \frac{\partial}{\partial y} (h\tau_{yy}) + \frac{\partial}{\partial x} (h\tau_{xy}) \quad (5.3)$$

Where h is the water depth (m), p and q are the specific flow in the x and y directions (m/s), z is the surface elevation (m), g is the acceleration due to gravity (m/s²), n is the Manning resistance, ρ is the water density (kg/m³), τ_{xx} , τ_{yy} and τ_{xy} are the components of the effective shear stress and f is the Coriolis (s⁻¹). When the diffusive wave is selected the inertial terms of the momentum equations Eq. (5.2) and (5.3) are neglected.

In HEC-RAS, the geometric data were imported which were exported from ArcGIS by HEC-GeoRAS tool. HEC-RAS V.5 can be used either as a fully 2D model or as a hybrid 1D, 2D model when the main rivers are modelled as 1D and the floodplains are modelled as 2D. Although a hybrid 1D, 2D model tends to be faster than a 2D model, such 1D, 2D model requires the user to define the connections between the 1D and the 2D models. Such connections require a prior definition of the overflow locations (Brunner, 2014).

The Extreme Value Type I distribution or Gumbel distribution is used to fit the observed or simulated annual maximum runoff by using below frequency factors (Chow et al., 1988).

$$K_T = -\frac{\sqrt{6}}{\pi} \left\{ 0.5772 + \ln \left[\ln \left(\frac{T}{T-1} \right) \right] \right\} \quad (5.4)$$

$$x_T = \bar{x} + K_T s \quad (5.5)$$

Where K_T is frequency factor, T is return period, x_T is magnitude of annual maximum at the given return period, \bar{x} is mean of annual maximum runoff and s the standard deviation of annual maximum runoff. For a given specific return period, the annual maximum flood can be estimated from these equations.

5.7 Results and discussion

5.7.1 Observed annual maximum discharge

The observed annual maximum discharge at gauge station (M.164) was analyzed by Gumbel distributions shown in Table 5.1. The daily discharge recorded is 123.9 m³/s on 18th October 2010 as around 8 years return period. The previous study (Maskong and Jothityangkoon, 2013) found that the recorded discharge were possibly underestimated values. However, it would be a condition data of the flood simulation.

Table 5.1 Observed annual maximum discharges for different return periods at M.164

T(year)	2	5	10	15	20	25	50	100
Q(m ³ /s)	52	105	140	159	173	184	217	249

5.7.2 Roughness coefficients (Manning's n)

The geometric data including stream line, bank stations, cross section and flow path line were digitized and generated from DEM by Hec-GeoRAS tool in ArcGIS application. The rating curve at M.164 on 2010 and 2013 from the Royal Irrigation Department data were used to calibrate and validate the geometric data along the river by varying the Manning's n values. As a result, Figure 5.6 clearly shows that the n values between 0.020-0.035 (vary with elevation of main channel) and it provides the simulated rating curve with good agreement to the observed rating curve as shown in table 5.2. Therefore, these ranged of n values were used as the suitable physical data of the further simulation. In addition, the n values for the floodplain consisting of different land-use type were selected based on the observed and recommended data as summarized in Table 5.3 (Brunner, 2014).

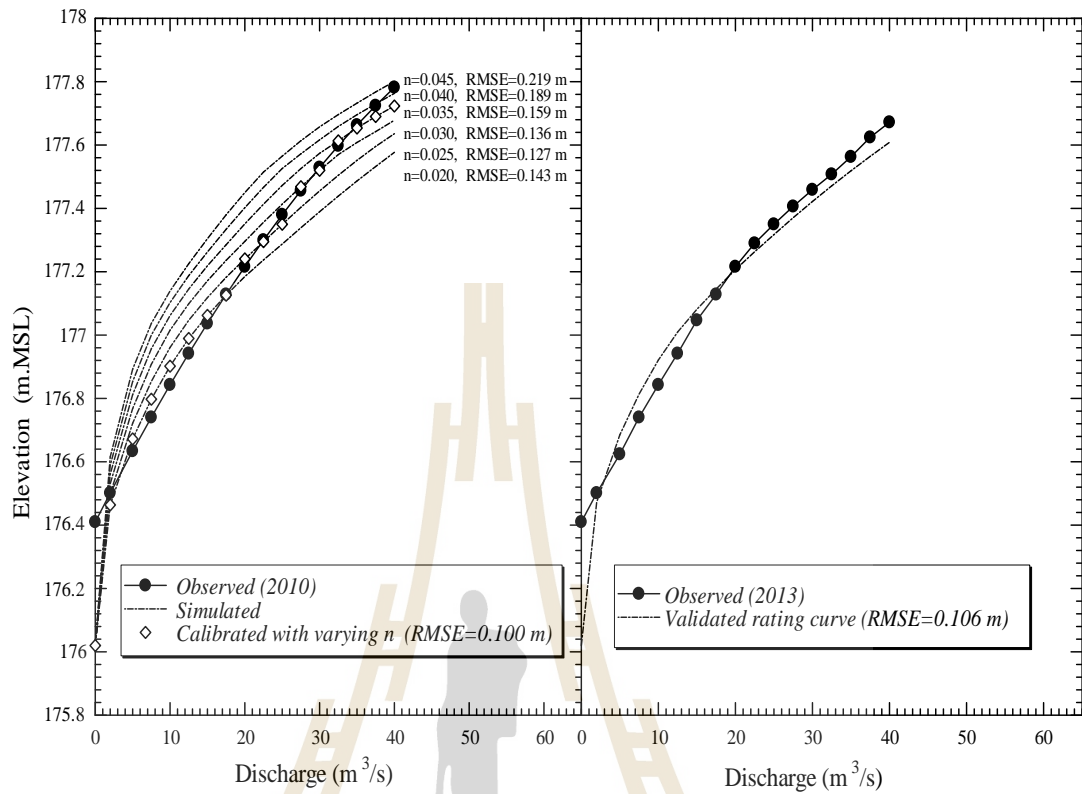


Figure 5.6 Comparison of Rating curve between calculated and simulated

Table 5.2 Comparison between calculated and simulated Rating curve

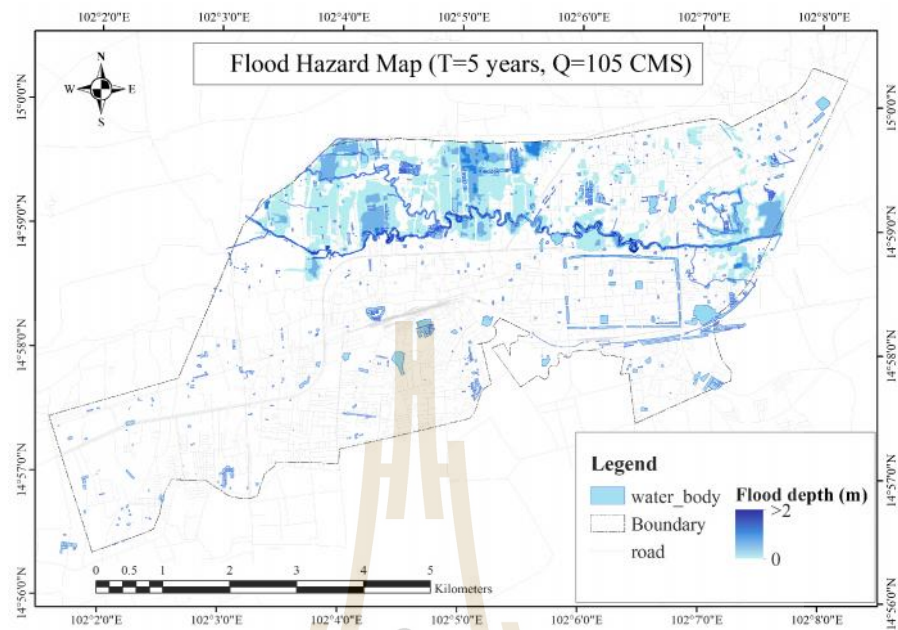
Manning's n	0.020	0.025	0.030	0.035	0.040	0.045	Vary (0.020-0.035)
RMSE	0.143	0.127	0.136	0.159	0.189	0.219	0.100

Table 5.3 The value of the manning roughness (n)

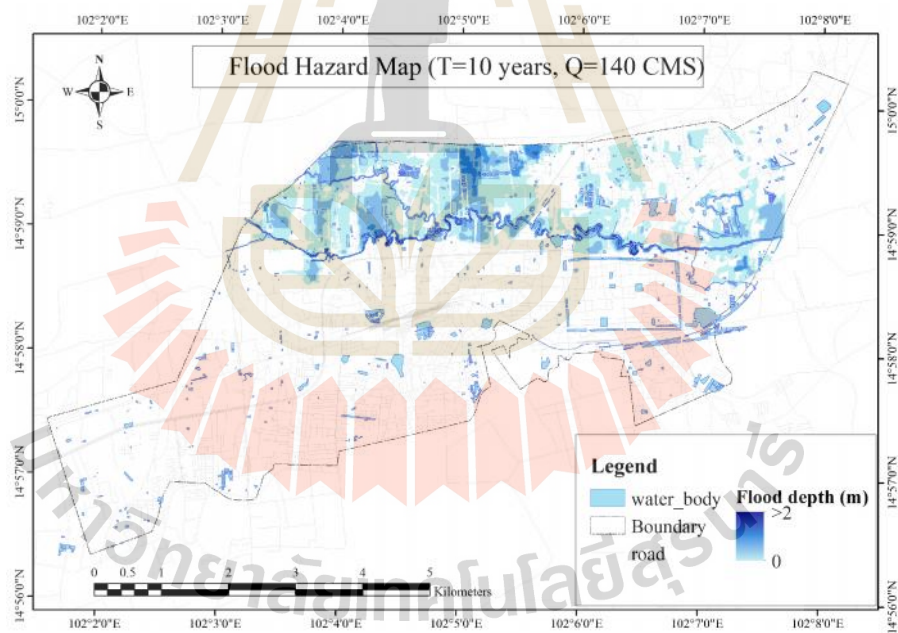
Land use	Value
Main channel of river	0.020-0.035
Land use on floodplain	
<i>Agriculture land (A)</i>	0.045
<i>Forest land (F)</i>	0.06
<i>Urban and built-up land (U)</i>	0.055
<i>Miscellaneous land (M)</i>	0.05
<i>Water Body (W)</i>	0.04

5.7.3 Flood hazard map

Figures 5.7 (a)-(f) illustrate flood hazard map subjected to various maximum discharges with different return periods (T=5, 10, 15, 25, 50 and 100 years) as mentioned in previous section. Flood extent for all return periods are shown as a similar pattern. The floods inundation areas are located at northern part of the river when the discharge is higher than the maximum capacity of the river ($40 \text{ m}^3/\text{s}$) and extend with increasing discharges. Figure 5.8 represent a comparison of flood depth between 2010 surveyed depth of flooding and simulated flood depth at annual maximum discharges for each different return period. The results also show that the simulated flood inundation areas of flood hazard map subjected to the 50 years return period (Figure 5.7 (e)) is almost identical with onsite saurveying flood map.

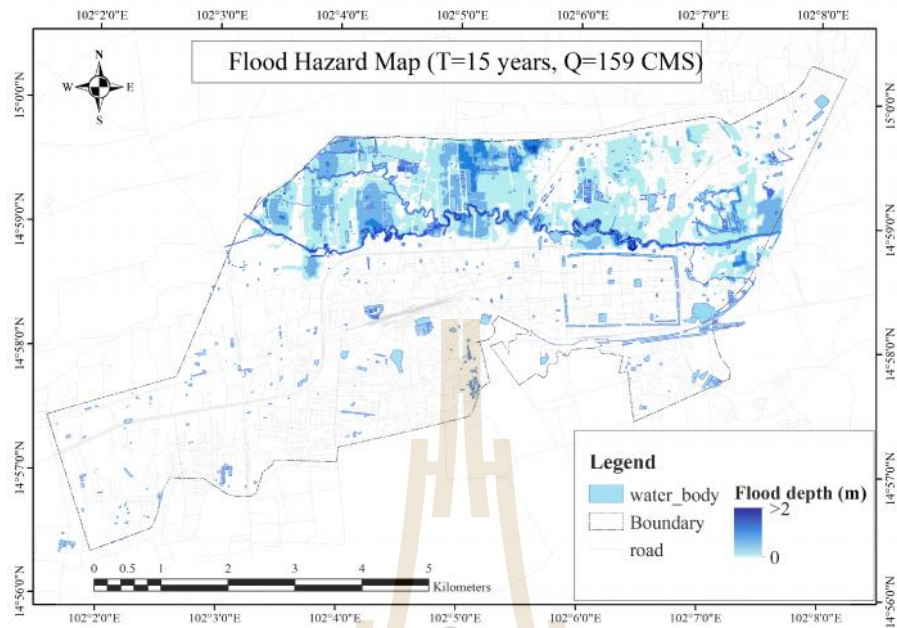


(a)

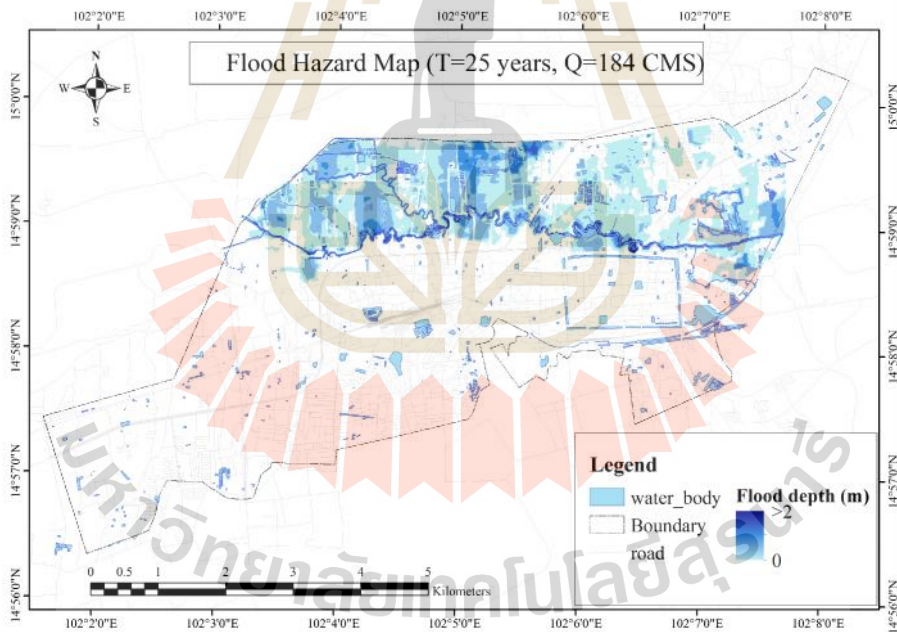


(b)

Figure 5.7 Simulated flood hazard area at the return periods (a) T=5 years, (b) T=10 years, (c) T=15 years, (d) T=25 years, (e) T=50 years and (f) T=100 years

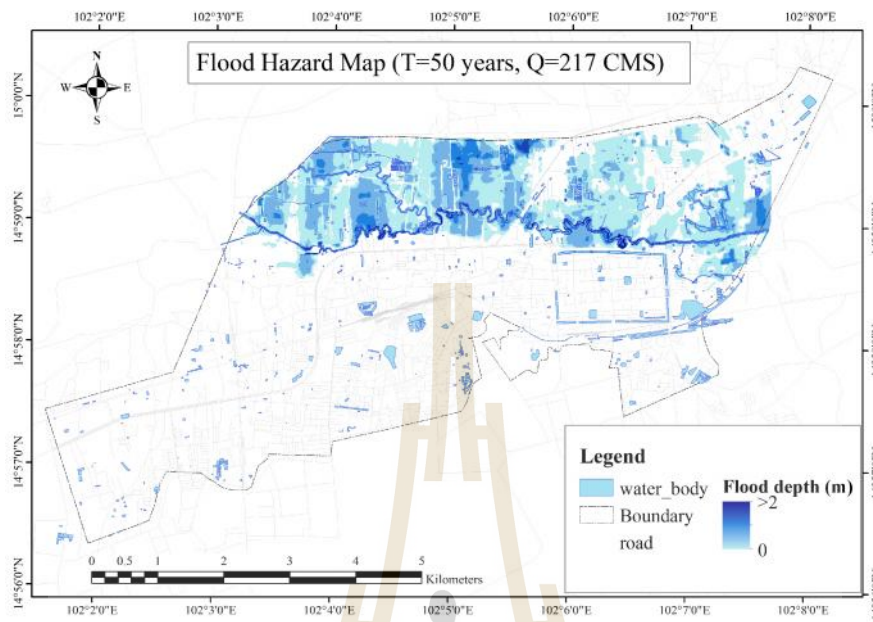


(c)

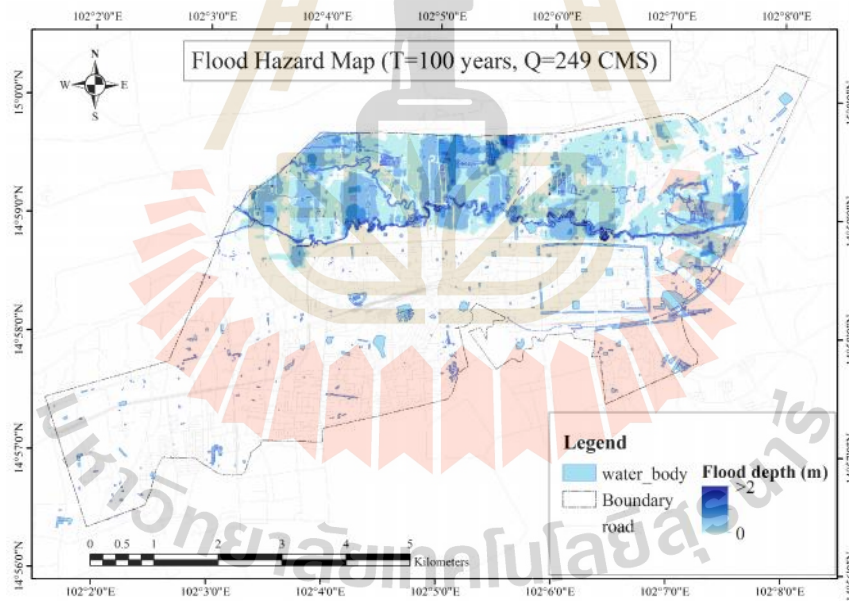


(d)

Figure 5.7 (Cont.) Simulated flood hazard area at the return periods (a) T=5 years, (b) T=10 years, (c) T=15 years, (d) T=25 years, (e) T=50 years and (f) T=100 years



(e)



(f)

Figure 5.7 (Cont.) Simulated flood hazard area at the return periods (a) T=5 years, (b) T=10 years, (c) T=15 years, (d) T=25 years, (e) T=50 years and (f) T=100 years

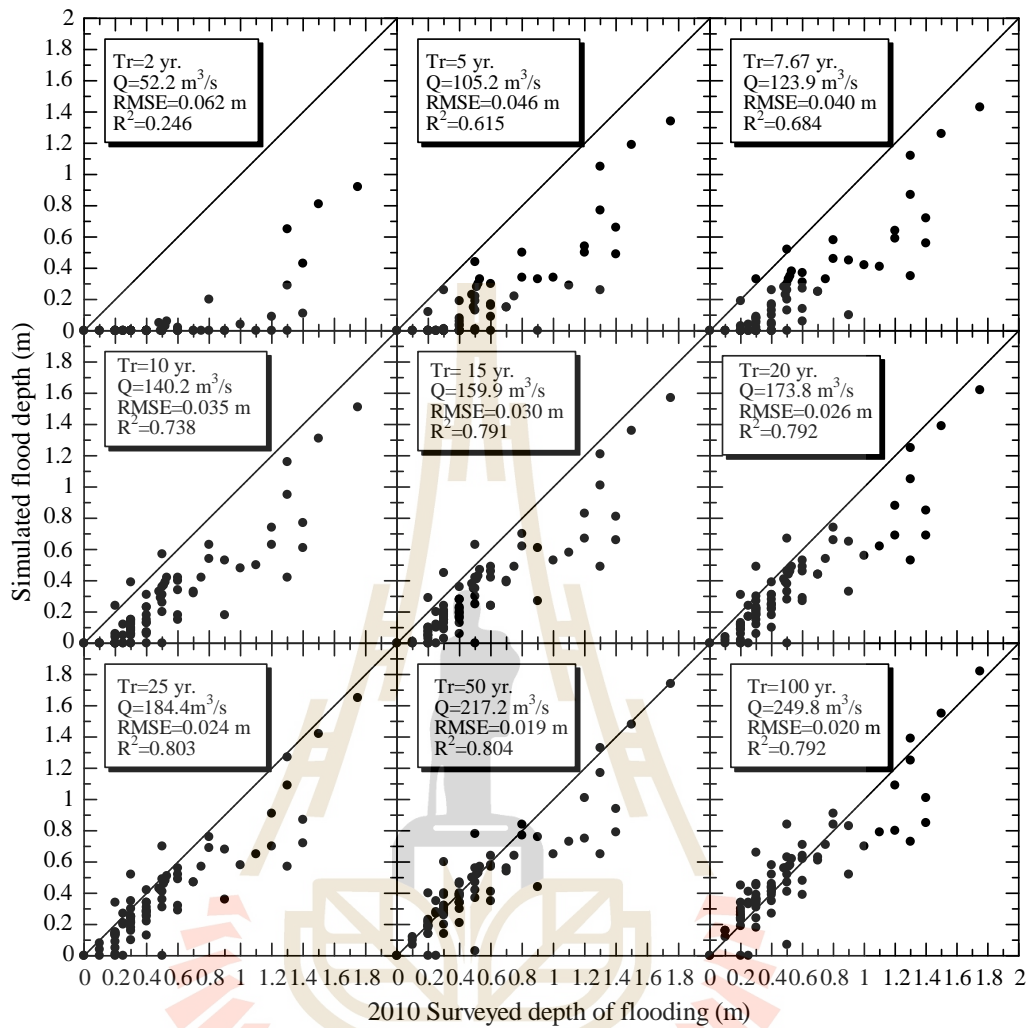


Figure 5.8 Comparison of flood depth between surveyed flood and simulated flood

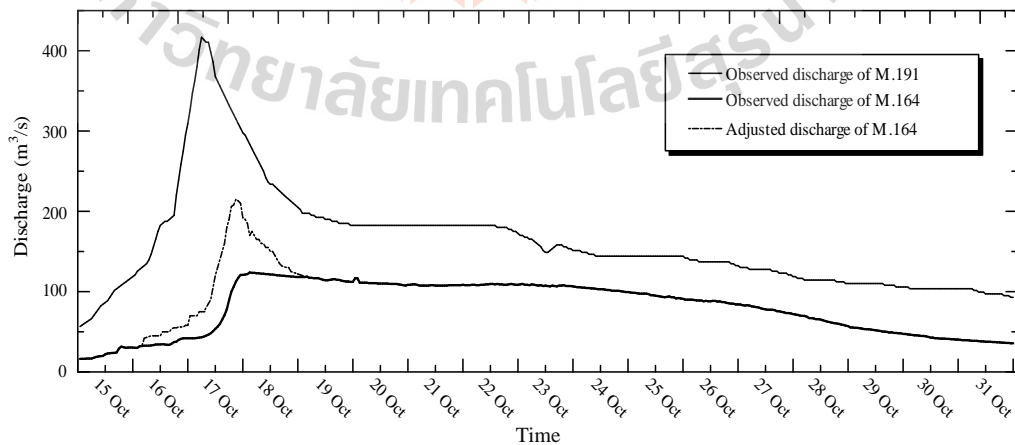


Figure 5.9 Adjusted hydrograph in 2010 flood event at M.164

5.8 Correction of flood hydrograph

During 2010 flood event, we suspected that there was an error of recorded hydrograph at station M.164. Peak discharge of observed hydrograph of M.191 upstream of M.164 was $410 \text{ m}^3/\text{s}$, whereas peak discharge of M.164 downstream was too low only $123 \text{ m}^3/\text{s}$ (Figure 5.1 and 5.9) (Maskong and Jothityangkoon, 2013). After successful mapping of the flood hazard map and found that the frequency of 2010 flood event was about 50 year return period. Based on this approach and simulation, a new hydrograph was generated and compared to recorded hydrograph. These results confirmed that the recorded hydrograph at M.164 was underestimated values. To correct this flood hydrograph, the new hydrograph represented by a dash line in Figure 5.9 was simulated to adjust the peak of observed hydrograph from 123 to $217 \text{ m}^3/\text{s}$.

5.9 Conclusion

To construct flood hazard map for a small flood affected area such as the Nakhon Ratchasima Municipality, studying step starts from (1) on-site surveying on 2010 flood event to construct observed flood map (2) applied HEC-RAS V.5 and GIS tool to receive high resolution geometric data ($\text{DEM } 5 \times 5 \text{ m}^2$) from HEC-GeoRAS in ArcGIS application and calibrated value of Manning's n for simulating 2D flood inundation extent and flood depth. Simulated flood hazard map based on input maximum discharge at different return periods confirmed that the simulated flood hazard area at 50 years return period is almost identical to 2010 observed flood event. One more application of the constructed flood hazard map is to correct the relative magnitude of peak discharges between upstream and downstream hydrographs to

realistic manner. Maximum discharges for different return periods from HEC-RAS V.5 were simulated based on the assumption of steady flow condition, therefore flooding duration of inundation for each grid cells were unable to estimate. From physical properties of flood characteristics presented by the flood hazard map will be developed further to construct a flood risk map by formulating flood risk index (i.e. flood properties, socio-economic factor, land-use) and using GIS raster index model. The flood risk map can be utilized as a tool to identify priority of the area for planning of flood prevention, flood mitigation and flood risk management.

5.10 References

- Aerts, J.C.J.H., and Botzen, W.J.W. (2011). **Climate change impacts on pricing long-term flood insurance: a comprehensive study for the Netherlands**, *Global Environ Change*, Vol. 21, pp. 1045-1060.
- Alaghmand, S. (2009). **River modelling for flood risk map prediction (a case study of Sungai Kayu Ara**, MSc thesis, Universiti Sains Malaysia (USM), Malaysia.
- Alaghmand, S., Abustan, R., Abustan, I., and Ealamian, S. (2012). **Comparison between capabilities of HEC-RAS and MIKE11 hydraulic models in river flood risk modelling (a case study of Sungai Kayu Ara River basin, Malaysia)**, *Hydrology Science and Technology*, Vol. 2, No. 3, pp.270–291.
- Asia Disaster Reduction Center (ARDC). (2009). **Natural disaster data book 2009 (An analytical review)**, Kobe, Japan, pp. 23.
- Brunner, G. (2014). **Combined 1D and 2D modelling with HEC-RAS**, USACE, p.130.

- Congressional Budget Office. (2009). **The National Flood Insurance Program: Factors Affecting Actuarial Soundness**, Washington DC, The United States.
- Chow, V.T., Maidment, D.R. and Mays, L.W. (1988). **Applied hydrology**. New York, p.391.
- DHI Group. (2016). **MIKE 11 river modelling package and applications**. Available: <https://www.mikepoweredbydhi.com/products/mike-11> [Accessed: 10 October 2016].
- FLO-2D Software, Inc., products. (2016). **Webinars and training**. Available: <https://www.flo-2d.com> [Accessed: 10 October 2016].
- Furdada, G., Calderón, L. E. and Marqués, M. A. (2008). **Flood hazard map of La Trinidad (NW Nicaragua). Method and results**, Natural Hazards, Vol. 45(2) pp.183-195.
- Ghimire, R., Ferreira S., and Dorfman, J.H. (2015). **Flood-induced displacement and civil conflict**, *World Development*, Vol. 66, pp. 614-628.
- Jia, L.S., and Wenjiao, S. (2015). **Effects of alpine swamp wetland change on rainfall season runoff and flood characteristics in the headwater area of the Yangtze River**, *CATENA*, Vol. 127, pp. 116-123.
- Kabenge, M., Elaru, J., Wang, H. and Fengting, Li. (2017). **Characterizing flood hazard risk in data-scarce areas, using a remote sensing and GIS-based flood hazard index**, *Natural Hazards*, Vol. 89(3) pp.1369-1387.
- Kongjun T., and Noypairoj, S. (2011). Flood disaster in Nakhon Ratchasima Province on 14-16 October 2010, **Report of Royal Irrigation Department of Thailand**.

- Knebl, M.R., Yang, Z.L., Hutchison, K., and Maidment, D.R. (2005). **Regional scale flood modeling using NEXRAD rainfall, GIS, and HEC-HMS/RAS: a case study for the San Antonio River Basin Summer 2002 storm event**, Journal of Environmental Management, Vol.75(4 special issue), pp. 325–36.
- Lian, J.J., Xu, K., and Ma, C. (2013). **Joint impact of rainfall and tidal level on flood risk in a coastal city with a complex river network: a case study of Fuzhou City, China**, Hydrology and Earth System Sciences (HESS), Vol. 17(2), pp.679–89.
- Luu, C., Meding, J. V. and Kanjanabootra, S. (2018). **Assessing flood hazard using flood marks and analytic hierarchy process approach: a case study for the 2013 flood event in Quang Nam, Vietnam**, Natural Hazards, Vol. 90(3) pp.1031-1050.
- Maskong, H. and Jothityangkoon, C. (2013). **Flood mapping for the municipality of Nakhon Ratchasima**, in Proceedings of the 18th National Convention on Civil Engineering (NCCE18), Chiang Mai, Thailand May 8-10, 2013.
- Mohammadi, S.A., Nazariha, M., and Mehrdadi, N. (2014). **Flood damage estimate (quantity), using HEC-FDA model. Case study: the Neka river**, Procedia Engineering, Vol.70, pp.1173–82.
- Moya, Q.V., Kure, S., Udo, K., and Mano, A. (2016). **Application of 2D numerical simulation for the analysis of the February 2014 Bolivian Amazonia flood: Application of the new HEC-RAS version 5**, RIBAGUA –Rev Iberoam Agua.
- Nakhon Ratchasima City Municipality. (2016). **Statistics of population**. Available: <http://www.koratcity.go.th/page/population> [Accessed: 1 November 2016].

Ponsan, P., and Panchana, S. (2011). **Summarizing the implementation of prevention and mitigation of disasters caused by 2010 flooding in Nakhon Ratchasima**, Report of Royal Irrigation Department of Thailand.

Reports of Members on the Impact of Tropical Cyclones, (2011). **WMO/ESCAP Panel on Tropical Cyclones**, New Delhi, India, pp. 2-3.

The Associated Programme on Flood Management (APFM), (2013). **Flood Management Tools Series (Conservation and Restoration of Rivers and Floodplains)**. World Meteorological Organization.

US Army Corps of Engineers, (2014). **Hydrologic Engineering Centers River Analysis System (HEC-RAS)**, available at: <http://www.hec.usace.army.mil/software/hecras/>[Accessed: 15 November 2014].

CHAPTER VI

THE DEVELOPMENT OF A GIS TOOL APPLICATION FOR FLOOD RISK MAPPING: A CASE STUDY OF NAKHON RATCHASIMA MUNICIPALITY, THAILAND

6.1 Summary

A flood risk model was modified from Zonensein et al. (2008) and the GIS application tool was created for flood risk mapping. Land use change was the scenario of the flood risk model. The flood depth and flood velocity were the product of flood hazard map that simulated as follow in Chapter V. Land use in each of flood indicators are included to represent the risk rating in spatial system (1-5 score). The future Land use was predicted by existed map in CA-Makov model and the result show the change of flood risk area in different Lansuse from past to future. It was found that the community and business area are increased from 9.05% and 11.59% year 2012 to 2022, respectively. Total flood risk area of community and business area are increased by 38.35% and 9.60% from year 2012 to 2022. Therefore, the flood risk model is a powerful tool for generating the flood risk map that can be utilized as a tool to identify priority of the area for planning of flood prevention, flood mitigation and flood risk management and urban planning. Moreover, the GIS flood risk application tool is user friendly interface.

6.2 Introduction

Flood risk map is integration of the potential hazards with the vulnerabilities of existing or potential economic activities when disclosed to the risk range of flood probabilities. The flood risk map can be defined as the probability of a loss, and this depends on three elements including hazard, vulnerability, and exposure. The flood risk map can be developed by applying average damage values per unit area (per land use type) on the preliminary hazard maps. However, in the detailed mapping stage, flood risk maps need high accuracy (APFM, 2013).

6.3 Methodology

6.3.1 Input data

The conceptual framework of the study step for flood risk mapping is shown in Figure 6.1 and its consists of 3 components: (1) Land use change prediction (2) Flood hazard map simulation and (3) Flood risk mapping.

From the previous study in Chapter V, the suitable Rating curve (Figure 6.2) and Hydrograph (Figure 6.3) at runoff station M.164 were simulated from the flood event. They were used to be unsteady flow condition for simulating a flood hazard map.

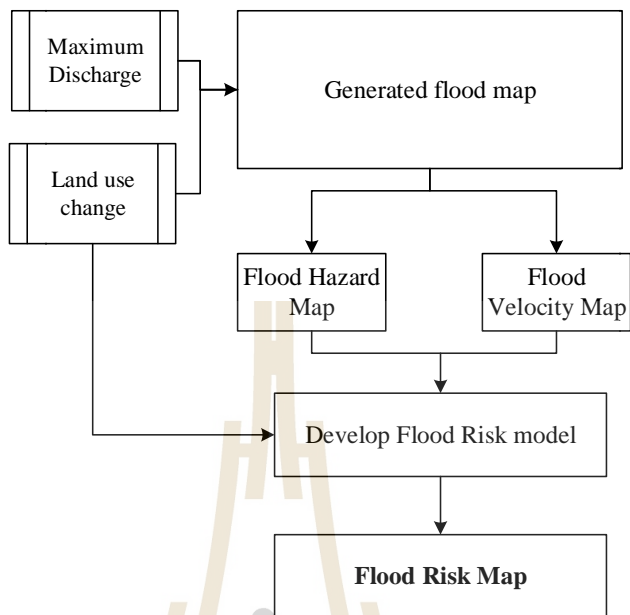


Figure 6.1 Flowchart of the study step for flood risk mapping

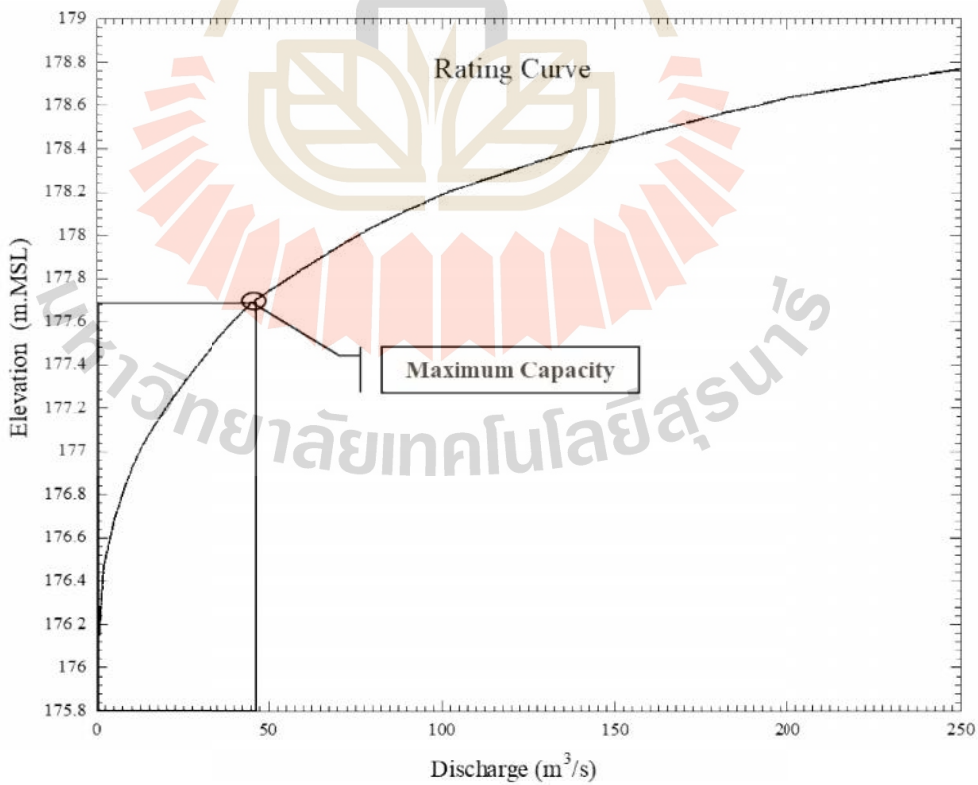


Figure 6.2 Simulated Rating curve at M.164

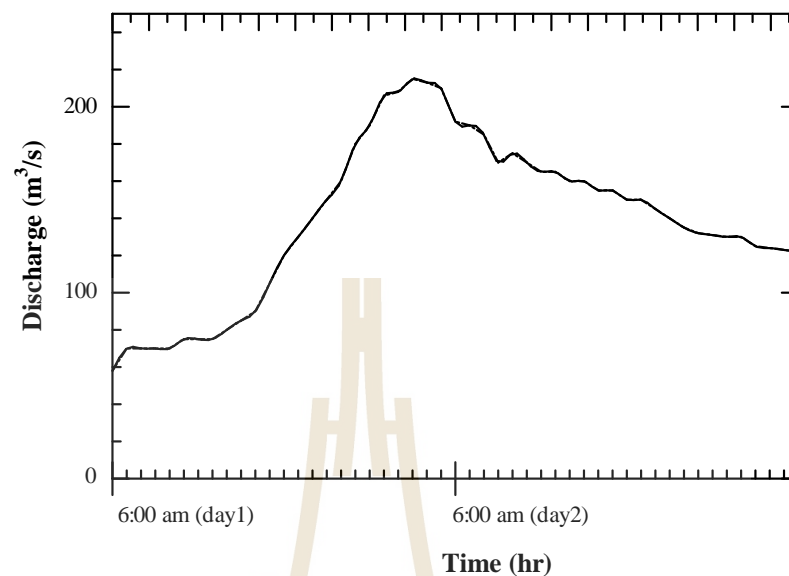


Figure 6.3 Generated runoff hydrograph for T=50 years (2010 flood event)

The land use maps as shown in Figure 6.4 and 6.5 were the classification of 2012 and 2017 Land use type of Nakhon Ratchasima Municipality, respectively. They were divided into 6 types including Water, Farm, Road, Empty, Community and Business. To perform Land use map prediction in the near future, the CA-Markov model was utilized and the obtained results was used as input data to quantify the consequent flood scenarios for that particular state of future Land use maps. The model is the result of integration between two individual modules, the Markov chain model and CA-Markov model that is available in the IDRISI software. The model can be used to generate such a transition probability matrix in which it takes two Land use maps as input data and then produces the output as the future Land use map (Eastman, 2003a, 2003b).

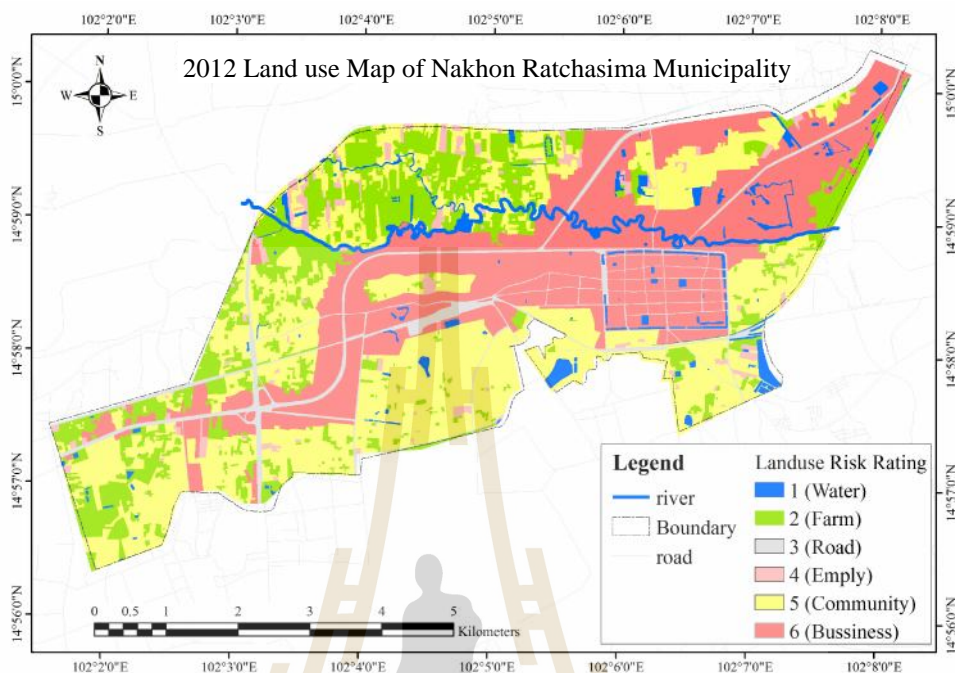


Figure 6.4 Land use Map in 2012 of Nakhon Ratchasima Municipality

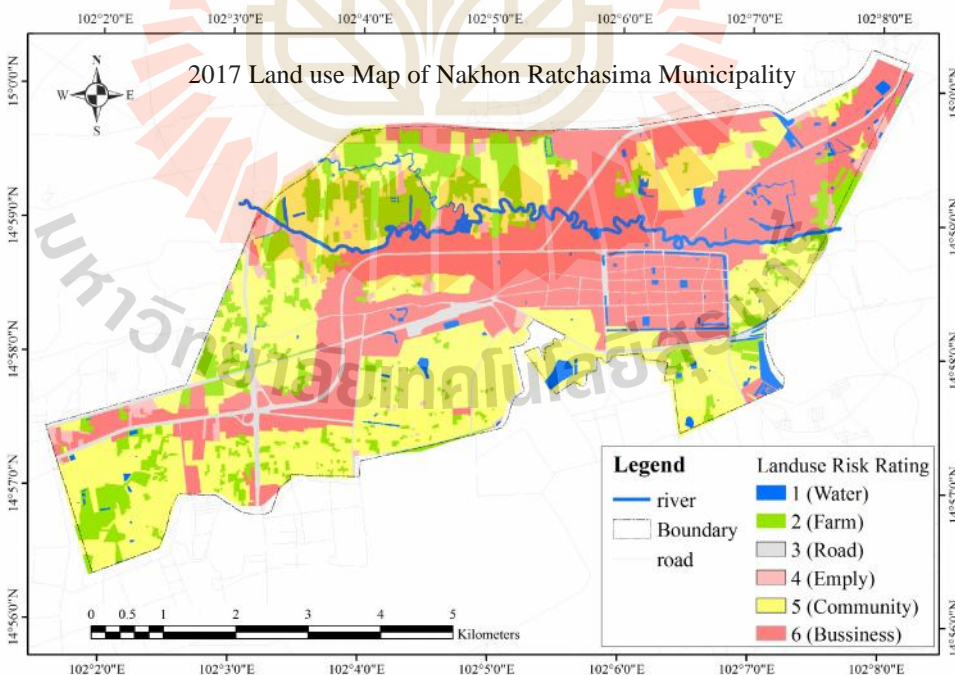


Figure 6.5 Land use in 2017 Map of Nakhon Ratchasima Municipality

6.3.2 Flood risk model

Flood risk is defined as the product of the probability and the consequences of flood event. Both components of risk are affected by multiple uncertainties but can conveniently divide between assessing the uncertainty associated with probabilities of the hazard and uncertainty associated with the consequences (the vulnerability). Both can be mapped individually, as well as the joint estimate of flood risk. Different types of vulnerability might require different types of visualizations. The risk of flood is based on three crucial elements which are related as the formula of flood risk shown in Equation 6.1 (Mongkonkerd et al.,2013).

$$\text{Flood risk} = \frac{\text{Vulnerability} \times \text{Characteristic}}{\text{Coping capacity}} \quad (6.1)$$

The best ways to reduce flood risk are reducing vulnerability and increasing coping capacity, which is a core common component of flood risk management. Figure 6.6 and 6.7 show the elements of flood risk which depend on vulnerability, flood characteristic, the ability of local people to cope with flood as follows.

Vulnerability refers to circumstances of a community or asset that make it susceptible to the damaging effects of a flood. There are many aspects of vulnerability, arising from various physical, social, economic, and environmental factors. Examples may include construction of buildings, inadequate protection of assets, lack of information and awareness.

Characteristic refers to natural disaster occurrence, frequency of damage, duration and maximum water level.

Coping capacity is the ability of people in the community to face and manage the flood using available skills and resources. The capacity to cope requires continuing awareness, resources and good management, both in normal times as well as during crisis or adverse conditions.

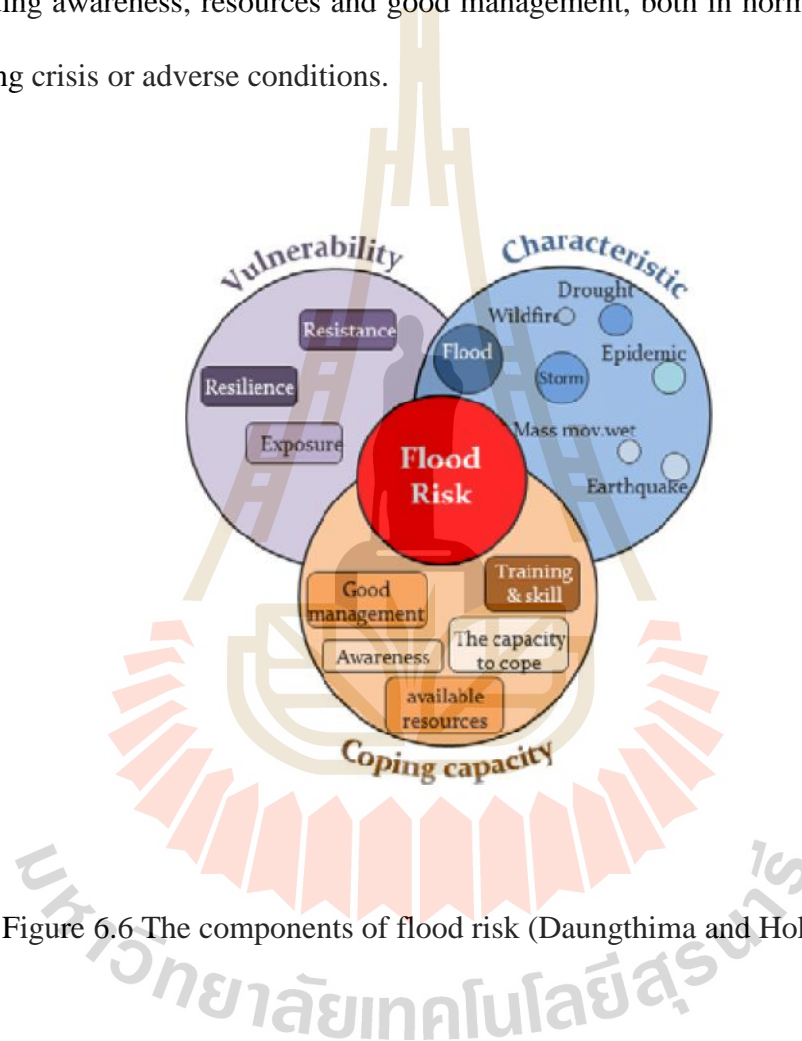


Figure 6.6 The components of flood risk (Daungthima and Hokao, 2013)

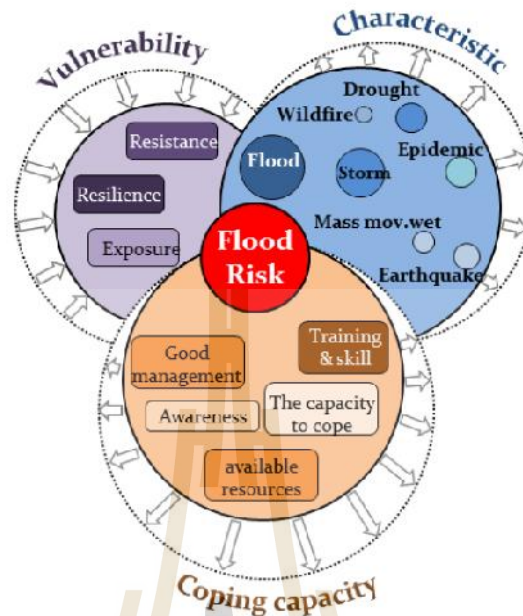


Figure 6.7 The reduction of flood risk (Daungthima and Hokao, 2013)

In this methodology, the probability component of flood risk is associated with the return period of a river flood event. This feature defines a basic information required to determine specific characteristics of a flood, such as its depth, land use type area, velocity. For the sake of simplicity and clarity, it was determined that the Flood Risk Index (FRI) should be a non-dimensional value, which could range between 1 and 5 the minimum and maximum risk, respectively (Modified from Zonensein et al.,2008). Moreover, in order to operate the indicators that compose flood risk rating, which have varied numbers and units, they must be normalized beforehand, converting them into a common range. According to the formulation established next, all indicators have to be adjusted to the same range, assuming values between 0 and 100.

The weighed product of these sub-indices results in the FRI, as presented in Equation 6.1. The weighted summation describes the relationship between the factors that constitute the sub-indices as show in Equation 6.2 (Zonensein et al.,2008), Faulkner et al.,2011).

$$FRI = FP^{q_{FP}} \times C^{q_c} \quad (6.1)$$

$$FRI = \left[\sum_{i=1}^n I_i^{FP} \cdot p_i^{FP} \right] \times \left[\sum_{j=1}^m I_j^C \cdot p_j^C \right] \quad (6.2)$$

Where:

FRI (Flood Risk Index) is the ranging between lowest risk and highest risk;

FP is the sub-index of the flood properties;

C is the sub-index of the flood consequences;

I_i^{FP} is i^{th} indicator for sub-index of the flood properties;

I_j^C is j^{th} indicator for sub-index of the flood consequences;

p_i^{FP} is the weighting factor associated with i^{th} indicator of sub-index FP,

$$0 \leq p_i^{FP} \leq 1 \text{ and } \sum_{i=1}^n p_i^{FP} = 1$$

p_j^C is the weighting factor associated with j^{th} indicator of sub-index C,

$$0 \leq p_j^C \leq 1 \text{ and } \sum_{j=1}^m p_j^C = 1$$

The risk of flood from the both of flood properties and flood consequences should be defined by each of the types of land use. In order to quantify the risk, the Equation 6.3 was modified from Zonensein et al. (2008), all indicators have to be adjusted to the same range, assuming risk values between 1 and 5.

$$FRI = \frac{\left[\sum_{i=1}^n I_i^{FP} \cdot p_i^{FP} \right] \times \left[\sum_{j=1}^m I_j^C \cdot p_j^C \right]}{5(n+m)} \quad (6.3)$$

Where: n is total number of indicators that compose sub-index FP and m total number of indicators that compose sub-index C.

The proposed Flood Risk Index (FRI) was developed according to these concepts and its properties were previously explained. The optimal of the constitutive indicators was conditioned by the availability of data, its precision and domain. Another restriction was that the FRI must be constituted by the minimum set of indicators proficient of sufficiently characterizing a particular scenario of risk. The indicators that compose the FRI mean to represent the main affects caused by flood. The classification of indicators is presented below in Table 6.1 to 6.3.

Table 6.1 Classification of the flood depth based on risk rating

Flood depth (m)	I_D^{FP}	Risk rating
<0.2	1	Very low
0.4	2	Low
0.7	3	Moderate
1.5	4	High
>1.5	5	Very high

Source: Adapted from Reiter (2000) and Chen (2007)

Table 6.2 Classification of the flood velocity based on risk rating

Flood velocity (m/s)	I_V^{FP}	Risk rating
<0.25	1	Very low
0.5	2	Low
1.0	3	Moderate
2.0	4	High
>2.0	5	Very high

Source: Adapted from Reiter (2000) and Chen (2007)

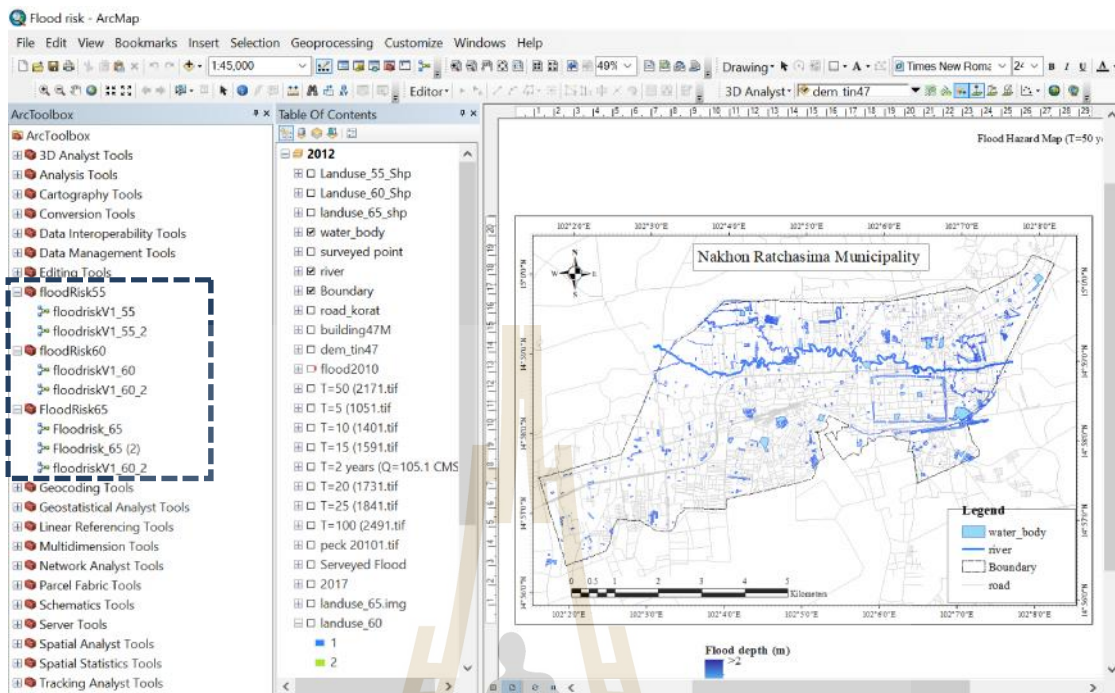


Figure 6.9 The flood risk application tool is applied in ArcGIS

6.4 Result and Discussion

The 2022 Land use map as shown in Figure 6.10 was predicted from 2012 and 2017 Land use map by CA-Makov model. Table 6.4 shows the change of covering area for different land use types in year 2012, 2017 and 2022. It was found that, in 2022 community and business areas are increased 9.05% and 11.59% from year 2012, respectively.

Table 6.4 Land use change from past 2012 and 2017 to future 2022 with different type of Land use

Land use type	2012		2017		2022	
	km ²	%	km ²	%	km ²	%
Water	1.32	3.54	1.22	3.27	1.19	3.16
Empty	6.9	18.46	5.02	13.43	3.79	10.06
Farm	2.02	5.4	2.02	5.4	2.02	5.35
Road	1.02	2.72	1.02	2.72	1.02	2.7
Community	13.48	36.1	14.35	38.41	14.7	39.55
Business	12.63	33.78	13.74	36.77	14.15	39.17
Total	37.37	100	37.37	100	37.37	100

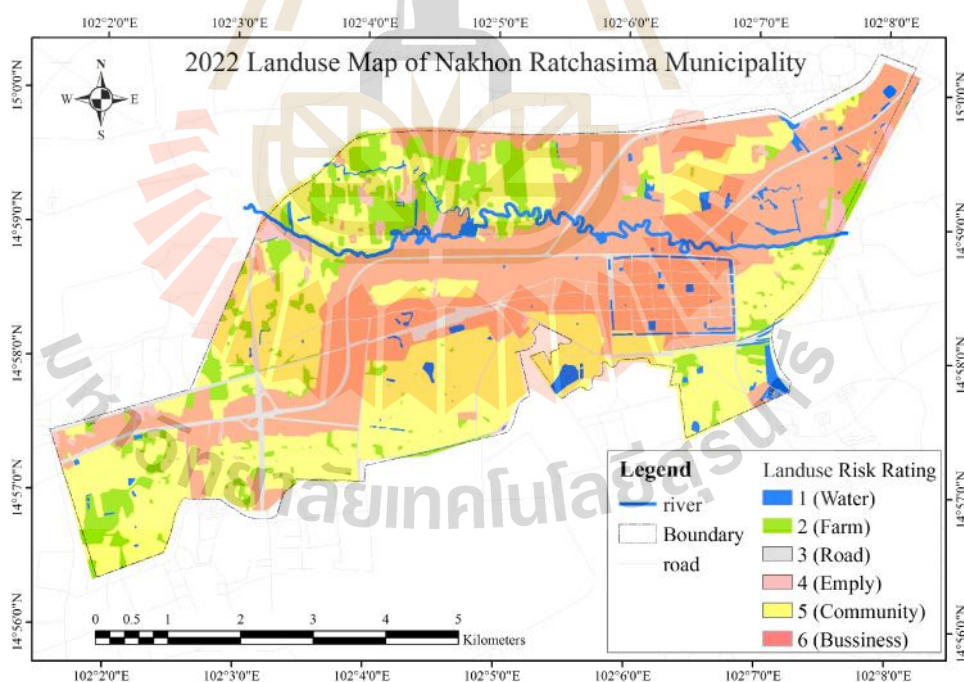


Figure 6.10 The 2022 Land use map of Nakhon Ratchasima Municipality

The flood hazard maps of years 2012, 2017 and 2022 based on Land use change were simulated by flood hazard model using an unsteady condition flow and geometrics data from Chapter V. The indicators of flood properties (The flood depth and flood velocity) are product of flood hazard map, shown in Figure 6.11 and 6.12. They are flood properties of year 2022 for Nakhon Ratchasima Municipality.

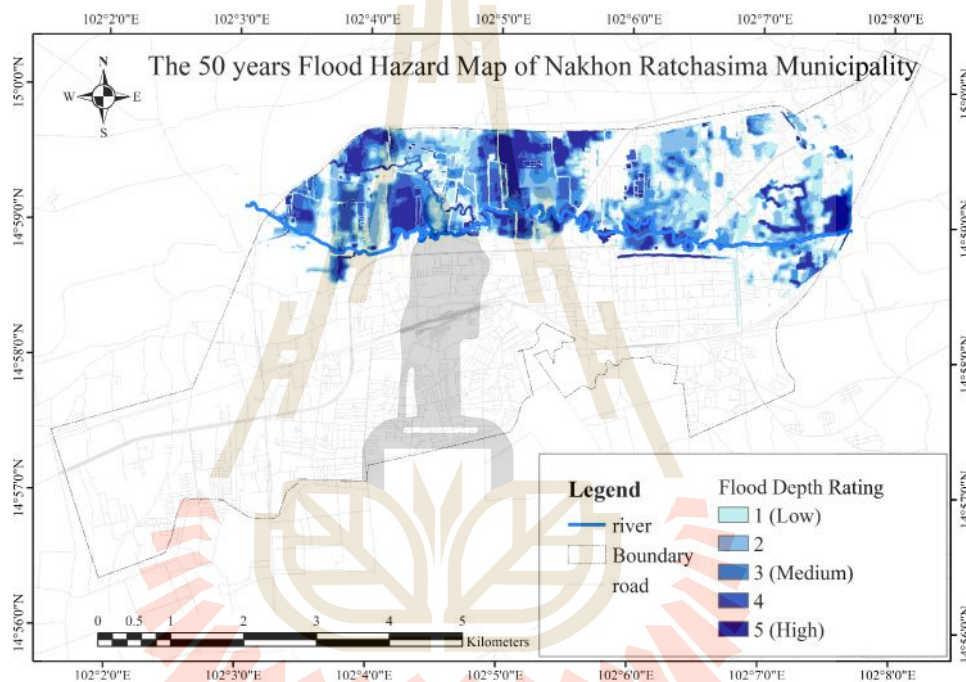


Figure 6.11 The 2022 classification of simulated flood depth at the return periods 50 years based on risk rating scale for Nakhon Ratchasima Municipality

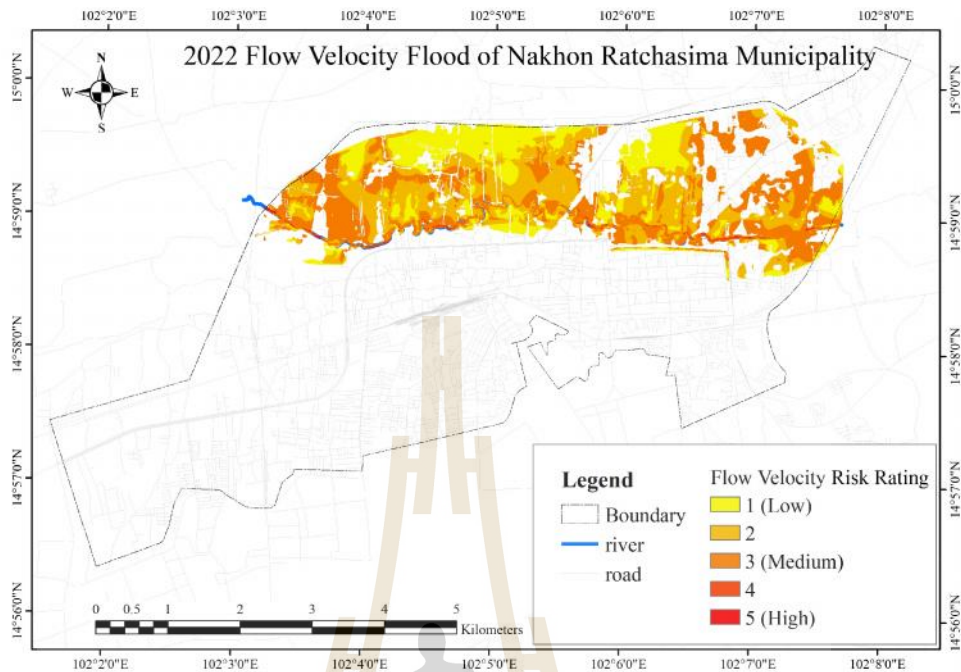


Figure 6.12 The 2022 classification of simulated flood velocity at the return periods 50 years based on risk rating scale for Nakhon Ratchasima Municipality

The Flood Risk map as shown in Figures 6.13, 6.14, and 6.15 were simulated from 2012, 2017 and 2022 flood indicators data by Flood risk model. Tables 6.5, 6.6 and 6.7 show the risk area for different land use in year 2012, 2017, and 2022, respectively. The total flood risk area of business, community and road zone are increased 38.35%, 9.60% and 8.08%, respectively from years 2012 to 2022.

Table 6.5 The rating risk area in year 2012 for different Land use types

Land use type	Total area (km ²)	Rating risk area					Total flood area (km ²)
		5 (km ²)	4 (km ²)	3 (km ²)	2 (km ²)	1 (km ²)	
Business	12.63	1.241	0	0.758	0.725	0	2.72
Community	13.49	0.62	0.491	0.64	0.666	0	2.42
Empty	1.02	0.06	0.092	0.102	0.122	0.089	0.46
Road	2.02	0	0.005	0.005	0.012	0.002	0.02
Farm	6.9	0	0	0.815	1.057	1.128	3
Water	1.32	0	0	0	0.379	0.256	0.64
Total	37.38	1.92	0.588	2.32	2.961	1.475	9.26

Table 6.6 The rating risk area in year 2017 for different Land use type

Land use type	Total area (km ²)	Rating risk area					Total flood area (km ²)
		5 (km ²)	4 (km ²)	3 (km ²)	2 (km ²)	1 (km ²)	
Business	13.76	1.627	0.177	0.92	0.856	0	3.58
Community	14.39	0.719	0.523	0.677	0.692	0	2.61
Empty	0.93	0.08	0.054	0.068	0.09	0.085	0.38
Road	2.02	0	0.005	0.005	0.012	0.005	0.03
Farm	5.02	0	0	0.656	0.835	0.584	2.07
Water	1.26	0	0	0	0.352	0.242	0.59
Total	37.38	2.425	0.759	2.326	2.837	0.915	9.26

Table 6.7 The rating risk area in year 2022 for different Land use type

Land use type	Total area (km ²)	Rating risk area					Total flood area (km ²)
		5 (km ²)	4 (km ²)	3 (km ²)	2 (km ²)	1 (km ²)	
Business	14.75	1.655	0.212	0.698	0.764	0.44	3.77
Community	14.9	0.271	0.453	0.533	0.689	0.701	2.65
Empty	0.72	0.147	0.041	0.032	0.069	0.08	0.37
Road	2.02	0.005	0.001	0.005	0.012	0.005	0.03
Farm	3.8	0.526	0.348	0.364	0.404	0.245	1.89
Water	1.19	0.342	0.059	0.048	0.04	0.074	0.56
Total	37.38	2.946	1.114	1.68	1.978	1.545	9.26

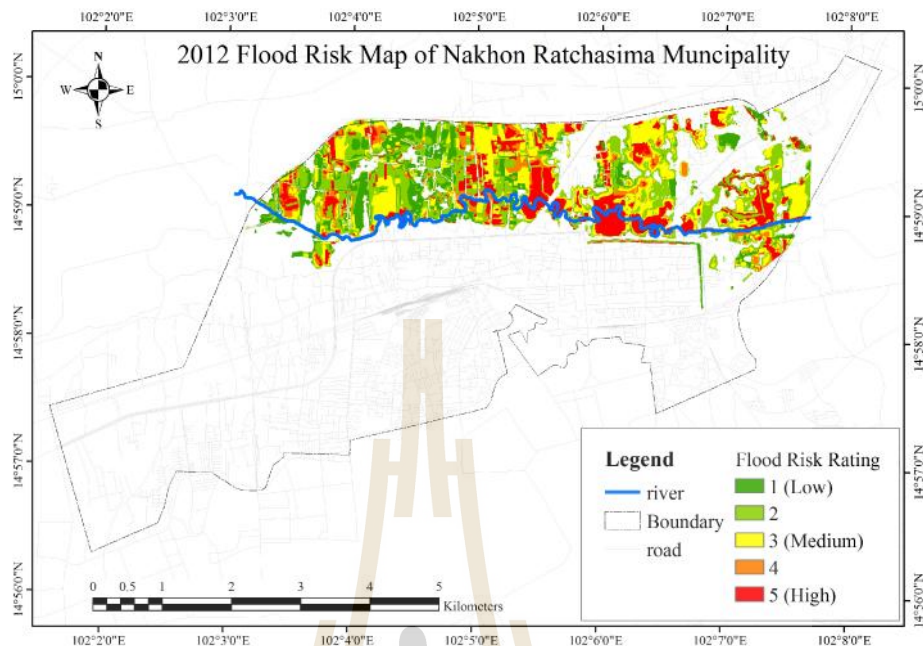


Figure 6.13 The 2012 Flood Risk Map of Nakhon Ratchasima Municipality

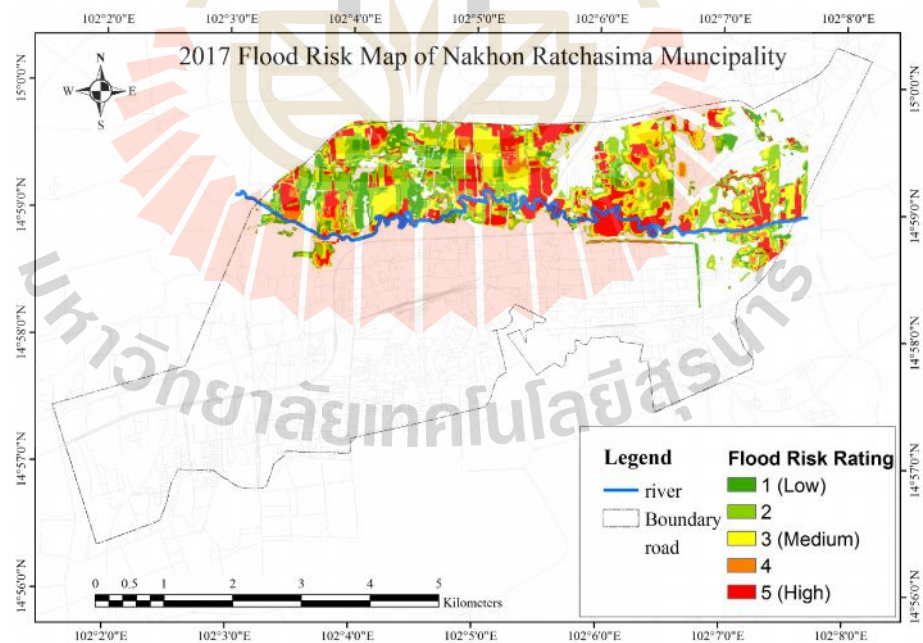


Figure 6.14 The 2017 Flood Risk Map of Nakhon Ratchasima Municipality

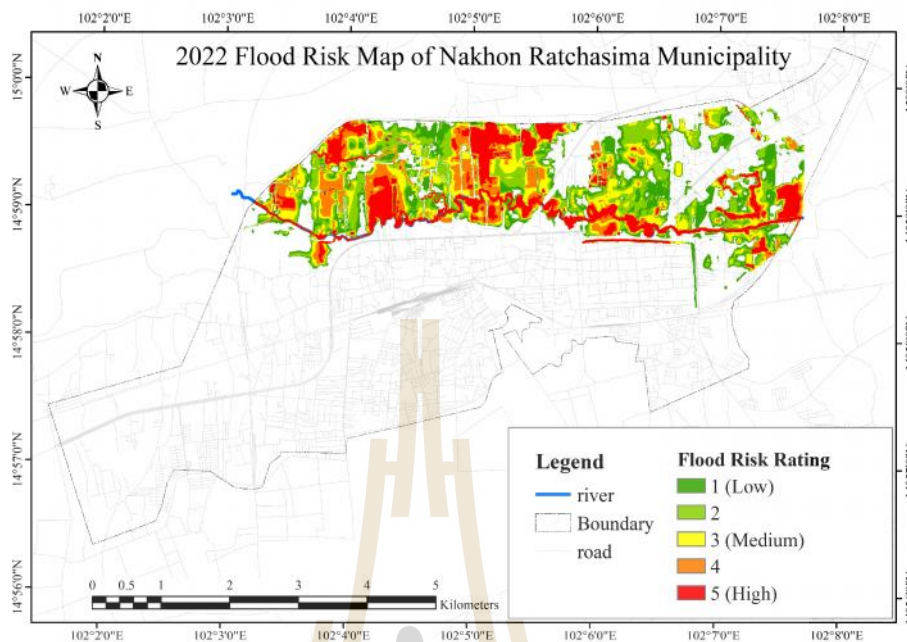


Figure 6.15 The 2022 Flood Risk Map of Nakhon Ratchasima Municipality



6.5 Conclusion

To construct a flood risk map, the flood risk model was modified from previous flood risk model of Zonensein et al. (2008) and the GIS application tool was created for flood risk mapping. The existing flood risk model was modified by considering the types of land use in each of flood indicators to represent the risk rating in spatial system. The future land use was predicted by existed map in CA-Makov model. The result shows the change of flood risk area in different land use from part to future. It was found that the total flood risk area of business, community and road zone are increased 38.35%, 9.60% and 8.08%, respectively from years 2012 to 2022 (10 years), respectively. For business area, very high flood risk area is increased 33.40% from years 2012 to 2022. The flood risk map can be utilized as a tool to identify priority of the area for planning of flood prevention, flood mitigation and flood risk management and urban planning.

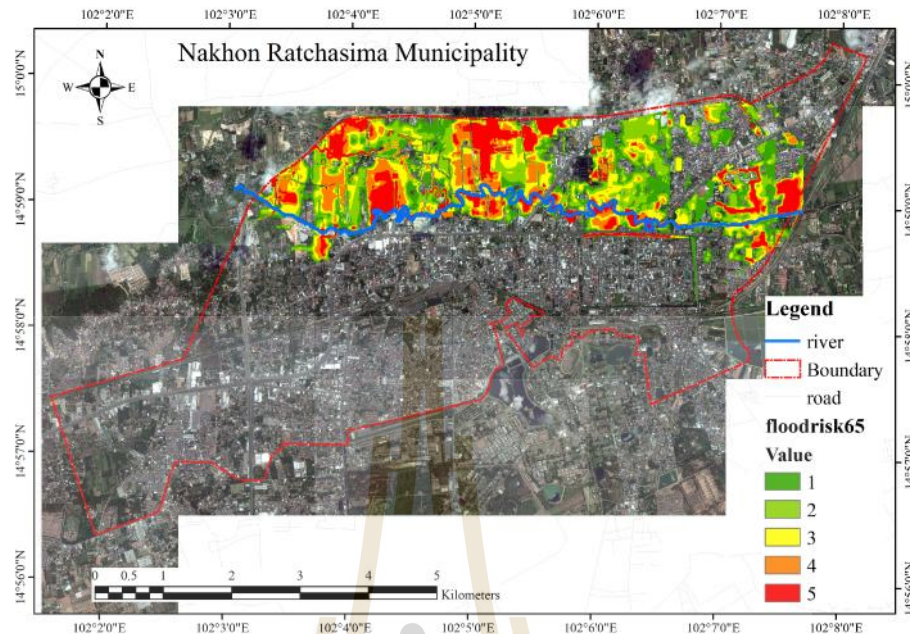


Figure 6.16 The 2022 Flood Risk Map with 2017 aerial photo of Nakhon Ratchasima Municipality

6.6 References

- Beven, K.J., and Kirkby, M.J. (1979). **A physically-based variable contributing area model of basin hydrology**, *Hydrol. Sci. J.*, 24(1), 43-69.
- Chen, P. (2007). **Flood impact assessment using hydrodynamic modelling in Bangkok, Thailand**. International Institute for Geo-Information Science and Earth Observation, Enschede, Netherlands.
- Daungthima, W. and Hokao, K. (2013). **Assessing the flood impacts and the cultural properties vulnerabilities in Ayutthaya, Thailand**. *Procedia Environmental Sciences*. 17: 739-748.
- Eastman, J.R. (2003a). **Idrisi Kilimajaro tutorial**. USA: Clark Laboratories, Clark University.

- Eastman, J.R. (2003b). **IDRISI Kilimanjaro: Guide to GIS and Image Processing**. USA: Clark Laboratories, Clark University.
- Faulkner, H., McCarthy, S., Tunstall, S., (2011). **Flood risk communication, in Flood Risk Science and Management**. edited by Pender, G. and Faulkner, H., pp. 386-406, Willey-Blackwell, UK.
- Mongkonkerd, S., Hirunsalee, S., Kanaegae, H. and Denpaiboon, C. (2013). **Comparison of direct monetary flood damage in 2011 to pillar house and non-pillar house in Ayuthhaya, Thailand**. *Procedia Environmental Sciences*, 17: 327-336.
- Reiter, P. (2000). **International methods of Risk Analysis, Damage Evaluation and Social Impact Studies concerning Dam-Break Accidents**, PR Water Consulting, Helsinki, Finland.
- The Associated Programme on Flood Management (APFM), (2013). **Flood Management Tools Series (Flood Mapping)**. World Meteorological Organization.
- Zonensein, J., Miguez, M.G., Magalhães, L.P.C., Valentin M.G. and Mascarenhas, F.C.B. (2008). **Flood Risk Index as an Urban Management Tool**. In:11th International Conference on Urban Drainage. Edinburgh, UK:/IWA,

CHAPTER VII

CONCLUSION AND RECOMMENDATION

7.1 Conclusion

In Chapter 4, a simple distributed hydraulic model is developed at the pixel/soil column scale and upscale to implement at the catchment scale. Applied water balance concept within the pixel and downstream interactions between each pixel allow the runoff generation by three mechanisms: HOF, DOF and SSF. Based on an actual building block of the selected DEM, the model can be parameterized for a large set of hypothetical catchments and input climate events. Simulation results are received when all processes are driven to reach a periodic steady state by a sequence of identical climate events. The advantage of this approach is simple, tractable and computationally efficiency that we can carry out for multiple realization of climate-soil- topography combination. This model will be used to simulate the effects of different combination of climate, soil, and topography on the runoff generation processes through hypothetical catchment and climate combination.

HEC-GeoRAS and ArcGIS are powerful tools as pre-processor for preparation for geospatial input data and also as a post-processor for visualization of the hydraulic model results for HEC-RAS models. In Chapter 5, the flood hazard map was simulated from the DEM and Land use using 1D2D hybrid method in HEC-RAS V.5. The improvement of rating curve in the floodplain was due to Land use condition

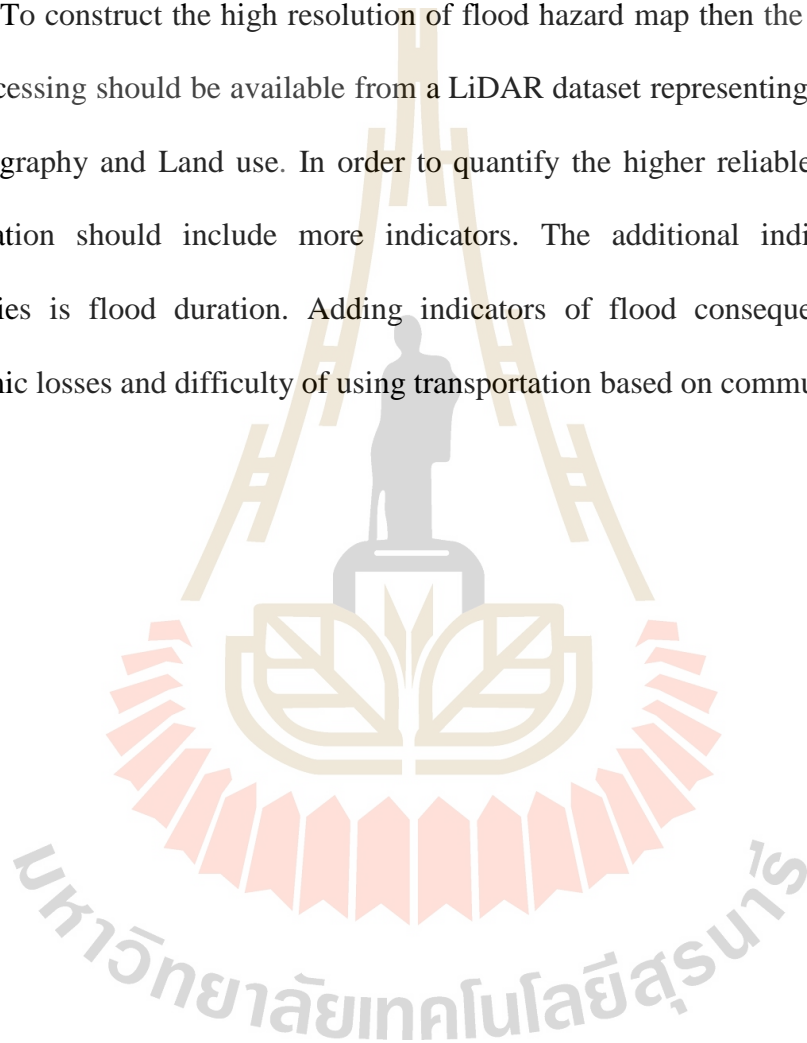
which leads to the increase of the river water level and volume and peak discharge of the simulated flooding. The runoff hydrograph in the flood event was generated to correct this flood hydrograph by the simulated flooding also. Flood depth and flood velocity are the product of flood hazard mapping that is the most important element to be the flood properties indicator for flood risk model.

In general, there are three limiting factors for the applicability of the flood risk model : (1) availability of data (2) existence of data with adequate precision and (3) limits of the normalization scales. In Chapter 6, the existing flood risk model (Zonensein et al. ; 2008) and the GIS application tool were applied to construct flood risk map by using input flood properties (flood depth and flood velocity) from Chapter 5. The Land use change is the scenario in this study and the flood risk rating can be defined for each of the Land use types. By using Markov chain model and CA-Markov model. The future community and business area are increased by 9.05% and 11.59% from year 2012 to 2022 (10 years), respectively. The predicted flood risk area of business, community and road zone from modified flood risk model are increased 38.35%, 9.60% and 8.08%, respectively from year 2012 to 2022. For business area, very high flood risk area is increased 33.40% from year 2012 to 2022. Therefore, the flood risk model is a powerful tool for generating the flood risk map for planning and management of flooding. Moreover, the GIS flood risk application tool is user friendly interface.

7.1 Recommendation

To develop the next step of a simple distributed hydraulic model to investigate the climate, soil and topographic controls on annual water balance in a qualitative way to define dimensionless functional relationships.

To construct the high resolution of flood hazard map then the terrain to raster geoprocessing should be available from a LiDAR dataset representing high resolution of topography and Land use. In order to quantify the higher reliable flood risk, the formulation should include more indicators. The additional indicator of flood properties is flood duration. Adding indicators of flood consequence are socio-economic losses and difficulty of using transportation based on community income.



BIOGRAPHY

Miss. Haruetai Maskong was born on November 26, 1982 in Nakhon Ratchasima Province, Thailand. She received her Bachelor's degree in Transportation Engineering from Suranaree University of Technology in 2005. She has worked as a Transportation engineer in Bangkok Marine Enterprises Company limited for a year after that she was a Teacher/Researcher assistant in School of Civil Engineering, Institute of Engineering, Suranaree University of Technology. In 2008, she received a scholarship awarding to graduate students whose lecturers are awarded research funding by outside sources (OROG) from Suranaree University of technology for Master degree study at Suranaree University of technology. In 2011, she received a Scholarship awarding to graduate student from Suranaree University of technology for Doctoral degree study at Suranaree University of technology. In 2015, she got a scholarship award from Austrian Government (OEAD) called Ernst Mach Grant, Ernst Mach-worldwide for research at Vienna University of Technology (1/11/2015-30/5/2016). She continued with her Ph.D. graduate studies in the Civil Engineering Program, School of Civil Engineering, Institute of Engineering, Suranaree University of Technology.

การสร้างแผนที่เสี่ยงภัยน้ำท่วมสำหรับเทศบาลนครราชสีมา



วิทยานิพนธ์นี้เป็นส่วนหนึ่งของการศึกษาตามหลักสูตรปริญญาวิศวกรรมศาสตรดุษฎีบัณฑิต

สาขาวิชาวิศวกรรมโยธา

มหาวิทยาลัยเทคโนโลยีสุรนารี

ปีการศึกษา 2560

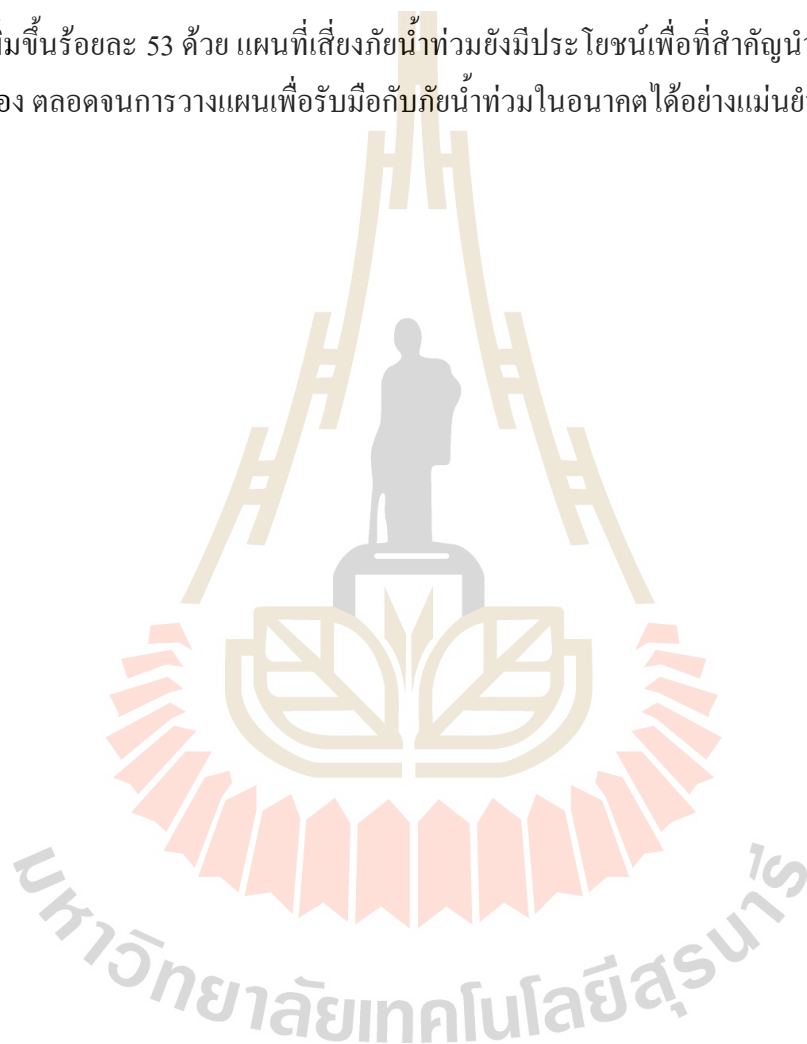
หตุทัย มาศโค้ง : การสร้างแผนที่เสี่ยงภัยน้ำท่วมสำหรับเทศบาลนครนครราชสีมา
(FLOOD RISK MAPPING FOR NAKHON RATCHASIMA MUNICIPALITY)

อาจารย์ที่ปรึกษา : รองศาสตราจารย์ ดร.ฉัตรชัย โชติษฐียงกูร, 138 หน้า

วิทยานิพนธ์ฉบับนี้มีวัตถุประสงค์เพื่อศึกษาสภาพปัญหา ทำความเข้าใจ เหตุการณ์น้ำท่วมในอดีตในพื้นที่เทศบาลเมืองนครราชสีมา โดยเฉพาะเหตุการณ์ปี พ.ศ.2553 และปรับแก้ข้อมูลสภาพการเกิดน้ำท่วมในอดีตให้มีความถูกต้องแม่นยำขึ้น ข้อมูลที่ได้นี้ได้ถูกนำมาใช้สำหรับการพัฒนาแบบจำลองน้ำท่วม เพื่อสร้างแผนที่น้ำท่วม (Flood Hazard Map) ที่คาบการเกิดซ้ำต่าง ๆ 5 10 15 25 50 และ 100 ปี ตลอดจนพัฒนาแบบจำลอง และเครื่องมือสำหรับสร้างแผนที่เสี่ยงภัยน้ำท่วม (Flood Risk Map) เพื่อใช้ในโปรแกรม ArcGIS

ข้อมูลความลึกน้ำท่วมสูงสุดจากการสำรวจหลังจากเหตุการณ์น้ำท่วมเมื่อปี พ.ศ.2553 ถูกนำมาสร้างเป็นแผนที่น้ำท่วม (Flood Event Map) เพื่อทำความเข้าใจสภาพปัญหาจริงของการเกิดน้ำท่วม รวมถึงการวิเคราะห์ข้อมูลทางอุตุ-อุทกวิทยาของพื้นที่ศึกษาด้วย พบว่าแผนที่น้ำท่วมจากสำนักงานพัฒนาเทคโนโลยีอวกาศและภูมิสารสนเทศ (องค์การมหาชน) เป็นแผนที่น้ำท่วมที่แสดงเพียงพื้นที่น้ำท่วม (Flood Extend Map) ไม่ได้แสดงถึงความลึกน้ำท่วม อีกทั้งยังไม่สามารถแสดงถึงพื้นที่น้ำท่วมที่เป็นจริงในพื้นที่ศึกษาได้ และข้อมูลอัตราการไหลในขณะที่เกิดน้ำล้นตลิ่งแล้ว ไม่สามารถตรวจวัดได้ ดังนั้นเพื่อสร้างแผนที่น้ำท่วมที่แสดงถึงผลกระทบที่มีความแม่นยำมากขึ้น จึงใช้แบบจำลองทางชลศาสตร์ คือ โปรแกรม HecRAS V5 จำลองแผนที่น้ำท่วม โดยสร้างข้อมูลกายภาพ (Geometric data) เช่น ร่องลำนน้ำ (Channel) และพื้นที่ราบน้ำท่วม (Floodplain) ของพื้นที่ศึกษาจากแผนที่ความสูงเชิงตัวเลข (DEM) ด้วยเครื่องมือ Hec-GeoRAS ในโปรแกรม ArcGIS ก่อนจะส่งออกข้อมูลทางกายภาพ เพื่อนำเข้าแบบจำลองแผนที่น้ำท่วม ซึ่งข้อมูลทางกายภาพของพื้นที่ศึกษา ได้นำเส้นโค้งความสัมพันธ์ระหว่างระดับน้ำและปริมาณน้ำ (Rating curve) ใช้เพื่อสอบเทียบการไหลในร่องน้ำ พบว่าค่าสัมประสิทธิ์ความขรุขระ (Manning's n) ที่เหมาะสมในแบบจำลองอยู่ระหว่าง 0.020-0.035 (ขึ้นอยู่กับระดับของร่องน้ำ) และของพื้นที่ราบน้ำท่วมขึ้นอยู่กับประเภทของการใช้ประโยชน์ที่ดิน จากผลการจำลองแผนที่น้ำท่วม และแผนที่น้ำท่วมจากการสำรวจ สามารถทำความเข้าใจกายภาพของการเกิดน้ำล้นตลิ่งในพื้นที่ที่ศึกษาได้ว่าเป็นเหตุการณ์น้ำท่วมที่มีอัตราการสูงสุดไหลในลำน้ำที่คาบการเกิดซ้ำ 50 ปี (อัตราการไหลเท่ากับ $217 \text{ m}^3/\text{s}$) และยังสามารถสร้างเส้นโค้งความสัมพันธ์ระหว่างระดับน้ำ และปริมาณน้ำ ที่ระดับน้ำล้นตลิ่งไปยังพื้นที่ราบน้ำท่วมของสถานีวัดน้ำท่า M.164 ได้ สามารถใช้ปรับแก้กราฟอุทก (Hydrograph) จากข้อมูลตรวจวัด ในช่วงเวลาเกิดน้ำล้นตลิ่งให้ถูกต้องแม่นยำยิ่งขึ้น

การจำลองแผนที่คุณลักษณะพื้นที่เสี่ยงภัยน้ำท่วมดำเนินการต่อจากข้อมูลแผนที่น้ำท่วมและการเปลี่ยนแปลงการใช้ประโยชน์ที่ดิน แผนที่น้ำท่วมที่ใช้ถูกจำลองจากข้อมูลการไหลแบบไม่คงที่ (Unsteady flow) ใช้กราฟอูทกที่ถูกปรับแก้แล้ว และแผนที่การใช้ประโยชน์ที่ดินของปี พ.ศ. 2565 ทำนายโดยแบบจำลอง CA-Markov จากแผนที่การใช้ประโยชน์ที่ดินปี พ.ศ.2555 และ ปี พ.ศ. 2560 ซึ่งพบว่า พื้นที่การใช้ประโยชน์ที่ดินประเภทที่อยู่อาศัย และพื้นที่เศรษฐกิจของปี พ.ศ.2565 เพิ่มขึ้น ร้อยละ 9.05 และ ร้อยละ 11.92 ตามลำดับ จากปี พ.ศ.2555 ส่งผลให้มีพื้นที่เสี่ยงภัยน้ำท่วมสูงสุด เพิ่มขึ้นร้อยละ 53 ด้วย แผนที่เสี่ยงภัยน้ำท่วมยังมีประโยชน์เพื่อที่ลำคัญนำไปใช้สำหรับการวางผังเมือง ตลอดจนการวางแผนเพื่อรับมือกับภัยน้ำท่วมในอนาคตได้อย่างแม่นยำ



สาขาวิชา วิศวกรรมโยธา

ปีการศึกษา 2560

ลายมือชื่อนักศึกษา _____

ลายมือชื่ออาจารย์ที่ปรึกษา _____

HARUETAI MASKONG : FLOOD RISK MAPPING FOR
NAKHON RATCHASIMA MUNICIPALITY. THESIS ADVISOR : ASSOC.
PROF. CHATCHAI JOTHITYANGKOON, Ph.D., 138 PP.

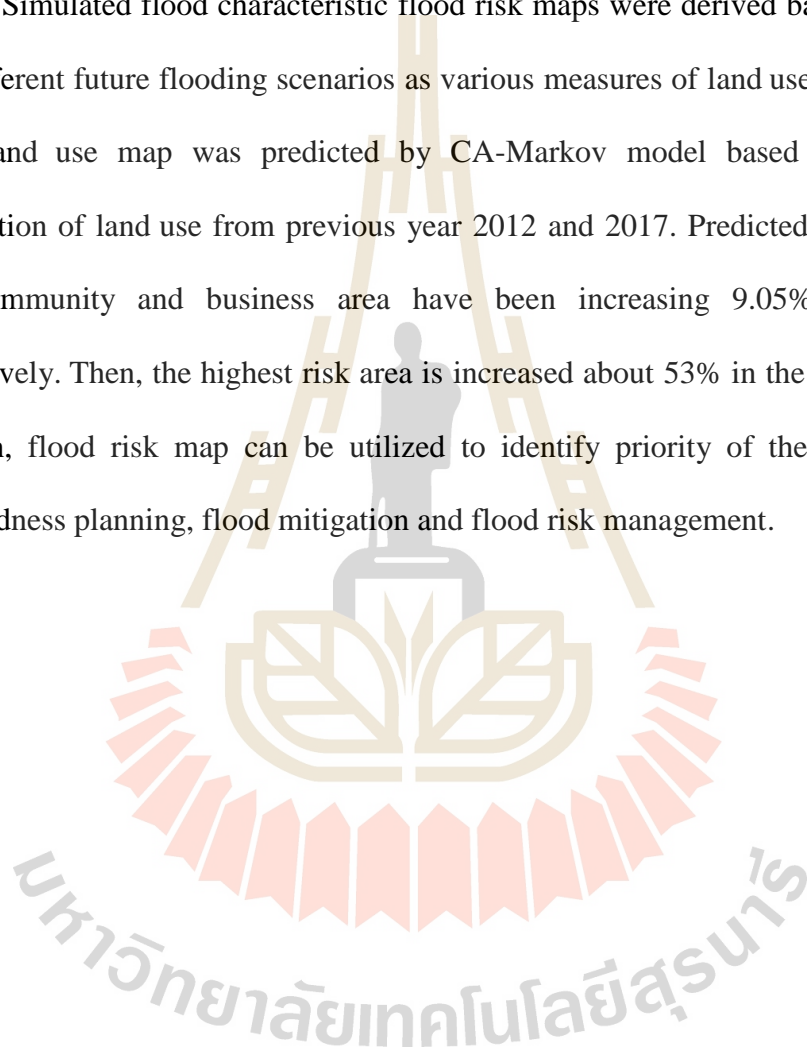
FLOOD MANAGEMENT / FLOOD HAZARD MAP / FLOOD RISK / RIVER
FLOOD / GIS APPLICATION TOOL /

The objectives of this dissertation are to collect historical flood properties, to understand flood behavior and to improve the accuracy of recorded flood in the municipality of Nakhon Ratchasima, particularly, past flood in 2010. This information has been used for developing flood inundation model to generate flood hazard maps with the maximum discharge value at the observed station (M.164) for return periods of 5, 10, 15, 25, 50, and 100 years. Then, develop an application tool in ArcGIS to generate flood risk map.

To construct the flood hazard map from available observed flood map of the small flood affected area, HecRAS V.5 and GIS tool are used to formulate and delineate flood hazard map for future scenarios of flood properties. For a simulation, input physical parameters were generated by Hec-GeoRAS in ArcGIS based on DEM ($5 \times 5 \text{ m}^2$). A range of calibrated Manning's n in a main channel was obtained from fitting exercise with observed Rating curve. It was found that the n values between 0.020-0.035 (vary with elevation of main channel) are suitable values. Manning's n in floodplain depending upon the type of land cover that were estimated by the land-use map. Observed and simulated flood map with precise information can be used to understand flood behavior in urban area and to improve the accuracy of recorded flood area from satellite images. For the 2010 flooding event in the concerning area, the

simulated flood hazard map subjected to the discharge of 50 years return period ($217 \text{ m}^3/\text{s}$) is almost identical with the observed flood map from the surveying. These results confirmed that the recorded hydrograph at M.164 was underestimated values then the new hydrograph was proposed.

Simulated flood characteristic flood risk maps were derived based on existing and different future flooding scenarios as various measures of land use change. Future 2022 land use map was predicted by CA-Markov model based on the spatial distribution of land use from previous year 2012 and 2017. Predicted results showed that community and business area have been increasing 9.05% and 11.92%, respectively. Then, the highest risk area is increased about 53% in the next decade. In addition, flood risk map can be utilized to identify priority of the area for flood preparedness planning, flood mitigation and flood risk management.



School of Civil Engineering

Academic Year 2017

Student's Signature _____

Advisor's Signature _____

ACKNOWLEDGEMENTS

I would like to express my highest gratitude to my supervisor, Assoc. Prof. Dr. Chatchai Jothityangkoon, for his supervision, encouragement and support, all of which have been given to me with his endless kindness. The examining committee has played a significant role in the completion of my thesis. I am grateful to Asst. Prof. Dr. Kittiwet Kuntiyawichai for serving as the chair of the Ph.D. thesis examining committee. I would also like to thank Asst. Prof. Dr. Preeyaphorn Kosa, Asst. Prof. Dr. Pornpot Tanseng, and Asst. Prof. Dr. Mongkol Jiravacharadet for serving as Ph.D. thesis examiners.

I would like to acknowledge the valuable supervision from Asst. Prof. Dr. Jurgen Komma and Prof. Dr. Gunter Bloeschl during my 8-month visit to the Vienna University of Technology, Austria.

I acknowledge the help and encouragement from Asst. Prof. Chow Hirunteeyakul, Dr. Nattaporn Charoentham, Dr. Chayakrit Phetchuay, Dr. Wisitsak Tabyang, Dr. Cherdsak Suksiripattanapong, Dr. Apichat Suddeepong, Miss. Nattiya Wonglakorn, Mr. Mathagul Metham, Mr. Nart Sooksil and Mr. Nivech Sertjantuk. I am very grateful to Mr. Thitikorn Aphibunsuwan for supporting, understanding and encouraging which made my study more than just successful.

Finally, I would like to appreciate my family and my brother Mr. Piyawut Maskong for their love, support, understanding, and providing me the opportunity to pursue my graduate studies.

Haruetai Maskong

TABLE OF CONTENTS

	Page
ABSTRACT IN THAI.....	I
ABSTRACT IN ENGLISH.....	III
ACKNOWLEDGEMENTS.....	V
TABLE OF CONTENTS.....	VI
LIST OF TABLES.....	XI
LIST OF FIGURES.....	XII
CHAPTER	
1 INTRODUCTION.....	1
1.1 Problem background and importance of the study.....	1
1.2 Research objective.....	7
1.3 Scope and limitations of study.....	8
1.4 Benefit of study.....	9
1.5 Thesis structure.....	9
1.6 References.....	10

TABLE OF CONTENTS (Continued)

	Page
2 BASIC CONCEPTS AND LITERATURE REVIEW	11
2.1 Introduction.....	11
2.2 Runoff generation processes.....	13
2.3 Hydrologic model.....	23
2.3.1 Type of the model.....	23
2.3.2 Rainfall-runoff model.....	27
2.3.3 Water balance concept.....	33
2.3.4 Water balance concept based on watershed	34
2.3.5 Channel Routing.....	36
2.4 Tool of Flood mapping.....	37
2.5 Review of the relevant research works.....	40
2.6 Reference.....	51
3 MATERIALS AND METHODS	57
3.1 Data preparation.....	57
3.1.1 Basin characteristic of study area.....	57
3.1.2 Hydrological and Geological data.....	64
3.1.3 Surveying and collecting data.....	64
3.2 Development of the flood map model.....	65
3.3 Development of the flood risk model.....	66

TABLE OF CONTENTS (Continued)

	Page
4 THE DEVELOPMENT OF A SIMPLE DISTRIBUTED HYDROLOGICAL MODEL BASED ON UP-SCALING FROM PIXEL TO CATCHMENT SCALE.....	68
4.1 Summary.....	68
4.2 Introduction.....	69
4.3 Methodology.....	71
4.3.1 Soil-water moisture and water balance.....	72
4.3.2 Evapotranspiration.....	74
4.3.3 Runoff generation process.....	75
4.3.4 Routing processes at the pixel scale.....	76
4.3.5 Topography.....	78
4.3.5 Soil properties.....	79
4.4 Results and discussion.....	80
4.5 Conclusions.....	83
4.6 References.....	85

TABLE OF CONTENTS (Continued)

	Page
5 FLOOD HAZARD MAPPING USING ON-SITE SURVEYED FLOOD MAP, HECRAS V.5 AND GIS TOOL: A CASE STUDY OF NAKHON RATCHASIMA MUNICIPALITY, THAILAND.....	87
5.1 Summary.....	87
5.2 Introduction.....	88
5.3 Study area and dataset.....	91
5.4 Methodology.....	94
5.5 Review of flood experiences.....	95
5.6 Modeling approach for numerical simulation	96
5.7 Results and discussion.....	98
5.7.1 Observed annual maximum discharge.....	98
5.7.2 Roughness coefficients (Manning's n)	99
5.7.3 Flood hazard map.....	101
5.8 Correction of flood hydrograph.....	106
5.9 Conclusions.....	106
5.10 References.....	107

TABLE OF CONTENTS (Continued)

	Page
6 THE DEVELOPMENT OF A GIS TOOL APPLICATION FOR FLOOD RISK MAPPING: A CASE STUDY OF NAKHON RATCHASIMA MUNICIPALITY, THAILAND.....	111
6.1 Summary.....	111
6.2 Introduction.....	112
6.3 Methodology.....	112
6.3.1 Input data.....	112
6.3.2 Flood Risk model.....	116
6.3.3 GIS application tool.....	122
6.4 Results and discussion.....	123
6.5 Conclusions.....	132
6.6 References.....	133
7 CONCLUSION AND RECOMMENDATION.....	135
7.1 Conclusions.....	135
7.2 Recommendation.....	137
BIOGRAPHY.....	138

LIST OF TABLES

Table	Page
2.1	The disaster vulnerability factors.....48
3.1	List of sub-basins of upper Mun River Basin and their properties.....60
3.2	Data types agencies and available records for upper Mun River Basin.....60
3.3	List of land use type and its area for Lam Takong River Basin.....63
5.1	Observed annual maximum discharges for different return period at M.164.....99
5.2	Comparison between calculated and simulated Rating curve.....100
5.3	The value of the manning roughness (n)101
6.1	Classification of the flood depth.....121
6.2	Classification of the flood velocity.....121
6.3	Classification of the type of Land use that affected by flood.....122
6.4	Covering area for different Land use type in years 2012, 2017 and 2022 based on Figure 6.4, 6.5 and 6.10.....124
6.5	The rating risk area in year 2012 for different Land use type.....127
6.6	The rating risk area in year 2017 for different Land use type.....128
6.7	The rating risk area in year 2022 for different Land use type.....129

LIST OF FIGURES

Figure	Page
1.1	Satellite image of 2011 flooding in Ayutthaya And Pathum Thani Provinces2
1.2	Boundary and location of Nakhon Ratchasima province and upper Mun river basin5
1.3	Boundary and location of study area in Nakhon Ratchasima Municipality, Nakhon Ratchasima province, Thailand6
2.1	Pathway Pathways followed by subsurface runoff on hillslopes.14
2.2	Classification of runoff generation processes15
2.3	Rainfall, runoff, infiltration and surface storage during a natural rainstorm.....19
2.4	Schematic of a watershed discretization and associated flow network in sub-watershed (left) and in grid-based artificial units (right).....24
2.5	Rainfall-runoff models using effective rainfall..... 26
2.6	Rainfall-runoff model using a surface water budget 26

LIST OF FIGURES (Continued)

Figure	Page
2.7 Flood prediction process	29
2.8 Relationship of runoff to rainfall in SCS method	32
2.9 Hydrological cycle	32
2.10 The components of flood risk	50
2.11 The reduction of flood risk.....	50
3.1 Conceptual framework of the research methodology and processes.....	58
3.2 Upper Mun river basin.....	59
3.3 DEM of Lam Takong basin	61
3.4 Land use of Lam Takong basin	61
3.5 Stream network of Lam Takong basin.....	62
3.6 Hydrological and geological station of Lam Takong basin.....	62
4.1 Conceptual description of the hydrological processes in hillslope pixels	71
4.2 Schematic diagram of the pixel-based model structure of single soil column.....	75
4.3 Multi inflow directions upstream of pixel E and only one outflow direction from pixel E depending on its elevation (100).	78

LIST OF FIGURES (Continued)

Figure	Page
4.4	Estimation of Hortonian overland flow based on Green-Ampt equation.....80
4.5	Water balance of input and output water from a pixel82
4.6	Output hydrograph form pixels based on combination of pixel and channel routing processes84
5.1	The boundary and location of the study area (a) Nakhon Ratchasima Province (b) Nakhon Ratchasima Municipality.....92
5.2	Land use of Nakhon Ratchasima Municipality93
5.3	DEM of Nakhon Ratchasima Municipality.....93
5.4	Flowchart of the study step, which is a conceptual framework of this study.....94
5.5	The 2010 surveyed point of flooding of Nakhon Ratchasima Municipality.....96
5.6	Comparison of Rating curve between calculated and simulated.100
5.7	Simulated flood hazard area at the return periods (a) T=5 years, (b) T=10 years, (c) T=15 years, (d) T=25 years, (e) T=50 years and (f) T=100 years.....102
5.8	Comparison of flood depth between surveyed flood and simulated flood.....105
5.9	Adjusted hydrograph in 2010 flood event at M.164105

LIST OF FIGURES (Continued)

Figure	Page
6.1	Flowchart of the study step for flood risk mapping.....113
6.2	Simulated Rating curve at M164.....113
6.3	Generated runoff hydrograph for T=50 years (2010 flood event).....114
6.4	Land use in 2012 Map of Nakhon Ratchasima Municipality115
6.5	Land use in 2017 Map of Nakhon Ratchasima Municipality115
6.6	The components of flood risk.....117
6.7	The reduction of flood risk118
6.8	The model structure in the flood risk application tool.....122
6.9	The flood risk application tool is applied in ArcGIS.....123
6.10	The 2022 Land use map of Nakhon Ratchasima Municipality.....124
6.11	The 2022 classification of simulated flood depth at the return periods 50 years based on risk rating scale for Nakhon Ratchasima Municipality.....125
6.12	The 2022 classification of simulated flood velocity at the return periods 50 years based on risk rating scale for Nakhon Ratchasima Municipality126
6.13	The 2012 Flood Risk Map of Nakhon Ratchasima Municipality.....130
6.14	The 2017 Flood Risk Map of Nakhon Ratchasima Municipality.....130
6.15	The 2022 Flood Risk Map of Nakhon Ratchasima Municipality.....131
6.16	The 2022 Flood Risk Map with 2017 avail photo of Nakhon Ratchasima Municipality.....133

CHAPTER I

INTRODUCTION

1.1 Problem background and importance of the study

The worst flood in five decades in Thailand occurred in 2011. It began in late July by the rainfall of tropical storm Nock-ten, flood water moved through the provinces of Northern and Central Thailand along the Mekong and Chao Phraya river basins. By October flood water reached the Chao Phraya river and inundated parts of the capital city of Bangkok. Figure 1.1 showed flood inundated area in Ayutthaya and Pathum Thani Provinces in Central Thailand on 23 October 2011 (right), compared to before the flooding on 11 July 2011 (left). In October, the Chao Phraya River had overflowed onto nearby floodplains, especially southwest of the river. Paddy fields, roads, and buildings had all been submerged by flood water. Fast flooding and flood water persevered inundation in some areas lasted until mid-January 2012. The flood resulted in a total of 815 deaths (with 3 missing) and 13.6 million people affected. Sixty-five of Thailand's 77 provinces were declared flood disaster zones, and over 20,000 square kilometers of farmland was damaged (Emergency Operation Center for Flood, 2012). The World Bank estimated that the economic loss exceeded 1,425 billion baht. Most of these were manufacturing industries, as seven major industrial estates were inundated by as much 3 meters depth during the floods (World Bank, 2011). Disruptions of manufacturing supply chains affected regional automobile production and caused a global shortage of hard disk drives which lasted throughout

2012. Thai government was unprepared for the long duration and severity of the floods, and many communities felt that the Flood Response Operation Center (FROC), which was established to coordinate emergency rescue and provide regular communications to the public, was inadequate. The Thai Government was blamed by the public that decision making on flood water management had done was carried out based on political interest and without reliable projection of flood inundated area for flood warning.



(a) 11 July 2011

(b) 23 October 2011

Figure 1.1 Satellite images of the 2011 flooding in Ayutthaya and Pathum Thani Provinces (NASA Earth Observatory, 2011)

Peak floods often occur with a frequency results in loss life and property, agricultures and industries. In 2010, Nakhon Ratchasima province located in the upper Mun River basin as shown in figure 1.2, received excessive rainfall in successive during day 14 – 16 October 2010. Majority of floodplain area in Nakhon Ratchasima province suffered from this serious flooding event. Heavy rains caused large amount of runoff flow into both upstream and downstream of all reservoirs in Nakhon Ratchasima province including Lamtakong and Lamphrapkloeng Dams. With ongoing water flowing into these reservoirs until excess it capacity, the water level was higher than the level of emergency service spillway which in turn caused severe uncontrolled flood flow into many municipalities downstream. Moreover, most of the rain could not be retarded by wetland, water then flow rapidly over lands into canals and combined with overflow water from many dams. The combination of these events caused widespread flooding on floodplain in lower basin including Muang Nakhon ratchasima district, Pukthongchai district and Chaloemphrakiat district etc. Flood water from tributary of Mun River was drained slowly into Mun River because the water level in Mun River was higher than the water level in tributary's canals and there are a lot of obstructions in the canal which resulted in reduce flow speed.

There are two types of flood protection methods to alleviate flood: (1) structural measures and (2) non-structural measures. The structural measures are a hard tool for flood control use levees and floodwalls, by-pass floodways, retarding basins and flood storage area, flood mitigation reservoirs and drainage systems modifications etc. to reduce flood peaks. The non-structural measures are a soft tool for flood management, including of land use management, flood forecasting and flood warning etc. Both measures should be used together to mitigate disaster efficiently.

After flood disaster in year 2011, there are a number of adhoc organizations were established by government. GISTDA (Geo-Informatics and Space Technology Development Agency) is a public organization under the Ministry of Science and Technology. GISTDA provides the satellite image archive for the Emergency Operation Center for Flood, Storm and Landslide (EOC). The EOC supports broad aspect of information for situation monitoring and evaluation to the provincial Flood Relief Operations Center (FROC). GISTDA not only supplies daily information from satellite images about the flooded areas but also sending experts in geo-informatics technology to help analyze satellites images, GISTDA also derives flood maps for other agencies working under FROC. Flood map can present spatial data of inundation area and expansion of flood boundary. However, it cannot evaluate flood depth and flood duration. In order to protect or at least mitigate the effect of flooding problems, physical characteristic of inundation area combine with consequent impact have to be defined in the form of a flood risk map. The flood risk map will help the responsible authorities to target on the area with higher risk where flood mitigation plan have to be effectively implemented. Flood map and flood risk map will give public tangible imagery of its impaction the flood on their community.



Figure 1.2 Boundary and location of Nakhon Ratchasima Province and upper Mun River Basin.

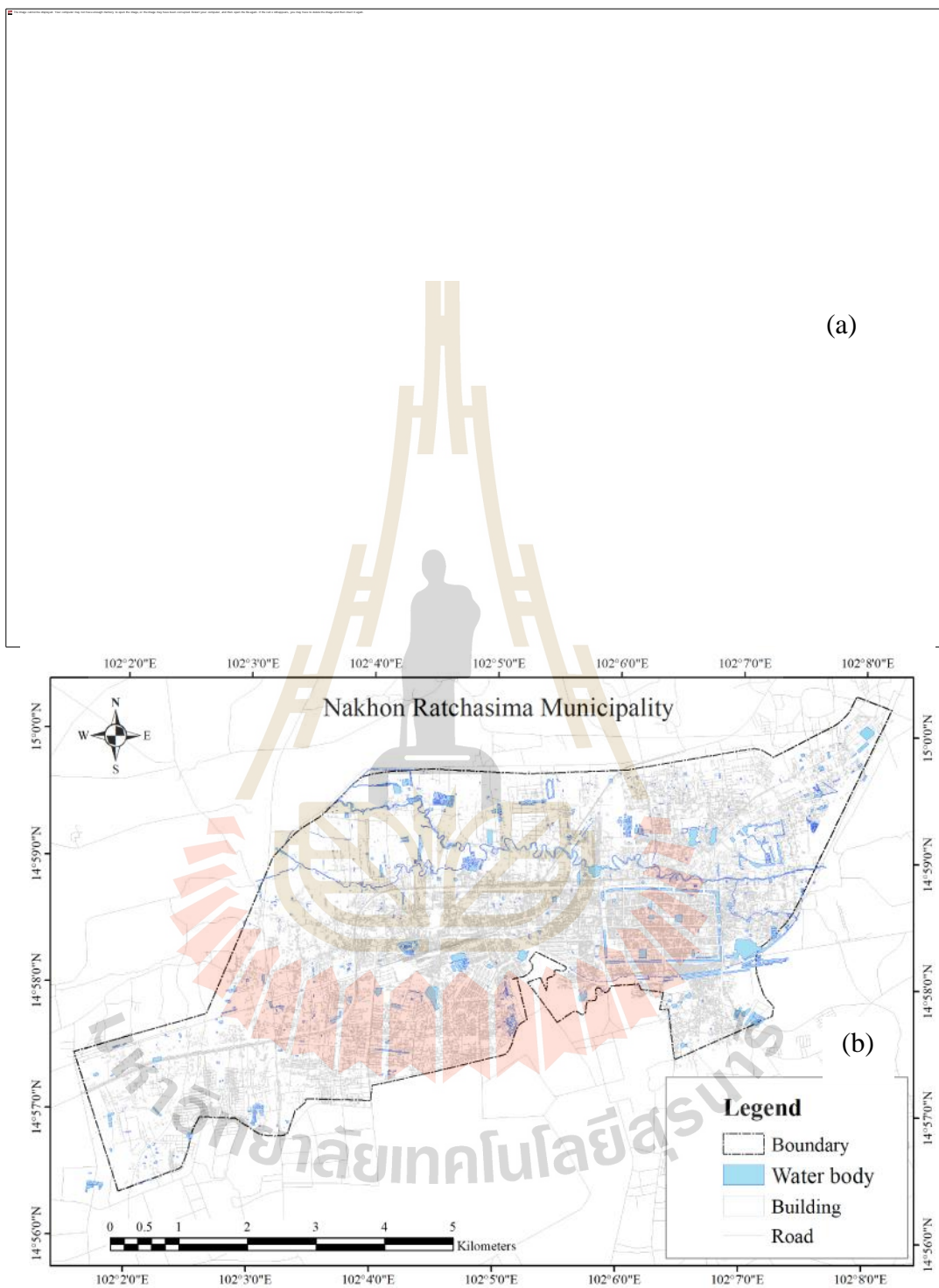


Figure 1.3 The boundary and location of the study area (a) Nakhon Ratchasima Province (b) Nakhon Ratchasima Municipality

1.2 Research objectives

Nakhon Ratchasima Municipality show in Figure 1.3 is located at the downstream of the Lam Ta Kong River as the urban center of Nakhon Ratchasima Province. There has suffered from flooding in 1978, 1996, 2002 and 2010 (Weeraya and Jirawat, 2012). Thus, the objectives of this study are as follows :

1.2.1 Collect historical flood extent and delineate observed flood map in the Nakhon Ratchasima Municipality, particularly, past flood in 2010.

1.2.2 Develop the simple distributed model that could investigate the combined effect of climate, soil, vegetation and topography on the runoff generation processes at the catchment scale in a quantitative way.

1.2.3 Construct a flood hazard map from available observed flood map of the small flood affected area with specified return periods.

1.2.4 Understand flood behavior in urban area and to improve the accuracy of recorded flood map.

1.2.5 Derive flood risk maps based on different future flooding scenarios including various measures of flood protection system land use change.

1.2.6 Develop an application tool in ArcGIS to generate flood risk map.

1.3 Scope and limitations of study

1.3.1 Study area is the Nakhon Ratchasima Municipality in Nakhon Ratchasima Province, Thailand. Upstream and downstream boundary are Khon Chum Watergates and Khoi Ngam Watergates, respectively.

1.3.2 HEC-RAS V.5 as a hybrid 1D2D model is used to quantified flood extent, depth and velocity. Flood map simulation are considered as steady flow at the observed station (M.164) for return period of 5, 10, 15, 25, 50 and 100 years.

1.3.3 The Topographic map with scale 1:50,000 (L7018 WGS84) is obtained from the Royal Thai Survey Department (RTSD) .

1.3.4 The Digital Elevation Model (DEM) 5x5 m² resolution is obtained from the Land Development Department (LDD) in the year 2008.

1.3.5 The soil data is collected from the Land Development Department (LDD) and the Department of Groundwater Resources (DGR).

1.3.6 The rainfall data and the weather data are provided by the Thai Meteorological Department (TMD) between the years 1982-2013. There are 23 rainfall stations and 6 weather stations.

1.3.7 The runoff data is provided by the Royal Irrigation Department (RID) between the years 1982-2013 for 12 stations.

1.4 Benefit of study

1.4.1 Observed flood map with precise information (i.e. area, depth, duration) can be used to understand flood behavior in urban area and to improve the accuracy of recorded flood map from satellite images.

1.4.2 Flood risk map can be identified and utilized as a tool for flood preparedness planning, flood mitigation, and flood risk management.

1.5 Thesis structure

The thesis is divided into 7 chapters Chapter I to VII are as follows:

Chapter I “Introduction” present the problem background and importance of the study, research objective, scope and limitation of study, benefits of study and thesis structure.

Chapter II “Basic concepts and literature review” consists of the descriptions of flooding and flood map, hydraulic model and literature reviews.

Chapter III “Data and methodology” summarize about collected data, surveyed data and description of methodology.

Chapter IV “The development of a simple distributed hydrological model based on up-scaling from pixel to catchment scale”

Chapter V “Flood hazard mapping using on-site surveyed flood map, HEC-RAS V.5 and GIS tool: a case study of Nakhon Ratchasima Municipality, Thailand”

Chapter VI “The development of a GIS tool application for flood risk mapping: a case study of Nakhon Ratchasima Municipality, Thailand”

Chapter VII “Conclusion and Recommendation” contains conclusion of the study and recommendations.

1.6 References

Emergency Operation Center for Flood, Storm and Landslide (2012). **Flood, storm and landslide situation report**. Retrieved 25 January 2012 (in Thai)

NASA Earth Observatory (2011). **2011 flooding in Ayutthaya Province-EO-1 merged** [Online]. Available:http://upload.wikimedia.org/wikipedia/commons/e/ec/2011_flooding_in_Ayutthaya_Province-EO-1_merged.jpg. [Accessed: 15 November 2013]

Weeraya,. M. and Jirawat, K. (2012). **The study of flood relief measures of upper Mun River Basin in Nakhon Ratchasima by Mike 11 Model**. In The 10th National Kasetsart University Kamphaeng Saen Conference, December 6-7, Kasetsart University Kamphaen, Nakhon Pathom.

World Bank (2011). **The World Bank Supports Thailand's Post-Floods Recovery Effort** [online]. Available: <http://www.worldbank.org/en/news/feature/2011/12/13/world-bank-supports-thailands-post-floods-recovery-effort>. [Accessed: 15 November 2013]

CHAPTER II

BASIC CONCEPTS AND LITERATURE REVIEW

This chapter summarizes the results of literature review carried out to understanding of the flood phenomenon, concepts of the flood risk model, which include recent research results and application of the flood risk map.

2.1 Introduction

Since the prehistoric times, floods interactions have evolved include a version to flood risk, flood defense and flood risk management, all serve as mindset or a paradigm. Flood is a general and temporary condition of partial or complete inundation of normally dry land from overflow of inland or tidal waters from the unusual and rapid accumulation or runoff of surface waters from any source. The impacts of major floods may considerably increase in the future, since society is becoming more vulnerable to the damage and disruption caused by floods, and because floods may become more serious and more frequent due to climatic changes.

Flood can be defined as an overflow, or accumulation, of substantial water volume that inundates the land (which is not normally submerged). Floods are well-known natural hazard that sometimes can lead to devastated consequences like loss of human lives or costly damage to the properties. In general, floods can be divided into 5 main types, which are (Ghosh, S.N., 2006) :

1. *River flood* is the major cause of flooding extensive areas as a result of heavy rains in the catchment areas as well as local areas thereby increasing the river level.

2. *Flash flood* occur due to heavy rain in hilly areas which cause local rivers and small streams to rise to dangerous level within a short period of time (6-12 hours). Heavy and continuous rains in local areas can cause flash floods.

3. *Urban flood* occur due to local heavy rain up to 100 mm or more in a day over the city and larger towns can cause damaging and disruptive flooding due to poor drainage and rapid runoff.

4. *Strom surge or tidal flooding* occurs during tropical disturbances, developing to cyclones and crossing surrounding coastlines. Cyclone induced storm surges have devastating consequences in coastal areas and such surge induced floods may extend many kilometers inland.

5. *Floods arising due to failure of dam* is the large number of large and small dams are constructed to store water for various purposes. Due to poor maintenance and due to exceptionally high precipitation, a severe flood may result causing failure of the dam. This causes a surging water front travelling with high velocity causing destruction of properties and loss of life.

Primary effects of flooding are physical damage to properties, buildings, roads, and to natural resources, due to the drowning and subsequence epidemics or water-borne diseases. Its secondary effects include, water-supply contamination, spread of the water-borne diseases, diminishing of crop supply. Moreover, flooding can cause long-term effect by corrupting natural resources and fertility of the ecosystem along with sustainable use of fertile land. High cost for recovering of the severely-damaged buildings, infrastructure and human illness is also a concerned issue.

2.2 Runoff generation processes

The rainfall – runoff question is also at the heart of the interface linking meteorology and hydrology. The temporal and spatial scales associated with surface water inputs, given as output from meteorological processes have profound effects on the hydrological processes that partition water inputs at the earth surface. High intensity short duration rainfall is much more likely to exceed the capacity of the soil to infiltrate water and result in overland flow than a longer less intense rainfall. A cross section (Figure 2.1) through a hillslope that demonstrate in detail of the pathways infiltrated water. Infiltrated water may flow through the matrix of the soil in the inter-granular pores and small structural voids. Infiltrated water may also flow through larger voids referred to as macropores. Macropores include pipes that are open passageways in the soil caused by decaying roots and burrowing animals. Macropores also include larger structural voids within the soil matrix that serve as preferential pathways for subsurface flow. The permeability of the soil matrix may differ between soil horizons and this may lead to the buildup of a saturated wedge above a soil horizon interface. Water in these saturated wedges may flow laterally through the soil matrix or enter macropores and be carried rapidly to the stream as subsurface storm flow in the form of interflow.

With background on the pathways followed by infiltrated water can inspect the processes involved in the generation of runoff (Figure 2.2). Each process has a different response to rainfall or snowmelt in the volume of runoff produced, the peak discharge rate, and the timing of contributions to stream flow in the channel. The relative importance of each process is affected by climate, geology, topography, soil

characteristics, vegetation, and land use. The dominant process may vary between large and small storms.

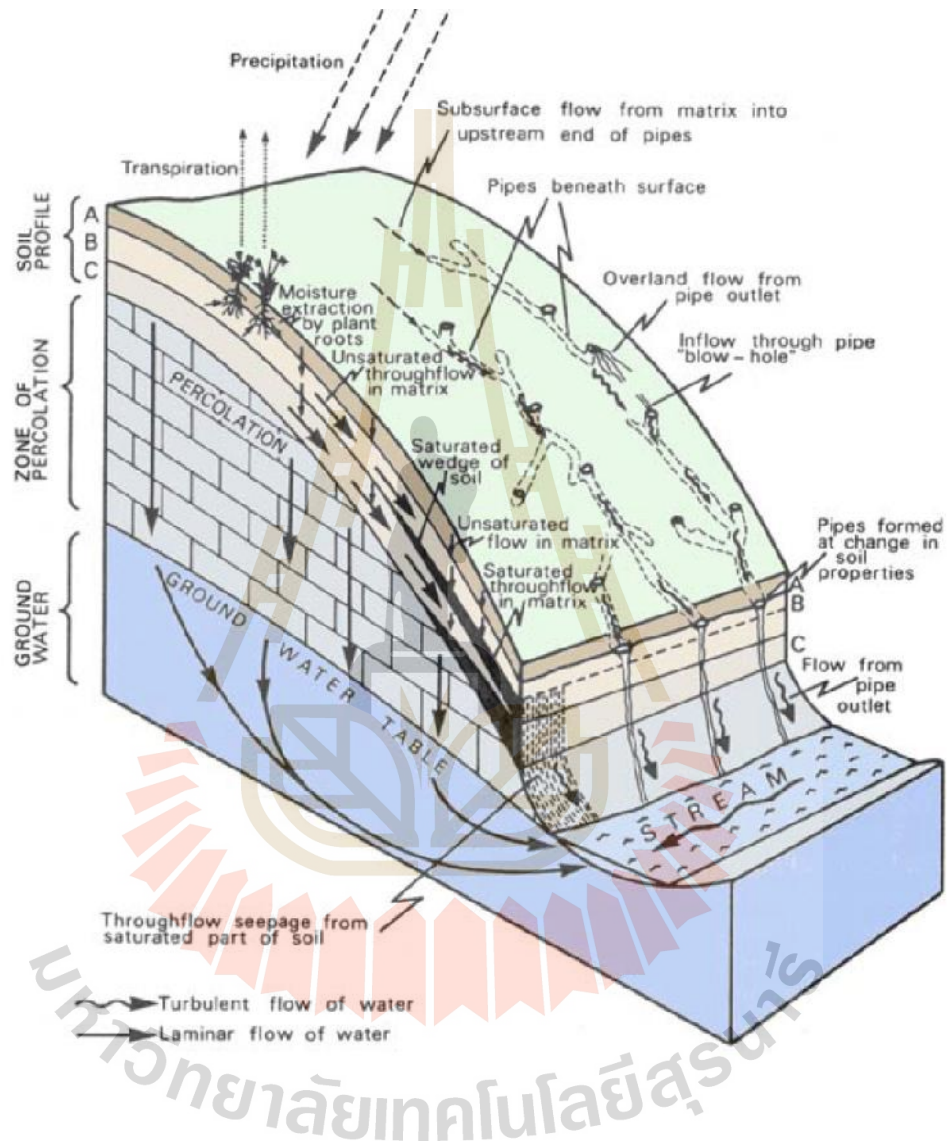


Figure 2.1 Pathway Pathways followed by subsurface runoff on hillslopes

(Tarboton, D.G., 2003)

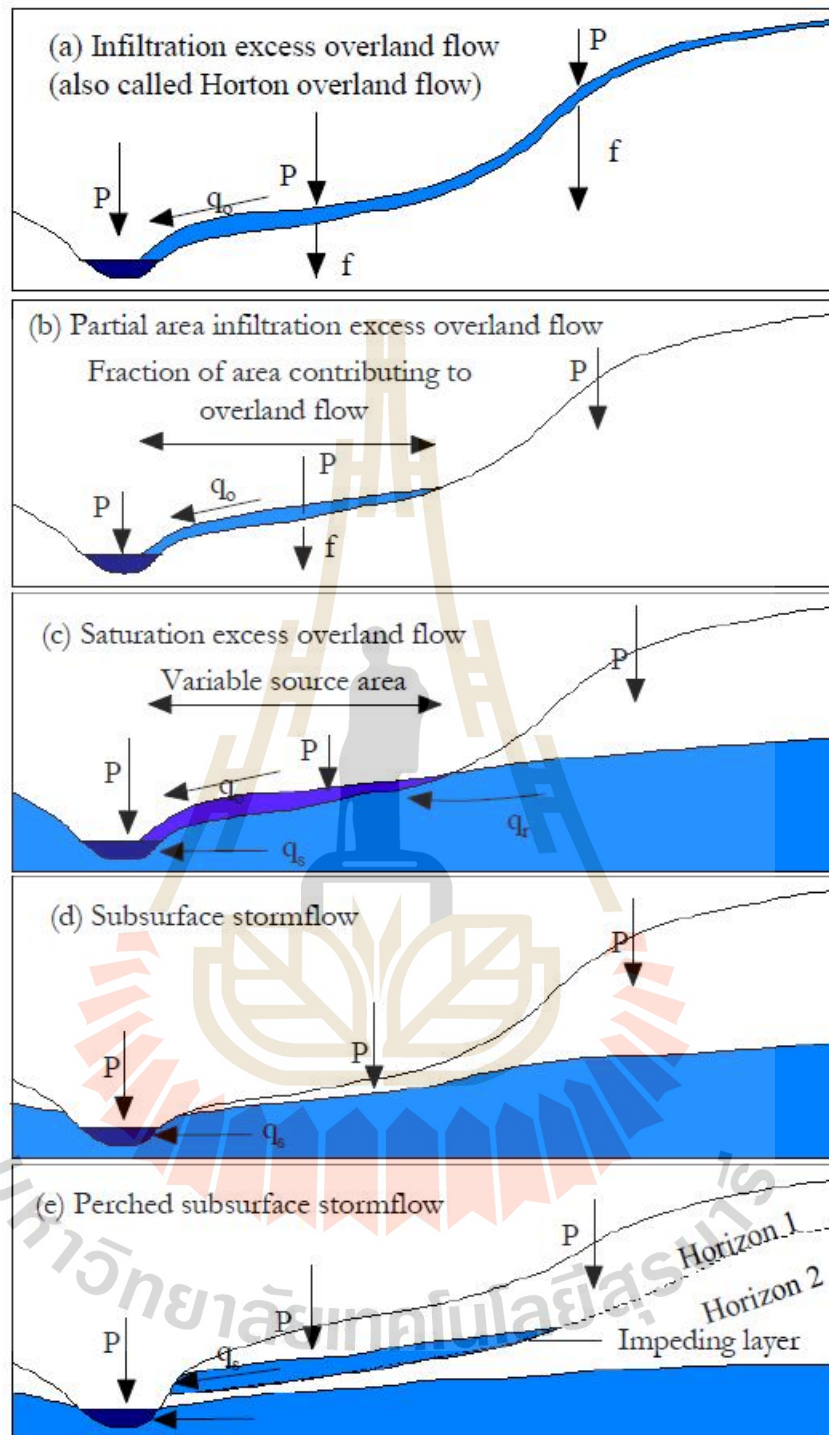


Figure 2.2 Classification of runoff generation processes (Beven, 2000)

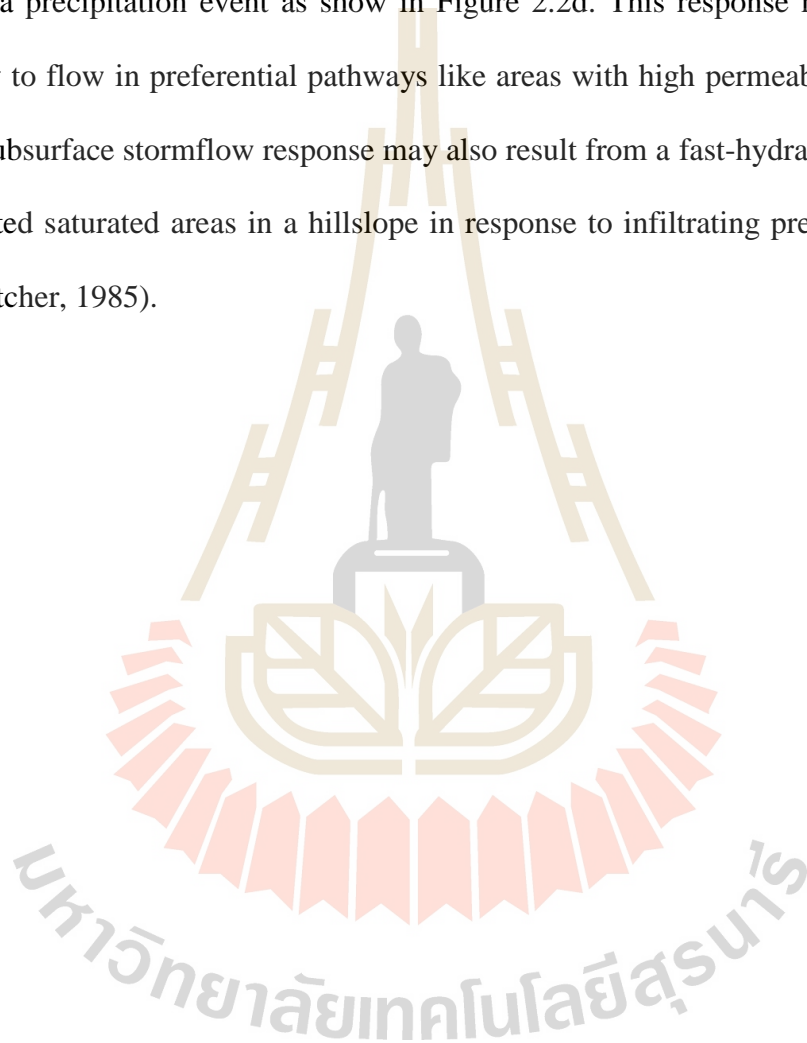
The infiltration excess overland flow processes is illustrated in Figure 2.2a. There is a maximum limiting rate at which a soil in a given condition can absorb surface water input. This process called “Horton” overland flow, named after one of the founding fathers of quantitative hydrology. As the infiltration capacity of the soil, infiltration capacity is also referred to as infiltrability. When surface water input exceeds infiltration capacity the excess water accumulates on the soil surface and fills small depressions. Water in depression storage does not directly contribute to overland flow runoff; it either evaporates or infiltrates later. With continued surface water input, the depression storage capacity is filled, and water spills over to run down slope as an irregular sheet or to converge into rivulets of overland flow. The amount of water stored on the hillside in the process of flowing down slope is called surface detention. The transition from depression storage to surface detention and overland flow is not sharp, because some depressions may fill and contribute to overland flow before others. Figure 2.3 illustrates the response, in terms of runoff from a hillside plot due to rainfall rate exceeding infiltration capacity with the filling of depression storage and increase in, and draining of, water in surface detention during a storm. Note, in Figure 2.3, that infiltration capacity declines during the storm, due to the pores being filled with water reducing the capillary forces drawing water into pores. Due to spatial variability of the soil properties affecting infiltration capacity and due to spatial variability of surface water inputs, infiltration excess runoff does not necessarily occur over a whole drainage basin during a storm or surface water input event. Betson (1964) pointed out that the area contributing to infiltration excess runoff may only be a small portion of the watershed. This idea has

become known as the partial-area concept of infiltration excess overland flow and is illustrated in Figure 2.2b.

Infiltration excess overland flow occurs anywhere that surface water input exceeds the infiltration capacity of the surface. This occurs most frequently in areas devoid of vegetation or possessing only a thin cover. Semi-arid rangelands and cultivated fields in regions with high rainfall intensity are places where this process can be observed. It can also be seen where the soil has been compacted or topsoil removed. Infiltration excess overland flow is particularly obvious on paved urban areas. In most humid regions infiltration capacities are high because vegetation protects the soil from rain-packing and dispersal, and because the supply of humus and the activity of micro fauna create an open soil structure. Under such conditions surface water input intensities generally do not exceed infiltration capacities and infiltration excess runoff is rare.

Overland flow can occur due to surface water input on areas that are already saturated. This is referred to as saturation excess overland flow, illustrated in Figure 2.2c. Saturation excess overland flow occurs in locations where infiltrating water completely saturates the soil profile until there is no space for any further water to infiltrate. The complete saturation of a soil profile resulting in the water table rising to the surface is referred to as saturation from below. Once saturation from below occurs at a location all further surface water input at that location becomes overland flow runoff.

Subsurface stormflow is a runoff producing mechanism operating in most upland terrains. Subsurface stormflow describes a runoff generation processes in the hillslope close to the soil surface that result in a stream channel hydrograph response during a precipitation event as show in Figure 2.2d. This response may be coupled directly to flow in preferential pathways like areas with high permeability. However, rapid subsurface stormflow response may also result from a fast-hydraulic response of connected saturated areas in a hillslope in response to infiltrating precipitation (Burt and Butcher, 1985).



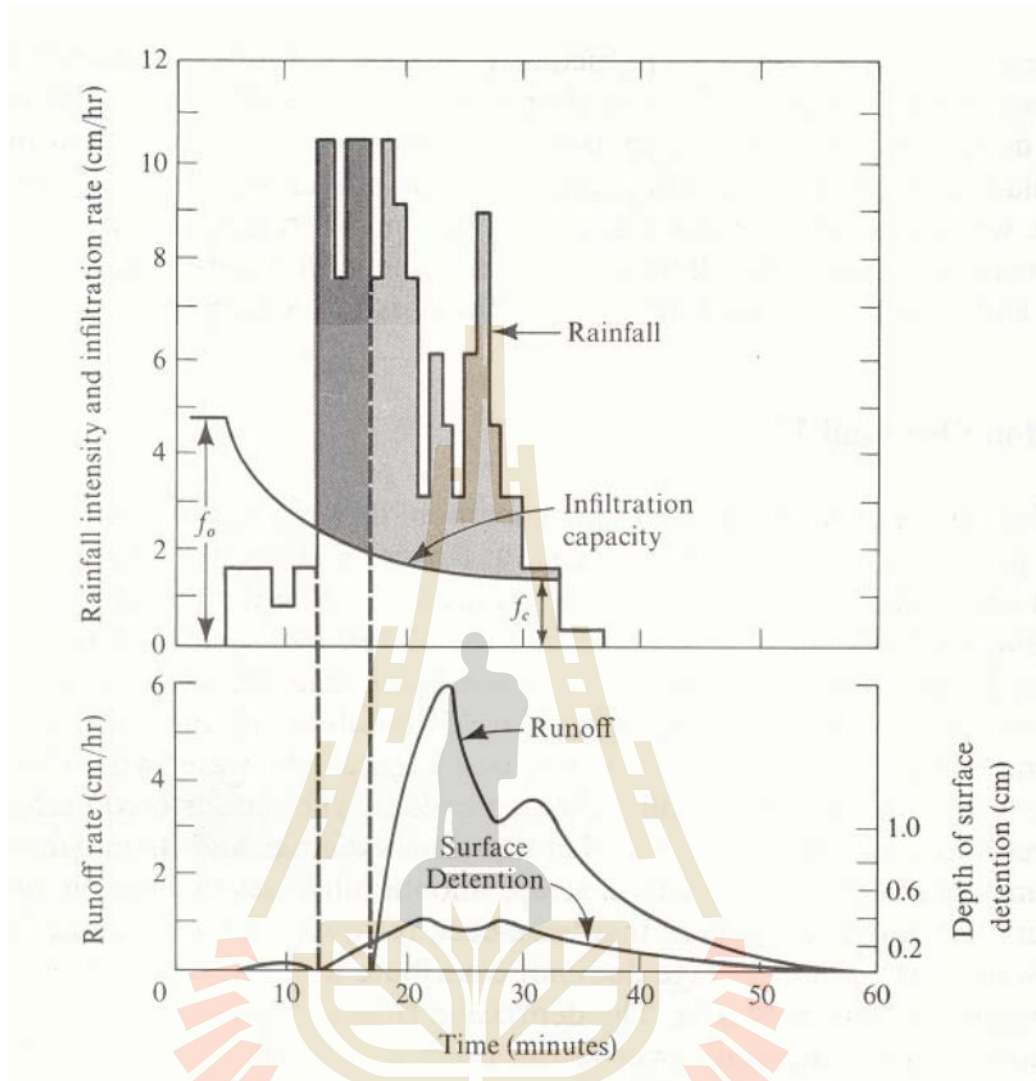


Figure 2.3 Rainfall, runoff, infiltration and surface storage during a natural rainstorm (Dunne and Leopold, 1978)

A hydrologic model was used development by Jothityangkoon et al (2001).

The water balance equation for revised, single bucket model is as follows:

$$\frac{ds(t)}{dt} = p(t) - q_{ss}(t) - q_{se}(t) - e_b(t) - e_v(t) \quad (2.1)$$

where $s(t)$ is the volume of soil moisture storage, $p(t)$ is the rainfall input rate, $q_{ss}(t)$ is subsurface runoff, $q_{se}(t)$ is saturation excess runoff rate, $e_b(t)$ is bare soil evaporation rate and $e_v(t)$ is the transpiration rate. Details of the four outflow rates (ones with a negative sign on the right hand side of Eq. 2.1) can be described as follows:

Subsurface runoff

The subsurface runoff term, q_{ss} , was determined using the relation:

$$q_{ss} = \frac{(s - s_f)}{t_c} \quad \text{if } s > s_f \quad (2.2a)$$

$$q_{ss} = 0 \quad \text{if } s < s_f \quad (2.2b)$$

Where s_f is the soil-moisture storage at field capacity, and t_c is a catchment response time with respect to the subsurface flow. The threshold storage, s_f , is assumed to be equal to $S_f = f_c D$, where f_c is soil's field capacity, and D is average effective soil depth. The reason for the use of field capacity is that often when the moisture content is less than the field capacity, capillary forces are larger than those of gravity and drainage is prevented.

In theory, the catchment response time, t_c , defines average traveling time of the induced runoff within the catchment to reach catchment's outlet. For the subsurface flow, this value can be estimated by the Darcy's law for idealized triangular representation of the unconfined aquifer within a hillslope, assuming that the hydraulic gradient can be approximated by slope of ground surface. This gives:

$$t_c = \frac{LW}{2K_s \tan S} \quad (2.3)$$

where W is the average soil porosity, L is the average hill slope length, $\tan S$ is the average ground surface slope, K_s is the average saturated hydraulic conductivity. However, due to the lack of necessary data, especially the hydraulic conductivity, for performing direct calculation of t_c from Eq. 2.3, its proper value was calibrated to provide the best fit of the simulated discharge to the observed one.

Saturation excess runoff rate

Similarly, the surface runoff term, $q_{se}(t)$, was determined using the relation:

$$q_{se} = (s - S_b) / \Delta t \quad \text{if} \quad s > S_b \quad (2.4a)$$

$$q_{se} = 0 \quad \text{if} \quad s < S_b \quad (2.4b)$$

where S_b is the bucket's soil-moisture storage capacity, given by $S_b = wD$ where w is the average soil porosity, and Δt is the time interval. Eq. 2.4 indicates that the excess surface runoff exists if amount of soil moisture storage is higher than bucket's soil-moisture storage capacity only, otherwise this term will be zero.

Bare soil evaporation rate

The evaporation term, e_b , was estimated through the relation:

$$e_b = \frac{s}{t_e} \quad (2.5)$$

$$t_e = \frac{S_b}{(1-M)e_p} \quad (2.6)$$

where t_e is a characteristic time scale associated with bare soil evaporation, estimated using Eq. 2.6, e_p is potential evaporation rate, and M is fraction of forest vegetation cover. In the original lumped model, M can vary between 0 and 1 as the forest cover can vary significantly basin to basin.

Transpiration rate

$$e_v = Mk_v e_p \quad \text{if} \quad s > s_f \quad (2.7a)$$

$$e_v = \frac{s_f}{t_g} \quad \text{if} \quad s < s_f \quad (2.7b)$$

$$t_g = \frac{s_f}{Mk_v e_p} \quad (2.8)$$

where t_g is a characteristic time scale associated with the transpiration and k_v is a plant transpiration efficiency.

2.3 Hydrologic model

2.3.1 Type of the model

The models are simplified conceptual framework of the water balance at some specific area. Most models were developed using complicated mathematical formulation to operate mainly at basin or catchment scale. They are mostly used for hydrologic prediction and for apposite understanding of hydrologic processes and their consequences. The hydrologic models commonly used nowadays can be divided into two broad categories (Seth, 2006):

(1) *Stochastic model* generates outputs that are at least partially random produces the different output from a given input. In essence, they are black-box systems in nature as their main aim is to link certain input (for instance rainfall) to model output (for instance stream runoff) using some chosen mathematical and statistical concepts where the commonly used are regression, transfer functions, and system identification. The simplest form is the linear model, but it is common to employ non-linear components to represent some general aspects of the catchment's response without moving deeply into real physical processes that might be involved (no/little physical basis required). A well-known example is the ANN model (artificial neural network) which has the ability to model both linear and nonlinear relationships without the need to make any implicit assumptions at first.

(2) *Deterministic models*, this model does not consider randomness. A given input always produces the same output. The model's processes are developed based on definite physical laws and no uncertainties in prediction are admitted. The models are based on our understanding of physics of the hydrological processes which control catchment response and use physically-based equations to describe these

processes. They basically try to represent main physical processes observed in the real world, especially those of surface runoff, subsurface flow, evapotranspiration, and channel flow, but these can go far more complicated.

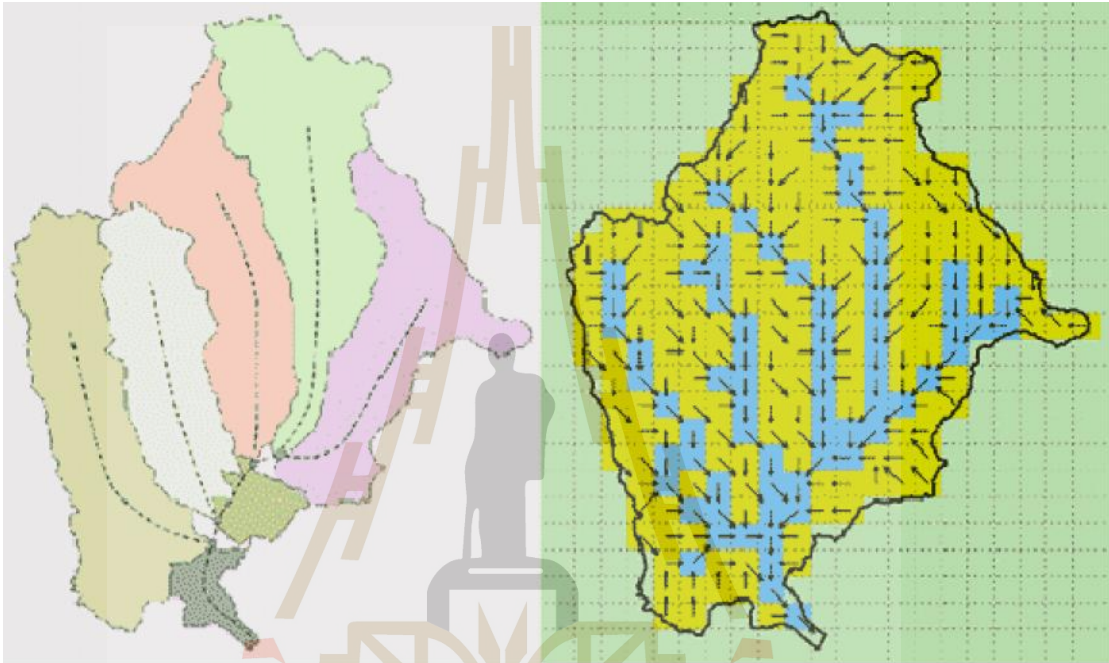


Figure 2.4 Schematic of a watershed discretization and associated flow network in sub-watershed (left) and in grid-based artificial units (right) (CRAHI, 2012).

Deterministic models can be further classified according to whether the model gives a spatially lumped or distributed description of the catchment area, and whether the description of hydrological processes is empirical, conceptual or fully physically based. Two groups of the models generally referred to in literature are (Figure 2.4) (CRAHI, 2012);

lumped model, these models conceptually assume that the transfer of water in the catchment taking place in only few well-defined storages (or lump), each of which has homogeneous property and represents a fundamental unit in the operating process (e.g. rainfall, soil characteristics, vegetation, land use practice). Though, this assumption is rarely fulfilled in reality, their concepts still provide some primary understanding in the water balance details of the examined area. These models can be regarded as in the intermediate position between the full grid-based approach and the empirical black box analysis. There are numerous lumped hydrologic models which are based on concept of a Unit Hydrograph (UH). This concept is valid within a framework which assumes that the watershed is a linear causative and time invariant system where only part of relevant excess rainfall that produces runoff.

The grid-based or distributed models, these models consider the hydrologic process that taking place within area divided into a large amount of small rectangular grids that enables them to describe the hydrologic processes with a fine resolution (e.g. 100-500 m). The equations of the processes are solved in each defined unit (grid) and combined with output from the neighbor. This structure leads to very complex models that require a great amount of information, and at least, up to present, the calibration of a tremendous amount of parameters, if not all the variables may be estimated from field data. This makes the use of the distributed models for realistic runoff forecasting is still rather difficult so far, particularly when performing in the large and heterogeneous area.

In general, the black-box model is appropriate for the preliminary study of the water balance process in the area due to its simple structure and no/little physical data of the area required. However, it gives little information about the actual process and several adjustments in the calculating algorithms might be needed just to fit the output data with the real observed ones. On the contrary, lumped model needs more physical data and knowledge of the hydrological process in the area to work properly. But its capacity is still limited to the analysis at basin/sub-basin scale only. To have model with better spatial resolution, the grid-based model is the most suitable alternative. However, the difficulties in developing such model lie in its need for huge amount of physical data and through knowledge of the hydrological process of the interested area. Therefore, it typically works well for the study in small area.

There are two strategic approaches to build the preferred hydrologic model, the downward (or top-down) and the upward (or bottom-up) approaches. As described by Klemes (1983), the downward (or top-down) approach was applied in the model's developing process. In essence, this kind of work tries to find a concept directly at the level or scale of interest (or higher) and then looks for steps that could have led to it. This is in the contrary to the upward (or bottom-up) approach which tries to combine, by mathematical synthesis, the empirical facts and theoretical knowledge available at a lower level of scale into the theories capable of predicting the response at the higher scale. As a consequence, the simple form of the preferred model will be considered and test first at the preferred scale of interest, then more complexity will be added to the original model to gain higher accuracy in the obtained result until it reaches level of accuracy required.

2.3.2 Rainfall-runoff model

The major input into the rainfall-runoff model is an estimate of rainfall and the output is an estimate of runoff. The intermediate steps that transform rainfall to runoff are the model processes. Among the hydrologic processes typically modeled are: interception, infiltration, evapotranspiration, snowpack and snowmelt, retention and detention storages, soil water movement, and filtration to ground water, overland flow, open channel flow, and subsurface flow (interflow and base flow).

Rainfall runoff models may be grouped in two general classifications that are illustrated in Figures 2.5 and 2.6. The first approach uses the concept of effective rainfall in which a loss model is assumed which divides the rainfall intensity into losses and an effective rainfall hyetograph. The effective rainfall is then used as input to a catchment model to produce the runoff hydrograph. It follows from this approach that the infiltration process ceases at the end of the storm duration. An alternative approach that might be termed a surface water budget model incorporates the loss mechanism into the catchment model. In this way, the incident rainfall hyetograph is used as input and the estimation of infiltration and other losses is made as an integral part of the calculation of runoff. This approach implies that infiltration will continue to occur as long as the average depth of excess water on the surface is finite. Clearly, this may continue after the cessation of rainfall.

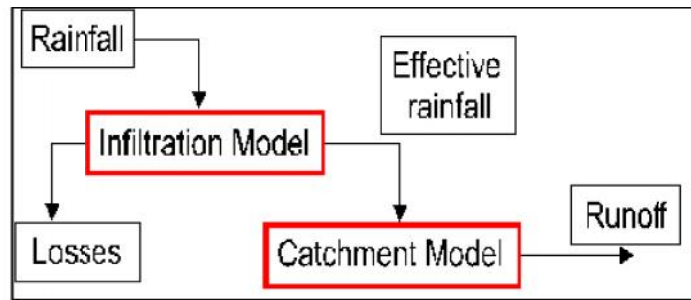


Figure 2.5 Rainfall-runoff models using effective rainfall (Alan, 2010)

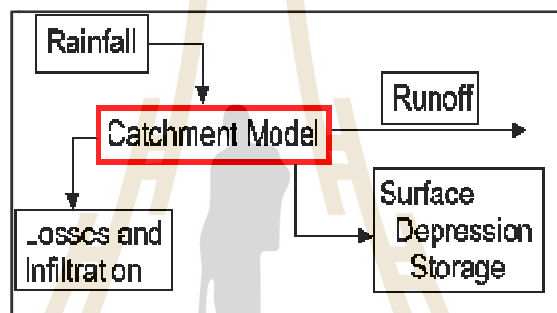


Figure 2.6 Rainfall-runoff model using a surface water budget (Alan, 2010)

Examples of the rainfall-runoff model

Unit hydrograph model

Unit hydrograph shows the temporal change in flow per unit of runoff.

The unit hydrograph is a useful tool in the process of predicting the impact of precipitation on streamflow. The role of unit hydrograph theory in the flood prediction process (Figure 2.7) is to provide an estimate of streamflow given an amount precipitation. The Unit Hydrograph provides us with a way to estimate runoff, and is an integral part of many hydrologic modeling systems.

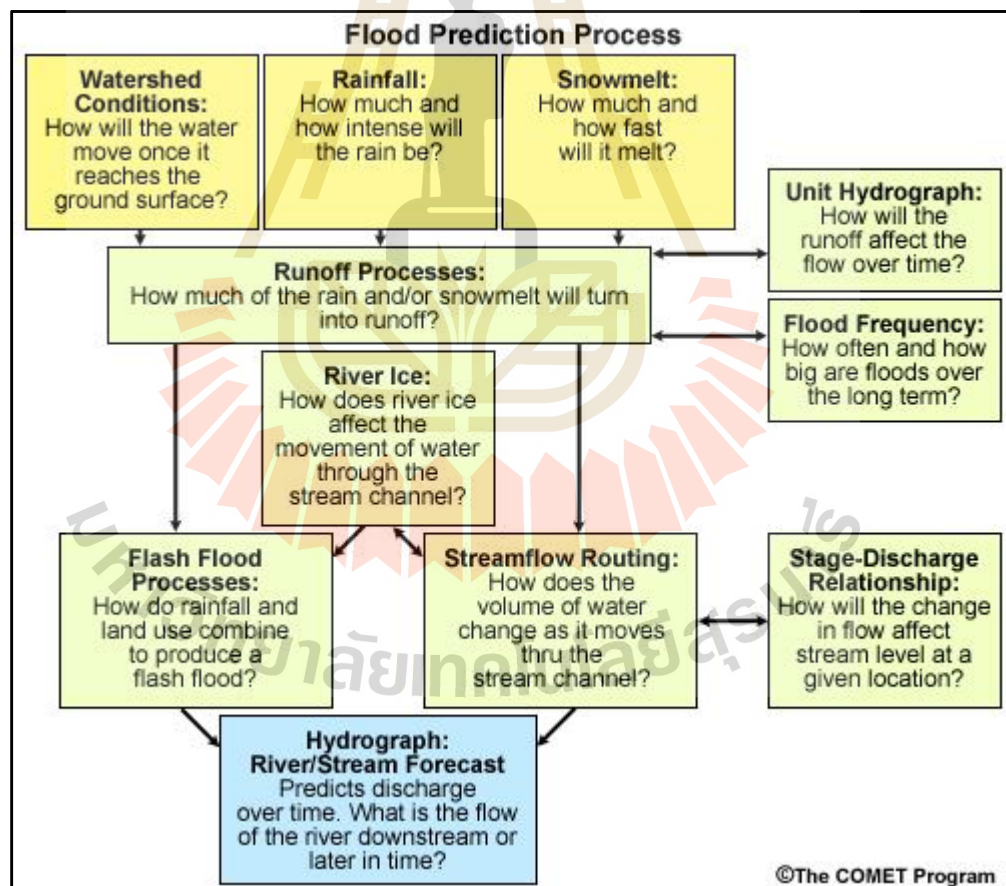


Figure 2.7 Flood prediction process (NOAA National Weather Service (NWS), 2010)

Curve Number model

The Curve Number (CN) method was developed to estimate total storm runoff from total storm rainfall. This method estimates direct runoff, which consists of channel runoff, surface runoff, and unknown proportion subsurface runoff. Generally, the CN method is well suited for small watershed (Tekeli et al., 2007). In contrast, it is not restricted to use for only small watersheds. It can be applied equally well to other large areas if the geographic variations of storm rainfall, soil, and land use are taken into account. So that with increasing availability of finer spatial resolution information from remote sensing data on land use, it is possible to use CN method for large areas with better accuracy (Chatterjee et al., 2001).

The model was developed to provide a consistent basis for estimating the amounts of runoff under varying land use and soil types (Rallison and Miller, 1981).

The SCS curve number equation is (Soil Conservation Service, 1972)

$$Q_{surf} = \frac{(R_{day} - I_a)^2}{(R_{day} - I_a + S)} \quad (2.9)$$

Where Q_{surf} is the accumulated runoff or rainfall excess (mm.H₂O),

R_{day} is the rainfall depth for the day (mm.H₂O), I_a is the initial abstractions which includes surface storage, interception and infiltration prior to runoff (mm.H₂O) and S is the retention parameter (mm.H₂O).

The retention parameter varies spatially due to changes in soils, land use, management and slope and temporally due to changes in soil water content. The retention parameter is defined as:

$$S = 25.4 \left[\frac{1000}{CN} - 10 \right] \quad (2.10)$$

Where CN is the curve number for the day. The initial abstractions, I_a is commonly approximated as $0.2S$ and equation 2.9 becomes:

$$Q_{surf} = \frac{(R_{day} - 0.2S)^2}{(R_{day} - 0.8S)} \quad (2.11)$$

Runoff will only occur when $R_{day} > I_a$. A graphical solution of equation 2.11 for different curve number values is presented in Figure 2.8.

มหาวิทยาลัยเทคโนโลยีสุรนารี

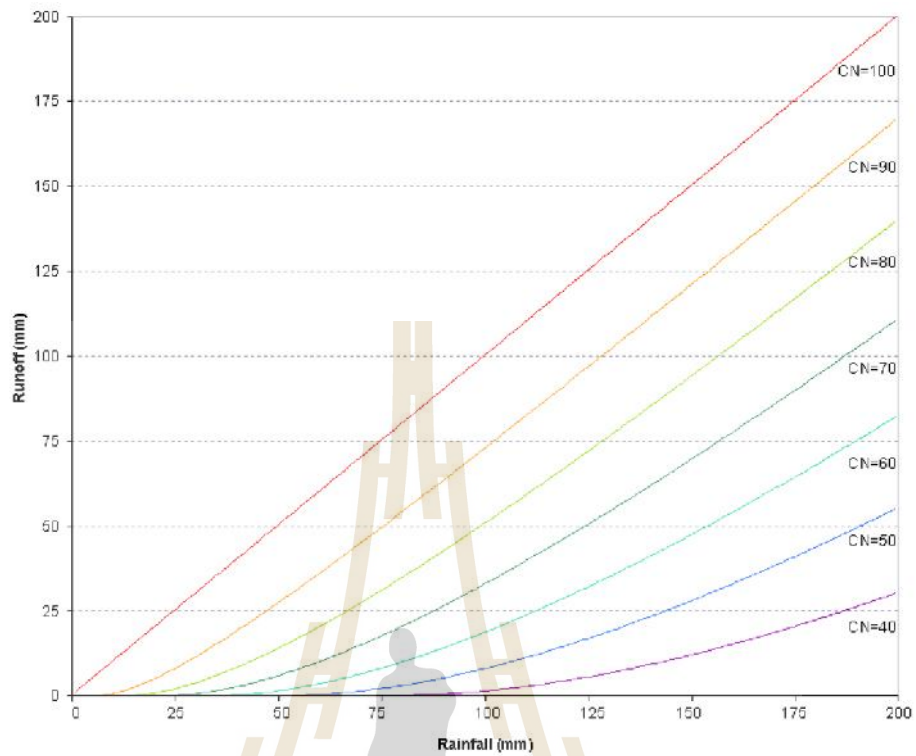


Figure 2.8 Relationship of runoff to rainfall in SCS method (Neitsch et al., 2011)

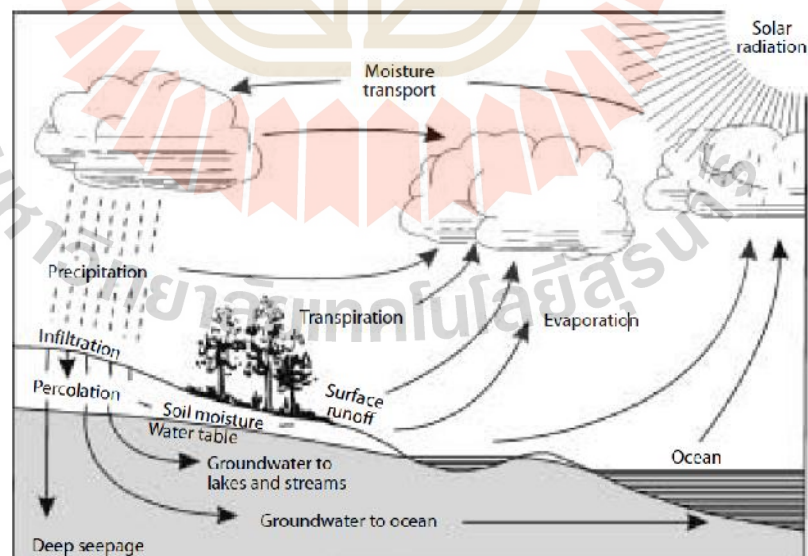


Figure 2.9 Hydrological cycle (Zhang, 2002)

2.3.3 Water balance concept

The natural occurrence of water circulation near the surface of the earth, the hydrological cycle is illustrated in Figure 2.9. The movement of water through the hydrological cycle varies significantly in both time and space. The hydrological cycle emphasizes the four phases: precipitation, evapotranspiration, surface runoff and groundwater. Water balance is based on the law of conservation of mass: any change in the water content of a given soil volume during a specified period must equal the difference between the amount of water added to the soil volume and the amount of water withdrawn from it. In principle, a water balance can be computed for any soil volume, ranging from a small sample of soil to an entire catchment.

When the control volume is the entire catchment, the surface water balance equation can be expressed as:

$$\Delta S = P - Q - ET - R \quad (2.12)$$

where ΔS is the change in spatially averaged catchment water storage, P is the spatially averaged precipitation, Q is the spatially averaged catchment surface runoff, ET is the spatially averaged evapotranspiration and R is the spatially averaged catchment recharge.

The water balance model in Eq. 2.12 is applied to determine amount of the total overland surface runoff over each considered unit area under the prior input data. It then simulates the runoff movement to the neighboring land units before finding its way to the stream channel situated nearby. Flow pattern of the existing

surface runoff usually determined by the topographic elements of the area, especially surface slope and aspect. Primary output from the hydrologic model is hydrographs at varying locations along the waterways to describe quantity, rate and timing of stream flow that results from the associated rain events. These hydrographs then become a key input into the hydraulic model. The hydraulic model simulates the movement of flood waters through waterway reaches, storage elements, and hydraulic structures. It calculates flood levels and flow patterns and also complex effects of backwater, overtopping of embankments, waterway confluences, bridge constructions and other hydraulic structure behavior.

2.3.4 Water balance concept based on watershed

Typically, the watershed can be defined as an enclosed region where the direct precipitation occurs within the confines of its drainage basin and collects into a stream channel, flowing downhill to a common basin outlet. A drainage basin is the physical boundary between watersheds where slope of the watershed diverts all surface runoff to the same drainage outlet. The boundary between watersheds is called a drainage divide. Watershed hydrology deals with the rainfall-runoff relationships found across a drainage basin (Singh 1992).

Watershed runoff is composed of three components: surface runoff, interflow, groundwater runoff (i.e. baseflow). Surface runoff flows over the surface of the watershed and downstream in stream channels to the watershed basin outlet. Interflow is the portion of runoff that infiltrates into the upper soil layers of the watershed and moves laterally until it reaches the stream channel. Interflow moves slower than surface runoff, reaching the stream channel later in time. Base flow percolates through soil until it reaches the water table and then moves laterally until

reaching the stream. Base flow is much slower than both surface runoff and interflow and has little to no impact on flood peaks resulting from a storm (Shultz, 2007).

Surface runoff is composed of two main components: overland flow and channel flow. Overland flow is the portion of runoff which flows over the land surface to the stream channel. Overland flow occurs when the precipitation rate from a storm exceeds the interception capacity of the vegetative canopy, the infiltration capacity of soil on the watershed, and surface storage. Channel flow is the translation of a flood wave as it moves downstream in a stream channel. As runoff moves across a watershed and then downstream to the outlet, it undergoes changes across both the overland flow plane and within the stream channel (Shultz, 2007).

Regarding to general concept of the hydrologic model stated earlier, there are five main factors that contribute the most to variation of the observed channel runoff:

1. Precipitation (e.g. duration, distribution, intensity) is used as the input water resource in the water balance model;
2. Topography (e.g. slope, geologic structure, drainage system) is used to determine general flow direction of the surface runoff;
3. Evapotranspiration (ET) is used to determine rate of water loss due to the evapotranspiration process (depends mostly on the climatic and soil conditions and vegetation cover pattern);
4. Soil infiltration capacity is used to determine the water loss due to the infiltration process (depends mostly on soil type);
5. Land use/land cover (LULC) pattern is used to assist the determination of flow movement, infiltration rate and AET rate the most.

2.3.5 Channel Routing

Hydraulic routing is based on the solution of partial differential equations of unsteady open-channel flow. The equations used are the St. Venant equations or the dynamic wave equations (Chow 1988). The hydraulic models (e.g. dynamic and diffusion wave models) require the gathering of a lot of data related to river geometry and morphology and consume a lot of computer resources in order to solve the Saint-Venant equations numerically.

Governing equations and numerical solution schemes

A complete set of governing equations for reduced complexity two-dimensional flood modelling comprises one of the simplified forms of the momentum equation, and a continuity equation. Continuity (or the law of conservation of mass) relates the volume in a given computational cell to the flows into and out of it during a time step:

$$\frac{\partial V^{i,j}}{\partial t} = Q_x^{i-1,j} - Q_x^{i,j} + Q_y^{i,j-1} - Q_y^{i,j} \quad (2.13)$$

where $V^{i,j}$ is the volume in cell (i, j) , t is the time and $Q_x^{i-1,j}$, $Q_x^{i,j}$, $Q_y^{i,j-1}$ and $Q_y^{i,j}$ describe the volumetric flow rates (either positive or negative) between adjacent floodplain cells in the x and y Cartesian directions respectively. The continuity equation for the cell (i, j) can therefore be written:

$$\frac{\partial h^{i,j}}{\partial t} = \theta \frac{Q_{x,t}^{i-1,j} - Q_{x,t}^{i,j} + Q_{y,t}^{i,j-1} - Q_{y,t}^{i,j}}{\Delta x \Delta y} + (1 - \theta) \frac{Q_{x,t+1}^{i-1,j} - Q_{x,t+1}^{i,j} + Q_{y,t+1}^{i,j-1} - Q_{y,t+1}^{i,j}}{\Delta x \Delta y} \quad (2.14)$$

Where $h^{i,j}$ is the flow depth, Δx and Δy are the grid cell dimensions. The weighting coefficient (θ) is used to determine whether the equation system is solved fully or partially implicitly for $\theta < 1$ or explicitly for $\theta = 1$ (Cunge et al., 1980).

2.4 Tools for Flood mapping

MIKE FLOOD

MIKE FLOOD is the complete toolbox for flood modelling available. It includes a wide selection of 1D and 2D flood simulation engines, which enable user to model virtually any flood problem - whether it involves rivers, floodplains, floods in streets, drainage networks, coastal areas, dam, levee and dike breaches or any combination of these. Where other tools give up, MIKE FLOOD gives results. The core elements in MIKE FLOOD are well-proven models, MIKE 11 for rivers, MIKE URBAN for collection systems and MIKE 21 for 2D surface flow. These are coupled to form a unique and trend-setting three-way coupled modelling tool. MIKE FLOOD is applicable at any scale from a single parking lot to regional models. Independent studies show that you can save months of efforts and create more reliable models by upgrading from standard 1D modelling to MIKE FLOOD.

HAZUS-MH software

HAZUS-MH was developed by the Federal Emergency Management Agency's (FEMA) of USA. HAZUS is a nationally applicable standardized methodology that contains models for estimating potential losses from earthquakes, floods and hurricanes. HAZUS uses Geographic Information Systems (GIS) technology to estimate physical, economic and social impacts of disasters. It graphically illustrates the limits of identified high-risk locations due to earthquake, hurricane and floods. Users can then visualize the spatial relationships between populations and other more permanently fixed geographic assets or resources for the specific hazard being modeled, a crucial function in the pre-disaster planning process. HAZUS is used for mitigation and recovery, as well as preparedness and response. Government planners, GIS specialists and emergency managers use HAZUS to determine losses and the most beneficial mitigation approaches to take to minimize them. HAZUS can be used in the assessment step in the mitigation planning process, which is the foundation for a community's long-term strategy to reduce disaster losses and break the cycle of disaster damage, reconstruction and repeated damage. Being ready will aid in recovery after a natural disaster. As the number of HAZUS users continues to increase, so do the types of uses. Increasingly, HAZUS is being used by states and communities in support of risk assessments that perform economic loss scenarios for certain natural hazards and rapid needs assessments during hurricane response. Other communities are using HAZUS to increase hazard awareness. Emergency managers have also found these map templates helpful to support rapid impact assessment and disaster response.

WMS software

The Watershed Modeling System (WMS) is a modelling system for watershed hydrology and hydraulics. WMS is capable of automated delineation of sub-watershed boundaries and flood extent, and includes graphic display options to aid in understanding the drainage characteristics of terrain surfaces as well as several computation features. WMS is a comprehensive graphical modeling environment for all phases of watershed hydrology and hydraulics. WMS can perform operations such as automated basin delineation, geometric parameter calculations; GIS overlay computations (CN, rainfall depth, roughness coefficients, etc.), cross-section extraction from terrain data, floodplain delineation and mapping, storm drain analysis, runoff, and more.

HEC-RAS

The Hydrologic Engineering Center River Analysis System (HEC-RAS) is free software with a friendly graphical user interface that was successfully used for flood studies (US Army Corps of Engineers, 2014). This software allows the user to perform one-dimensional steady flow, one and two-dimensional unsteady flow calculations, sediment transport/mobile bed computations, and water temperature/water quality modeling. In 2014, a new version of HEC-RAS (HEC-RAS-v5) was released including 2D capabilities. HEC-RAS-v5 can be used either as a fully 2D model or as a hybrid 1D2D model when the main rivers are modelled as 1D and the floodplains are modelled as 2D. Although a hybrid 1D2D model tends to be faster than a 2D model, such 1D2D model requires the user to define the connections between the 1D and the 2D models. Such connections require a prior definition of the overflow locations.

2.5 Review of the relevant research works

Flooding is a critical, yet natural phenomenon with severe economic, social and environmental consequences. Recent years, the results of severe flood events underline the requirements for reliable flood modelling tools that enable us to analyses flood events and develop flood protection measures or flood mitigation strategies in the attempt to prevent the losses of human lives and property, as well as to minimize significant destruction of infrastructure and landscape. Several hydrologic models have been developed and applied to the study of surface runoff characteristics and the associated flooding analysis for the interested areas. Examples of these works are reviewed here as follows.

Werner (2000) indicated that the flood hazard in areas adjacent to rivers may be estimated by applying hydrological/hydraulic models to calculate parameters such as flood extent, depth and duration. However, by using a two-dimensional flow model based on the topography has the drawback that computational requirements are high, making this approach unattractive when applying in, e.g., a decision support system.

Sinnakaudan et al. (2002) found that the Geographic Information System (GIS) is an efficient and interactive spatial decision support tool for flood risk analysis. They had developed the ArcView GIS extension namely AVHEC-6.avx to integrate the HEC-6 hydraulic model within GIS environment. It has the capability of analyzing the computed water surface profiles generated from HEC-6 model and producing a related flood map for the Pari River in the ArcView GIS. The flood risk model was tested using the hydraulic and hydrological data from the Pari River catchment area. The results of this study clearly show that GIS provides an effective environment for flood risk analysis and mapping.

Liu et al. (2003) studied a diffusive transport approach for flow routing in GIS-based flood modelling. This research proposes a GIS-based diffusive transport approach for the determination of rainfall runoff response and flood routing through a catchment. The watershed is represented as a grid cell mesh and routing of runoff from each cell to the basin outlet is accomplished using first passage time response function based on the mean and variance of the flow time distribution derived from the advection–dispersion transport equation. The flow velocity is location dependent and calculated in each cell by using the Manning equation based on the local slope, roughness coefficient and hydraulic radius. The total direct runoff at the basin outlet is obtained by superimposing all contributions from every grid cell.

Jothityangkoon and Sivapalam (2003) developed the distributed rainfall-runoff model to predict extreme flood. It was found from this work that when increase of normal flood condition to the extreme flood condition, the model's results showed that process of the runoff occurrence has changed by increasing of saturation excess overland flow from the increase of the saturated area. The overflowing process of the river bank had the role more than the flowing in the waterway.

Werner et al. (2005) explored the potential for identifying roughness values for distributed land use types using a comprehensive calibration data set of the 1995 flood event in the River Meuse, including gauged levels, flood extent maps and distributed flood plain level observations. The reach studied was modelled using an integrated 1D–2D hydrodynamic model, with floodplain flow modelled in the 2D domain. Detailed information on floodplain land use types is aggregated to form one, two or five classes of floodplain roughness. Sensitivity analysis of model performance against the calibration data shows that as the number of floodplain classes increases,

sensitivity to these roughness values decreases, given allocation of prior roughness values on the basis of constituent land use types and associated roughness values found from literature. Evaluating the identifiability of the roughness in these classes using the Generalised Likelihood Uncertainty Estimation (GLUE) method confirms this insensitivity. As a consequence, application of complex formula to establish roughness values for changed floodplain land use would seem inappropriate, and evaluation of such changes within a probabilistic framework are suggested.

Jothityangkoon et al. (2006) applied the distributed rainfall-runoff model developed in Australia to analyze daily water balance in Lum Pang Chu Watershed, which is sub-catchment of Mun River in the northeast of Thailand. Result of the daily model being developed by using long term water balance concept found that, it was necessary to add more complexity to runoff generation processes from soil-water storage to increase base flow in the stream and receive a better fit to the observed flow duration curve.

Ramlal and Baban (2007) developed a GIS-based hydrologic model to flood management in Trinidad, West Indies. This work uses GIS to map the extent of the flooding, estimate soil loss due to erosion and estimate sediment loading in the rivers in the Caparo River Basin. The results indicate that flooding was caused by several factors including clear cutting of vegetative cover, especially in areas of steep slopes that lead to sediment filled rivers and narrow waterways. Other factors include poor agricultural practices and uncontrolled development in floodplains.

Merwade et al. (2008) studied of GIS techniques for creating river terrain models for hydrodynamic modelling and flood inundation mapping. The objectives of them study are to highlight key issues associated with creating an integrated river terrain, and propose GIS techniques to overcome these issues. Multiple approaches are used to create river terrain models for 2D/3D hydrodynamic modelling and flood inundation mapping. Creating surface representations of river systems is a challenging task because of issues associated with interpolating river bathymetry, and then integrating this bathymetry with surrounding topography. The techniques are presented by mapping and analyzing river channel data in a channel fitted coordinate system; interpolation of river cross-sections to create a 3D mesh for main channel; and integration of interpolated 3D mesh with surrounding topography. Creation of a 3D mesh for the main channel using a channel-fitted coordinate system and subsequent integration with surrounding topography produces a coherent river terrain model, which can be used for 2D/3D hydrodynamic modelling and flood inundation mapping. Since the results from hydraulic and hydrodynamic models are greatly affected by the geometric description of the river channel bathymetry and surrounding topography, an integrated river terrain that accurately describes the main channel and the floodplain along with geomorphologic and engineering features is an important dataset that will improve our ability to accurately model and understand river flow and surrounding hydrologic processes such as surface water/ground water interaction.

Zonensein et al. (2008) presented a quantitative multi-criteria index, named Flood Risk Index (FRI), which is able to overcome some off the inconveniences of traditional flood risk assessment methodologies. The two components of risk (Probability and consequences) are represented by sub-indices, related both to flood properties and to local vulnerability and exposure characteristics, and each sub-index results from the interaction of a number of factors, expressed by indicators. The relative importance of indicators and sub-indices is represented by weights associated to each of them. The concept of risk has variable meaning according to the context in which it is employed and, for that reason, the adopted interpretation must be elucidated prior to any analysis. In engineering, risk is divided in two basic components: one related to the probability of occurrence of a hazardous event and another regarding its consequences. Concerning flood risk, in particular, this is the definition mostly accepted being. Range of the FRI were set up for the sake of simplicity and clarity, it was determined that the FRI should be a dimensionless value, which could range between 0 and 100 – the minimum and maximum risk, respectively. Moreover, in order to operate the indicators that compose FRI, which have varied natures and units, they must be normalized beforehand, converting them into a common range. According to the formulation established next, all indicators have to be adjusted to the same range, assuming values between 0 and 100. Finally, weighted summations and products compose the formulation of FRI. The index constitutes a decision support tool, allowing the rating, identification, and comparison of critical zones, the assessment of different flood risk scenarios, the development of flood risk maps, among other potential uses. The FRI was applied in a GIS.

Chen et al. (2009) developed a GIS-based urban flood inundation model called GUFIM which consists of two components: a storm-runoff model and an inundation model. Cumulative surface runoff, output of the storm-runoff model, serves as input to the inundation model. The storm-runoff model adapts the Green-Ampt model to compute infiltration based on rainfall characteristics, soil properties, and drainage infrastructure conveyance. The basis of the inundation model is a flat-water model. This effort uses publicly available elevation data, storm data, and insurance claim data to develop, implement and verify the model approach.

Rozalis et al. (2010) studied of the assessment of flood hazard by developing a flood hazard map for mid-eastern Dhaka of Bangladesh was carried out by 1D hydrodynamic simulation using both topographic remote sensing data and hydrologic field-observed data. The study demonstrates a simple and effective way to modify the collected DEM. The aim of flood hazard map is to provide residents with the information on the range of possible damage and the disaster prevention activities. The effective use of hazard map can decrease the magnitude of disasters. On the other hand, flood risk map represents the current scenario of that area according to degree of risk. The map provides helpful information about flood risk management and should be useful in assigning priority for the development of high-risk areas.

Masood and Takeuchi (2010) studied of flash floods prediction. Flash floods cause some of the most severe natural disasters. The complexity of flash flood generation processes and their dependency on different factors related to watershed properties and rainfall characteristics make flash flood prediction a difficult task. They used an uncalibrated hydrological model to simulate flow events. The model is based on the well-known SCS curve number method for rainfall–runoff calculations

and on the kinematic wave method for flow routing. Existing data available from maps, GIS and field studies were used to define model parameters, and no further calibration was conducted to obtain a better fit between computed and observed flow data. The model rainfall input was obtained from the high temporal and spatial resolution radar data adjusted to rain gauges. The model shows a generally good capability in predicting flash flood peak discharge in terms of their general level, classified as low, medium or high (all high level events were correctly predicted). It was found that the model mainly well predicts flash floods generated by intense, short-lived convective storm events while model performances for lowland moderate flows generated by more widespread winter storms were quite poor. The degree of urban development was found to have a large impact on runoff amount and peak discharge, with higher sensitivity of moderate and low flow events relative to high flows. Flash flood generation was also found to be very sensitive to the temporal distribution of rain intensity within a specific storm event.

Khatibi (2011) used historical data to model these transitions and to explain. This is a new bottom-up modelling capability based on a set of postulates integrating: (i) systemic thinking where systems are effected by four types of feedback loops to be described in the paper, which include positive/negative feedback; and (ii) evolutionary thinking, where each feedback loop is associated with a “risk mindset.” These mindsets can undergo evolutionary transition from one to the next and the transition is largely driven by natural selection. After an evolutionary transition, lower mindsets do not necessarily disappear but can adapt and coexist with higher order loops. Based on the insight gained, the paper argues that (i) as the loops coexist pluralistically, systems increase in their complexity; (ii) there may be unexpected

dynamic behaviors when a system is interacted with different types of feedback loops; and (iii) currently, these dynamic behaviors are overlooked, suggesting possible loopholes, bottlenecks or barriers and hence the motivation.

Jothityangkoon et al. (2013) studied of the assessing the impact of climate and land use changes on extreme floods in a large tropical catchment. They concern about the safety of large dams designed and built some 50 years ago. In this study distributed rainfall–runoff model appropriate for extreme flood conditions is used to generate revised estimates of the Probable Maximum Flood (PMF) for the Upper Ping River catchment in northern Thailand, upstream of location of the Bhumipol Dam. The model has two components: a continuous water balance model based on a configuration of parameters estimated from climate, soil and vegetation data and a distributed flood routing model based on non-linear storage discharge relationships of the river network under extreme flood conditions. The model is implemented under several alternative scenarios regarding the Probable Maximum Precipitation (PMP) estimates and is also used to estimate the potential effects of both climate change and land use and land cover changes on the extreme floods. These new estimates are compared against estimates using other hydrological models, including the application of the original prediction methods under current conditions. Model simulations and sensitivity analyses indicate that area reasonable Probable Maximum Flood (PMF) at the dam site is $6,311 \text{ m}^3/\text{s}$, which is only slightly higher than the original design flood of $6000 \text{ m}^3/\text{s}$. As part of an uncertainty assessment, the estimated PMF is sensitive to the design method, input PMP, land use changes and the flood plain inundation effect.

Daungthima and Hokao (2013) studied of the Analyzing the Possible Physical Impact of Flood Disasters on Cultural Heritage in Ayutthaya, Thailand. They was reviews of disaster vulnerability factors, found that the most crucial factors may be organized as six groups of factors which are: topography, slope, density of building, distance from the river, drainage system and soil type, and distance to road. Topography refers to current elevation and surface water flow paths. Slope refers to upstream source of flooding, flood susceptibility and overflow sensibility. Density of building refers to land value per floor space and land use. The distance from the river refers to distance of area flooding risk to river. Drainage system and soil refer to vulnerable community and critical, soil erodibility, soil drainage, soil moisture, soil scape in fragile environmental balance and soil composition. Distance to road refers to distance of historical sites to road.

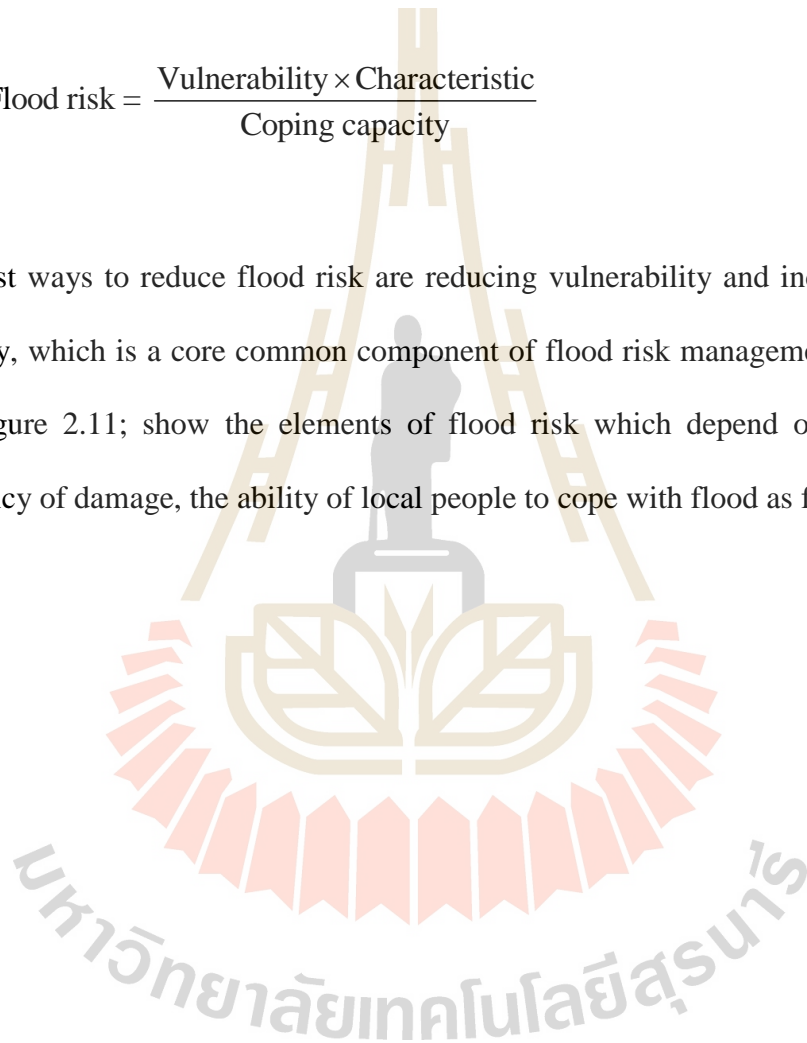
Table 2.1. The disaster vulnerability factors

Factors	Detail of factors
Topography	Current elevation Surface water flow paths
Slope	Upstream source of flooding Flood susceptibility Overflow sensibility
Density of building	Land value per floor space Land use
Distance from the river	Area at risk from flooding
Drainage system & Soil	Vulnerable community and critical infrastructure Soil erodibility Soil drainage Soil moisture Soil scape in fragile environmental balance Soil composition
Distance to road	Distance of historical site to road

Mongkonkerd et al. (2013) determined flood risk not only by vulnerability but also by characteristics and coping capacity to flood exposure. Therefore, the risk of flood is based on three crucial elements which are related as shown in equation 2.15 (the formula of flood risk).

$$\text{Flood risk} = \frac{\text{Vulnerability} \times \text{Characteristic}}{\text{Coping capacity}} \quad (2.15)$$

The best ways to reduce flood risk are reducing vulnerability and increasing coping capacity, which is a core common component of flood risk management. Figure 2.10 and Figure 2.11; show the elements of flood risk which depend on vulnerability, frequency of damage, the ability of local people to cope with flood as follows:



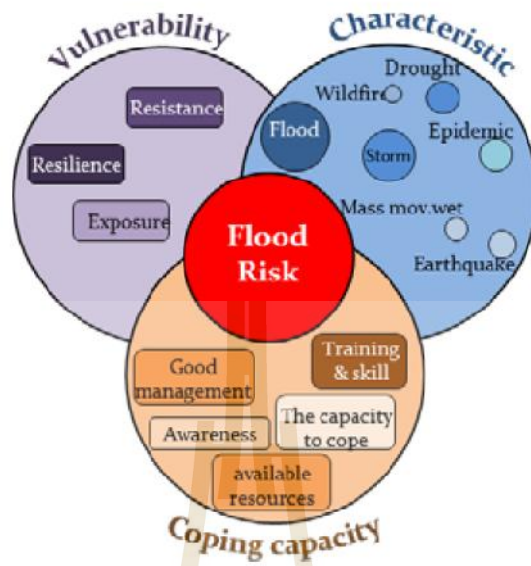


Figure 2.10 The components of flood risk (Daungthima and Hokao., 2013)

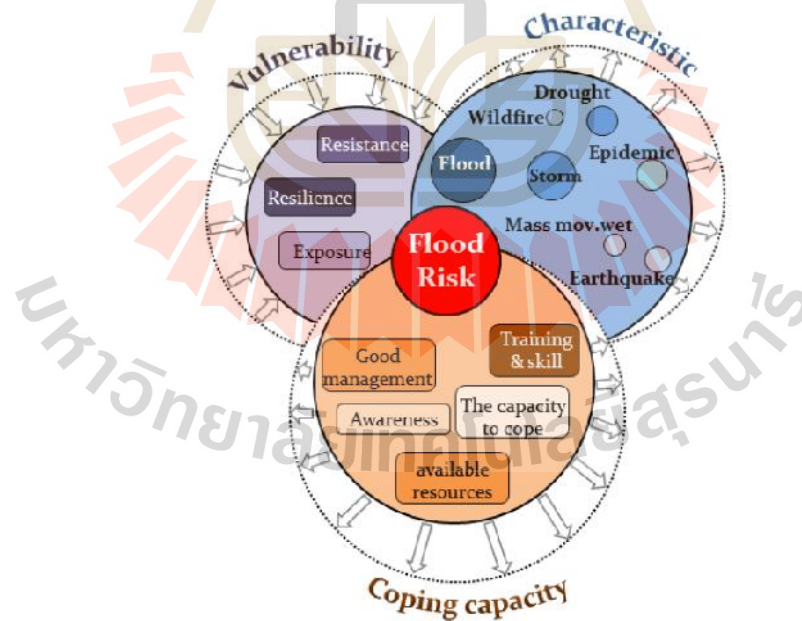


Figure 2.11 The reduction of flood risk (Daungthima and Hokao., 2013)

Vulnerability refers to circumstances of a community or asset that make it susceptible to the damaging effects of a flood. There are many aspects of vulnerability, arising from various physical, social, economic, and environmental factors. Examples may include construction of buildings, inadequate protection of assets, lack of information and awareness.

Characteristic refers to natural disaster occurrence, frequency of damage, duration and maximum water level.

Coping capacity is the ability of people in the community to face and manage the flood using available skills and resources. The capacity to cope requires continuing awareness, resources and good management, both in normal times as well as during crises or adverse conditions.

2.6 References

- Alan A.S. (2010). **Hydrological Theory: Rainfall Runoff Models** [online]. Available: <http://www.alanasmith.com/theory-Calculating-Runoff-Rainfall-Runoff-Models.html>.
- Beven, K. J. (2000). **Rainfall Runoff Modelling: The Primer**, John Wiley, Chichester.
- Betson, R. P. (1964). **What Is Watershed Runoff**. Journal of Geophysical Research, 68: 1541-1552.
- Burt T.P. and Butcher D.P. (1985), **Topographic controls of soil moisture distributions**. Journal of Soil Science, 36(3), 469 – 486.

- Chatterjee, C., Jha, R., Lohani, A. K., Kumar, R., and Singh, R. (2001). **Run-off curve number estimation for a basin using remote sensing and GIS**. Asian-Pacific Remote Sensing and GIS Journal. 14: 1-8.
- Chen, J., Hill, A.A. and Urbano, L.D. (2009). **A GIS-based model for urban flood inundation**. Journal of Hydrology. 373: 184-192.
- Chow, V. T., Maidment, D. R. and Mays L.W (1988). **Applied Hydrology**. McGrawHill International Editions: Singapore. 569 pp.
- CRAHI. (2012). **Type of hydrological models**. [Online]. Available: <http://www.crahi.upc.edu/en/projects/areas-of-expertise/78-tipus-de-models-hydrologics>.
- Cunge, J.A., Holly, F.M., Verwey, A. (1980). **Practical Aspects of Computational River Hydraulics**. Pitman Publishing, London. 420 pp.
- Daungthima, W. and Hokao, K. (2013). **Assessing the flood impacts and the cultural properties vulnerabilities in Ayutthaya, Thailand**. Procedia Environmental Sciences. 17: 739-748.
- Dunne, T. and Leopold, L. B. (1978). **Water in Environmental Planning**. W H Freeman and Co, San Francisco, 818 p.
- Tarboton, D.G. (2003). **Rainfall-Runoff Processes**. Water Research Laboratory, Civil and Environmental Engineering, Utah State University
- Ghosh, S.N. (2006). **Flood Control and Drainage Engineering** 3th edition. Taylor & Francis Group. 357 pp.
- Jothityangkoon, C. and Sivapalan, M. and Farmer, D.L. (2001). **Process controls of water balance variability in a large semiarid catchment: Downward**

- approach to hydrological model development.** Journal of Hydrology. 254: 174-198.
- Jothityangkoon, C. and Sivapalan, M. (2003). **Towards estimation of extreme flood: Examination of the roles of runoff process changes and floodplain flows.** Journal of Hydrology. 281: 206-229.
- Jothityangkoon, C. and Hirunteeyakul, C. (2006). **Hydrological model development for water balance study in subcatchment of Mun River.** School of civil engineering, Suranaree University of Technology.
- Jothityangkoon, C., Hirunteeyakul, C., Boonraed, K. and Sivapalan, M. (2013). **Assessing the impact of climate and land use changes on extreme floods in a large tropical catchment** Journal of Hydrology. 490: 88-105.
- Khatibi, R. (2011). Evolutionary systemic modelling of practices on flood risk, Journal of Hydrology, 401 36–52
- Klemes, V. (1983). **Conceptualisation and scale in hydrology.** Journal of Hydrology. 65: 1-23.
- Liu, Y.B., Gebremeskel, S., Smedt, F.D., Hoffmann, L. and Pfister, L. (2003). **A diffusive transport approach for flow routing in GIS-based flood modeling.** Journal of Hydrology. 283: 91-106.
- Masood, M. and Takeuchi, K. (2010). **Assessment of flood hazard, vulnerability and risk of mid-eastern Dhaka using DEM and 1D hydrodynamic model,** Nat Hazards, 61:757–770.
- Merwade, V., Cook, A., Coonrod, J. (2008). **GIS techniques for creating river terrain models for hydrodynamic modelling and flood inundation mapping,** Environmental Modelling & Software, 23:1300-1311.

- Mongkonkerd, S., Hirunsalee, S., Kanaegae, H. and Denpaiboon, C. (2013). **Comparison of direct monetary flood damage in 2011 to pillar house and non-pillar house in Ayuthhaya, Thailand.** *Procedia Environmental Sciences*, 17: 327-336.
- Neil, M.H., Paul, D.B., Matthew, S.H. and Matthew, D.W.(2007). **Simple spatially-distributed models for predicting flood inundation: A review.** *Geomorphology*, Vol.90, pp.208-225.
- Neitsch, S. L., Arnold, J. G., Kiniry, J. R., and Williams, J. R. (2011). **Soil and Water Assessment Tool theoretical documentation version 2009.** Texas Water Resources Institute, College Station, Texas.
- NOAA National Weather Service (2010). **Unit Hydrograph Theory** [online]. Available:http://stream2.cma.gov.cn/pub/comet/HydrologyFlooding/UnitHydrographTheoryInternationalEdition/comet/hydro/basic_int/unit_hydrograph/print.htm#page_1.0.0.
- Rallison. R. E. and Miller, N. (1981). **Past, present and future SCS runoff procedure.** In V.P. Singh (Ed.), *Rainfall runoff relationship* (pp.353-364). Water Resources Publication, Littleton, Colorado.
- Ramlal, B. and Baban, S.M.J. (2007). **Developing a GIS based integrated approach to flood management in Trinidad, West Indies.** *Journal of Environmental Management*. 88: 1131-1140.
- Rozalis, S., Morin, E., Yair, Y. and Price, C. (2010), **Flash flood prediction using an uncalibrated hydrological model and radar rainfall data in a**

- Mediterranean watershed under changing hydrological conditions**,
Journal of Hydrology, 394:245–255
- Seth, S.M. (2006). **Role of Remote Sensing and GIS inputs in physically based Hydrological Modelling** [Online]. Available: <http://www.gisdevelopment.net/application/nrm/water/overview/wato0006pf.htm>
- Shultz, M.J. (2007). **Comparison of Distributed Versus Lumped Hydrologic Simulation Models Using Stationary and Moving Storm Events Applied to Small Synthetic Rectangular Basins and an Actual Watershed Basin**. Ph.D. THESIS, The University of Texas at Arlington.
- Singh, V.P. (1992). **Elementary Hydrology**. New Jersey: Prentice Hall, Englewood Cliffs.
- Sinnakaudan, S.K., Ghani, A.A., Ahmad, M.S.S. and Zakaria, N.A. (2002). Flood risk mapping for Pari River incorporating sediment transport. **Environmental Modelling & Software**. 18: 119-130.
- Soil Conservation Service (SCS). (1972). **National Engineering Handbook, Section 4: Hydrology**. Department of Agriculture, Washington DC, 762 p.
- Tekeli, T. I., Akgul, S., Dengiz, O., and Akuzum, T. (2007). **Estimation of flood discharge for small watershed using SCS curve number and geographic information system**. International Congress on River Basin Management. Antalya, Turkey.
- US Army Corps of Engineers, (2014). **Hydrologic Engineering Centers River Analysis System (HEC-RAS)**, available at: <http://www.hec.usace.army.mil/software/hec-ras/>[Accessed: 15 November 2014].

Werner, M.G.F. (2000). **Impact of Grid Size in GIS Based Flood Extent Mapping Using a 1D Flow Model**. Elsevier Science Ltd.

Werner, M.G.F., Hunter, N.M. and Bates, P.D. (2005). **Identifiability of distributed floodplain roughness values in flood extent estimation**. Journal of Hydrology, 314 : 139–157

Zhang,L., Walker, G.R and Dawes, W.R.(2002). **Water balance modelling: concepts and applications**. Regional Water and Soil Assessment for Managing Sustainable Agriculture in China and Australia, ACIAR Monograph. No. 84: 31–47.

Zonensein, J., Miguez., M.G., de Magalhaes, L.P.C., Valentin, M.G., and Mascarenhas, F.C.B. (2008). **Flood Risk Index as an Urban Management Tool**. 11th International Conference on Urban Drainage, Edinburgh, Scotland, UK.

CHAPTER III

DATA AND METHODOLOGY

This chapter describes the materials and methodology of risk mapping. Conceptual framework of the research is shown in Figure 3.1. Table 3.1 is represented physical data for basin in the study area. Upper Mun river basin consist of 6 subbasins shown in Figure 3.2 to demonstrate primary collected data, Lam Takong subbasin is chosen to represent methodology process.

3.1 Data preparation

3.1.1 Physical characteristic of study area

Digital Elevation Model (DEM)

The topography of land surface substantially influence on the magnitude and dynamics of surface runoff. To illustrate the shape of land surface, DEM can be used to generate topographic map. The Digital Elevation Model (DEM) (Figure 3.3) contains spatially distributed elevation information to allow an automatic delineation of watershed boundary. Topographic maps from the Royal Thai Survey Department (RTSD) at the scale 1:50,000 and 1:4,000 are used to generate DEM. The relevant parameters can be generated from DEM: slope, flow direction, flow accumulation and stream network. In general, increasing level of spatial resolution can increase the accuracy of the simulated results. Values assigned to any grid cell represent an average value over a number of grid elements.

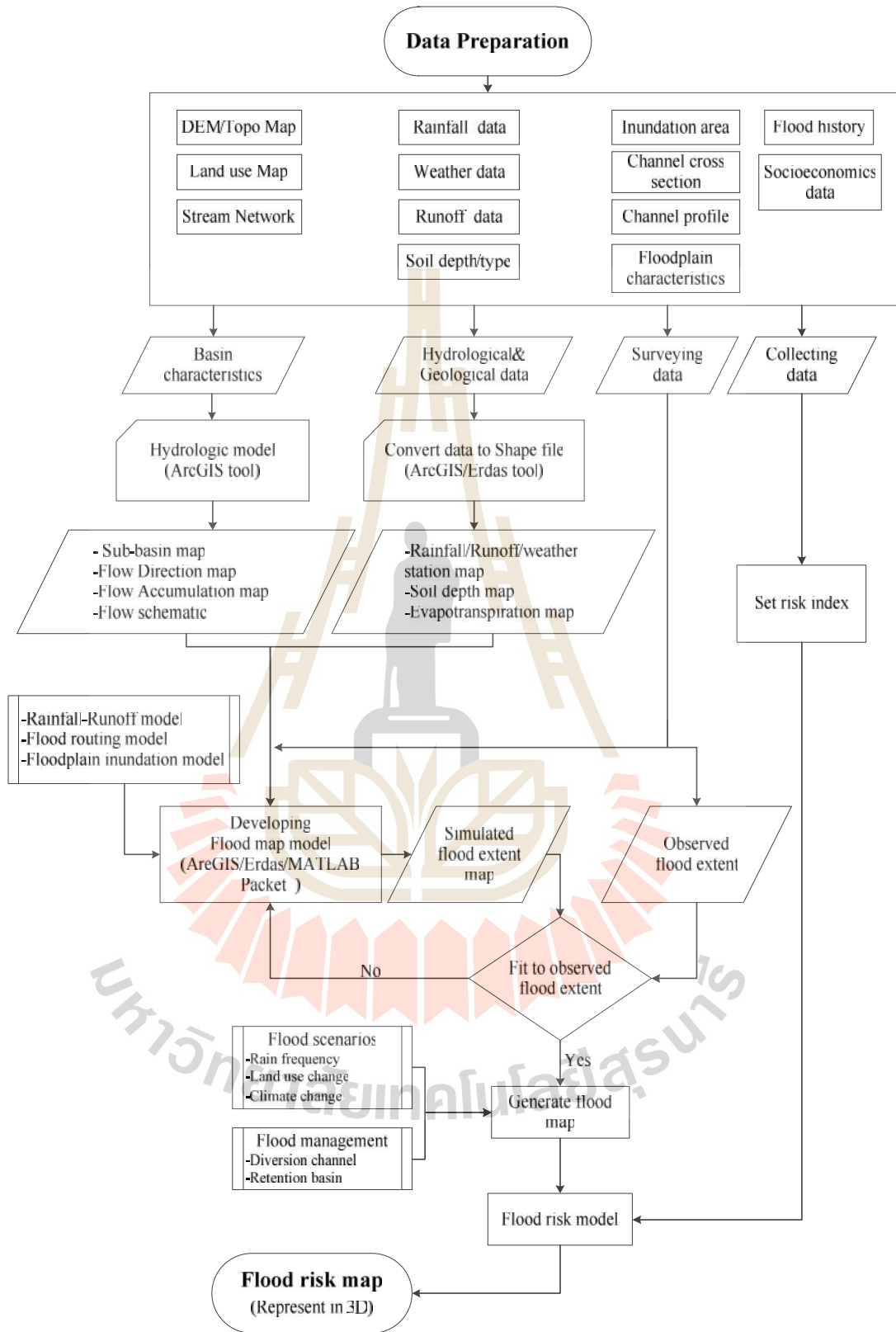


Figure 3.1 Conceptual framework of the research methodology and processes

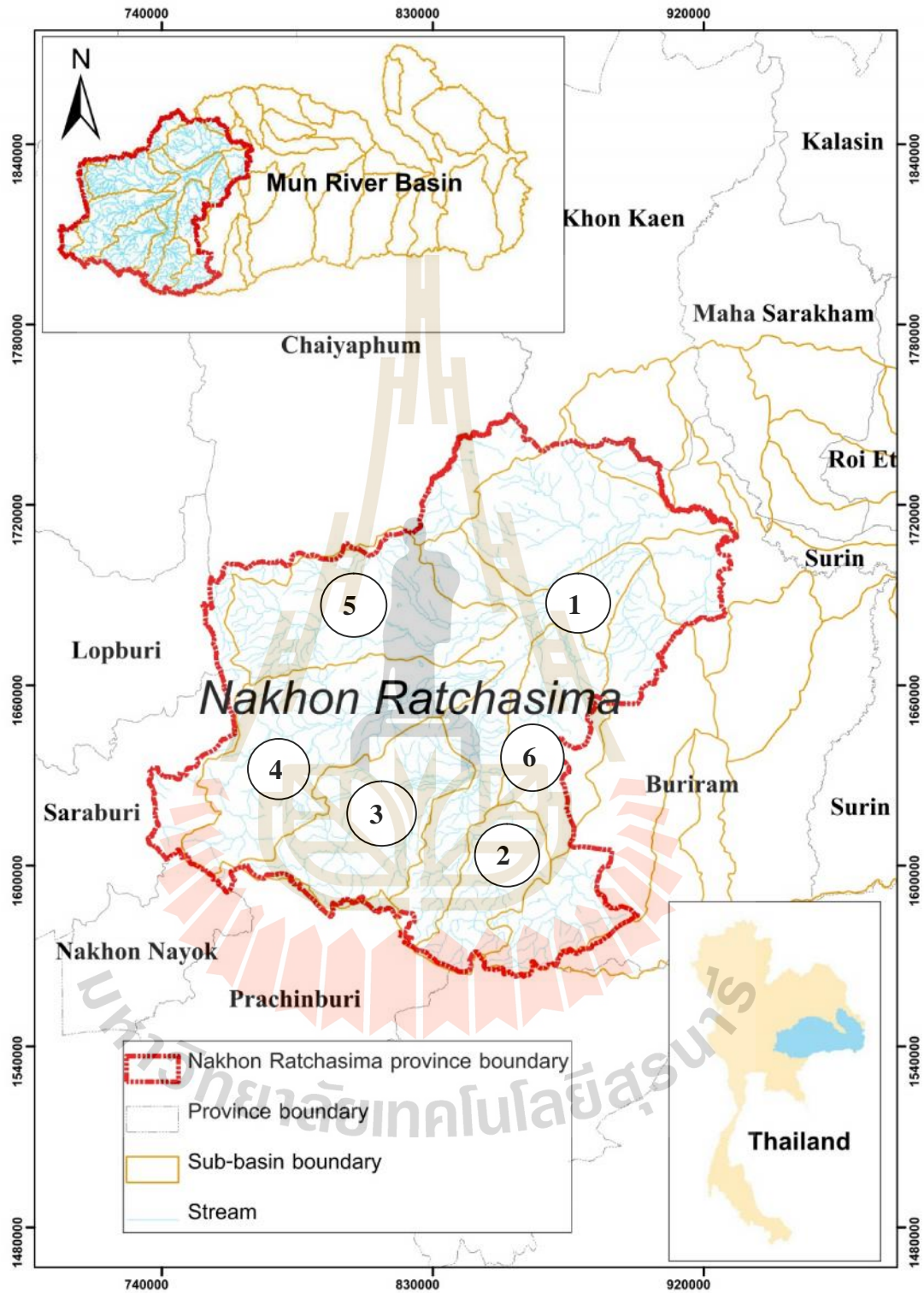


Figure 3.2 Upper Mun River Basin

Table 3.1 List of subbasins of upper Mun River Basin and their properties

Sub-basin no.	Sub-basin name	Area (km ²)	Stream Length (m)
1	Upper part of Lam nam mun	2,811	224
2	Lam sae	1,197	
3	Lam phra phlong	2,277	
4	Lam ta khong	3,315	220
5	Lam Chiang krai	2,617	178
6	Lam Chak karat	1,642	
Total		13,859	-

Table 3.2 Data types agencies and available records for upper Mun River Basin

Data type	Agency	Period of time
Digital Elevation Model	Land Development Department (LDD)	2004
Land use	Land Development Department (LDD)	2008
Stream network	Land Development Department (LDD)	2008
Rainfall	Thai Meteorology Department (TMD)	1990-2013
Weather	Thai Meteorology Department (TMD)	1990-2013
Runoff	Royal Irrigation Department (RID)	1990-2013
Soil	Land Development Department (LDD)	2008
	Department of Groundwater Resources (DGR)	-

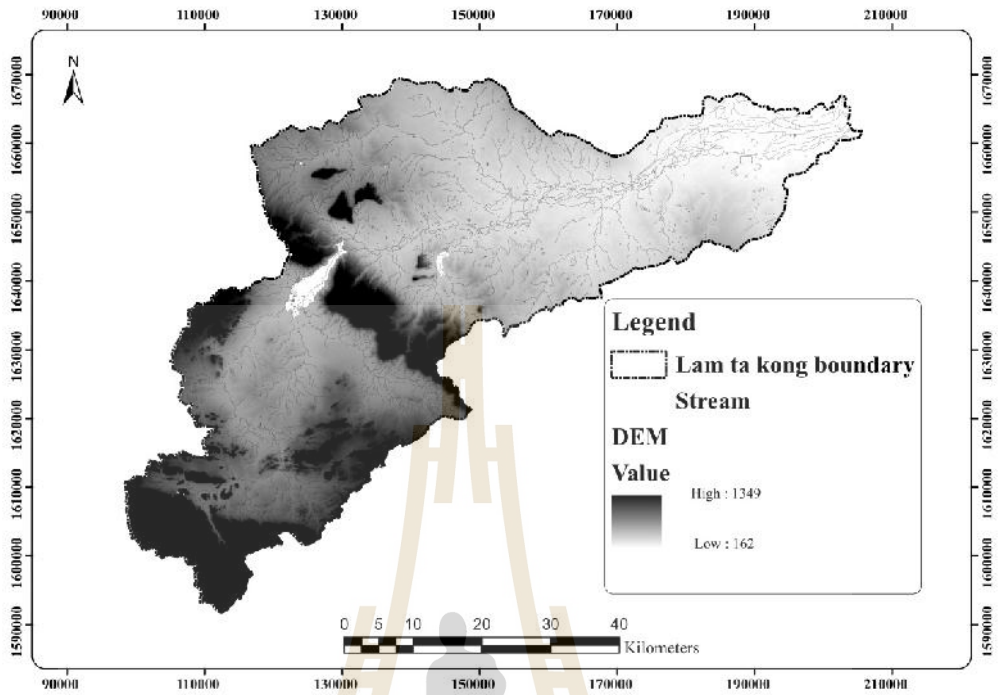


Figure 3.3 DEM of Lam Takong River Basin

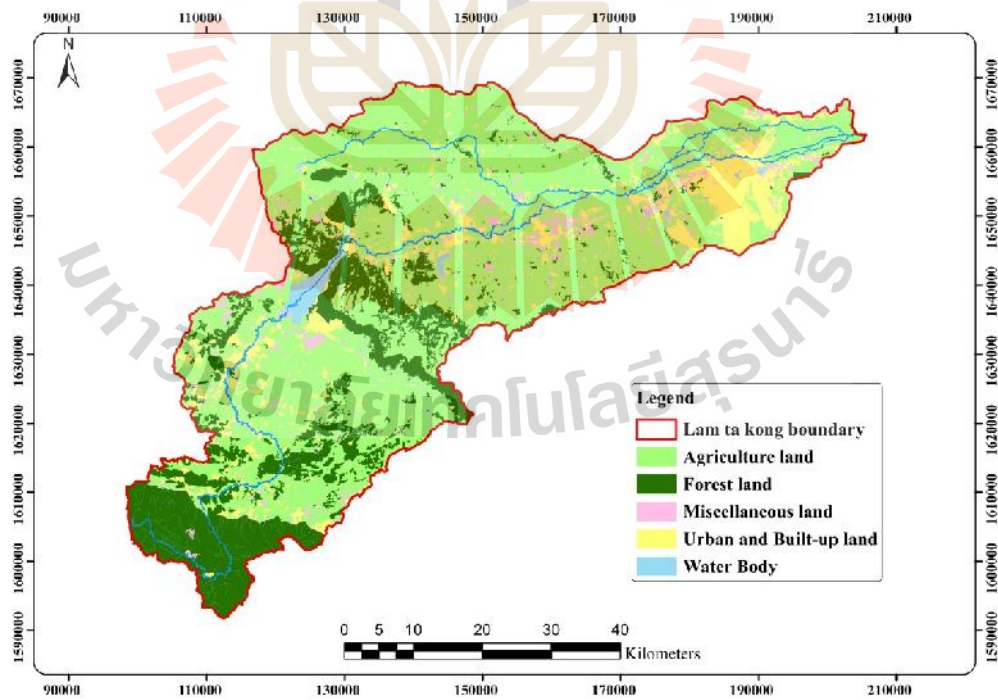


Figure 3.4 Land use of Lam Takong River Basin

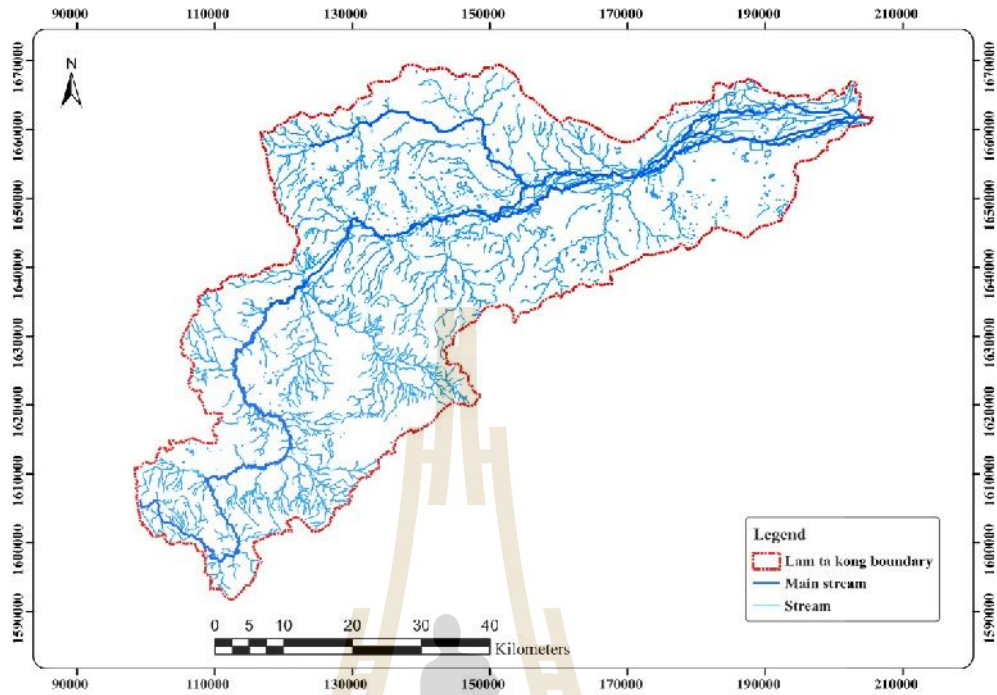


Figure 3.5 Stream network of Lam Takong River Basin

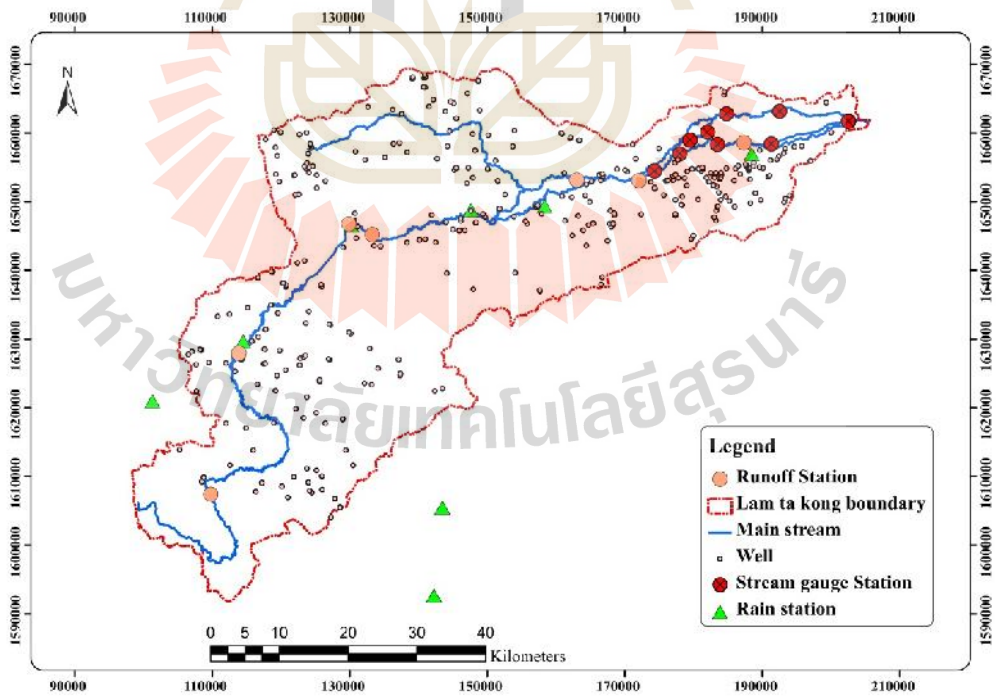


Figure 3.6 Hydrological and geological station of Lam Takong River Basin

Land use and Land cover

Land use and Land cover data are required for rainfall-runoff processes and flood assessment because they indicate the activities on land with different level of flood risk. The digital land use data on scale of 1:50,000 and 1:4000 were obtained from Land Development Department (LDD) in 2008. Five land use types are used in this study (Table 3.3).

Table 3.3 List of land use type and its area for Lam Takong River Basin

Land use types	Area (km²)	% of total area
Agriculture land (A)	2,022	61
Forest land (F)	675	20
Urban and built-up land (U)	400	12
Miscellaneous land (M)	158	5
Water Body (W)	60	2
Total	3,315	100

3.1.2 Hydrological and Geological data

To obtain accurate a real rainfall for the whole basin, rainfall data from a number of rain gauges are required to capture the variability of rainfall in the watershed. In this study in Lam Takong River Basin, rainfall data were collected from 8 stations (Figure 3.6) located within and around the watershed by Thai Meteorology Department (TMD). The runoff data are obtained from Royal Irrigation Department (RID). These data were used for calibrate and validate model parameter. For soil data, there are two main properties to be considered: effective depth of soil layer and soil texture (in term of the soil porosity). Soil data was obtained at the scale of 1:25,000 from LDD. These data were mapped based on original data extracted from 360 boring log of ground water wells (surveyed the Department of Groundwater Resources (DGR) within the Lam Takong area. The effective soil depth for each well is defined as distance from ground to the bedrock level of the well. The porosity will be calculated from the average porosity value of relevant soil textures found at each. Knowledge of effective soil depth and soil porosity data can be used to calculate soil water storage for water balance model.

3.1.3 Surveying and collecting data

Surveying data consist of channel cross section, channel profile, inundation area and floodplain characteristics. Collecting data consist of a simple and accurate method of collating and displaying the relevant extent and level information. After the data has been collected. It was used to produce a map of the flooded area, with peak flood levels at particular locations, if available. A brief accompanying report can detail additional information such as flood mechanism, time and duration of flooding, emergency response and estimated damage. Data and

information on historic flood events is essential to identify where flood risk management measures are required and to efficiently design the most effective system for mitigating the risk. This data is also of benefit to local authorities and other state agencies in functions such as land-use planning, developing the emergency response to future flood events, and assisting in the development of flood map model.

3.2 Construct the flood hazard map model

This part contributes to generating of flood maps for study area during October's flood 2010 based on the simulated flood hazard map. A flood hazard map is simulated by flood map model (Hec-RAS V.5) which is developed from geometric data with ArcGIS/Erda software packet. The simulated flood hazard map are compared with the observed flood hazard map (of the same event) calibrated with surveying data and collecting data. The result to be re-developed until outcome is significant and acceptable. If the result of flood extent map is acceptable, the product can use for generate flood map process. Flood map is assumed as the flood scenarios (Rain frequency, Land use change and Climate change) and flood management (Diversion channel and Retention basin) for generating the flood map.

3.3 Development of the flood risk model

The purpose of flood risk such assessment is to identify the areas within a development plan that are at risk of flooding base on factors that are relevant to flood risks. Flood risk model was developed by flood map from previous step using GIS raster index model. An index model calculates the index value for each unit area and produces a classified map based on the index values. An index model is similar to a binary model in that both involve multi-criteria evaluation and both depend on map overlay operations in data processing. The concept of risk has variable meaning according to the context in which it is employed and, for that reason, the adopted interpretation must be elucidated prior to any analysis. In engineering, risk is divided in two basic components: one related to the probability of occurrence of a hazardous event and another regarding its consequences. Concerning flood risk, in particular, this is the definition mostly accepted being. Multi-criteria analysis enables a combined assessment, in which aspects of different natures and its relative importance are taken into account without the need of monetary valuation, this approach is recommended for the analysis of flood risk. Indices are an example of multi-criteria analyses and are especially useful and well suited to aid the resolution of decision problems. It is a way to combine information associated to indicators of distinct natures and significances, translating them into a single value. This effect, which must be representative of a real situation, means to reproduce the joint effect of the set of indicators. The properties that characterize an index include:

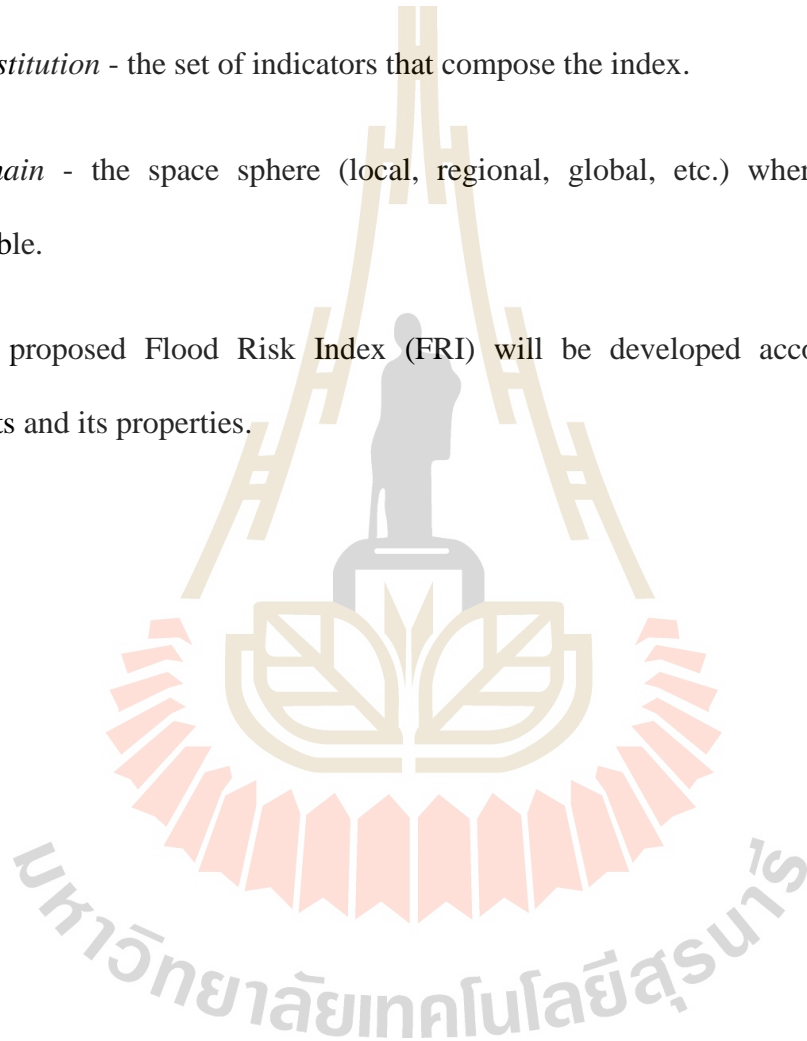
Range - defined by its maximum and minimum extremes, which comprise all the values the index can assume.

Formulation - the mathematical expression that represents the relationship between the set of indicators, which compose the index.

Constitution - the set of indicators that compose the index.

Domain - the space sphere (local, regional, global, etc.) where the index is applicable.

The proposed Flood Risk Index (FRI) will be developed according to these concepts and its properties.



CHAPTER IV

THE DEVELOPMENT OF A SIMPLE DISTRIBUTED HYDROLOGICAL MODEL BASED ON UP-SCALING FROM PIXEL TO CATCHMENT SCALE

4.1 Summary

Spatial units used in the modeling are rectangular grids with 30m-resolution grouped into hillslope and channel pixels. For each hillslope pixel, a simple two-layer soil model is used to simulate the dynamics of soil-water between unsaturated and saturated zones. Soil column of each pixel receives water in form of infiltration into unsaturated zone from precipitation, lateral overland and subsurface discharge from neighboring upstream pixels. It loss water through evapotranspiration and lateral overland and subsurface discharge to downstream pixel. Water column moves out of the grid in only one direction, depending to the steepest slope. Runoff generation is estimated at every pixel including Horton Overland Flow (HOF), Dunne overland flow (DOF), Subsurface Storm Flow (SSF) and infiltration excess runoff given by the Green-Ampt method. The upstream-downstream aggregated interaction of hydrological processes through the catchment scale forming of DOF, SSF and partial saturation area which occurs in the river network. Advantage of this approach is simple, tractable and computationally efficiency that we can carry out for multiple realization of climate- soil- topography combination. This model will be used to

simulate the effects of different combination of climate, soil, and topography on the runoff generation processes through hypothetical catchment and climate combination.

4.2 Introduction

Infiltration excess runoff (or Hortonian Overland Flow, HOF), saturation excess runoff (or Dunne Overland Flow, DOF) and Subsurface Storm Flow (SSF) are the three main and well-known runoff generation processes occurring in headwater catchments (Horton, 1933; Dunne, 1978). Dunne (1978) explained that the relative dominance of given runoff generation mechanisms is controlled by the combination of climate, soil, vegetation and topography. However, this holistic conceptual illustration of climate and landscape controls on runoff generation processes is still explained in a qualitative way. A quasi-distributed model based on TOPMODEL concepts (Beven and Kirkby, 1979) is used to investigate the relative dominance of Hortonian and Dunne overland flow mechanisms (Sivapalan et al., 1987; Larsen et al., 1994; Robison and Sivapalan, 1995). Their work was limited to two mechanisms and operated at event scales, and could not include the effect of antecedent condition and the effect of all conditions of catchments (e.g. steep topography or complex subsurface as assumed in TOPMODEL). Several studies applied semi or fully distributed catchment model in actual catchments that includes all three mechanisms of runoff generation. Mirus and Loague (2013) used a physics-based coupled surface and subsurface model, *InHM*, to investigate climatic and landscape controls on runoff generation. Carrillo et al. (2011) also used a physics-based model, *hsB*, to perform regressions of calibrated parameters associated with vegetation cover, demonstrating the role of vegetation in the co-evolution of catchment properties with climate. Torch

et al. (2013) extended this model to show the response and adaptation of vegetation to climate difference reflected in the long-term water balance exhibited by catchment in respect to Budyko curve. Li et al. (2014) developed a simple distributed hydrologic model to simulate the effects of different combinations of climate, soil, and topography on the runoff generation processes. Limitation of available observed data from highly instrumented catchments and most parameters are obtained by calibration. This prevented the ability of these models to apply to a large population of sites and catchments to obtain general knowledge on what are underlying physical controls on the runoff generation processes. Inspired by the work of (Li et al., 2014), the aim of this study is to further develop the simple distributed model that could investigate the combined effect of climate, soil, vegetation and topography on the runoff generation processes at the catchment scale in a quantitative way.

4.3 Methodology

A schematic illustration of the model is shown in Figure 4.1. Brief description of the procedure for runoff generation simulation are as follows:

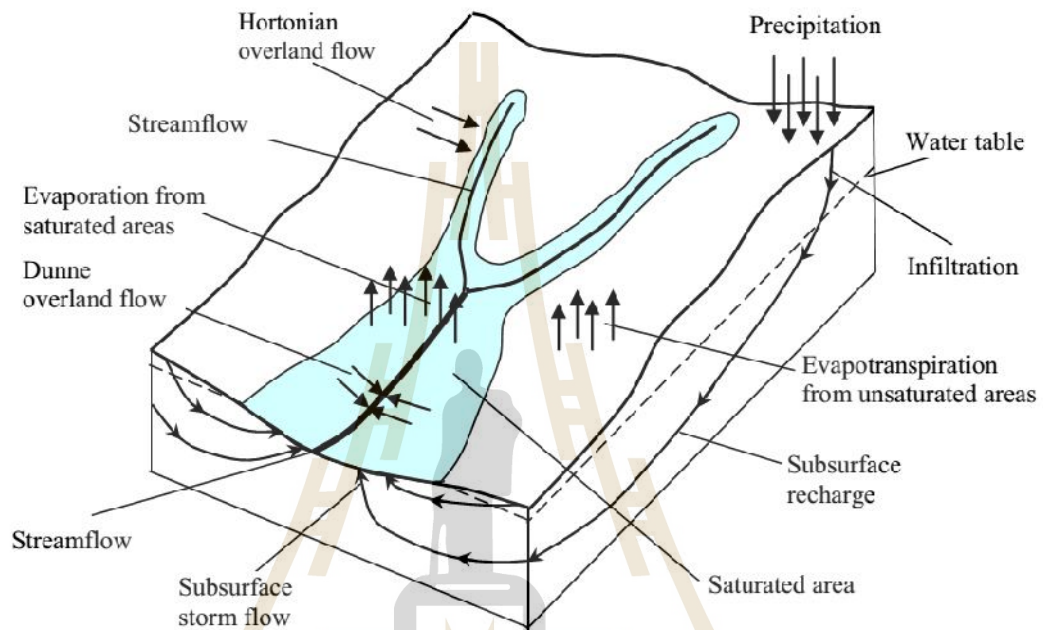


Figure 4.1 Conceptual description of the hydrological processes in hillslope pixels (Li et al., 2014)

- (1) The spatial units are DEM pixels grouped into hillslope pixels and channel pixels. Soil depth and soil hydraulic properties (hydraulic conductivity, porosity etc.) are assigned to each pixel.
- (2) For every pixel and every time step, HOF is estimated based on local infiltration capacity given by Green-Ampt method (1911). Later on soil moisture content is changed and the other two runoff generation mechanisms are possible: DOF and SSF.

(3) A simple two-layer soil model is used to simulate soil-water processes both in unsaturated and saturated layers.

(4) Overland flow is routed to downstream pixels at open channel velocity estimated by Manning's equation and subsurface is routed downstream at a subsurface velocity given by Darcy's law. Apart from river network geometry and soil depth, heterogeneity of other parameters is ignored such as soil properties, vegetation pattern, preferential pathways on the surface and in the subsurface. The details of the model and description of procedure and underlying equation and concepts are provided as following.

4.3.1 Soil-water moisture and water balance

To represent the dynamics of soil-water moisture in the pixel, a water balance equation can be applied at the pixel scale. In this study, the soil-water moisture in the soil column is divided into a ponding, unsaturated and saturated zone. Saturated soil-water moisture in the saturated zone is below the water table in the soil column. There are exchanges between the saturated zone and above unsaturated zone through capillary action and allow the retention of water in the unsaturated zone. Given the depth of unsaturated zone, the steady-state soil moisture profile in the unsaturated zone can be estimated by,

$$\theta_w(Z) = w \left(\frac{D_{us} - Z}{\zeta_a} + 1 \right)^{-\lambda} \quad (4.1)$$

Where $\theta_w(Z)$ is soil moisture in the soil column with a depth Z from the ground surface, ζ_a is bubbling pressure head, and λ is the pore-size distribution index

(Brooks and Corey, 1966). The average soil moisture in the unsaturated zone can be estimated by integrating Equation (4.1),

$$\bar{n} = \frac{w}{1-\beta} \frac{\Gamma_a}{D_{us}} \left[\left(\frac{D_{us}}{\Gamma_a} + 1 \right)^{1-\beta} - 1 \right] \quad (4.2)$$

The total soil water storage is given by,

$$S_{total} = D_{us} \bar{n} + D_s w \quad (4.3)$$

Where D_{us} is variable depth of the unsaturated zone, D_s is variable depth of the saturated zone and summation of D_{us} and D_s is the local soil depth (D), \bar{n} is the average soil moisture in unsaturated zone, and w is the effective porosity of the soil.

$$\frac{dS_s}{dt} = i - q_f - q_{se} - q_{ss} - e \quad (4.4)$$

$$D_{us} = (D - D_s) / \bar{n} \quad (4.5)$$

Where S_s is soil-water moisture in saturated zone ($= D_s w$), i is precipitation rate, q_f is infiltration excess runoff, q_{se} is saturation excess runoff, q_{ss} is subsurface storm flow and e is evapotranspiration rate. Equation (4.2) (4.4) (4.5) are solved for a new set of S_s D_s D_{us} \bar{n} , which satisfy the water balance condition. The new set of these parameters will be used for the next time step to estimate infiltration, evaporation and runoff generation.

4.3.2 Evapotranspiration

During inter-storm period, evapotranspiration is assumed to occur in three types with sequential order from surface unsaturated and saturated zone of the soil. Evaporation from water on the soil surface (if exists) is given by,

$$e_{ss} = \begin{cases} e_p & \text{if } d_w \geq e_p \Delta t \\ d_w / \Delta t & \text{if } d_w < e_p \Delta t \end{cases} \quad (4.6)$$

Where d_w is the local depth of surface water and e_p is the potential evaporation rate. If soil moisture is available for evaporation in the unsaturated zone of the soil column, evapotranspiration is given by,

$$e_{us} = \begin{cases} (e_p - e_{ss}) F_r \frac{n}{W} & \text{if } D_{us}^- \geq (e_p - e_{ss}) \Delta t \\ D_{us}^- / \Delta t & \text{if } D_{us}^- < (e_p - e_{ss}) \Delta t \end{cases} \quad (4.7)$$

Where F_r is the fraction of roots zone in the soil column, assumed to be unity. If soil moisture is still available for evapotranspiration in deeper saturated zone of the soil column. This evapotranspiration is given by,

$$e_{sat} = \begin{cases} 0 & \text{if } D_{us}^- \geq (e_p - e_{ss}) \Delta t \\ (e_p - e_{ss}) - D_{us}^- / \Delta t & \text{if } D_{us}^- < (e_p - e_{ss}) \Delta t \end{cases} \quad (4.8)$$

Potential evaporation demand is fully satisfied when the water table is close to the ground surface or soil surface is saturated during ponding period. Total evapotranspiration from all three zones will not exceed the potential evaporation rate.

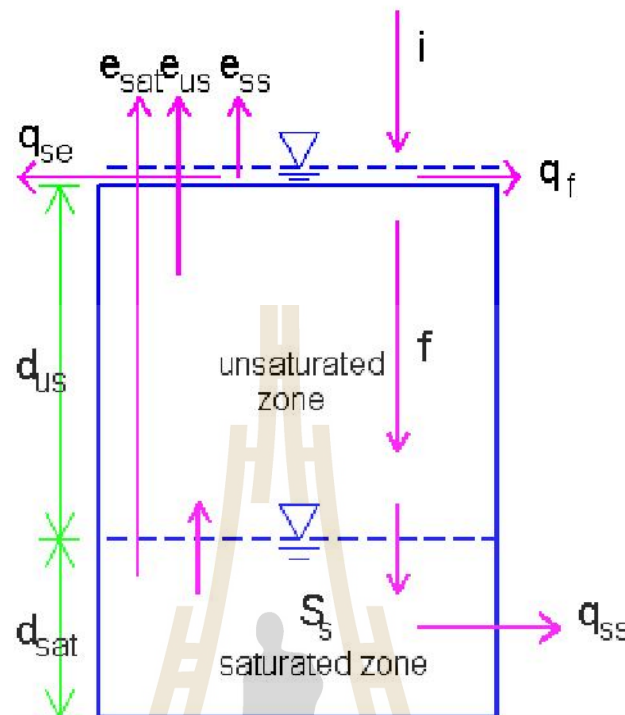


Figure 4.2 Schematic diagram of the pixel-based model structure of single soil column

4.3.3. Runoff generation process

Horton Overland Flow (HOF), saturation excess or Dunne Overland Flow (DOF), Subsurface Storm Flow (SSF) are three mechanisms of runoff generation processes. HOF occurs in a pixel when rainfall intensity exceeds the infiltration capacity. The dynamics of soil moisture in the unsaturated zone influence infiltration rate are estimated by using the Green-Ampt equation. DOF occurs in any pixel when the soil column is completely saturated from bottom, and forming the variable contributing area from a number of saturated pixels. Subsurface storm flow is generated from saturated zone of the pixels governed by saturated soil depth and downstream hydraulic gradient. At the same time, if the soil column receives water

more than lost it, saturated zone in the soil column may increase through the ground surface to generate DOF. In this situation, DOF and SSF are co-exist processes (Figure 4.2).

4.3.4. Routing processes at the pixel scale

The soil column of each pixel receives external water including lateral overland flow and subsurface discharge from neighboring upstream pixels. Routing of both surface and subsurface runoff is carried out based on two assumptions (1) outflow from each pixel will not be affected by inflow water over a short time step, (2) there is only one direction for outflow from each pixel, corresponding to the steepest slope with constant velocity (u), whereas there are 7 possible directions for inflow from its neighboring upstream pixels. Figure 4.3 presents outflow of pixel A, B, G into pixel E and only one outflow of pixel E into pixel I.

Over a short time interval (Δt), the volume of outflow from the grid is $u \cdot \Delta t \cdot \Delta x \cdot h$ equal the change of storage volume in the grid, $\Delta h \cdot \Delta x \cdot \Delta x$, where Δx is grid size in square shape, h is the water depth in the grid, Δh is the change of water depth. Integrating over Δt , the volume of outflow of a grid to downstream grid is,

$$\Delta V = h \left(1 - \exp \left(-u \cdot \frac{\Delta t}{\Delta x} \right) \right) \Delta x^2 \quad (4.9)$$

This routing scheme is applied to both ground surface and saturated zone. Overland flow velocity are estimated based on Manning 's equation as follows:

$$u_s = \frac{1}{n} S_0^{1/2} h_s^{2/3} \quad (4.10)$$

Where u_s is local velocity of overland flow, n is Manning 's coefficient, S_0 is the local surface slope and h_s is the surface water depth. Manning n for hill-slope pixels is 0.1 for grass/pasture range and is 0.06 for channel pixels.

Surface velocity is given by Darcy 's velocity as follows:

$$u_{ss} = k_s S_1 \quad (4.11)$$

Where S_1 is local bedrock slope, k_s is saturated hydraulic conductivity. We assume that subsurface water flows across pixels in only the saturated zone with water table slope parallel to the bedrock slope.

$$q_{ss} = u_{ss} A = k_s S_1 s_s(t) dx / dx^2 \quad (4.12)$$

Where q_{ss} is subsurface flow with the unit in L/T, $s_s(t)$ is soil-water moisture in saturated zone and dx is pixel size in m.

Finally, runoff from HOF, DOF and SSF reach the stream network and then is routed downstream through the channel pixels forming river network. The river network is assumed to be rectangular, width of the channel is estimated based on the hydraulic geometry relationship (Menabde and Sivapalan, 2001):

$$W = aA^b \quad (4.13)$$

Where A is the upstream catchment area corresponding to each river pixel at the catchment outlet, b is a constant parameter, which is 0.45, and a is a coefficient which can be adjusted to provide appropriate channel widths.

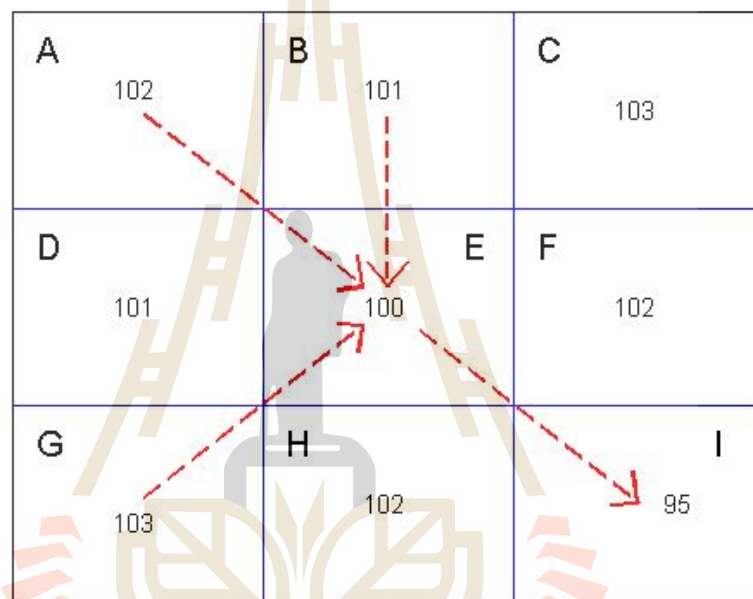


Figure 4.3 Multi inflow directions upstream of pixel E and only one outflow direction from pixel E depending on its elevation (100)

4.3.5. Topography

The topographic structure of a catchment is an important control on the dominance of runoff generation mechanisms. Overall steepness of the hillslope is chosen for this study which is the most dominant control compare to the other distribution of hillslope including convergence/divergence and convexity/concavity. A single realistic catchment is used to create new virtual catchment based on the 30 x

30 m DEM for a small catchment (4,019 pixels, 3.62 km²) located in Lam Ta Klong River Basin, Nakhon Ratchasima province, Thailand. Three types of slope distribution (flat, medium, steep) are generated by multiplying the original pixel slope by a factor.

4.3.6 Soil properties

Required soil properties for the model including saturated hydraulic conductivity, soil depth, effective porosity, wetting front soil suction head, bubbling pressure and pore-size distribution index. These properties vary in space and in multiple scales, and its variability can control the response. Only the first-order control of soil texture is chosen to investigate and leave the other effects to be considered in future research. Soil hydraulic properties are varied according to three texture classes: sand, silt loam and clay loam. Variation of soil depth (Z_x) is assumed to be a linear function of the topographic wetness index ($\ln(a/\tan s)$) (Stieglitz et al., 2003).

$$Z_x = \bar{Z} - (1/f) [\ln(a/\tan s)_x - \bar{\}}] \quad (4.14)$$

Where a is area drained per unit contour length, s is local slope angle, \bar{Z} is mean water table depth (WTD), $\bar{\}}$ is mean watershed value of $\ln(a/\tan s)$, and f is rate of decline of saturated hydraulic conductivity with depth in the soil column. The slope parameter of this function is adjusted to keep the main soil depth over entire catchment under three representative cases of soil depth: shallow, medium and deep with 1.0, 2.5 and 4.0 meters, respectively.

4.4 RESULTS AND DISCUSSION

Figure 4.4 presents simulated results from an infiltration model based on Green-Ampt equation to estimate excess rainfall hyetograph or HOF if the total rainfall of 11.37 cm. falls on a sandy loam soil ($K=1.09$ cm/h, $\Phi = 11.01$ cm and $n_e = 0.412$) of initial effective saturation 40%.

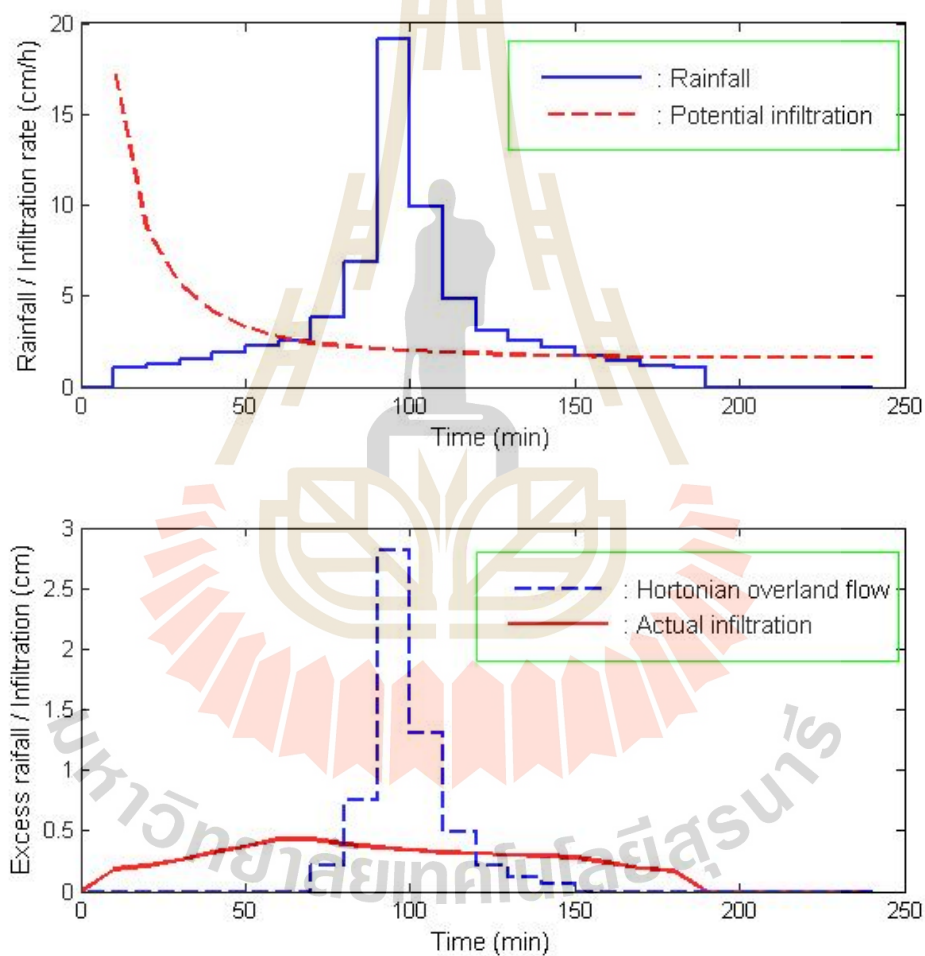


Figure 4.4 Estimation of Hortonian overland flow based on Green-Ampt equation

Model results of water balance in a soil column of pixel show in Figure 4.5. Testing soil is sand with effective porosity = 0.417, bubbling pressure = 0.0726 m, pore-size distribution index = 0.694, hydraulic conductivity = 10^{-6} m/s, soil depth = 1 m and surface slope = 0.10. Climate regime is generated with annual rainfall = 1,000 mm, annual potential evaporation = 500 mm, number of storm = 90 events/year, average rainfall intensity is 0.673 mm/hr. Simulated results in Figure 4.5 shows only 4 input storm events in steady state condition when initial and final saturation soil-water storages are equal. Figure 4.5(b) presents accumulated input and output from soil column of the pixel. Model results in Figure 4.5(b) indicated that HOF hardly coexist with DOF and SSF, very little HOF is generated under condition that supports DOF and SSF.

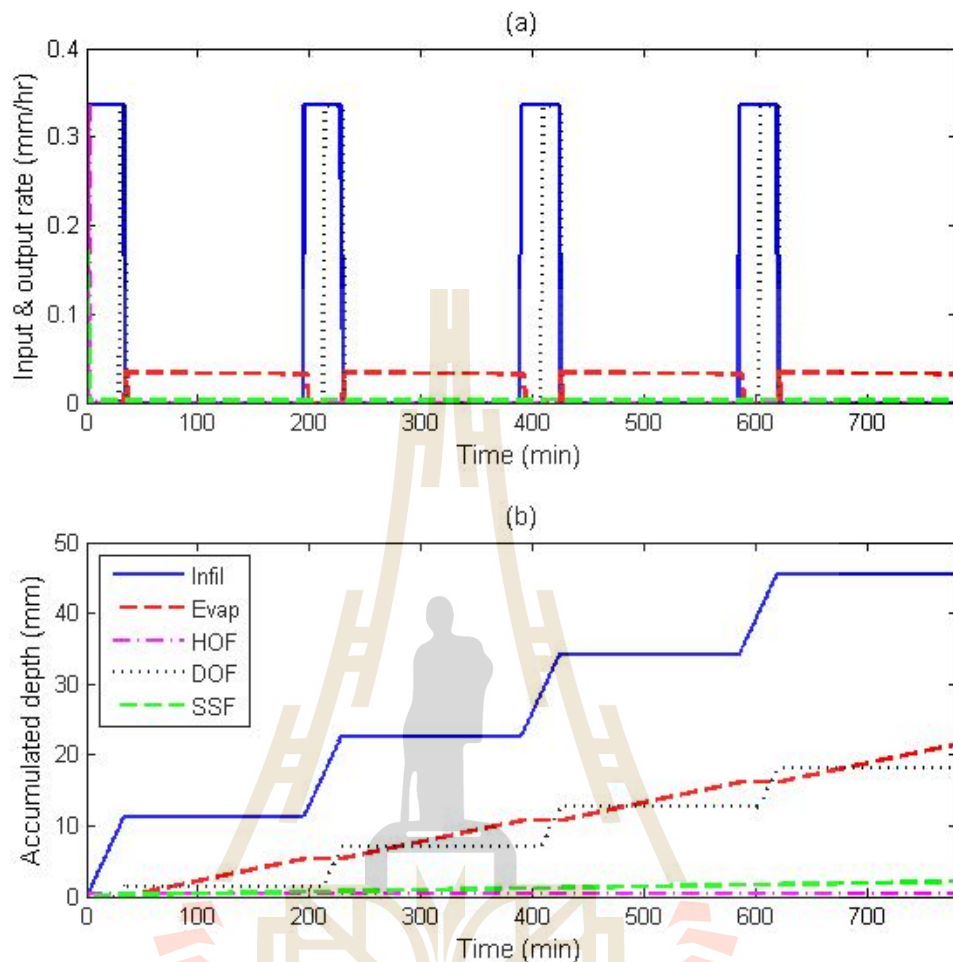


Figure 4.5 Water balance of input and output water from a pixel

Figure 4.6(a) shows topographic map of original DEM from Lam Ta Klong River Basin, the range of soil surface elevation is between 370 to 842 m. If combined overland flow from each pixel is 10 mm/h with duration 10 h, average soil depth = 2.5 m, $K = 10^{-4}$ m/s, $\Delta t = 10$ min, $\bar{Z} = 2$ m, $f = 1$ and $\beta = 5.38$ (for Equation 10). Hillslope and channel routing are carried out with the sequence of its elevation from upstream to downstream, providing downstream discharge at each pixel. For channel geometry,

parameters in Equation (13) $a = 25$ and $b = 0.45$. Figure 4.6 (b) presents discharge hydrograph (in mm) from pixel No.1 the most upstream pixel, pixel No.1652 (344 grids, 0.31 km²), pixel No.3104 (1814 grids, 1.63 km²), pixel No. 3806 (3590 grids, 3.23 km²) and the outlet of the basin, pixel No.4019 (4018 grids, 3.62 km²). Attenuation of downstream hydrographs show realistic manner.

4.5 CONCLUSIONS

A simple distributed hydraulic model is developed at the pixel/soil column scale and upscale to implement at the catchment scale. Applied water balance concept within the pixel and downstream interactions between each pixel allow the runoff generation by three mechanisms: HOF, DOF and SSF. Based on an actual building block of selected DEM, the model can be parameterized for a large set of hypothetical catchments and input climate events. Simulation results are received when all processes are driven to reach a periodic steady state by a sequence of identical climate events. In the next step, this model will be used to investigate the climate, soil and topographic controls on annual water balance in a qualitative way to define dimensionless functional relationships.

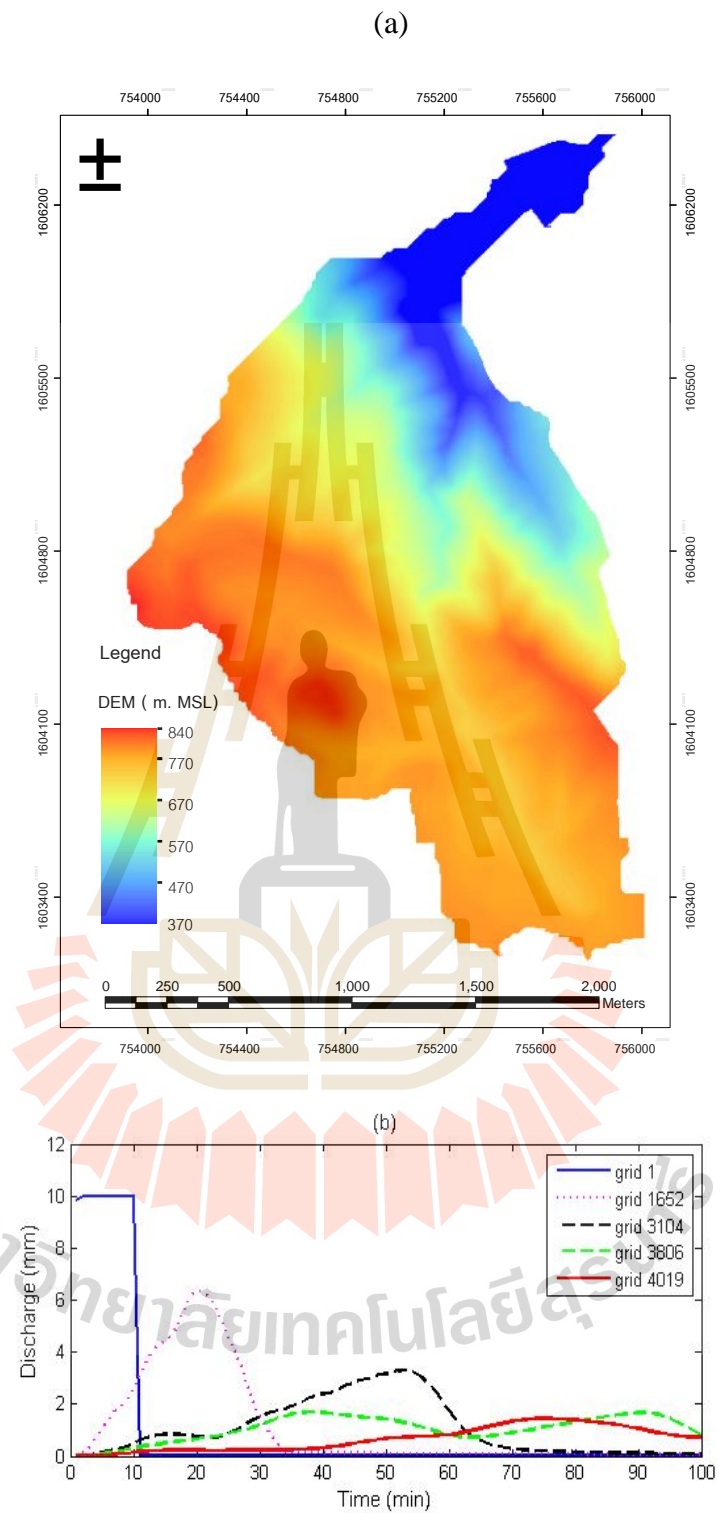


Figure 4.6 Output hydrograph form pixels based on combination of pixel and channel routing processes

4.6 References

- Beven, K.J., and Kirkby, M.J. (1979). **A physically-based variable contributing area model of basin hydrology**, *Hydrol. Sci. J.*, 24(1), 43-69.
- Brooks, R.H., and Corey A.T. (1966). **Properties of porous media affecting fluid flow**, *J. Irrig. Drain. Div. Am. Soc. Civ. Eng.*, IR2, 61–88.
- Carrillo, G., Torch, P.A., Sivapalan, M., Wagener, T., Harman, C., and Sawicz, K. (2011). **Catchment classification: hydrological analysis of catchment behavior through process-based modeling along a climate gradient**, *Hydrol. Earth Syst. Sci.*, 15, 3411-3430, doi:10.5194/hess-15-3411-2011,2011.
- Dunne, T. (1978). **Field studies of hillslope flow processes**, In: *Hillslope Hydrology* (M.J. Kirby, Editor), 227-293, J. Wiley & Son.
- Green, W.H., and Ampt, G.A. (1911). **Studies on soil physics, I. The flow of air and water through soils**, *J. Agric. Sci.*, 4, 1–24.
- Horton, R.E. (1933). **The role of infiltration in the hydrologic cycle**. *Trans. Am. Geophys. Union*.
- Larsen, J.E., Sivapalan, M., Coles, N.A., and Linnet, P.E. (1994). **Similarity analysis of runoff generation processes in real world catchments**, *Water Resour. Res.*, 30(6), 1641-1652.
- Li, H.Y., Sivapalan, M., Tian, F., and Harman, C. (2014). **Functional approach to exploring climatic and landscape controls of runoff generation: 1. Behavioral constraints on runoff volume**, *Water Resour. Res.*, 50, 9300–9322, doi:10.1002/2014WR016307.2014WR016307.

- Menabde, M., and Sivapalan, M. (2001). **Linking space-time variability of river runoff and rainfall fields: a dynamic approach**, *Adv. Water Resour.*, 24(9-10), 1001–1014.
- Mirus, B.B. and Loague, K. (2013). **How runoff begins (and ends): Characterizing hydrologic response at the catchment scale**, *Water Resour. Res.*, 49, 2987-3006, doi:10.1002/wrcr.20218.
- Robinson, J.S., and Sivapalan, M. (1995). **Catchment scale model of runoff generation by aggregation and similarity analysis**, *Hydrol. Process.*, 9, 5/6, 555-574.
- Sivapalan, M., Beven, K. and Wood E.F., (1987). **On hydrologic similarity, 2. A scaled model of storm runoff production**. *Water Resour. Res.*, 23(12), 2266-2278.
- Stieglitz, M., Sherman, J., McNamara, J., Engel, V., Shanley, J. and Kling, G.W. (2003). **An approach to understanding hydrologic connectivity on the hillslope and the implication for nutrient transport**. *Global Biogeochem. Cycles*, 17(4), 1105, doi: 10.1029/ 2003 GB002041.
- Troch, P.A., Carrillo, G., Sivapalan, M., Wagener, T. and Sawicz, K. (2013). **Climate-vegetation-soil interactions and long-term hydrologic partitioning: Signatures of catchment co-evolution**, *Hydrol. Earth Syst. Sci.*, 17, 2209–2217, doi:10.5194/hess-17-2209-2013.

CHAPTER V

**FLOOD HAZARD MAPPING USING ON-SITE
SURVEYED FLOOD MAP, HECRAS V.5 AND
GIS TOOL: A CASE STUDY OF
NAKHON RATCHASIMA MUNICIPALITY,
THAILAND**

5.1 Summary

For a small flood affected area, satellite data normally provides physical properties of flood event with low accuracy information (location and boundary). Flood depth and flood duration cannot be identified from a snapshot of satellite image. Therefore, on-site surveying of historical flood properties and its impact are still essential and this observed flood map is realistic and reliable information for future flood management. The objective of this study is to constructing flood hazard map from available observed flood map of the small flood affected area and use HEC-RAS V.5 and GIS tool to formulate flood hazard map for future scenarios. This method was applied for the municipality of Nakhon Ratchasima, Thailand. For a simulation, input physical parameters were generated by Hec-GeoRAS in ArcGIS based on DEM ($5 \times 5 \text{ m}^2$). A range of calibrated Manning's n in a main channel was obtained from fitting exercise with observed Rating curve. Land-use map was used to

estimate the Manning's n in floodplain depending upon the type of land cover. Simulated results were exported to ArcGIS to delineate water surface on floodplain. Then, the maximum discharge value at the observed station (M.164) for return periods of 5, 10, 15, 25, 50, and 100 years were used as upstream input flood to simulate the flood map. It is found that, for the 2010 flooding event in the concerning area, the simulated flood hazard map subjected to the discharge of 50 years ($217 \text{ m}^3/\text{s}$) return period which is almost identical with the observed flood map from the surveying.

5.2 Introduction

Floods can be considered as the most important natural disaster with higher frequency of occurrence higher than any other natural disaster and affecting more people than the other natural hazards together (ARDC, 2009). Floods are related to social–civil conflicts (Ghimire et al., 2015) environmental problems (Jia and Wenjiao, 2015) and economic losses (Aerts and Botzen, 2011). Floodplains can be defined as the areas that are periodically inundated by the overflow of river (Maskong and Jothityangkoon, 2013). In 2010, Nakhon Ratchasima province received excessive rainfall in successive day during 14 – 16 October 2010. A majority of the floodplain area in Nakhon Ratchasima province suffered from this serious flooding event. Heavy rains caused a large amount of runoff flow into both upstream and downstream of all reservoirs in Nakhon Ratchasima province including Lam Takong and Lam Prapleng Dams. With ongoing water flowing into these reservoirs until excess its capacity, the water level was higher than the level of emergency service spillway which in turn causes severe uncontrolled flood flow into many municipalities downstream. Moreover, most of water flow rapidly over lands into the canal and combined with the

overflow water from many dams. The combination of these events caused widespread flooding on the floodplain in lower basin, including Muang Nakhon Ratchasima district, Pukthongchai district and Chaloeprakiat district, etc. Flood water from tributary of Mun River was drained slowly into Mun River because the water level in Mun River was higher than the water level in tributary canals and there are a lot of obstructions in the canal which resulted in reducing flow speed (Kongjun and Noypairoj, 2011; Ponsan and Panchana, 2011; Reports of Members on the Impact of Tropical Cyclones, 2011).

The river flood modelling is a tool for evaluation and prediction of river flood risk in different scenarios. River flood risk modelling comprise of hydrological modelling, hydraulic modelling, river flood visualization and river flood mapping (Alaghmand, 2009). A flood hazard map is a graphical representation of flood inundation (inundation depths, extent, flow velocity etc.) expected for an event of given probability or several probabilities (APFM, 2013). The flood hazard map will help responsible authorities to target on the area with higher hazard where flood mitigation plans have to be effectively implemented. The flood hazard map will give public tangible imagery of its impact on their community. Flood hazard maps will not prevent floods from occurring, but they are an essential tool for warning and mitigation the damage of property and loss of life caused by floods, and for communicating flood risk. Nowadays, hydraulic simulation tools are available to model channel discharge and flooding in floodplains with 1D and 2D approaches. The Hydrologic Engineering Center River Analysis System (HEC-RAS) is free software with a friendly graphical user interface that was successfully used for flood studies (US Army Corps of Engineers, 2014; Knell et al., 2005; Lian et al., 2013;

Mohammadi et al., 2014), commercial software packages are widely used and distributed such as FLO-2D to simulate floods and flows (FLO-2D software, 2016) and the MIKE packets modelling tools (DHI Group, 2016). One of the most popular hydraulic models is HEC-RAS which announced and released its new HEC-RAS version 5 with 2D capabilities is a great innovation for flood studies (Brunner, 2014). The Flood map event was simulated by the 2D of the HEC-RAS 5 beta that shows good performance when compared with flood extent registered by satellite images (Moya et al., 2016). Furthermore, HEC-RAS has more accurate results of river flood map (flood extent and water depth) in comparison with MIKE11 in urban area. In recent years GIS integrated modelling applications have been made to integrate hydraulic models and GIS to facilitate the manipulation of the model output which led to the establishment of a new branch of hydraulics and hydrology. There are strong grounds for believing that GIS has an important function because natural hazards are multi-dimensional phenomena which have a spatial component [Alaghmand et al., 2013; Congressional Budget Office, 2009; Nakhon Ratchasima City Municipality, 2016]. The flood hazard map can be generated from a variety of tools, for example, (1) using vertical aerial photographs due to lacking of detailed topographic maps (Furdada et al., 2008), (2) using a remote sensing and GIS based flood index (Kabenge et al., 2017), using flood mark data (including flood depth and flood duration) and analytic hierarchy process (Luu et al., 2018).

The available flood map in Thailand from Geo-Informatics and Space Technology Development Agency (GISTDA) can present spatial data of inundation area and expansion of flood boundary. However, it cannot exhibit high resolution of flood depth and flood duration (Maskong and Jothityangkoon, 2013). In order to protect or at least mitigate the effect of flooding problems, physical characteristic of inundation area combining with consequent impact has to be defined in the form of flood hazard map. Therefore, this study aims to simulate flood hazard map from the 2010 flood event in Nakhon Ratchasima Municipality using the 2D capabilities of HEC-RAS V.5 application. The model provides the simulation of the flood extent and flood depth.

5.3 Study area and dataset

Nakhon Ratchasima Municipality is an urban center of Nakhon Ratchasima Province, Thailand where is located at the downstream of the Lam Ta Kong River, which is a tributary of Mun River Basin. The length of main stream of river is 17 km, and study area is 37.5 km² shown in Figure 5.1. The observed daily discharge data of the Lam Ta Kong River at station M.164 is provided by Royal Irrigation Department of Thailand. Mean annual rainfall is 1,373 mm and contributes to 510×10^6 m³ of the total average annual runoff. Figure 5.2 shows that majority of the areas are urban and built-up land-uses, where the population is approximately 136,153 people (Nakhon Ratchasima City Municipality, 2016). The geographic data based on the digital elevation model (DEM) from the Land Development Department of Thailand has a grid cell size of 5×5 m² demonstrating elevation between 172.6-204.6 m.MSL, shown in Figure 5.3.

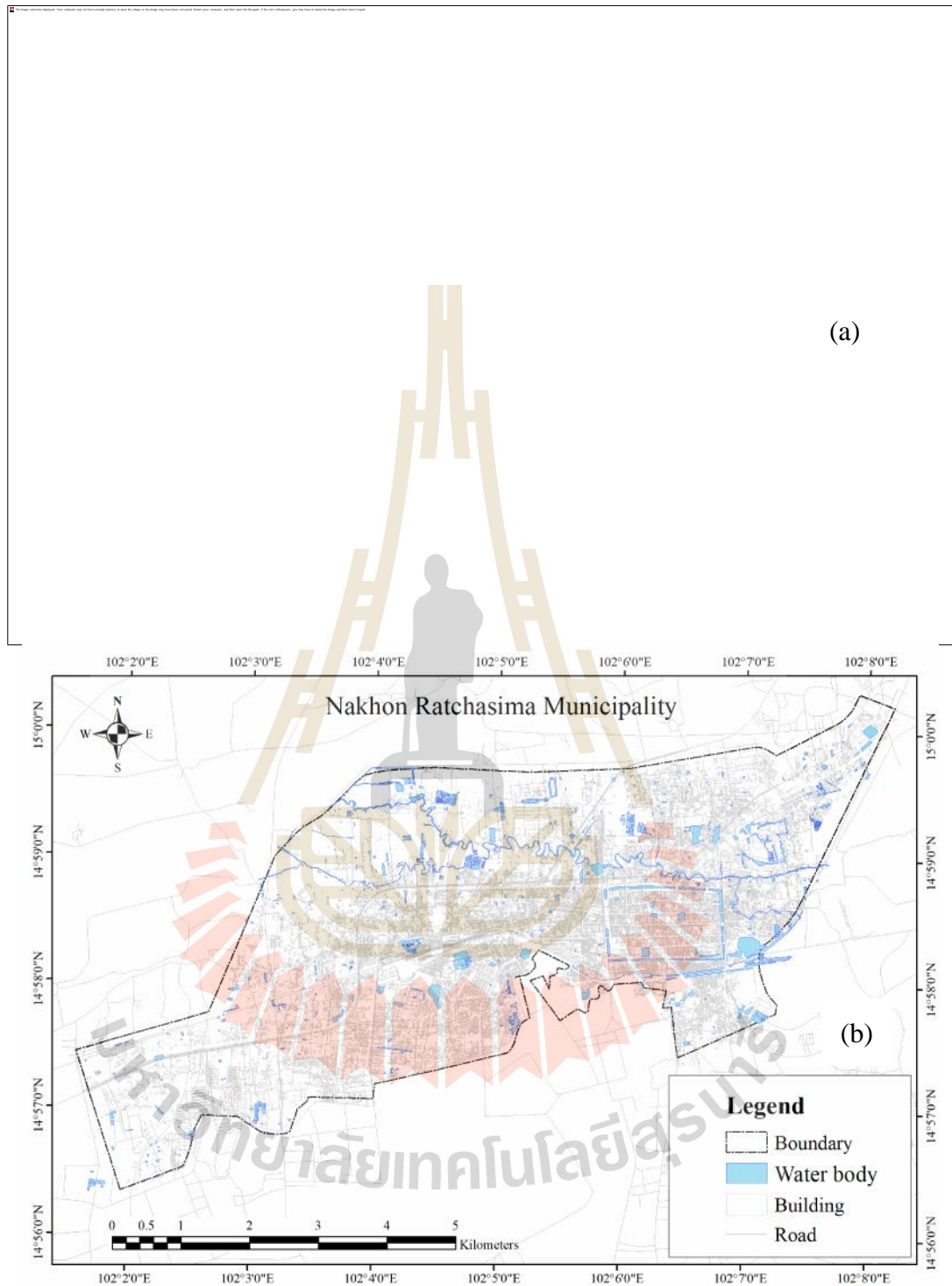


Figure 5.1 The boundary and location of the study area (a) Nakhon Ratchasima Province (b) Nakhon Ratchasima Municipality

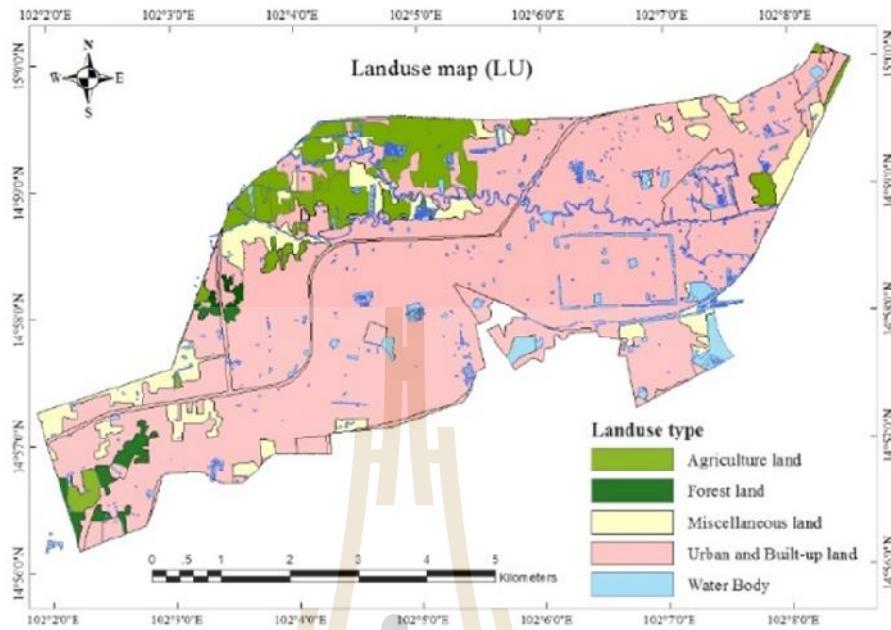


Figure 5.2 Land use of Nakhon Ratchasima Municipality

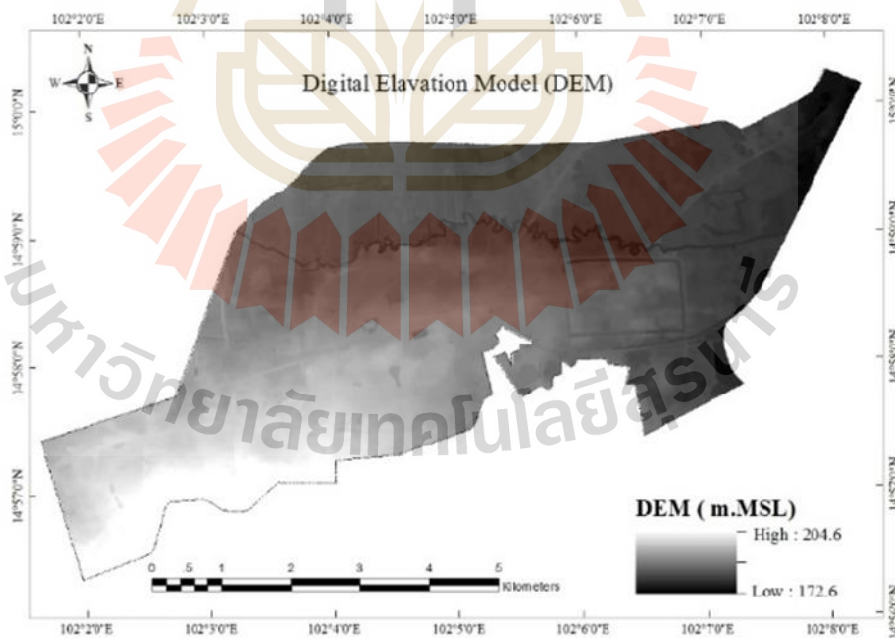


Figure 5.3 DEM of Nakhon Ratchasima Municipality

5.4 Methodology

The methodology for mapping a flood hazard map (shown in Figure 5.4) can be divided into two parts: review of flood and modeling approach for numerical simulation. Important step of these parts has been described below.

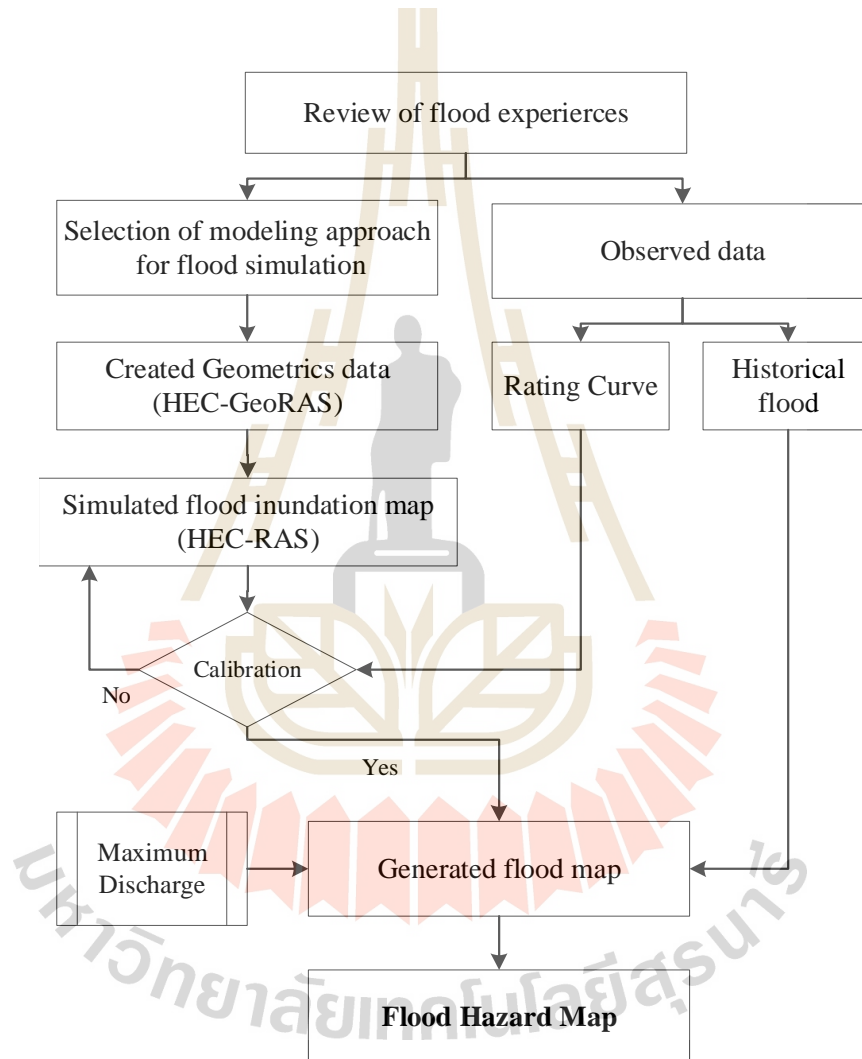


Figure 5.4 Flowchart of the study step, which is a conceptual framework of this study

5.5 Review of flood experiences

The lower northeastern part of Thailand was under low pressure groove during 1-19 October 2010. There was continuous heavy rain, especially in the Khao Yai National Park and covered very large surrounding areas. The accumulated areal rainfall was about 450 mm, which was about 40 % of the annual amount. The maximum 3-day rainfall (14-16 October 2010) in the upstream of Lam Ta Khong Dam was 180.3 mm, while in the downstream was 211.6 mm. The storage of Lam Ta Khong Dam and volume in all reservoirs rose very quickly and its downstream was extensively flooded. The dam operator failed to keep flood water in the reservoir. Since 17 October 2010, excess volume of flood began to overflow the service spillway at +277.30 m.MSL (Kongjun and Noypairoj, 2011; Ponsan and Panchana, 2011; Reports of Members on the Impact of Tropical Cyclones, 2011). Previous study (Maskong and Jothityangkoon, 2013) analyzed water balance of runoff found that accumulated depth of rainfall and volume of surface water in the year 2010 is higher than the other years. The severe scaling of flooding problem can be captured in the form of inundation map. Although, the boundary and location of 2010 flood inundation area is provided by GISTDA, its accuracy is low for small urban area. Figure 5 shown the surveyed point of flooding and the flood map obtained from field surveyed data represents is an inundation area and flood depth of Nakhon Ratchasima Municipality on 2010 flood event. This map can be developed further to include spatial variability of the depth and area and can be used to evaluate the hazard area and mitigation measures.

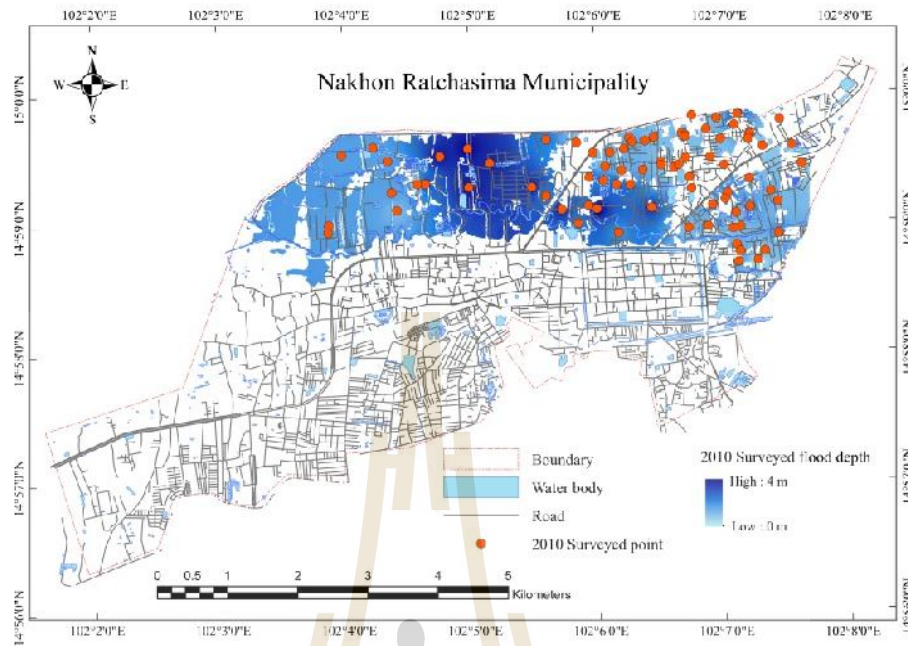


Figure 5.5 The 2010 surveyed point of flooding of Nakhon Ratchasima Municipality (modified from Maskong and Jothityangkoon, 2013)

5.6 Modeling approach for numerical simulation

A number of hydraulic simulation tools are available to model channel discharge and flooding in a flood plain with 1D and 2D approaches. One of the tools is provided by the Hydrology Engineering Center River Analysis System (HEC-RAS) which is available in public domain. Hence, a new HEC-RAS V.5 model developed by the United States Army Corps of Engineers (USACE) is used in this study to simulate the flood event in Nakhon Ratchasima Municipality. The new HEC-RAS V.5 can solve either the full 2D Saint Venant equations or the 2D diffusive wave equations.

$$\frac{\partial u}{\partial t} + \frac{\partial p}{\partial x} + \frac{\partial q}{\partial y} = 0 \quad (5.1)$$

$$\frac{\partial p}{\partial t} + \frac{\partial}{\partial x} \left(\frac{p^2}{h} \right) + \frac{\partial}{\partial y} \left(\frac{pq}{h} \right) = \frac{n^2 pg \sqrt{p^2 + q^2}}{h^2} - gh \frac{\partial u}{\partial x} + pf + \frac{\partial}{\partial x} (h\tau_{xx}) + \frac{\partial}{\partial y} (h\tau_{xy}) \quad (5.2)$$

$$\frac{\partial q}{\partial t} + \frac{\partial}{\partial y} \left(\frac{q^2}{h} \right) + \frac{\partial}{\partial x} \left(\frac{pq}{h} \right) = \frac{n^2 qg \sqrt{p^2 + q^2}}{h^2} - gh \frac{\partial u}{\partial y} + qf + \frac{\partial}{\partial y} (h\tau_{yy}) + \frac{\partial}{\partial x} (h\tau_{xy}) \quad (5.3)$$

Where h is the water depth (m), p and q are the specific flow in the x and y directions (m/s), z is the surface elevation (m), g is the acceleration due to gravity (m/s²), n is the Manning resistance, ρ is the water density (kg/m³), τ_{xx} , τ_{yy} and τ_{xy} are the components of the effective shear stress and f is the Coriolis (s⁻¹). When the diffusive wave is selected the inertial terms of the momentum equations Eq. (5.2) and (5.3) are neglected.

In HEC-RAS, the geometric data were imported which were exported from ArcGIS by HEC-GeoRAS tool. HEC-RAS V.5 can be used either as a fully 2D model or as a hybrid 1D, 2D model when the main rivers are modelled as 1D and the floodplains are modelled as 2D. Although a hybrid 1D, 2D model tends to be faster than a 2D model, such 1D, 2D model requires the user to define the connections between the 1D and the 2D models. Such connections require a prior definition of the overflow locations (Brunner, 2014).

The Extreme Value Type I distribution or Gumbel distribution is used to fit the observed or simulated annual maximum runoff by using below frequency factors (Chow et al., 1988).

$$K_T = -\frac{\sqrt{6}}{\pi} \left\{ 0.5772 + \ln \left[\ln \left(\frac{T}{T-1} \right) \right] \right\} \quad (5.4)$$

$$x_T = \bar{x} + K_T s \quad (5.5)$$

Where K_T is frequency factor, T is return period, x_T is magnitude of annual maximum at the given return period, \bar{x} is mean of annual maximum runoff and s the standard deviation of annual maximum runoff. For a given specific return period, the annual maximum flood can be estimated from these equations.

5.7 Results and discussion

5.7.1 Observed annual maximum discharge

The observed annual maximum discharge at gauge station (M.164) was analyzed by Gumbel distributions shown in Table 5.1. The daily discharge recorded is 123.9 m³/s on 18th October 2010 as around 8 years return period. The previous study (Maskong and Jothityangkoon, 2013) found that the recorded discharge were possibly underestimated values. However, it would be a condition data of the flood simulation.

Table 5.1 Observed annual maximum discharges for different return periods at M.164

T(year)	2	5	10	15	20	25	50	100
Q(m ³ /s)	52	105	140	159	173	184	217	249

5.7.2 Roughness coefficients (Manning's n)

The geometric data including stream line, bank stations, cross section and flow path line were digitized and generated from DEM by Hec-GeoRAS tool in ArcGIS application. The rating curve at M.164 on 2010 and 2013 from the Royal Irrigation Department data were used to calibrate and validate the geometric data along the river by varying the Manning's n values. As a result, Figure 5.6 clearly shows that the n values between 0.020-0.035 (vary with elevation of main channel) and it provides the simulated rating curve with good agreement to the observed rating curve as shown in table 5.2. Therefore, these ranged of n values were used as the suitable physical data of the further simulation. In addition, the n values for the floodplain consisting of different land-use type were selected based on the observed and recommended data as summarized in Table 5.3 (Brunner, 2014).

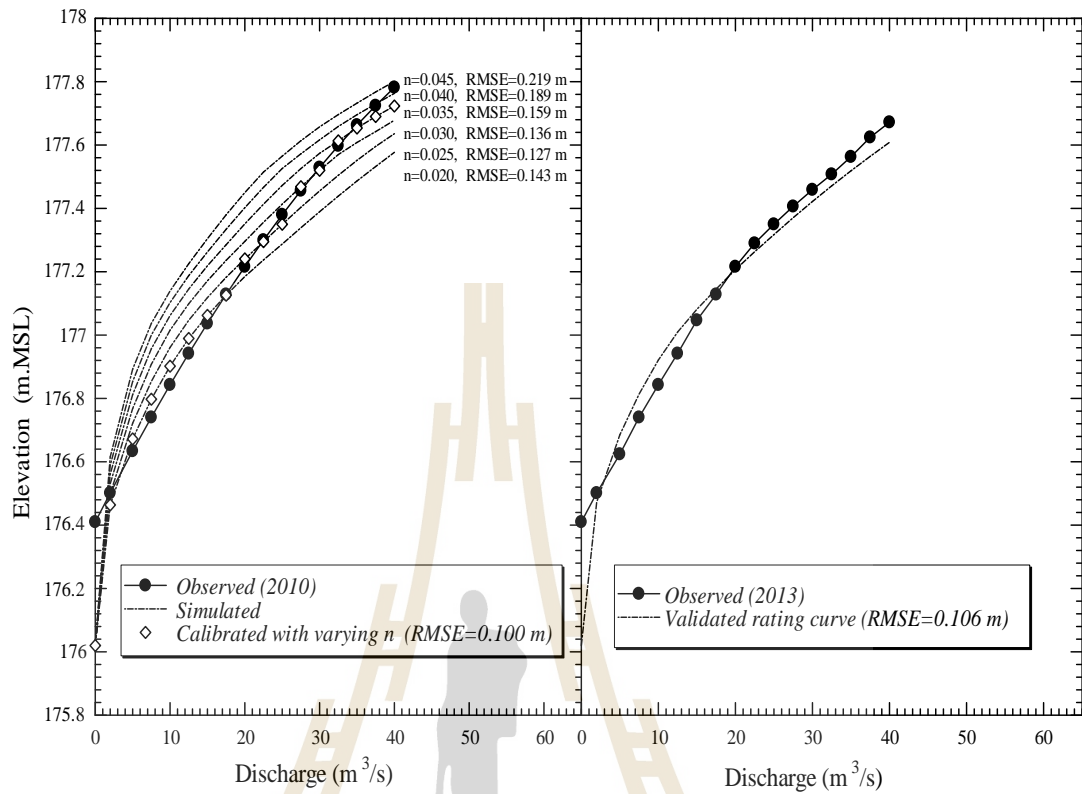


Figure 5.6 Comparison of Rating curve between calculated and simulated

Table 5.2 Comparison between calculated and simulated Rating curve

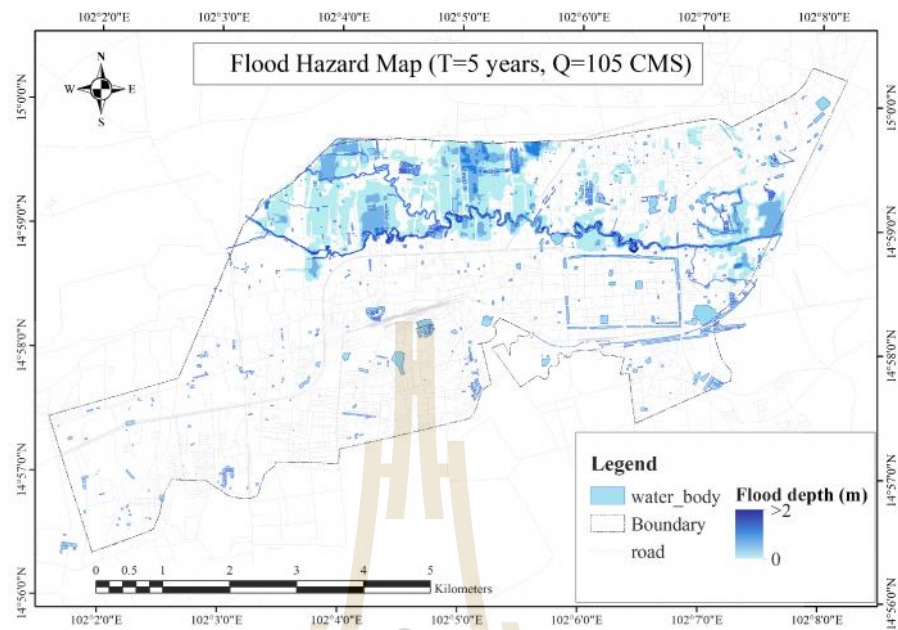
Manning's n	0.020	0.025	0.030	0.035	0.040	0.045	Vary (0.020-0.035)
RMSE	0.143	0.127	0.136	0.159	0.189	0.219	0.100

Table 5.3 The value of the manning roughness (n)

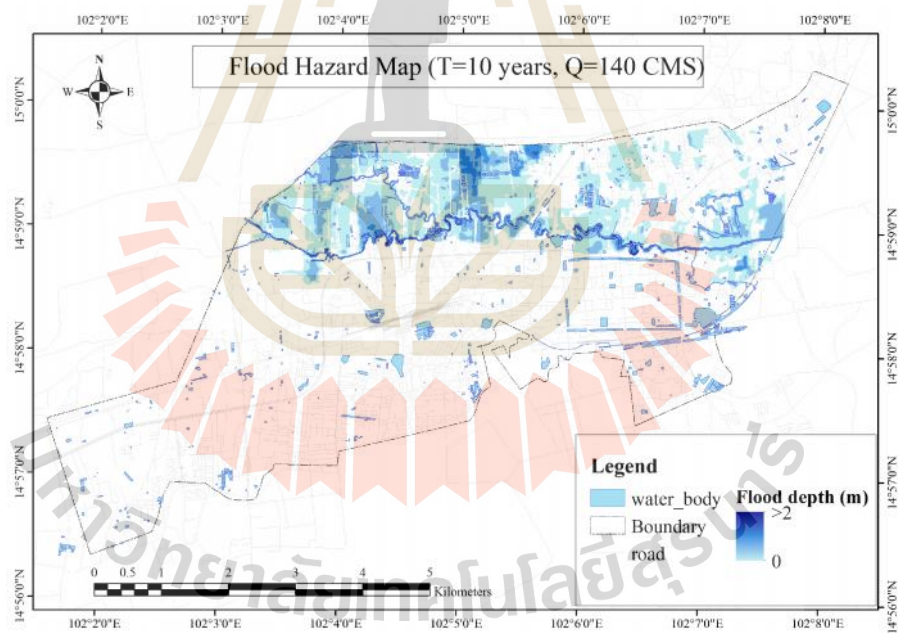
Land use	Value
Main channel of river	0.020-0.035
Land use on floodplain	
<i>Agriculture land (A)</i>	0.045
<i>Forest land (F)</i>	0.06
<i>Urban and built-up land (U)</i>	0.055
<i>Miscellaneous land (M)</i>	0.05
<i>Water Body (W)</i>	0.04

5.7.3 Flood hazard map

Figures 5.7 (a)-(f) illustrate flood hazard map subjected to various maximum discharges with different return periods (T=5, 10, 15, 25, 50 and 100 years) as mentioned in previous section. Flood extent for all return periods are shown as a similar pattern. The floods inundation areas are located at northern part of the river when the discharge is higher than the maximum capacity of the river ($40 \text{ m}^3/\text{s}$) and extend with increasing discharges. Figure 5.8 represent a comparison of flood depth between 2010 surveyed depth of flooding and simulated flood depth at annual maximum discharges for each different return period. The results also show that the simulated flood inundation areas of flood hazard map subjected to the 50 years return period (Figure 5.7 (e)) is almost identical with onsite saurveying flood map.

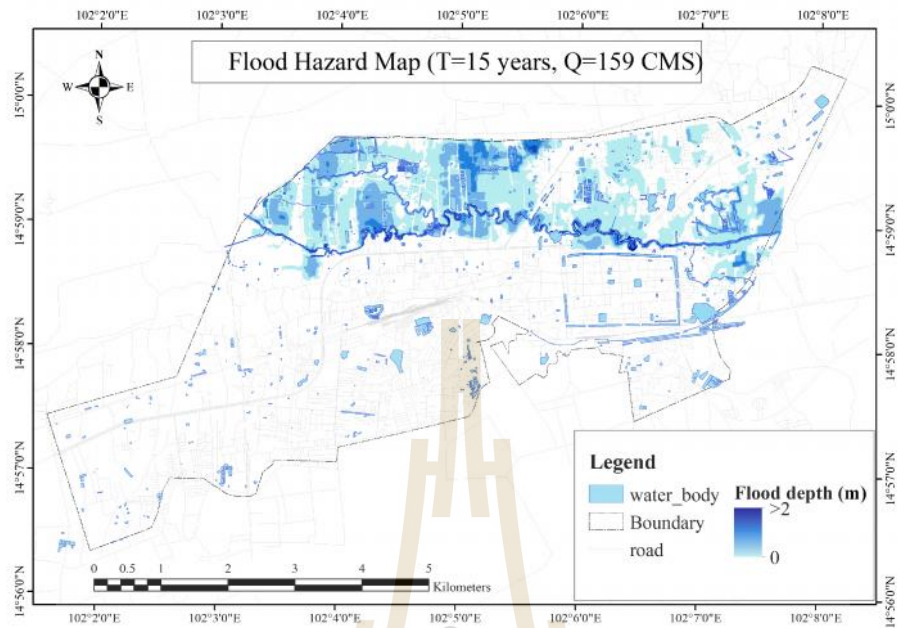


(a)

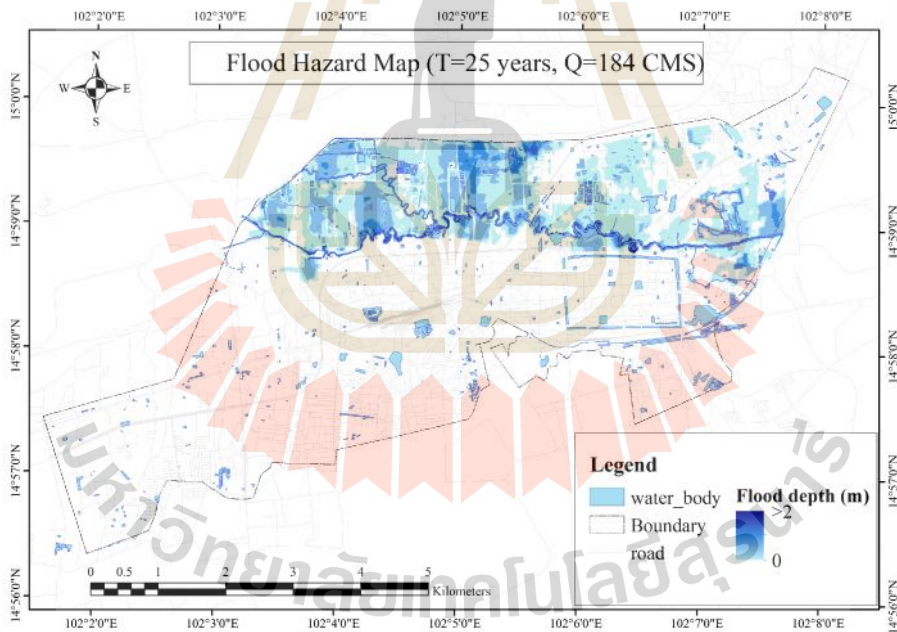


(b)

Figure 5.7 Simulated flood hazard area at the return periods (a) T=5 years, (b) T=10 years, (c) T=15 years, (d) T=25 years, (e) T=50 years and (f) T=100 years

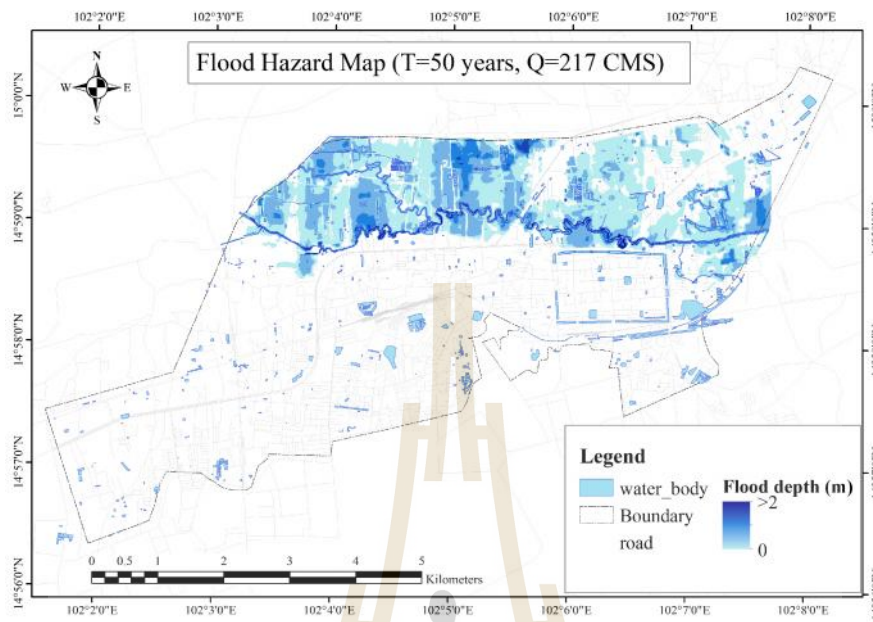


(c)

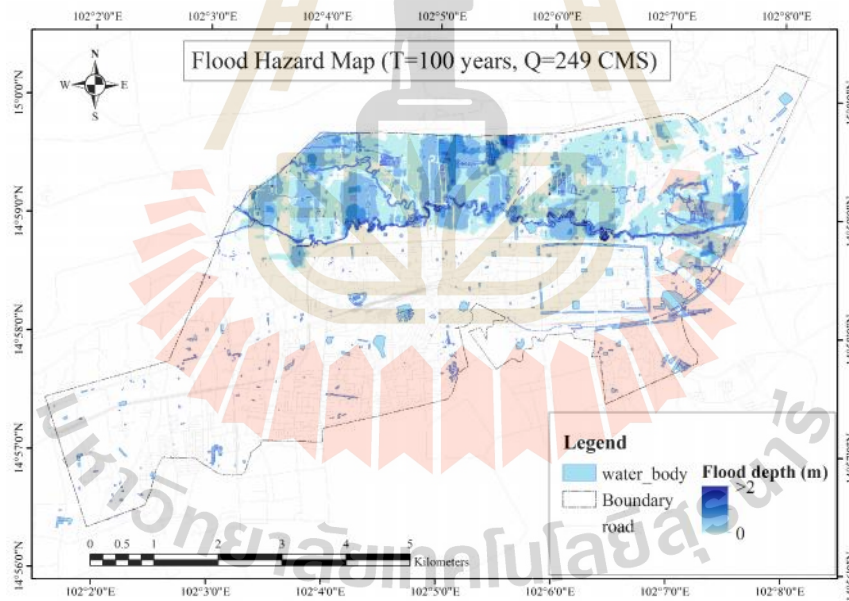


(d)

Figure 5.7 (Cont.) Simulated flood hazard area at the return periods (a) T=5 years, (b) T=10 years, (c) T=15 years, (d) T=25 years, (e) T=50 years and (f) T=100 years



(e)



(f)

Figure 5.7 (Cont.) Simulated flood hazard area at the return periods (a) T=5 years, (b) T=10 years, (c) T=15 years, (d) T=25 years, (e) T=50 years and (f) T=100 years

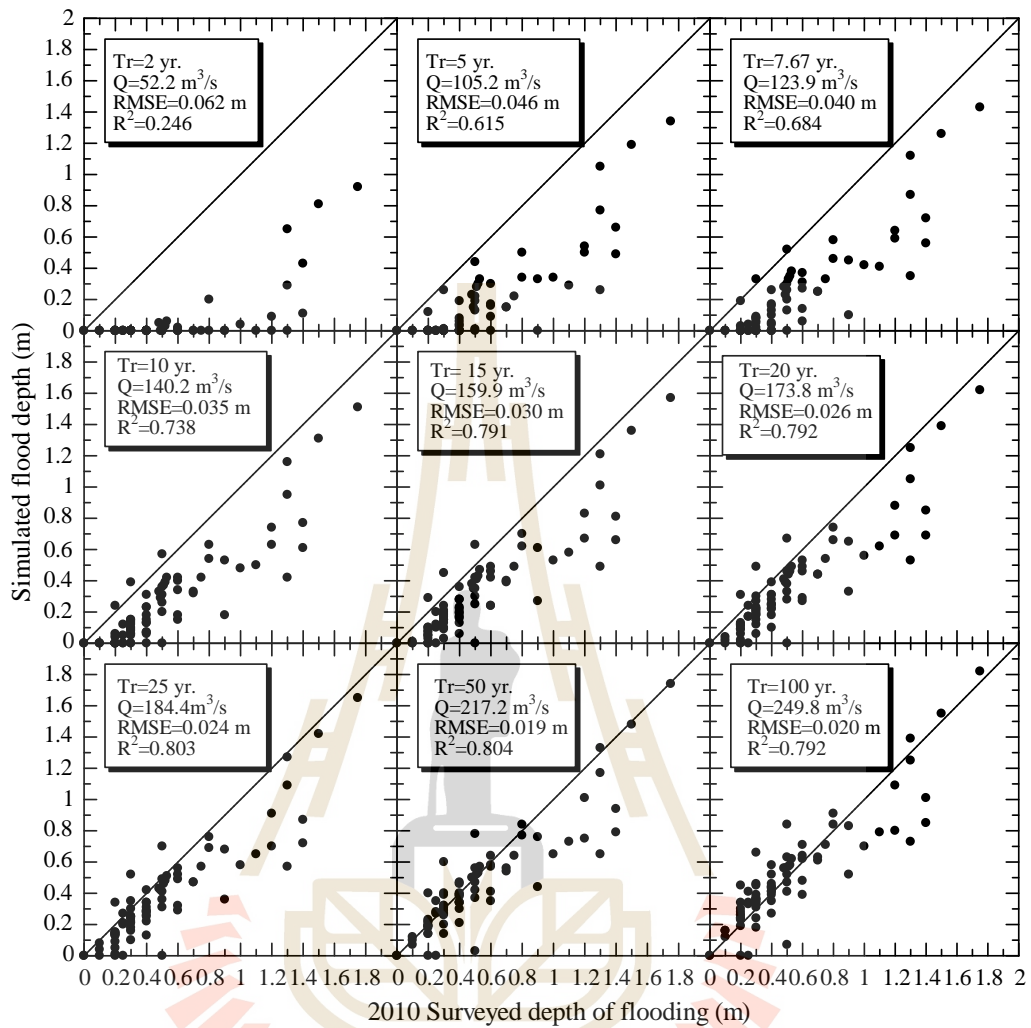


Figure 5.8 Comparison of flood depth between surveyed flood and simulated flood

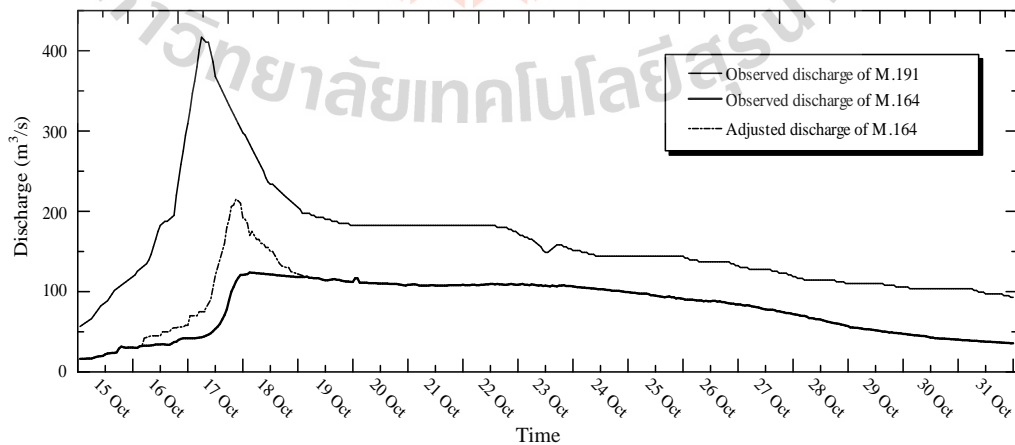


Figure 5.9 Adjusted hydrograph in 2010 flood event at M.164

5.8 Correction of flood hydrograph

During 2010 flood event, we suspected that there was an error of recorded hydrograph at station M.164. Peak discharge of observed hydrograph of M.191 upstream of M.164 was $410 \text{ m}^3/\text{s}$, whereas peak discharge of M.164 downstream was too low only $123 \text{ m}^3/\text{s}$ (Figure 5.1 and 5.9) (Maskong and Jothityangkoon, 2013). After successful mapping of the flood hazard map and found that the frequency of 2010 flood event was about 50 year return period. Based on this approach and simulation, a new hydrograph was generated and compared to recorded hydrograph. These results confirmed that the recorded hydrograph at M.164 was underestimated values. To correct this flood hydrograph, the new hydrograph represented by a dash line in Figure 5.9 was simulated to adjust the peak of observed hydrograph from 123 to $217 \text{ m}^3/\text{s}$.

5.9 Conclusion

To construct flood hazard map for a small flood affected area such as the Nakhon Ratchasima Municipality, studying step starts from (1) on-site surveying on 2010 flood event to construct observed flood map (2) applied HEC-RAS V.5 and GIS tool to receive high resolution geometric data ($\text{DEM } 5 \times 5 \text{ m}^2$) from HEC-GeoRAS in ArcGIS application and calibrated value of Manning's n for simulating 2D flood inundation extent and flood depth. Simulated flood hazard map based on input maximum discharge at different return periods confirmed that the simulated flood hazard area at 50 years return period is almost identical to 2010 observed flood event. One more application of the constructed flood hazard map is to correct the relative magnitude of peak discharges between upstream and downstream hydrographs to

realistic manner. Maximum discharges for different return periods from HEC-RAS V.5 were simulated based on the assumption of steady flow condition, therefore flooding duration of inundation for each grid cells were unable to estimate. From physical properties of flood characteristics presented by the flood hazard map will be developed further to construct a flood risk map by formulating flood risk index (i.e. flood properties, socio-economic factor, land-use) and using GIS raster index model. The flood risk map can be utilized as a tool to identify priority of the area for planning of flood prevention, flood mitigation and flood risk management.

5.10 References

- Aerts, J.C.J.H., and Botzen, W.J.W. (2011). **Climate change impacts on pricing long-term flood insurance: a comprehensive study for the Netherlands**, *Global Environ Change*, Vol. 21, pp. 1045-1060.
- Alaghmand, S. (2009). **River modelling for flood risk map prediction (a case study of Sungai Kayu Ara**, MSc thesis, Universiti Sains Malaysia (USM), Malaysia.
- Alaghmand, S., Abustan, R., Abustan, I., and Ealamian, S. (2012). **Comparison between capabilities of HEC-RAS and MIKE11 hydraulic models in river flood risk modelling (a case study of Sungai Kayu Ara River basin, Malaysia)**, *Hydrology Science and Technology*, Vol. 2, No. 3, pp.270–291.
- Asia Disaster Reduction Center (ARDC). (2009). **Natural disaster data book 2009 (An analytical review)**, Kobe, Japan, pp. 23.
- Brunner, G. (2014). **Combined 1D and 2D modelling with HEC-RAS**, USACE, p.130.

- Congressional Budget Office. (2009). **The National Flood Insurance Program: Factors Affecting Actuarial Soundness**, Washington DC, The United States.
- Chow, V.T., Maidment, D.R. and Mays, L.W. (1988). **Applied hydrology**. New York, p.391.
- DHI Group. (2016). **MIKE 11 river modelling package and applications**. Available: <https://www.mikepoweredbydhi.com/products/mike-11> [Accessed: 10 October 2016].
- FLO-2D Software, Inc., products. (2016). **Webinars and training**. Available: <https://www.flo-2d.com> [Accessed: 10 October 2016].
- Furdada, G., Calderón, L. E. and Marqués, M. A. (2008). **Flood hazard map of La Trinidad (NW Nicaragua). Method and results**, Natural Hazards, Vol. 45(2) pp.183-195.
- Ghimire, R., Ferreira S., and Dorfman, J.H. (2015). **Flood-induced displacement and civil conflict**, *World Development*, Vol. 66, pp. 614-628.
- Jia, L.S., and Wenjiao, S. (2015). **Effects of alpine swamp wetland change on rainfall season runoff and flood characteristics in the headwater area of the Yangtze River**, *CATENA*, Vol. 127, pp. 116-123.
- Kabenge, M., Elaru, J., Wang, H. and Fengting, Li. (2017). **Characterizing flood hazard risk in data-scarce areas, using a remote sensing and GIS-based flood hazard index**, *Natural Hazards*, Vol. 89(3) pp.1369-1387.
- Kongjun T., and Noypairoj, S. (2011). Flood disaster in Nakhon Ratchasima Province on 14-16 October 2010, **Report of Royal Irrigation Department of Thailand**.

- Knebl, M.R., Yang, Z.L., Hutchison, K., and Maidment, D.R. (2005). **Regional scale flood modeling using NEXRAD rainfall, GIS, and HEC-HMS/RAS: a case study for the San Antonio River Basin Summer 2002 storm event**, Journal of Environmental Management, Vol.75(4 special issue), pp. 325–36.
- Lian, J.J., Xu, K., and Ma, C. (2013). **Joint impact of rainfall and tidal level on flood risk in a coastal city with a complex river network: a case study of Fuzhou City, China**, Hydrology and Earth System Sciences (HESS), Vol. 17(2), pp.679–89.
- Luu, C., Meding, J. V. and Kanjanabootra, S. (2018). **Assessing flood hazard using flood marks and analytic hierarchy process approach: a case study for the 2013 flood event in Quang Nam, Vietnam**, Natural Hazards, Vol. 90(3) pp.1031-1050.
- Maskong, H. and Jothityangkoon, C. (2013). **Flood mapping for the municipality of Nakhon Ratchasima**, in Proceedings of the 18th National Convention on Civil Engineering (NCCE18), Chiang Mai, Thailand May 8-10, 2013.
- Mohammadi, S.A., Nazariha, M., and Mehrdadi, N. (2014). **Flood damage estimate (quantity), using HEC-FDA model. Case study: the Neka river**, Procedia Engineering, Vol.70, pp.1173–82.
- Moya, Q.V., Kure, S., Udo, K., and Mano, A. (2016). **Application of 2D numerical simulation for the analysis of the February 2014 Bolivian Amazonia flood: Application of the new HEC-RAS version 5**, RIBAGUA –Rev Iberoam Agua.
- Nakhon Ratchasima City Municipality. (2016). **Statistics of population**. Available: <http://www.koratcity.go.th/page/population> [Accessed: 1 November 2016].

Ponsan, P., and Panchana, S. (2011). **Summarizing the implementation of prevention and mitigation of disasters caused by 2010 flooding in Nakhon Ratchasima**, Report of Royal Irrigation Department of Thailand.

Reports of Members on the Impact of Tropical Cyclones, (2011). **WMO/ESCAP Panel on Tropical Cyclones**, New Delhi, India, pp. 2-3.

The Associated Programme on Flood Management (APFM), (2013). **Flood Management Tools Series (Conservation and Restoration of Rivers and Floodplains)**. World Meteorological Organization.

US Army Corps of Engineers, (2014). **Hydrologic Engineering Centers River Analysis System (HEC-RAS)**, available at: <http://www.hec.usace.army.mil/software/hecras/> [Accessed: 15 November 2014].

CHAPTER VI

THE DEVELOPMENT OF A GIS TOOL APPLICATION FOR FLOOD RISK MAPPING: A CASE STUDY OF NAKHON RATCHASIMA MUNICIPALITY, THAILAND

6.1 Summary

A flood risk model was modified from Zonensein et al. (2008) and the GIS application tool was created for flood risk mapping. Land use change was the scenario of the flood risk model. The flood depth and flood velocity were the product of flood hazard map that simulated as follow in Chapter V. Land use in each of flood indicators are included to represent the risk rating in spatial system (1-5 score). The future Land use was predicted by existed map in CA-Makov model and the result show the change of flood risk area in different Lansuse from past to future. It was found that the community and business area are increased from 9.05% and 11.59% year 2012 to 2022, respectively. Total flood risk area of community and business area are increased by 38.35% and 9.60% from year 2012 to 2022. Therefore, the flood risk model is a powerful tool for generating the flood risk map that can be utilized as a tool to identify priority of the area for planning of flood prevention, flood mitigation and flood risk management and urban planning. Moreover, the GIS flood risk application tool is user friendly interface.

6.2 Introduction

Flood risk map is integration of the potential hazards with the vulnerabilities of existing or potential economic activities when disclosed to the risk range of flood probabilities. The flood risk map can be defined as the probability of a loss, and this depends on three elements including hazard, vulnerability, and exposure. The flood risk map can be developed by applying average damage values per unit area (per land use type) on the preliminary hazard maps. However, in the detailed mapping stage, flood risk maps need high accuracy (APFM, 2013).

6.3 Methodology

6.3.1 Input data

The conceptual framework of the study step for flood risk mapping is shown in Figure 6.1 and its consists of 3 components: (1) Land use change prediction (2) Flood hazard map simulation and (3) Flood risk mapping.

From the previous study in Chapter V, the suitable Rating curve (Figure 6.2) and Hydrograph (Figure 6.3) at runoff station M.164 were simulated from the flood event. They were used to be unsteady flow condition for simulating a flood hazard map.

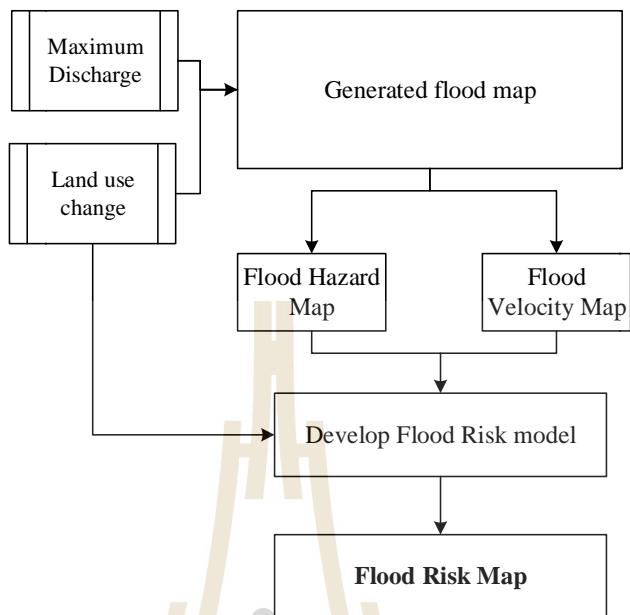


Figure 6.1 Flowchart of the study step for flood risk mapping

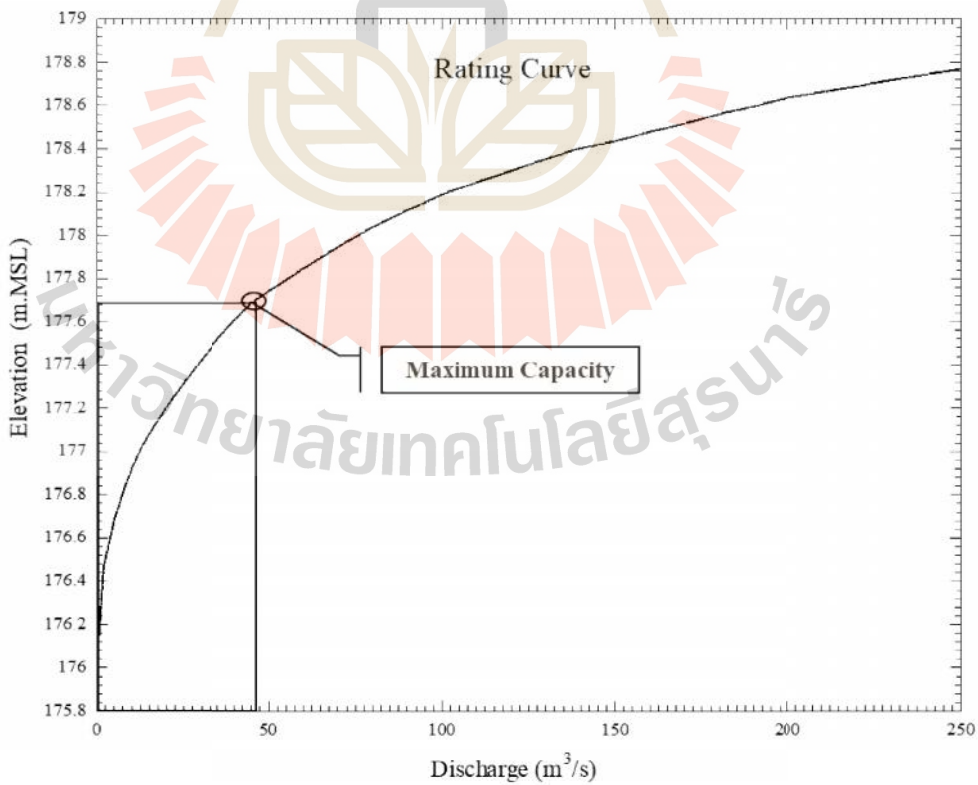


Figure 6.2 Simulated Rating curve at M.164

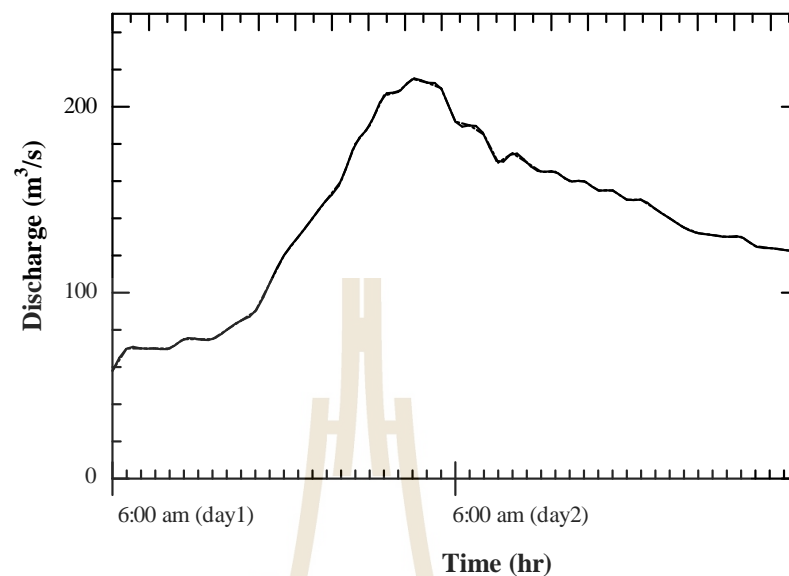


Figure 6.3 Generated runoff hydrograph for T=50 years (2010 flood event)

The land use maps as shown in Figure 6.4 and 6.5 were the classification of 2012 and 2017 Land use type of Nakhon Ratchasima Municipality, respectively. They were divided into 6 types including Water, Farm, Road, Empty, Community and Business. To perform Land use map prediction in the near future, the CA-Markov model was utilized and the obtained results was used as input data to quantify the consequent flood scenarios for that particular state of future Land use maps. The model is the result of integration between two individual modules, the Markov chain model and CA-Markov model that is available in the IDRISI software. The model can be used to generate such a transition probability matrix in which it takes two Land use maps as input data and then produces the output as the future Land use map (Eastman, 2003a, 2003b).

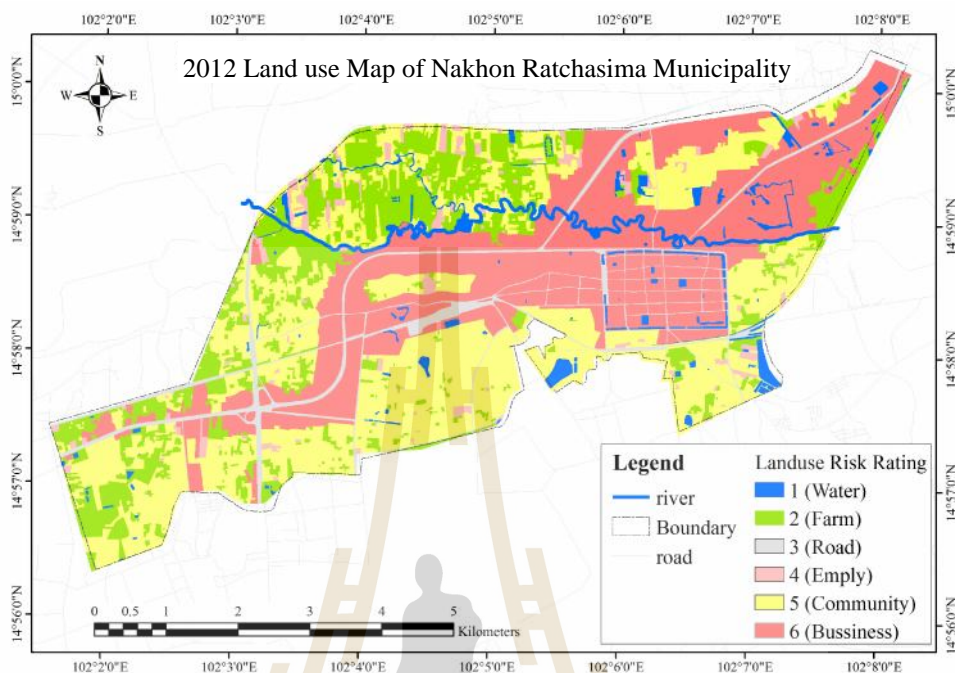


Figure 6.4 Land use Map in 2012 of Nakhon Ratchasima Municipality

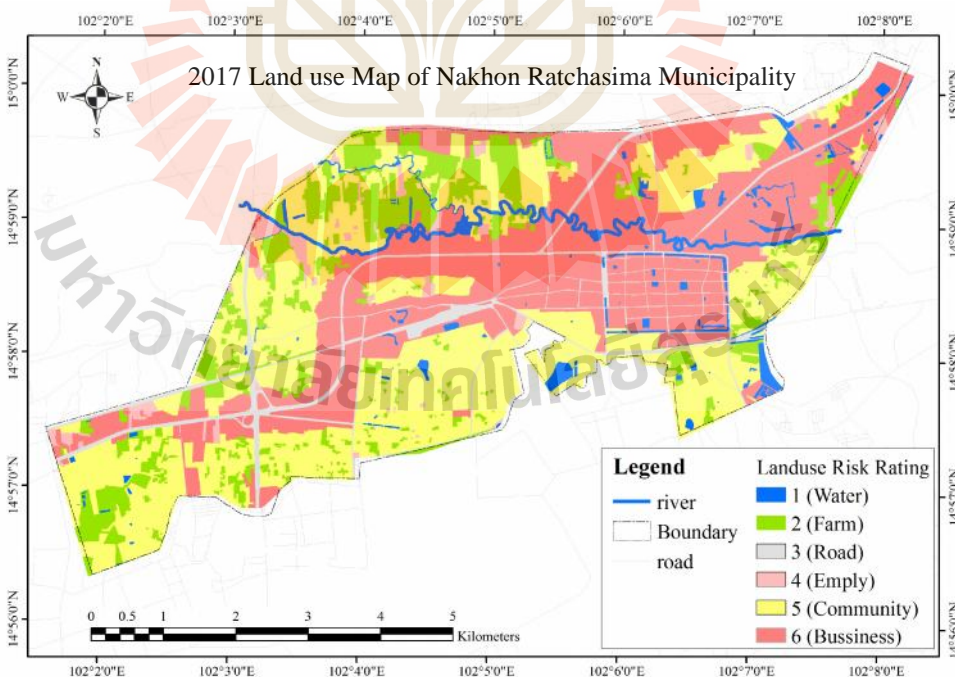


Figure 6.5 Land use in 2017 Map of Nakhon Ratchasima Municipality

6.3.2 Flood risk model

Flood risk is defined as the product of the probability and the consequences of flood event. Both components of risk are affected by multiple uncertainties but can conveniently divide between assessing the uncertainty associated with probabilities of the hazard and uncertainty associated with the consequences (the vulnerability). Both can be mapped individually, as well as the joint estimate of flood risk. Different types of vulnerability might require different types of visualizations. The risk of flood is based on three crucial elements which are related as the formula of flood risk shown in Equation 6.1 (Mongkonkerd et al.,2013).

$$\text{Flood risk} = \frac{\text{Vulnerability} \times \text{Characteristic}}{\text{Coping capacity}} \quad (6.1)$$

The best ways to reduce flood risk are reducing vulnerability and increasing coping capacity, which is a core common component of flood risk management. Figure 6.6 and 6.7 show the elements of flood risk which depend on vulnerability, flood characteristic, the ability of local people to cope with flood as follows.

Vulnerability refers to circumstances of a community or asset that make it susceptible to the damaging effects of a flood. There are many aspects of vulnerability, arising from various physical, social, economic, and environmental factors. Examples may include construction of buildings, inadequate protection of assets, lack of information and awareness.

Characteristic refers to natural disaster occurrence, frequency of damage, duration and maximum water level.

Coping capacity is the ability of people in the community to face and manage the flood using available skills and resources. The capacity to cope requires continuing awareness, resources and good management, both in normal times as well as during crisis or adverse conditions.

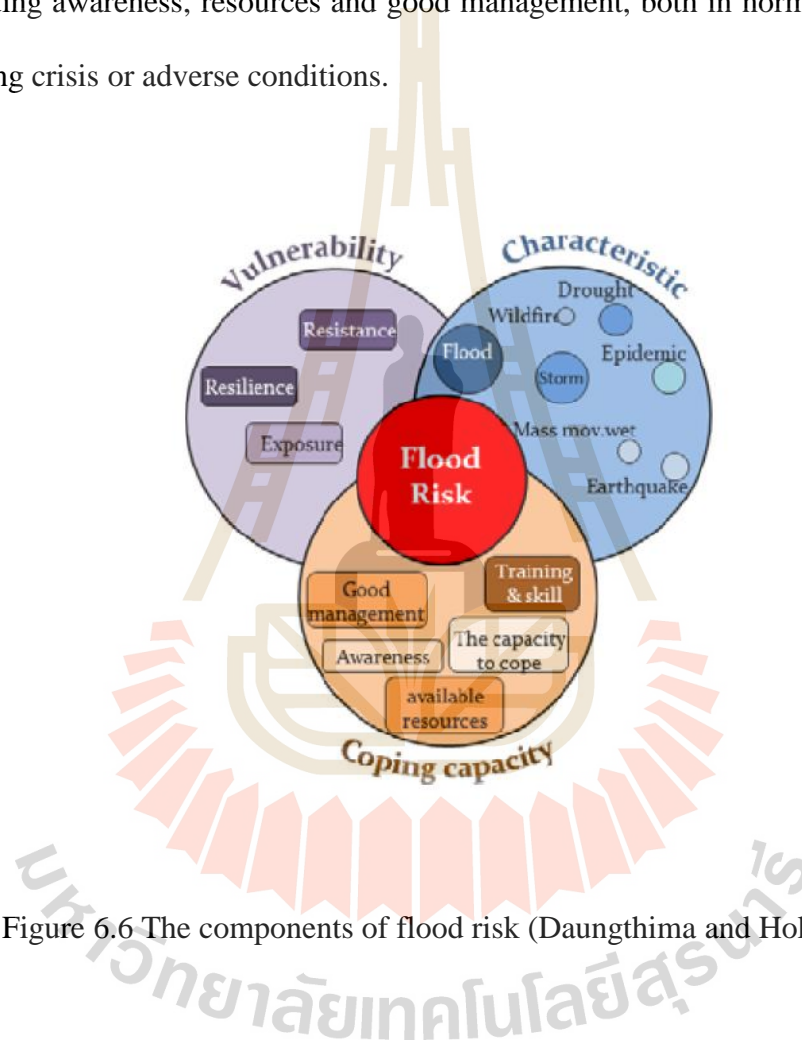


Figure 6.6 The components of flood risk (Daungthima and Hokao, 2013)

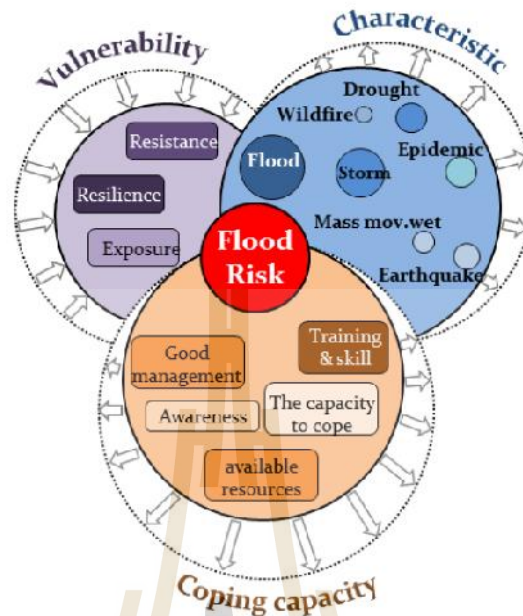


Figure 6.7 The reduction of flood risk (Daungthima and Hokao, 2013)

In this methodology, the probability component of flood risk is associated with the return period of a river flood event. This feature defines a basic information required to determine specific characteristics of a flood, such as its depth, land use type area, velocity. For the sake of simplicity and clarity, it was determined that the Flood Risk Index (FRI) should be a non-dimensional value, which could range between 1 and 5 the minimum and maximum risk, respectively (Modified from Zonensein et al.,2008). Moreover, in order to operate the indicators that compose flood risk rating, which have varied numbers and units, they must be normalized beforehand, converting them into a common range. According to the formulation established next, all indicators have to be adjusted to the same range, assuming values between 0 and 100.

The weighed product of these sub-indices results in the FRI, as presented in Equation 6.1. The weighted summation describes the relationship between the factors that constitute the sub-indices as show in Equation 6.2 (Zonensein et al.,2008), Faulkner et al.,2011).

$$FRI = FP^{q_{FP}} \times C^{q_c} \quad (6.1)$$

$$FRI = \left[\sum_{i=1}^n I_i^{FP} \cdot p_i^{FP} \right] \times \left[\sum_{j=1}^m I_j^C \cdot p_j^C \right] \quad (6.2)$$

Where:

FRI (Flood Risk Index) is the ranging between lowest risk and highest risk;

FP is the sub-index of the flood properties;

C is the sub-index of the flood consequences;

I_i^{FP} is i^{th} indicator for sub-index of the flood properties;

I_j^C is j^{th} indicator for sub-index of the flood consequences;

p_i^{FP} is the weighting factor associated with i^{th} indicator of sub-index FP,

$$0 \leq p_i^{FP} \leq 1 \text{ and } \sum_{i=1}^n p_i^{FP} = 1$$

p_j^C is the weighting factor associated with j^{th} indicator of sub-index C,

$$0 \leq p_j^C \leq 1 \text{ and } \sum_{j=1}^m p_j^C = 1$$

The risk of flood from the both of flood properties and flood consequences should be defined by each of the types of land use. In order to quantify the risk, the Equation 6.3 was modified from Zonensein et al. (2008), all indicators have to be adjusted to the same range, assuming risk values between 1 and 5.

$$FRI = \frac{\left[\sum_{i=1}^n I_i^{FP} \cdot p_i^{FP} \right] \times \left[\sum_{j=1}^m I_j^C \cdot p_j^C \right]}{5(n+m)} \quad (6.3)$$

Where: n is total number of indicators that compose sub-index FP and m total number of indicators that compose sub-index C.

The proposed Flood Risk Index (FRI) was developed according to these concepts and its properties were previously explained. The optimal of the constitutive indicators was conditioned by the availability of data, its precision and domain. Another restriction was that the FRI must be constituted by the minimum set of indicators proficient of sufficiently characterizing a particular scenario of risk. The indicators that compose the FRI mean to represent the main affects caused by flood. The classification of indicators is presented below in Table 6.1 to 6.3.

Table 6.1 Classification of the flood depth based on risk rating

Flood depth (m)	I_D^{FP}	Risk rating
<0.2	1	Very low
0.4	2	Low
0.7	3	Moderate
1.5	4	High
>1.5	5	Very high

Source: Adapted from Reiter (2000) and Chen (2007)

Table 6.2 Classification of the flood velocity based on risk rating

Flood velocity (m/s)	I_V^{FP}	Risk rating
<0.25	1	Very low
0.5	2	Low
1.0	3	Moderate
2.0	4	High
>2.0	5	Very high

Source: Adapted from Reiter (2000) and Chen (2007)

Table 6.3 Classification of the type of Land use that affected by flood

Land use type	I_{LU}^C	Risk rating
Empty	1	Very low
Farm	2	Low
Road	3	Moderate
Community	4	High
Business	5	Very high

6.3.3 GIS application tool

Flood risk model tool was created by model builder in ArcGIS. Flood properties from simulated flood hazard map and Land use change are the input data as a scenario. Flood risk map is generated by the flood risk model (Equation 6.3) from GIS application tool that shown in Figure 6.8 and Figure 6.9.

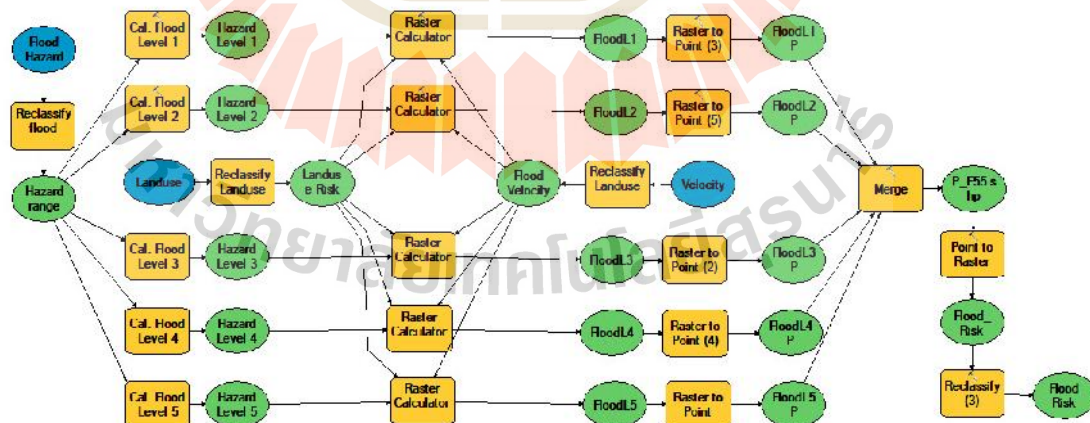


Figure 6.8 The model structure in the flood risk application tool

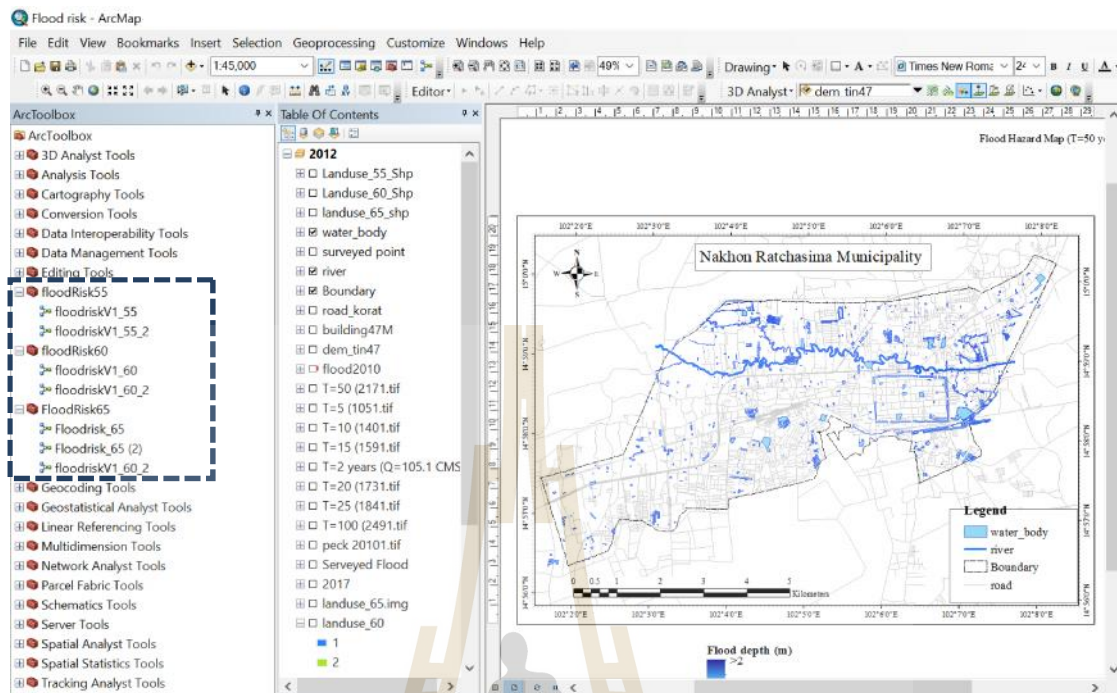


Figure 6.9 The flood risk application tool is applied in ArcGIS

6.4 Result and Discussion

The 2022 Land use map as shown in Figure 6.10 was predicted from 2012 and 2017 Land use map by CA-Makov model. Table 6.4 shows the change of covering area for different land use types in year 2012, 2017 and 2022. It was found that, in 2022 community and business areas are increased 9.05% and 11.59% from year 2012, respectively.

Table 6.4 Land use change from past 2012 and 2017 to future 2022 with different type of Land use

Land use type	2012		2017		2022	
	km ²	%	km ²	%	km ²	%
Water	1.32	3.54	1.22	3.27	1.19	3.16
Empty	6.9	18.46	5.02	13.43	3.79	10.06
Farm	2.02	5.4	2.02	5.4	2.02	5.35
Road	1.02	2.72	1.02	2.72	1.02	2.7
Community	13.48	36.1	14.35	38.41	14.7	39.55
Business	12.63	33.78	13.74	36.77	14.15	39.17
Total	37.37	100	37.37	100	37.37	100

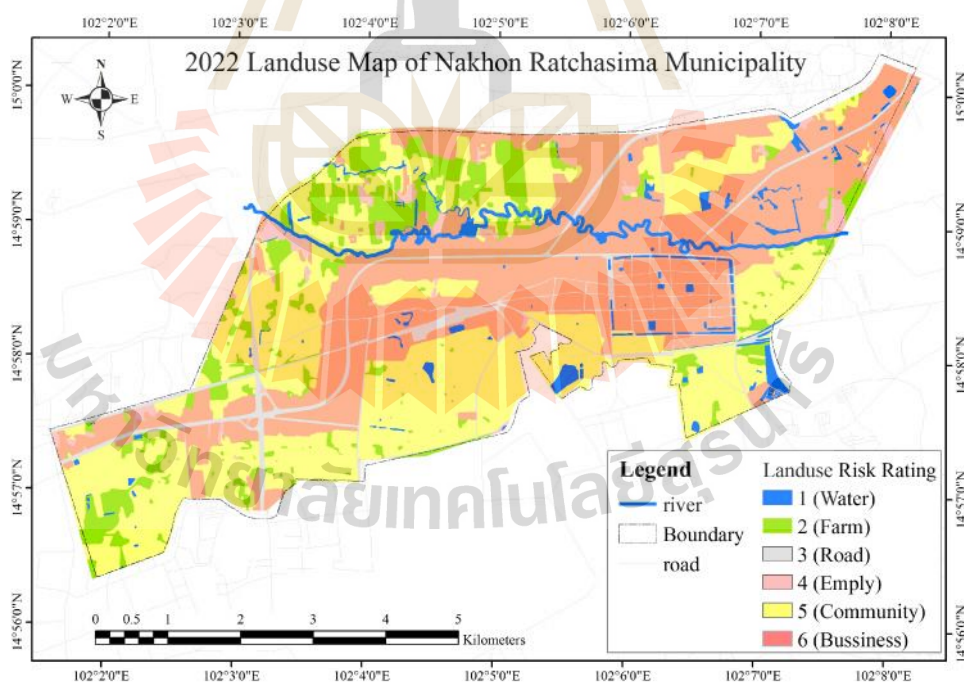


Figure 6.10 The 2022 Land use map of Nakhon Ratchasima Municipality

The flood hazard maps of years 2012, 2017 and 2022 based on Land use change were simulated by flood hazard model using an unsteady condition flow and geometrics data from Chapter V. The indicators of flood properties (The flood depth and flood velocity) are product of flood hazard map, shown in Figure 6.11 and 6.12. They are flood properties of year 2022 for Nakhon Ratchasima Municipality.

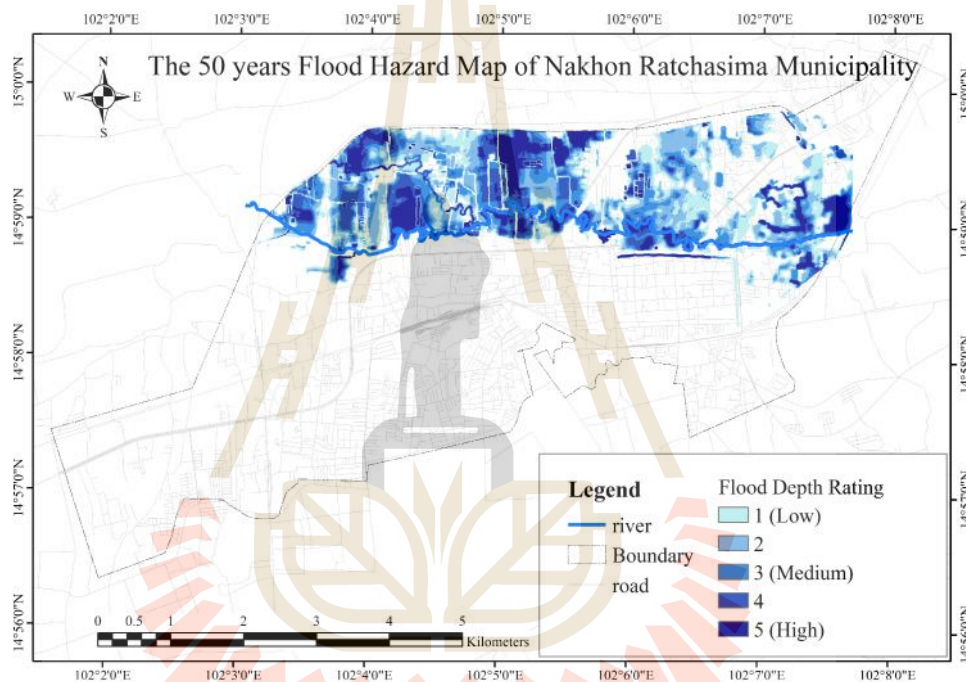


Figure 6.11 The 2022 classification of simulated flood depth at the return periods 50 years based on risk rating scale for Nakhon Ratchasima Municipality

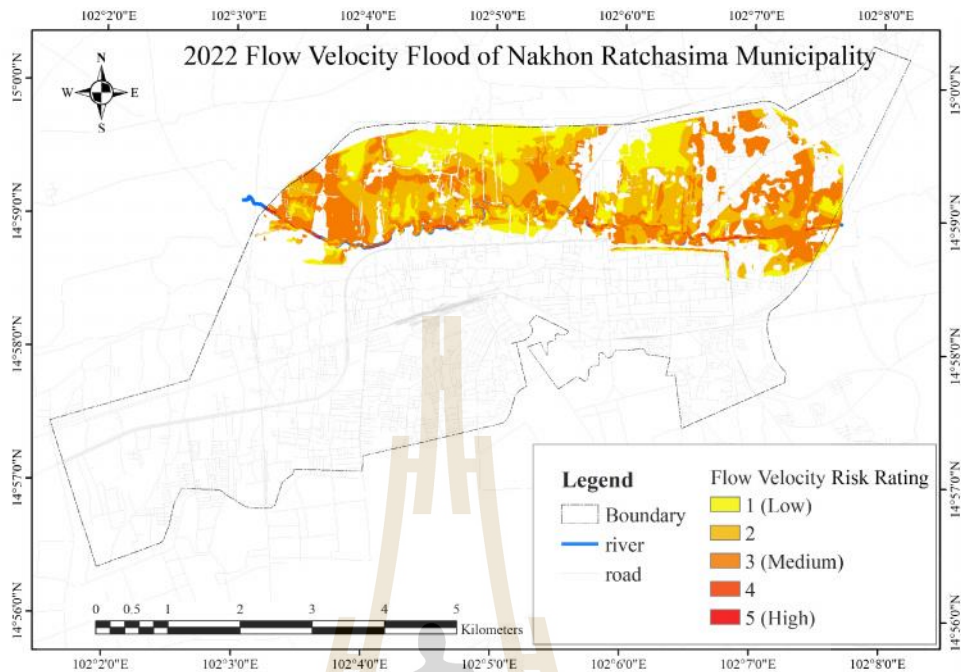


Figure 6.12 The 2022 classification of simulated flood velocity at the return periods 50 years based on risk rating scale for Nakhon Ratchasima Municipality

The Flood Risk map as shown in Figures 6.13, 6.14, and 6.15 were simulated from 2012, 2017 and 2022 flood indicators data by Flood risk model. Tables 6.5, 6.6 and 6.7 show the risk area for different land use in year 2012, 2017, and 2022, respectively. The total flood risk area of business, community and road zone are increased 38.35%, 9.60% and 8.08%, respectively from years 2012 to 2022.

Table 6.5 The rating risk area in year 2012 for different Land use types

Land use type	Total area (km ²)	Rating risk area					Total flood area (km ²)
		5 (km ²)	4 (km ²)	3 (km ²)	2 (km ²)	1 (km ²)	
Business	12.63	1.241	0	0.758	0.725	0	2.72
Community	13.49	0.62	0.491	0.64	0.666	0	2.42
Empty	1.02	0.06	0.092	0.102	0.122	0.089	0.46
Road	2.02	0	0.005	0.005	0.012	0.002	0.02
Farm	6.9	0	0	0.815	1.057	1.128	3
Water	1.32	0	0	0	0.379	0.256	0.64
Total	37.38	1.92	0.588	2.32	2.961	1.475	9.26

Table 6.6 The rating risk area in year 2017 for different Land use type

Land use type	Total area (km ²)	Rating risk area					Total flood area (km ²)
		5 (km ²)	4 (km ²)	3 (km ²)	2 (km ²)	1 (km ²)	
Business	13.76	1.627	0.177	0.92	0.856	0	3.58
Community	14.39	0.719	0.523	0.677	0.692	0	2.61
Empty	0.93	0.08	0.054	0.068	0.09	0.085	0.38
Road	2.02	0	0.005	0.005	0.012	0.005	0.03
Farm	5.02	0	0	0.656	0.835	0.584	2.07
Water	1.26	0	0	0	0.352	0.242	0.59
Total	37.38	2.425	0.759	2.326	2.837	0.915	9.26

Table 6.7 The rating risk area in year 2022 for different Land use type

Land use type	Total area (km ²)	Rating risk area					Total flood area (km ²)
		5 (km ²)	4 (km ²)	3 (km ²)	2 (km ²)	1 (km ²)	
Business	14.75	1.655	0.212	0.698	0.764	0.44	3.77
Community	14.9	0.271	0.453	0.533	0.689	0.701	2.65
Empty	0.72	0.147	0.041	0.032	0.069	0.08	0.37
Road	2.02	0.005	0.001	0.005	0.012	0.005	0.03
Farm	3.8	0.526	0.348	0.364	0.404	0.245	1.89
Water	1.19	0.342	0.059	0.048	0.04	0.074	0.56
Total	37.38	2.946	1.114	1.68	1.978	1.545	9.26

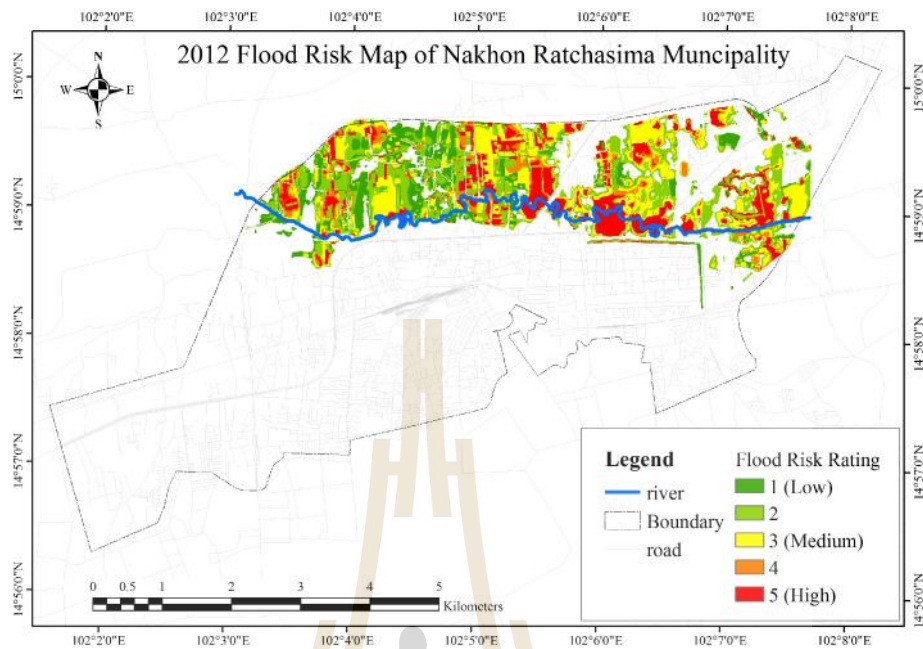


Figure 6.13 The 2012 Flood Risk Map of Nakhon Ratchasima Municipality

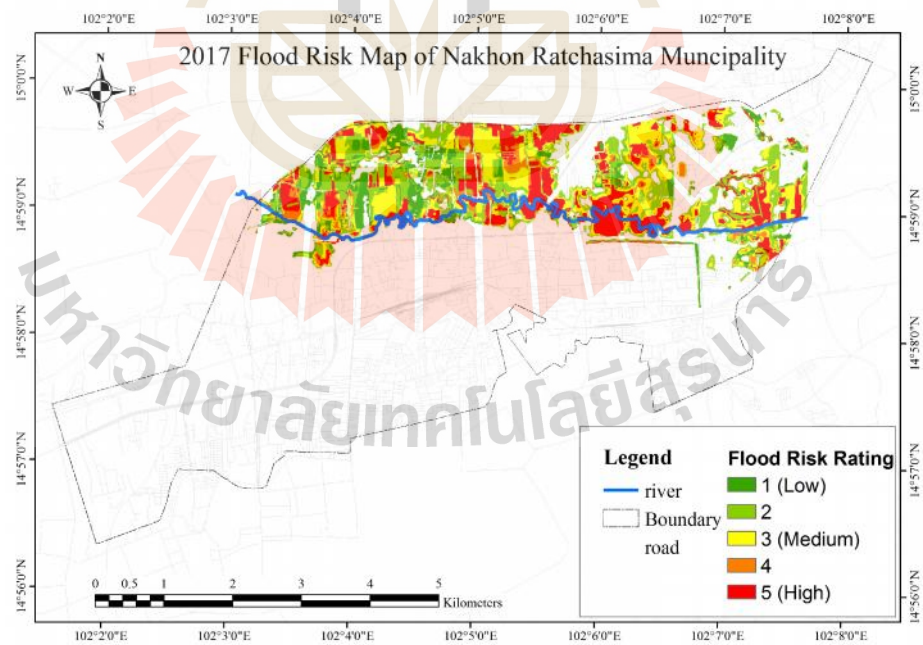


Figure 6.14 The 2017 Flood Risk Map of Nakhon Ratchasima Municipality

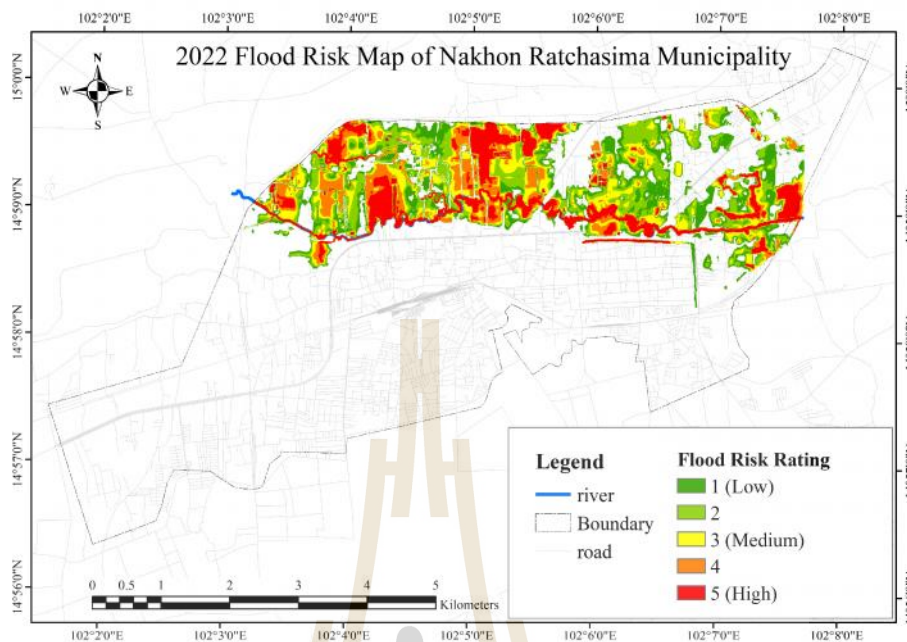


Figure 6.15 The 2022 Flood Risk Map of Nakhon Ratchasima Municipality



6.5 Conclusion

To construct a flood risk map, the flood risk model was modified from previous flood risk model of Zonensein et al. (2008) and the GIS application tool was created for flood risk mapping. The existing flood risk model was modified by considering the types of land use in each of flood indicators to represent the risk rating in spatial system. The future land use was predicted by existed map in CA-Makov model. The result shows the change of flood risk area in different land use from part to future. It was found that the total flood risk area of business, community and road zone are increased 38.35%, 9.60% and 8.08%, respectively from years 2012 to 2022 (10 years), respectively. For business area, very high flood risk area is increased 33.40% from years 2012 to 2022. The flood risk map can be utilized as a tool to identify priority of the area for planning of flood prevention, flood mitigation and flood risk management and urban planning.

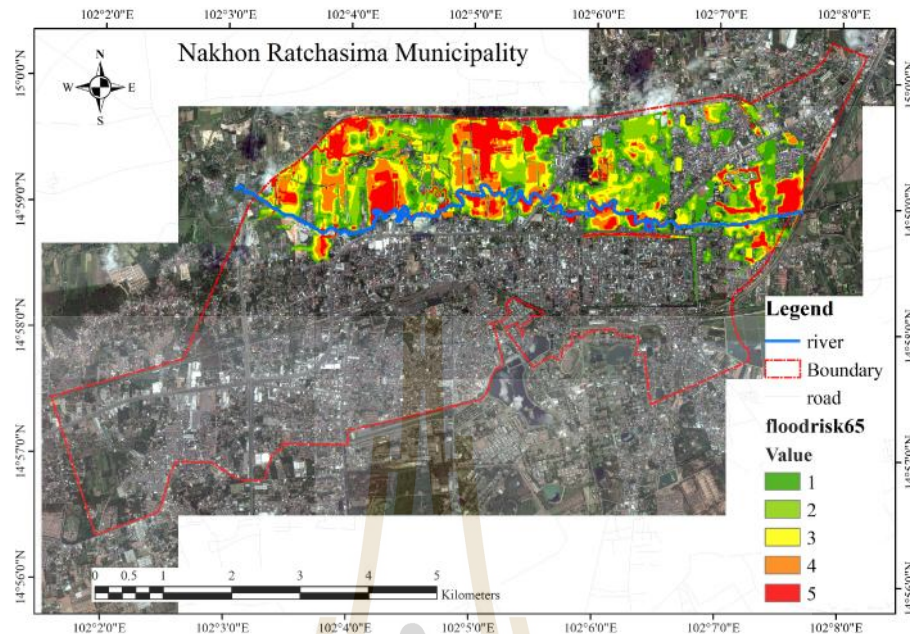


Figure 6.16 The 2022 Flood Risk Map with 2017 aerial photo of Nakhon Ratchasima Municipality

6.6 References

- Beven, K.J., and Kirkby, M.J. (1979). **A physically-based variable contributing area model of basin hydrology**, *Hydrol. Sci. J.*, 24(1), 43-69.
- Chen, P. (2007). **Flood impact assessment using hydrodynamic modelling in Bangkok, Thailand**. International Institute for Geo-Information Science and Earth Observation, Enschede, Netherlands.
- Daungthima, W. and Hokao, K. (2013). **Assessing the flood impacts and the cultural properties vulnerabilities in Ayutthaya, Thailand**. *Procedia Environmental Sciences*. 17: 739-748.
- Eastman, J.R. (2003a). **Idrisi Kilimajaro tutorial**. USA: Clark Laboratories, Clark University.

- Eastman, J.R. (2003b). **IDRISI Kilimanjaro: Guide to GIS and Image Processing**. USA: Clark Laboratories, Clark University.
- Faulkner, H., McCarthy, S., Tunstall, S., (2011). **Flood risk communication, in Flood Risk Science and Management**. edited by Pender, G. and Faulkner, H., pp. 386-406, Willey-Blackwell, UK.
- Mongkonkerd, S., Hirunsalee, S., Kanaegae, H. and Denpaiboon, C. (2013). **Comparison of direct monetary flood damage in 2011 to pillar house and non-pillar house in Ayuthhaya, Thailand**. *Procedia Environmental Sciences*, 17: 327-336.
- Reiter, P. (2000). **International methods of Risk Analysis, Damage Evaluation and Social Impact Studies concerning Dam-Break Accidents**, PR Water Consulting, Helsinki, Finland.
- The Associated Programme on Flood Management (APFM), (2013). **Flood Management Tools Series (Flood Mapping)**. World Meteorological Organization.
- Zonensein, J., Miguez, M.G., Magalhães, L.P.C., Valentin M.G. and Mascarenhas, F.C.B. (2008). **Flood Risk Index as an Urban Management Tool**. In:11th International Conference on Urban Drainage. Edinburgh, UK:/IWA,

CHAPTER VII

CONCLUSION AND RECOMMENDATION

7.1 Conclusion

In Chapter 4, a simple distributed hydraulic model is developed at the pixel/soil column scale and upscale to implement at the catchment scale. Applied water balance concept within the pixel and downstream interactions between each pixel allow the runoff generation by three mechanisms: HOF, DOF and SSF. Based on an actual building block of the selected DEM, the model can be parameterized for a large set of hypothetical catchments and input climate events. Simulation results are received when all processes are driven to reach a periodic steady state by a sequence of identical climate events. The advantage of this approach is simple, tractable and computationally efficiency that we can carry out for multiple realization of climate-soil- topography combination. This model will be used to simulate the effects of different combination of climate, soil, and topography on the runoff generation processes through hypothetical catchment and climate combination.

HEC-GeoRAS and ArcGIS are powerful tools as pre-processor for preparation for geospatial input data and also as a post-processor for visualization of the hydraulic model results for HEC-RAS models. In Chapter 5, the flood hazard map was simulated from the DEM and Land use using 1D2D hybrid method in HEC-RAS V.5. The improvement of rating curve in the floodplain was due to Land use condition

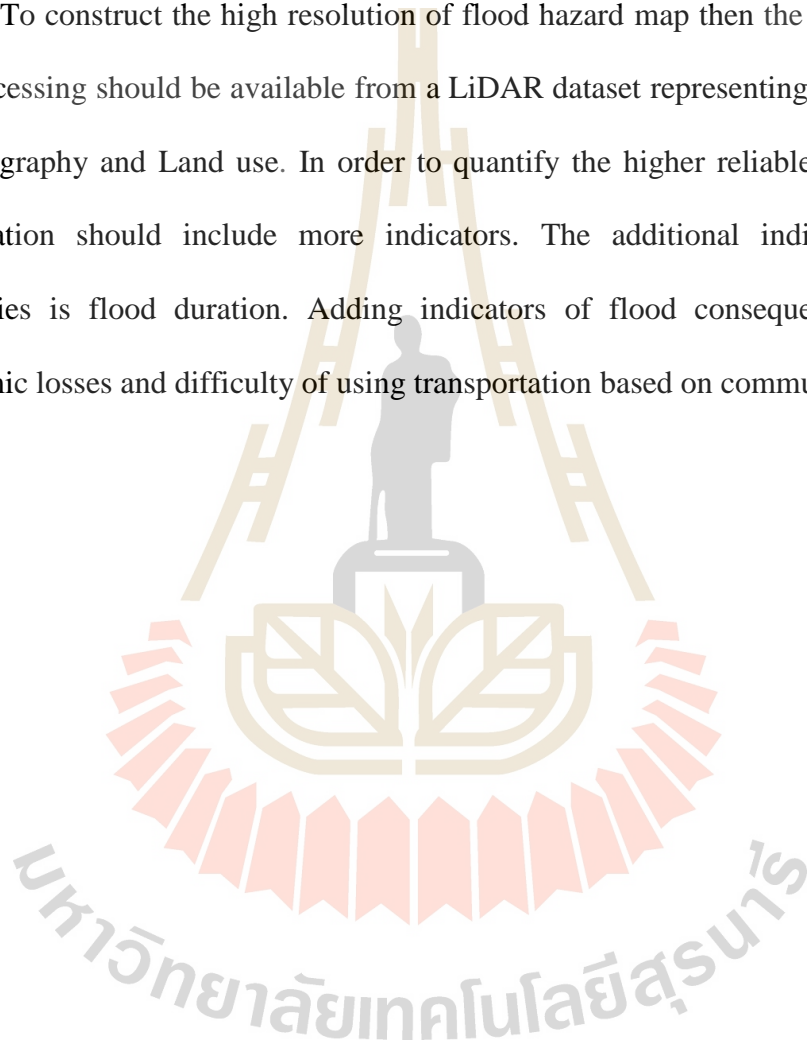
which leads to the increase of the river water level and volume and peak discharge of the simulated flooding. The runoff hydrograph in the flood event was generated to correct this flood hydrograph by the simulated flooding also. Flood depth and flood velocity are the product of flood hazard mapping that is the most important element to be the flood properties indicator for flood risk model.

In general, there are three limiting factors for the applicability of the flood risk model : (1) availability of data (2) existence of data with adequate precision and (3) limits of the normalization scales. In Chapter 6, the existing flood risk model (Zonensein et al. ; 2008) and the GIS application tool were applied to construct flood risk map by using input flood properties (flood depth and flood velocity) from Chapter 5. The Land use change is the scenario in this study and the flood risk rating can be defined for each of the Land use types. By using Markov chain model and CA-Markov model. The future community and business area are increased by 9.05% and 11.59% from year 2012 to 2022 (10 years), respectively. The predicted flood risk area of business, community and road zone from modified flood risk model are increased 38.35%, 9.60% and 8.08%, respectively from year 2012 to 2022. For business area, very high flood risk area is increased 33.40% from year 2012 to 2022. Therefore, the flood risk model is a powerful tool for generating the flood risk map for planning and management of flooding. Moreover, the GIS flood risk application tool is user friendly interface.

7.1 Recommendation

To develop the next step of a simple distributed hydraulic model to investigate the climate, soil and topographic controls on annual water balance in a qualitative way to define dimensionless functional relationships.

To construct the high resolution of flood hazard map then the terrain to raster geoprocessing should be available from a LiDAR dataset representing high resolution of topography and Land use. In order to quantify the higher reliable flood risk, the formulation should include more indicators. The additional indicator of flood properties is flood duration. Adding indicators of flood consequence are socio-economic losses and difficulty of using transportation based on community income.



BIOGRAPHY

Miss. Haruetai Maskong was born on November 26, 1982 in Nakhon Ratchasima Province, Thailand. She received her Bachelor's degree in Transportation Engineering from Suranaree University of Technology in 2005. She has worked as a Transportation engineer in Bangkok Marine Enterprises Company limited for a year after that she was a Teacher/Researcher assistant in School of Civil Engineering, Institute of Engineering, Suranaree University of Technology. In 2008, she received a scholarship awarding to graduate students whose lecturers are awarded research funding by outside sources (OROG) from Suranaree University of technology for Master degree study at Suranaree University of technology. In 2011, she received a Scholarship awarding to graduate student from Suranaree University of technology for Doctoral degree study at Suranaree University of technology. In 2015, she got a scholarship award from Austrian Government (OEAD) called Ernst Mach Grant, Ernst Mach-worldwide for research at Vienna University of Technology (1/11/2015-30/5/2016). She continued with her Ph.D. graduate studies in the Civil Engineering Program, School of Civil Engineering, Institute of Engineering, Suranaree University of Technology.